

# THESE DE DOCTORAT

Présentée à

L'UNIVERSITE DE LILLE  
ECOLE DOCTORALE DE BIOLOGIE SANTE-LILLE

## **“Deciphering biosynthesis mechanisms of *O*-acetylated GD2 in breast cancer”**

**« Étude des mécanismes de biosynthèse de la forme *O*-acétylée du GD2  
dans le cancer du sein »**

Pour l'obtention du titre de Docteur de l'Université de Lille par

**Sumeyye CAVDARLI**

Discipline : Aspects moléculaires et cellulaires de la biologie

Spécialité : Biochimie et biologie moléculaire

Soutenue le 23 janvier 2020 devant la commission d'examen :

Président : Pr Philippe Delannoy, Université de Lille, UGSF CMR 8576

Rapporteur : Pr Jacques Le Pendu, Université de Nantes, CRCINA UMR\_S\_1232

Rapporteur : Pr Koichi Furukawa, Chubu University, Japan

Examineur : Dr François Trottein, Inserm U1019, CNRS UMR 8204

Examineur : Dr Jean-Marc Le Doussal, OGD2 pharma, Nantes

Directeur : Dr Sophie Groux-Degroote, Université de Lille, UGSF CMR 8576

## AVANT-PROPOS

This work has been performed in UGSF UMR 8576 supervised by Dr Groux-Degroote in partnership with OGD2 Pharma Company.



“This is ten percent luck, twenty percent skills  
Fifty percent concentrated power of will  
Five percent pleasure, fifty percent pain  
And a hundred percent reason to remember the name “  
Fort Minor, Remember the name.

# ACKNOWLEDGMENTS

As a PhD thesis is a collaborative work, it naturally implies the personal and professional commitment of many people standing by my side: supervisors, colleagues, friends and family. I would like to thank all of them in these few lines for these past 3 years in “bâtiment C9” as “Céneuvien” and “Céneuvienne”.

**Philippe Delannoy & Sophie Groux-Degroote & Jean Marc Le Doussal**, I would like to thank all of you for giving me the opportunity to work on this “gangliosides initiation” project. Affiliated as an academician and industrial partner at the same time, I took this opportunity as a way of becoming a better scientific than I was. I am grateful to the confidence that you gave me since the beginning of my thesis.

**Koichi Furukawa**, thank you for accepting to be a member of my thesis’ jury. I am deeply grateful to be evaluated by such a master like you in gangliosides’ field. It is an utter honor.

**Jacques Le Pendu** and **François Trottein**, I am grateful for the follow-up of my thesis since the end of my first year. I really appreciate all the advice you both gave me in each meeting that led to the improvement of my work. In this final step of my thesis, I want to thank you for accepting to evaluate my work by being the member of my jury.

And I would like to pursue my acknowledgments as a Céneuvienne in French.

J’aimerai remercier **Anne Harduin-Lepers**, chef d’équipe du 017 pour toutes nos discussions sur mon projet de recherche, mes projets professionnels, et de croire en mes capacités de chercheur. Merci de m’avoir permis de gagner confiance en moi surtout sur la fin de ce parcours.

**Yann Guérardel**, un très grand merci pour tout : ton aide, ta disponibilité, tes conseils avisés, et la formation à la paillasse. Je ne serais jamais assez reconnaissante pour le temps que tu m’as dédié pour m’initier à la chimie structurale et de m’avoir aidée tout au long de ma thèse.

**François Foulquier**, je ne serais assez te remercier. Tu m’as permis de garder le cap de la thèse et de ne pas abandonner aux moments les plus compliqués. Je n’oublierai jamais que si j’ai pu en arriver là, c’est grâce à toi et aux déblocages du marquage des gangliosides par immunofluorescence ☺

**Nao Yamakawa**, tu as été ma formatrice en analyse structurale des gangliosides que j’ai développé chez Pagès. Nous avons développé beaucoup de projets « gangliosides » ensemble. Tu m’as énormément aidée à parfaire l’analyse et l’interprétation des résultats. Merci énormément.

**Guillaume Brysbaert**, mon bioinformaticien préféré !!! Le parcours des gangliosides et de CASD1 a été plus qu'éprouvant, merci pour tout le temps et l'effort que tu as consacré. L'initiation à la bioinformatique et Cytoscape n'aurait pas été aussi fun sans toi.

**Frédéric Bard**, Merci de m'avoir accueillie au sein de ton laboratoire « FB lab » et de m'avoir permis de réaliser le criblage à haut débit dans un endroit de rêve. Je te remercie pour tes conseils et de m'avoir challengé lors du « lab meeting ». J'ai vraiment apprécié ce court séjour à Singapour.

**Xavier Le Guézennec**, tu as été pour moi « the » personne indispensable et responsable du succès de screening à Singapour. J'ai beaucoup appris de tes conseils et de ton exigence à la perfection. Merci beaucoup pour tout : la formation, les analyses, les discussions, l'apprentissage de l'exécution parfaite et l'initiation à la culture singapourienne.

**Corentin Spriet**, pour moi voulais dire « expert en imagerie ». Merci d'avoir trouvé le temps pour la formation en microscopie, les scripts pour la quantification de fluorescence dans ton planning « over-surbooké » et toujours dans la bonne humeur.

**Christophe Mariller**, merci encore pour tous tes conseils scientifiques et informatiques.

**Martine et Laurence** sans vous mesdames, je n'aurais jamais appris à manier les lignes budgétaires de l'Université et du CNRS, à réaliser mes commandes, à envoyer mes colis, aux fiches de mission pour partir en congrès et à Singapour. Merci ;)

Je tiens à remercier **Manu, Charlotte et Bernie** de la plateforme Pagès ainsi que **Fred** affilié au bureau Pagès pour leur accueil dans la bonne humeur, le partage de leur expertise scientifique et leur service de localisation GPS pour retrouver Nao ☺

Merci la Team 017 avec **Virginie, Céline et Dorothée** pour vos conseils pratiques et techniques qui m'a accompagné tout au long de la thèse.

**Et le Trio du 017+3 : Justine, Maxence + Mathieu, Audrey et Laurine.** Je tiens à faire vivre notre adage comme l'a dit Maxence « Lab partnership has no end ! ». Grande pensée à tous nos moments, aux délires, aux fous rires, aux karaoké-labo, aux séances de nettoyage, aux pauses café, aux congrès et j'en passe, votre soutien m'a été vital les amis... Maxence tu m'as toujours impressionné par ta patience et ta bonne humeur constante, même dans les moments où tu n'en pouvais plus de nous ☺. Justine, ma complémentaire, ma blonde préférée, merci d'avoir été à mes côtés. Je te souhaite tout ce qu'il y a de meilleur. Mathieu, mon pioupiou, je t'ai vu grandir depuis ta licence 3 chez nous. Passionné par la science, tu as réussi à conquérir notre cœur et à assurer ta place parmi nous dans le trio du 017. Ainsi que **Audrey**, alias pioupiou clone 2 ☺ pour tous les bons moments

au labo. Je vous souhaite tout le bonheur et la réussite pour la suite de votre thèse. Laurine, tu es ma petite stagiaire préférée, devenue maintenant amie, je ne peux souhaiter que ton bonheur.

Une petite pensée pour **Agata** sans qui je n'aurai jamais été initié à la boxe et aux sports de combats et à **Elodie** et **Angelina** toujours motivée à me suivre pour une séance ou deux dans la semaine pour faire le plein de sérotonine avant de terminer sur une pause salée chez « Salad'&Co ». Elo, ma superwoman du C9 et du CHU, je te souhaite une très bonne fin de thèse. Et Nana, je suis sûre que tu vas finir par en faire une, peut-être bien au C9 ? ;)

D'une manière générale, Merci aux potos Céneuvien qui ont contribué à la bonne humeur : **Marzia, Charles, Lin, Anne-So, Marine, Vincent, Louis-David, Kenji, Sandrine, Marlène, James, Shin-Yi, Sylvain** et **Malika**.

et aux potos du FB lab : **Belinda, Son, Trinda, Jeremy, Felicia, Alex, Poonam**.

Je n'oublie pas non plus OGD2 pharma,

**Mylène**, la Wonder Woman de chez OGD2 pharma, tu es la personne la plus multitâche que je connaisse et surtout celle à qui j'ai recourt pour le moindre souci. Sincèrement, merci !

**Brigitte**, merci pour ton soutien durant cette thèse. En temps qu'électron libre de la société, j'ai beaucoup appris sur la manière de penser « private company » suite à tes interventions pendant nos réunions.

Et merci aux anciens **Julie, Samuel, Mickaël, Denis, Elise**, qui ont fait partie de cette thèse à distance et dans les moments Nantais. Je tiens à porter une attention particulière à **Samuel** pour avoir contribué à la réalisation du screening à Singapour et à mon Scientific Advisor **Mickaël** initiateur de ce projet de thèse.

*D'un point de vue personnel,*

Je me dois de remercier **mes parents** sans qui je ne serais la personne, la femme, la scientifique que je suis aujourd'hui. Un grand merci à ma petite **Merve** et **Sinan** d'avoir été toujours à mes côtés. Je suis reconnaissante de tous vos efforts, votre soutien et votre encouragement qui m'ont permis d'aboutir toute mes entreprises et à l'occurrence cette thèse. Vous allez pouvoir enfin répondre à la question : « Que fait votre fille dans la vie ? »

*"If there's magic in boxing, it's the magic of fighting battles beyond endurances...*

*It's the magic of risking everything for a dream that nobody sees but you...*

*But step back too far and you ain't fighting at all."*

Eddie Dupris, Million Dollar Baby.

## PUBLICATIONS

Cavdarli S., Yamakawa N., Clarisse C., Brysbaert G., Le Doussal JM., Delannoy P., Guérardel Y., Groux-Degroote S.,

**“Profiling of *O*-acetylated gangliosides expressed in neuroectoderm derived cells “**

International Journal of Molecular Science, January 2020.

doi:10.3390/ijms21010370

Cavdarli S., Groux-Degroote S., Delannoy P.,

**“Gangliosides: double edge-sword of neuroectodermal derived cancers”**

Biomolecules, July 2019.

doi:10.3390/biom9080311

Groux-Degroote S., Cavdarli S., Uchimura K., Allain F., and Delannoy P.,

**“Glycosylation changes in inflammatory diseases “**

Advanced in Protein in Chemistry and Structural Biology, November 2019.

<https://doi.org/10.1016/bs.apcsb.2019.08.008>

Cavdarli S., Dewald J.H., Yamakawa N., Guérardel Y., Terme M., Le Doussal JM., Delannoy P., and Groux-Degroote S.,

**“Identification of 9-*O*-Acetyl-N-Acetylneuraminic Acid (Neu5,9Ac2) as Main *O*-Acetylated Sialic Acid Species of GD2 in Breast Cancer Cells.”**

Glycoconjugate Journal, January 2019.

<https://doi.org/10.1007/s10719-018-09856-w>.

Dewald, JH., Cavdarli S., Steenackers A., Delannoy CP., Mortuaire M., Spriet C., Noël M., Groux-Degroote S., and Delannoy P.,

**“TNF Differentially Regulates Ganglioside Biosynthesis and Expression in Breast Cancer Cell Lines.”**

PloS One 13 (4), April 2018: e0196369.

<https://doi.org/10.1371/journal.pone.0196369>.

# COMMUNICATIONS

## **ORAL**

**International Symposium on Glycoconjugates, Milan, Italy** “Is CASD1 responsible for GD2 *O*-acetylation? Cavdarli S., Dewald, JH., Yamakawa, N., Guérardel, Y., Terme, M., Le Doussal, JM., Delannoy, P., Groux, S, August 2019.

**UGSF Seminar, Lille, France** “Deciphering biosynthesis mechanisms of *O*-acetylated GD2 in breast cancer” Cavdarli S., March 2019

**Glycobiology Gordon Research Seminar, Lucca, Italy** “Biosynthesis mechanism of *O*-acetylated GD2 in breast cancer cells” Cavdarli, S., Dewald, JH., Yamakawa, N., Guérardel, Y., Terme, M., Le Doussal, JM., Delannoy, P., Groux, S, March 2019.

## **POSTER**

**30<sup>th</sup> Joint Glycobiology Meeting, Lille, France 2019:** “Is CASD1 responsible for GD2 *O*-acetylation? Cavdarli S., Dewald, JH., Yamakawa, N., Guérardel, Y., Terme, M., Le Doussal, JM., Delannoy, P., Groux, S,

**Glycobiology Gordon Research Conference, Lucca, Italy:** “Biosynthesis mechanism of *O*-acetylated GD2 in breast cancer cells” Cavdarli, S., Dewald, JH., Yamakawa, N., Guérardel, Y., Terme, M., Le Doussal, JM., Delannoy, P., Groux, S, 2019.

**29<sup>th</sup> Joint Glycobiology Meeting, Ghent, Belgium 2018.** Identification of Neu5,9Ac2 as the main acetylated form of GD2 in breast cancer cells. Cavdarli, S., Dewald, JH., Yamakawa, N., Guérardel, Y., Terme, M., Le Doussal, JM., Delannoy, P., Groux, S, 2019.

**Alfred Benzon Symposium- Glycotherapeutics- Emerging roles of glycans in Medicine, Copenhagen 2018.** Identification of Neu5,9Ac2 as the main acetylated form of GD2 in breast cancer cells. Cavdarli, S., Dewald, JH., Yamakawa, N., Guérardel, Y., Terme, M., Le Doussal, JM., Delannoy, P., Groux, S, 2019.

**28<sup>th</sup> Joint Glycobiology Meeting, Aachen, Germany 2017** “Expression, and biosynthesis of *O*-Acetylated GD2 in breast cancer.” Cavdarli, S., Dewald, JH., Yamakawa, N., Guérardel, Y., Terme, M., Le Doussal, JM., Delannoy, P., Groux, S.

# SUMMARY

<b>ABSTRACT .....</b>	<b>14</b>
<b>RESUME.....</b>	<b>15</b>
<b>ABBREVIATION .....</b>	<b>16</b>
<b>INTRODUCTION.....</b>	<b>17</b>
GENERAL INTRODUCTION.....	18
1-Neuroectoderm: from development to tumorigenesis.....	18
2- Breast Cancer .....	19
<b>PART I: IMMUNOTHERAPY TARGETING GANGLIOSIDES .....</b>	<b>23</b>
1- Structural characterization of antibodies.....	23
2- Immunotherapy and therapeutic antibody.....	27
3-Anti-cancer therapeutic antibody activities .....	31
A- Immune system independent mechanisms.....	31
B- Immune system dependent mechanisms .....	32
4- Anti-GD2 therapeutic mAb against Neuroblastoma .....	33
A- Neuroblastoma.....	33
B- Anti-GD2 antibodies.....	34
C- Dinutuximab/ Qarziba .....	37
<b>PART II- GANGLIOSIDES CHEMISTRY AND BIOLOGY.....</b>	<b>40</b>
1- Expression and Roles.....	40
2- Structure.....	55
A- Glycosphingolipids .....	55
B- Gangliosides .....	56
C- Sialic Acids.....	58
3- Metabolism.....	59
A- De novo biosynthesis.....	59
B- Catabolism.....	62
C- Regulation of ganglioside metabolism .....	65
D- O-acetylated gangliosides.....	70



<b>STATE OF THE ART .....</b>	<b>78</b>
<b>THESIS OBJECTIVES .....</b>	<b>79</b>
<b>RESULTS.....</b>	<b>80</b>
PART I: ROLE OF CASD1 IN GD2 <i>O</i> -ACETYLATION IN BREAST CANCER CELL LINES .....	81
1-Introduction .....	81
2-Material and methods.....	81
3-Results.....	84
A-Depletion of <i>CASD1</i> expression .....	84
B- Transient overexpression of <i>CASD1</i> in SUM159PT cells.....	85
C- Effect of stable CASD1 overexpression in SUM159PT cells .....	87
4-Discussion & Conclusion.....	88
PART II: IDENTIFICATION OF 9- <i>O</i> -ACETYL-N-ACETYLNEURAMINIC ACID AS THE MAIN <i>O</i> -ACETYLATED SIALIC ACID SPECIES OF GD2 IN BREAST CANCER CELLS. ....	90
PART III: <i>O</i> -ACETYLATED GANGLIOSIDES PROFILING IN BREAST CANCER CELL LINES BY MASS SPECTROMETRY .....	103
PART IV: IDENTIFICATION OF GENES INVOLVED IN OAcGD2 BIOSYNTHESIS USING PHOSPHATOME/ KINOME siRNA HIGH THROUGHPUT SCREENING. ....	125
1- Introduction .....	125
2-Material & Methods .....	126
3-Results.....	129
A- Workflow of phosphatome/kinome siRNA screen .....	129
B- Selection of hits.....	132
4-Discussion.....	136
5-Conclusion.....	140
<b>DISCUSSION &amp; PERSPECTIVES.....</b>	<b>142</b>
<b>REFERENCES.....</b>	<b>153</b>

# ILLUSTRATIONS TABLE

<i>Figure 1 : Estimation of numbers of incident and death worldwide among women.</i>	19
<i>Figure 2: Structural organization of Immunoglobulin G in two-dimensional model.</i>	24
<i>Figure 3: Structure of murine, human, chimerized and humanized antibody.</i>	29
<i>Figure 4: Structure of a GSL composed of a ceramide backbone and a carbohydrate moiety: the example of GD2 ganglioside.</i>	56
<i>Figure 5: Major sialic acid species: Neu5Ac, Neu5Gc, KdN.</i>	58
<i>Figure 6: Glucosylceramide synthesis pathway. Adapted from Van Echten et Sandhoff, 1993.</i>	60
<i>Figure 7: Biosynthesis pathway for gangliosides. Adapted from Julien et al., 2013.</i>	62
<i>Figure 8: Subcellular traffic and metabolic turnover of gangliosides.</i>	63
<i>Figure 9: Ganglioside catabolism pathway. Adapted from Tettamanti et al., 2004</i>	65
<i>Figure 10: Proposed CASD1 acetyltransferase activity. A- CASD1 SOAT activity on CMP-Neu5Ac. B- Biosynthesis pathway for OAcGD3 ganglioside by directly acetylation of GD3.</i>	73
<i>Figure 11: Organization of CASD1 gene and protein.</i>	74
<i>Figure 12: CASD1 gene expression in healthy tissues according to the Human Protein Atlas.</i>	75
<i>Figure 13: CASD1 expression in cancer tissues and cell lines on the Human Protein Atlas.</i>	76
<i>Figure 14: Kaplan Meier survival plotter in BC patients.</i>	77
<i>Figure 15: Reduced OAcGD2 expression in SUM159PT depleted for CASD1 expression using siRNA strategy.</i>	84
<i>Figure 16: Increased OAcGD2 expression in CASD1 overexpressing SUM159PT cells using plasmid transfection.</i>	86
<i>Figure 17: CASD1 expression in SUM159PT CASD1+ clones after stable transfection.</i>	87
<i>Figure 18: Biological properties of selected SUM159PT CASD1+ clones.</i>	89
<i>Figure 19: Workflow of phosphatome/kinome screen on OAcGD2 expression in MDA-MB-231 GD3S+ cells.</i>	128
<i>Figure 20: Identification of the transfection efficiency on both replicates.</i>	129
<i>Figure 21: OAcGD2 staining in control wells.</i>	130
<i>Figure 22: Kinome/phosphatome screening of replicate 1 formatted with Alternative score.</i>	131
<i>Figure 23: Correlation of replicates.</i>	132
<i>Figure 24: Representative images of selected genes modulating OAcGD2 expression.</i>	134

# TABLE LIST

<i>Table 1: TNM classification of BC according to AJCC.....</i>	<i>20</i>
<i>Table 2: Molecular classification of BC.....</i>	<i>21</i>
<i>Table 3: Histological grade of BC according to the Scarff-Bloom-Richardson classification.....</i>	<i>21</i>
<i>Table 4: Properties of immunoglobulins isotypes. Adapted from Schroder et al., 2010.....</i>	<i>26</i>
<i>Table 5: Properties of IgG subtypes. Adapted from Bruhns et al., 2012.....</i>	<i>26</i>
<i>Table 6: List of anti-GD2and OAcGD2 antibodies. ....</i>	<i>35</i>
<i>Table 7: Oligosaccharidic cores of GSL-series. Cer: ceramide; Glc: glucose; Gal: galactose; GalNAc: N-acetylgalactosamine.....</i>	<i>55</i>
<i>Table 8: Nomenclature of gangliosides.....</i>	<i>57</i>
<i>Table 9: Hit list of genes modulating OAcGD2 expression in MDA-MB-231 GD3S+ cells.....</i>	<i>135</i>

# ABSTRACT

*O*-Acetylated GD2 (*O*AcGD2) ganglioside is neo-expressed in neuroectodermal derived tumors as neuroblastoma and breast cancer. This oncofetal marker is an essential target for immunotherapy. Dinutuximab (Unitixin TM), a therapeutic antibody targeting GD2 has recently obtained Food Drug Administration and European Medicines Agency approval for neuroblastoma treatment. Nevertheless, Dinutuximab causes toxicity due to the expression of GD2 on peripheral nerve fibers. In that way, targeting *O*AcGD2 seems more beneficial because of absence of this antigen in normal tissues. The activities of OGD2 Pharma Company, partner of this project, are focused on therapeutic antibody development against *O*AcGD2. OGD2 Pharma developed an antibody specifically targeting *O*AcGD2 with no cross reaction with GD2. Absent from the normal mammary gland, complex gangliosides especially GD2 and its *O*-acetylated form have been detected in breast cancer. This expression is correlated with poor patient outcome. The aim of this thesis project was to decipher the molecular mechanisms of *O*AcGD2 biosynthesis, expression and its role in breast cancer, in order to highlight the therapeutic and diagnostic value of targeting *O*AcGD2 in breast cancer.

## RESUME

Le ganglioside GD2, ré-exprimé dans les cancers d'origine neuro-ectodermique, a été caractérisé comme un antigène oncofetal constituant une cible pour l'immunothérapie. L'anticorps anti-GD2 dinutuximab (Unitixin, TM) a récemment obtenu l'agrément de la Food Drug Administration et de l'Agence Européenne du Médicament pour le traitement des neuroblastomes pédiatriques. Cependant, l'utilisation de cet anticorps se heurte à de forts problèmes de toxicité due à l'expression du GD2 dans les nerfs périphériques sains. La forme *O*-acétylée du GD2 (OAcGD2) n'est exprimé que dans les tissus cancéreux représentant ainsi une cible thérapeutique moins toxique que le GD2. Les activités de la société OGD2 Pharma, partenaire de ce projet, sont axées sur le développement d'anticorps thérapeutiques dirigés contre le GD2 *O*-acétylé. L'anticorps développé cible spécifiquement au GD2 *O*-acétylé sans réaction croisée avec GD2. Dans le cancer du sein, les gangliosides complexes, notamment le GD2 et sa forme *O*-acétylé sont ré-exprimés. Cette expression est corrélée à un mauvais pronostic chez les patientes atteintes de cancer du sein. L'objectif principale de ma thèse est d'identifier les mécanismes moléculaires régissant l'*O*-acétylation du GD2 dans le cancer du sein afin de mettre en évidence l'intérêt thérapeutique et diagnostique du ciblage de cet antigène.

## ABBREVIATION

- AA: Amino Acid
- ADC: Antibody Drug Conjugates
- ADCC: Antibody Dependent Cell Cytotoxicity
- BC: Breast Cancer
- CDC: Complement Dependent Cytotoxicity
- CDK: Cyclin Dependent kinase
- CDR: Complement Determining Region
- CNS: Central Nervous System
- CSC: Cancer Stem Cell
- ER: Endoplasmic Reticulum
- EMA: European Medicines Agency
- Ig: Immunoglobulin
- IgG: Immunoglobulin G
- Fab: Fragment antigen binding
- Fc: Fragment crystallizable
- FDA: Food Drug Administration
- FcR: Fragment crystallizable receptor
- FCS: Fetal Calf Serum
- GlcCer: Glucosylceramide
- GlcCerT: Glucosylceramide synthase
- GM2-AP: GM2 Activator Protein
- GM-CSF: Granulocytes Macrophages-colony stimulating factor
- GSL: Glycosphingolipids
- GT: Glycosyltransferase
- HACA: Human Anti-Chimeric Antibody
- HAMA: Human Anti-Mouse Antibody
- HPRT: Hypoxanthine guanine PhosphoRibosyl Transferase
- KdN: 3-deoxy-non-2-ulosonic acid
- LacCer: Lactosylceramide
- Lse: Lysosomal Sialic Acid *O*-acetyltransferase
- mAb: monoclonal Antibody
- NB: Neuroblastoma
- Neu5Ac: N-acetylneuraminic acid
- Neu5Gc: N-glycolylneuraminic acid
- PBMC: Peripheral Blood Mononuclear Cells
- PNS: Peripheral nervous system
- SAP: Sphingolipid Activator Protein
- SCLC: Small Cell Lung Carcinoma
- Sia: Sialic Acid
- sLex: Sialyl Lewis x
- SOAE: Sialyl-*O*-acetyltransferase
- SOAT: Sialyl-*O*-acetyltransferase
- scFv: single chain variable Fragment
- TACA: Tumor Associated Carbohydrate Antigen

## INTRODUCTION

## General Introduction

### *1-Neuroectoderm: from development to tumorigenesis*

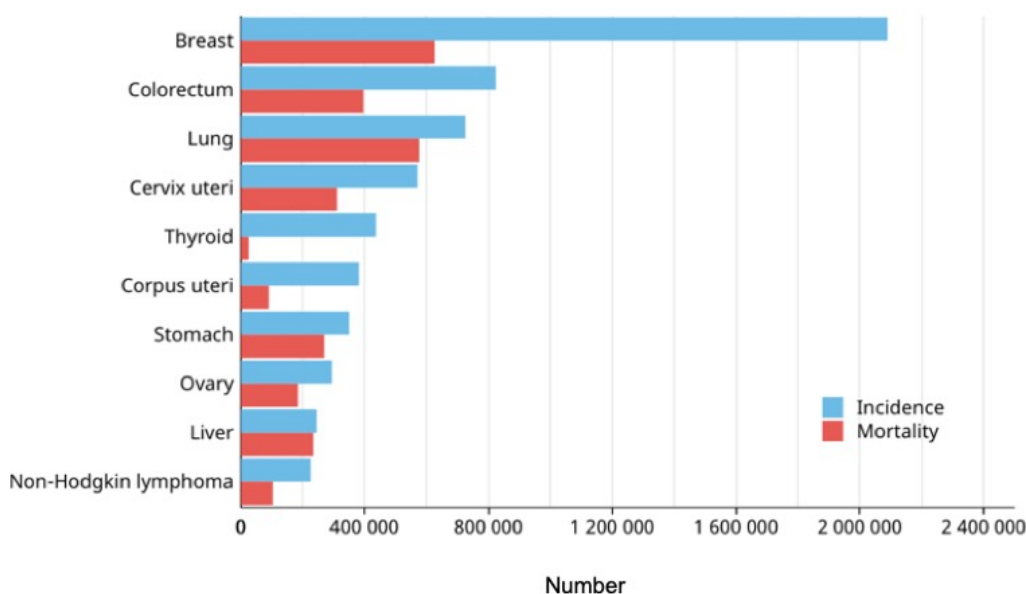
At the end of the third week of development, the three embryonic leaflets are developed giving rise to endoderm, mesoderm and primary ectoderm. The organogenesis process occurs from week 3 to 8 (Elshazzly and Caban, 2019). The primary ectoderm will split into the external ectoderm and the neuroectoderm respectively from the extremity to the inner dorsal embryonic leaflet. The neuroectoderm will form the neural tube and neural crests. The neural tube will generate the central nervous system (CNS), and the spinal cord. From the neural crest, the peripheral nervous system (PNS), the bones and cartilage of visceral arches will be produced (Etchevers *et al.*, 2019). Neural crest cells are multipotent cells which differentiate in many organs according to their migratory capabilities. They can differentiate into nervous and glial cell of sensorial and autonomous ganglions, adrenal gland cells, epidermis cells, neuroendocrine cells of gastrointestinal tract, lung cells, odontoblasts, and connective tissues. The neural tube generates mostly neurons, glial cells, and oligodendrocytes. The external ectoderm derives mainly into the epidermis, the integumentary system, and the mammary glands (Watson and Khaled, 2008).

Neuroectoderm-derived tumors embed cancers of all organs deriving from ectoderm leaflet organogenesis due to a similar molecular patterning of tumors exhibited by those different cancers. These tumors comprise mainly Neuroblastoma (NB), Glioblastoma, Melanoma, Osteosarcoma, Small Cell Lung Cancer (SCLC), and Breast Cancer (BC). This project was focused on the study of ganglioside molecular patterns of neuroectoderm-derived tumors, with a particular focus on breast cancer.



## 2- Breast Cancer

Breast cancer is the most frequent women cancer worldwide impacting 2,1 million women each year. In 2018, it is estimated by the World Health Organization that 627 000 women died from breast cancer, representing thus the leading cause of death among women (Figure 1). BC metastasizes to lymph nodes, bones, liver, lung, and brain. Early diagnosis of the disease can lead to a better prognosis and a higher survival rate. Whereas surgical resection and chemotherapy can cure primary tumors and early stage metastasis, metastatic disease causes death in 90% of cases (Valastyan and Weinberg, 2011). BC tumors characterization is needed for the determination of systemic therapy. Systemic therapies for the treatment of BC are chemotherapy, endocrine therapy and targeted therapy such as therapeutic antibodies.



**Figure 1 : Estimation of numbers of incident and death worldwide among women.**

Adapted from Globocan 2018, global cancer observatory (<http://gco.iarc.fr/>), International agency for cancer research on 2019.

The breast is composed of a bilayer epithelium constituted by two main epithelial cell types: luminal and basal. Luminal cell forms ductal structures that ensure milk transportation to nipples during lactation. Basal cells surround luminal cells and are in contact with the membrane that separate the parenchyme from the stromal component of the tissues (Gusterson and Stein,

2012). BC tumorigenesis occurs in a sequential manner from the malignant transformation of a normal cell line to a cancer one. Clinicopathological features allow to make the difference between benign and tumoral lesions. Benign lesions are local lesions growing slowly whereas tumoral lesions proliferate faster and are not localized. In the case of ductal carcinoma development, accumulation of abnormal chromosomal changes transforms benign lesions into atypical hyperplasia, then into *in situ* carcinoma, and invasive carcinoma (Burstein *et al.*, 2004). Nevertheless, BC is not a single disease, it corresponds to multiple diseases that have highly diverse histopathologies, genetics and genomics variations, and clinical outcomes (Vargo-Gogola and Rosen, 2007). Thus, the characterization of the disease had been performed according to different criteria.

The anatomic features are used for biological classification of tumors according to T, N, M categories corresponding respectively to the size of tumor (T), lymph node invasion (N) and distant metastases (M). First developed in 1959, the TNM classification is used as a prognostic guide to select whether to apply systemic therapy. T, N, and M are graded from 0 to 4 according to the gravity of disease (Amin *et al.*, 2017). The notation occurs from T0 in the case of the absence of the primary lesion, to T4 which is the most extensive tumor represented by the maximum diameter of the lesion. Lymph node status is classified from N0 to N3 for assessing the presence and the distribution of proximal metastasis into lymph nodes. The presence of distal metastasis is defined by M1 regardless of the number of metastasis or proximity to the primary lesion. M0 defines the absence of metastases of tumors (Table 1).

**Table 1: TNM classification of BC according to AJCC**

Stade	Tumors Size	Lymph Node Invasion	Metastasis
I	>2 cm	N0	None
II	2-5 cm	N1	None
III	<5 cm	N1; N2; N3	None
IV	$\geq 2$ cm - $\leq 5$ cm	N0; N1; N2; N3	Yes

Nowadays, a TNM classification based solely on anatomical features for tumors characterization is not sufficient for the choice of the adapted systemic treatment. BC is classified in 4 molecular sub-types: luminal, basal, Her2-like and normal breast-like based on the genomic profile of tumors. Luminal subtype is characterized by estrogen receptor (ER) and progesterone receptor (PR) expression. Her2-like subtype is associated mainly to Her2 receptor overexpression and also to ER and PR expression. Basal subtype (also named triple negative BC) is characterized by the absence of expression of previously mentioned receptors. Normal breast-like subtype is negative for ER, PR and Her2 similarly to triple negative breast subtype, but keeps the expression of genes expressed by normal breast tissue (Table 2).

**Table 2: Molecular classification of BC**

Subtype	Immunocytochemical markers	Additional features	Grade	Prevalence	Outcome
<b>Luminal A</b>	ER+/PR+/Her2-	Low Ki67	I or II	19-39%	Good
<b>Luminal B</b>	ER+/PR+/ Her2+	High Ki67	II or III	10-23%	Intermediary or Poor
<b>Basal like (Triple negative)</b>	ER-/PR-/Her2-	CK5/6 + CK14+ EGFR+	III	30-45%	Poor
<b>ERBB2/Her2+</b>	ER-/PR-/Her2+		III	4-10%	Poor
<b>Normal breast-like</b>	ER-/PR-/Her2-	CK5/6- CK14- EGFR-	III	10%	Poor

The histologic grade of tumors is assigned for all invasive breast carcinoma according to the Scarff-Bloom-Richardson (sbr) grading system (Table 2). The grade for a tumor is determined by assessing the morphological features from 1 to 3 respectively favorable to unfavorable (Table 3).

**Table 3: Histological grade of BC according to the Scarff-Bloom-Richardson classification**

Grade	Sbr score	Prognostic
<b>I</b>	3-5	Favorable
<b>II</b>	6-7	Moderately favorable
<b>III</b>	8-9	Unfavorable
<b>IV</b>	<9	Unfavorable

The American Joint community of cancer (AJCC) designed 3 types of BC classification: anatomic stage, clinical prognostic stage, pathological prognostic stage. In 2018, the expert panel suggested that clinical and pathological stage are the two stages needed to define the systemic therapy. Clinical prognostic stage is used for all patients and pathological prognostic stage for patient who undergo surgical resection as the initial treatment of BC. The clinical prognostic stage takes into account the history of the patients, the physical examination, imaging analysis, cytology and histology of biopsies collected before treatment. This stage includes TNM classification, hormone receptor status and HER2 status. The pathological prognostic stage includes TNM, grade, Her2, ER and PR status, and also genomic assays if tumors belong to ER positive, Her2 negative or T1-2 N0 group (Amin *et al.*, 2017).

Despite all the efforts made for the early detection of the disease, BC remains the leading cause of death among women. Strategies targeting the primary tumor have markedly improved but systemic treatments to prevent metastasis are less effective, drug resistance and metastatic disease remain the underlying cause of death in the majority of patients with BC (Hawley *et al.*, 2018). Substantial evidence gathered since 10 years suggest that BC initiation, progression and recurrence is supported by cancer stem cell (CSC) (Owens and Naylor, 2013). Liang and coworkers have shown co-expression of ganglioside GD2 on BC stem cells which are CD44<sup>high</sup>/CD24<sup>low</sup> (Battula *et al.*, 2012; Liang *et al.*, 2013). GD2 expression activates c-Met receptor and induces an increase of tumor aggressiveness by potentiating the epithelial-mesenchymal transition (Cazet *et al.*, 2012; Liang *et al.*, 2017; Sarkar *et al.*, 2015). Furthermore, GD2 ganglioside is characterized as a Tumor Associated Carbohydrate Antigen (TACA) in NB and melanoma (Furukawa *et al.*, 2006). Since they are not expressed in healthy adult tissues/cells, TACA, such as GD2 ganglioside, are considered as good targets for cancer immunotherapy.

## PART I: Immunotherapy targeting gangliosides

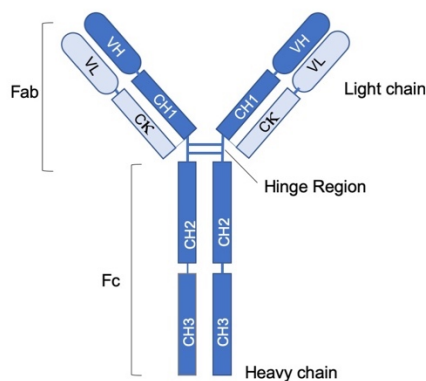
GD2 is widely expressed during developmental stages and decreases progressively and is lost in almost every tissue in healthy adults. Only traces amount of GD2 are expressed in melanocytes, neurons and peripheral nerve fibers in healthy adults. During tumorigenesis, complex gangliosides are re-expressed, especially in neuroectoderm derived tumors. In that way, GD2 is considered as oncofetal marker in SCLC, melanoma and NB (Sun *et al.*, 2017). GD2 neo-expression had been also detected in BC and osteosarcoma (Orsi *et al.*, 2017; Roth *et al.*, 2014; Shibuya *et al.*, 2012). In 2015, the anti-GD2 immunotherapy Dinutuximab (Unituxin™; ch14.18) developed by United Therapeutics Corporation and the National Cancer Institute has been approved by the Food Drug Administration (FDA) for the use in a combination therapy for the treatment of pediatric high-risk NB (Dhillon, 2015). In 2017, Qarziba (Dinutuximab beta EUSA; Dinutuximab beta Apeiron; ch14.18/CHO) has been approved by European Medicines Agency (EMA) for the treatment of NB. Nevertheless, the use of this antibody for treatment induces side toxicity due to GD2 expression on peripheral nerve fibers. The infusion of the antibody is associated with pain, which cannot be entirely controlled by morphine injection (Wallace *et al.*, 1997). As an alternative strategy, targeting the *O*-acetylated form of GD2 (*O*AcGD2) seems to be a better option than GD2 since *O*AcGD2 is not expressed in healthy cells nor on peripheral nerve fibers (Alvarez-Rueda *et al.*, 2011).

In this part of the introduction, we will focus on anti-GD2 ganglioside immunotherapy developed to treat neuro-ectoderm derived cancers.

### *1- Structural characterization of antibodies*

Antibodies are glycoproteins belonging to the Immunoglobulin family (Ig). Ig consist of two sandwiched  $\beta$ -pleated sheets pinned together by a disulfide bridge between the hinge region (Williams and Barclay, 1988). Ig are heterodimeric proteins composed by 2 heavy (H) and 2 light chains (L). The L chain consist of a  $\kappa$  or  $\lambda$  chain. Each component chain consists of one NH<sub>2</sub>-

terminal variable (VL) or one COOH-terminal constant (C) domains (Schroeder and Cavacini, 2010). The L chain contains 1 C domain ( $C_{\kappa}$  or  $C_{\lambda}$ ) and 1 VL domain for a total mass of 25 kDa whereas the H chain contains 3 or 4 CH domains and 1 VH domain for a mass of about 55 kDa. The H chain with 3 domains also includes a hinge domain between the CH1 and CH2 domains (Figure 1). An antibody can be functionally separated into the variable domain that binds the antigen and the constant domain(s) that specify effector function (Figure 2).



**Figure 2: Structural organization of Immunoglobulin G in two-dimensional model.**

Adapted from Schroder *et al.*, 2010. IgG antibody is composed by two heavy and two light chains. The fragment antigen-binding (Fab) is composed of CH1, and  $C_{\kappa}/C_{\lambda}$  constants domains, VL light variable domain and VH heavy variable domain. The Fragment crystallizable (Fc) domain is composed by CH2 and CH3 constants domains.

The variable domain defines the fragment antigen-binding (Fab) region which is composed by the CH1 domain and all the variable domains. Structurally, a variable domain is composed by three sequences encoding hypervariable domain defining the Complementary determining region (CDR) situated between four regions of stable sequence which are the framework regions. The constant domain carries the effector function such as the activation of complement or binding to the fragment crystallizable receptor (FcR). The H chain constant domain is mainly composed by CH1-CH2-CH3 with the additional CH4 domain dependent of the Ig class. Each CH domain is folded into 3-strands/4-strands  $\beta$  sheets pinned together by intrachain disulfide bonds. This fragment crystallizable (Fc) fragment defines the isotype and the subclass of immunoglobulin. Isotypes are common antigenic determinants defining the constant domain of

the antibody allowing the grouping of Ig into classes. Each class defines an individual type of C domain and are located on the same transcriptional orientation on chromosome 14.

Five isotypes ( $\mu$ ,  $\delta$ ,  $\epsilon$ ,  $\gamma$ ,  $\alpha$ ) are classified according to their size, protein composition, expression, properties for FcR binding and complement fixation. The H chain generally contains CH1-CH2-CH3 for IgG, IgA or IgD (Table 4). It contains the additional CH4 domain for IgM and IgE (Schroeder and Cavacini, 2010). IgM is the first Ig expressed in early B-cell development. While its monomeric form exhibits low affinity due to its immature form, the pentameric form of IgM has higher avidity in antigen targeting, especially when the antigen contains repeated epitopes. IgM production is considered as primary immune response. The main functions of IgM are opsonizing antigen for destruction and fixing complement. IgM are natural antibodies which are frequently used to diagnose acute exposure to an immunogen or pathogen. This isotype is more polyreactive than other isotypes (Boes, 2000). IgD are circulating antibodies detected at low levels in serum due to their short half-life. IgD are co-expressed on the membrane of B-cells when they leave the bone marrow and populate the secondary lymphoid organs. Nevertheless, its immunogenic function is still unclear. IgG is the most prevalent isotype exhibiting the longest serum half-life among all isotypes. IgA isotypes are highly expressed on mucosal surfaces and in secretions such saliva and milk, and to a lesser extent in serum. IgA are divided in two sub-classes according to the size of the hinge domain which is longer in IgA1 than IgA2. This longer hinge domain confers to IgA1 a higher sensitivity to bacterial proteases. IgA2 monomers predominate in mucosal secretions whereas dimers of IgA1 constitute 90% of IgA expressed in serum. IgE is a short-life component of serum, present at a low concentration and associated to hypersensitivity and allergic reactions (Chang *et al.*, 2007). IgE is upregulated and exhibits a strong binding to FcRI expressed on mast cells, basophils, eosinophils and Langerhans cells contributing to its immunologic potency (Chang *et al.*, 2007).

**Table 4: Properties of immunoglobulins isotypes.** Adapted from Schroder *et al.*, 2010

Isotype	% Serum	1/2 life	Structure	CDC	ADCC	Opsonizing	FcR	Other functions
<b>IgG</b>	75	++++	Monomer	Yes	Yes	Yes	Fc $\gamma$ R	Secondary response. Neutralize toxins and virus
<b>IgM</b>	10	++	Pentamer	Yes	-	-	Neonatal FcR	Primary response
<b>IgD</b>	<0.5	++	Monomer	-	-	-	Fc $\delta$ R	
<b>IgA</b>	15	++	Monomer	-	-	-	Fc $\alpha$ R	Mucosal response
<b>IgE</b>	<0.01	+	Monomer	-	-	-	Fc $\epsilon$ R	Allergy

IgG are divided into subclasses according to their structural, antigenic, functional differences in the constant domains. They are ranked according to their expression in the serum of healthy European subjects: IgG1 > IgG2 > IgG3 > IgG4 (Table 5). IgG exhibit different functional activities. All IgG subtypes except IgG4 can activate the complement cascade through C1q binding.. For immunotherapy, IgG are the prevalent isotype used for anti-cancer therapeutic antibody development. The activation of immune response by IgG is directed by FcR which links the humoral response to the immune cell. Each isotype has its proper FcR: Fc $\gamma$ R, Fc $\epsilon$ R, Fc $\alpha$ R, Fc $\delta$ R, neonatal FcR which bind to the Fc domain of IgG, IgE, IgA, IgD and IgM, respectively (Heijnen and van de Winkel, 1997).

**Table 5: Properties of IgG subtypes.** Adapted from Bruhns *et al.*, 2012

IgG subtype	Molecular Weight (kDa)	½ life (day)	Binding to protein A	ADCC	CDC	Opsonization	Fc $\gamma$ R
<b>IgG1</b>	146	21	+++	+++	++	+++	Fc $\gamma$ RI, II, III
<b>IgG2</b>	146	21	+++	-	+	+	Fc $\gamma$ RII
<b>IgG3</b>	165	7	-	++	+++	++	Fc $\gamma$ RI, II, III
<b>IgG4</b>	146	21	+++	-	-	+	Fc $\gamma$ RI, II



These isotypes have different functions in immune system regulation. The IgG is the isotype actively used for the development of anti-cancer therapeutics.

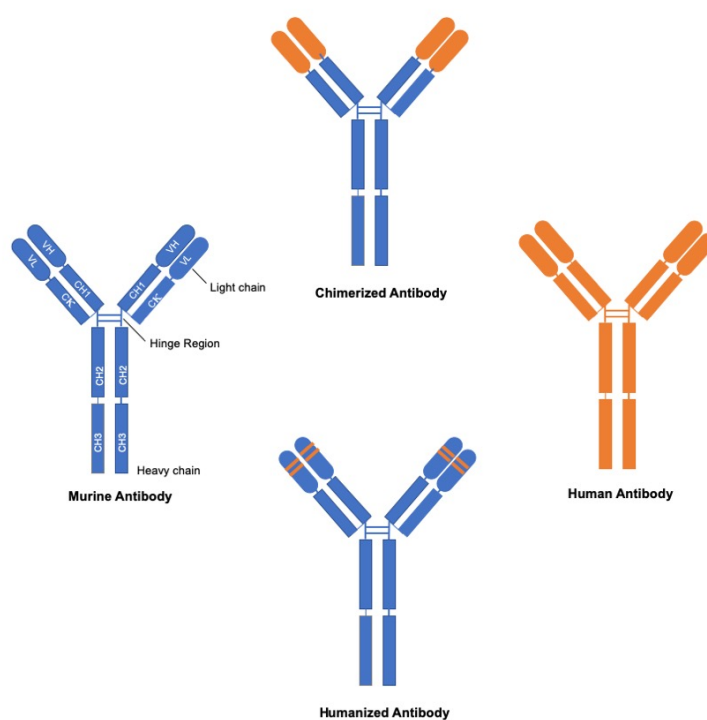
## *2- Immunotherapy and therapeutic antibody*

Immunotherapy is a rapidly growing field for cancer therapy joining surgery, cytotoxic chemotherapy, radiation and targeted therapy (Oiseth and Aziz, 2017). Immunotherapy induces the activation of immune system by two approaches: passive and active immunotherapy. Active immunotherapy aims at using the patient's immune system by two-ways: Non-specific active immunotherapy or specific active immunotherapy tending to prepare the organism to a wide target panel or to target just one antigen respectively. Passive immunotherapy consists in the administration of monoclonal antibodies (mAb) targeting specific antigen. Currently, more than 80 mAb have been granted to marketing approvals and 570 antibody therapeutics are at various clinical phases including 62 antibodies in late-stage clinical study (Kaplon and Reichert, 2019).

Following the development of the hybridoma technology by Kohler and Milstein, first mAbs have been developed in mice. Hybridoma are obtained by the fusion of plasmocytes, i.e. antibody generating spleen cells from immunized mice, rat or rabbit, to immortal myeloma cell lines. The myeloma cells are deficient for hypoxanthine-guanine phosphoribosyl transferase (HPRT). This property is used for clonal selection of hybridoma expressing mAb in hypoxanthine aminopterin thymidine (HAT) supplemented media. These selected clones are immortal and secrete indefinitely mAb (Köhler and Milstein, 1975). B-series gangliosides are expressed during developmental stages and their expression is extremely low in healthy adults. Because of their low immunogenicity, the development of antibodies targeting gangliosides remains a challenging issue. However, the detection of mAb targeting ganglioside such GM1a or GD1b in peripheral neuropathy bearing patients' renders the ganglioside immunogenicity status sufficient for the development of mAbs (Willison and Yuki, 2002). Indeed, some strategies have been set-up to produce specific antibodies targeting gangliosides, especially GD2, such as repeated injections of gangliosides or PBMC (Peripheral blood mononuclear cells), adjuvants administration, irradiation

of hybridoma with interferon  $\gamma$  for exacerbation of the immune reaction in mice (Cheung *et al.*, 1985; Gross *et al.*, 1989; Livingston *et al.*, 1989). In that way, murine anti-GD2 antibodies have been developed for a therapeutic use. Among the 4 subtypes of murine antibodies (IgG1, IgG2a, IgG2b, IgG3), IgG3 subtype preferentially recognize TACA and is developed as therapeutic antibody targeting ganglioside (<http://www.ebook777.com/kuby-immunology-7th-edition>). However, the development of the immune response of patients to murine antibody induces a rapid clearance of the mAb by Human anti-Mouse antibody (HAMA) limiting the effector functions (Sahagan *et al.*, 1986). That is why humanized anti-GD2 antibodies have been developed to avoid anti-idiotypic response of patients (Ahmed and Cheung, 2014). Humanization is a process leading to the bioengineering of an antibody produced from xenogeneic sources to a human version for a better effector function and a lower immunogenicity (Hwang and Foote, 2005), aiming at a better therapeutic response (Figure 3). Commons methods for humanization include framework-homology-based-humanization, germline humanization, complementary determining region-homology based humanization and specificity-determining residues grafting (Safdari *et al.*, 2013) producing chimeric or humanized antibodies. All of these methods developed for therapeutic antibody production tend to limit immunogenicity due to the murine, rabbit or rat origin of antibody production (Hwang and Foote, 2005). Basically, chimeric antibodies are obtained by the fusion of variable murine domain to human constant portion for a better potentiation of effector function (Morrison *et al.*, 1984; Sahagan *et al.*, 1986) for limiting the clearance of the antibody by the HAMA. The framework-homology-based-humanization is one the main method employed for chimerization. Limited HAMA increases the half-life in serum and induces a better conservation of pharmacological properties of the antibody compared to mice antibody (Boulianne *et al.*, 1984), which together lead to a better response immune response by patients. Nevertheless, chimeric antibodies could also be responsible of the production of human anti-chimeric antibody (HACA) responses which opened a field for the full humanization of therapeutic antibodies. The complete humanization of an antibody is more complex and needs the use of methods like germline humanization, complementary determining region-homology based humanization and

specificity-determining residues grafting for replacing mice fragment of antibodies by human ones as much as possible. The generation of humanized antibodies requires additional strategies such as phage display techniques or the use of transgenic mice (Deckert, 2009). Basically, in humanized antibodies, the main part of murine variable domain is also replaced by the human one (Morrison *et al.*, 1984). Humanization process is essential for the development of therapeutic antibodies in order to decrease humoral response of patients and increase mAbs pharmacological properties.



**Figure 3: Structure of murine, human, chimerized and humanized antibody.**

Murine antibody is represented in blue, while human antibody is represented in orange. In the chimeric and humanized antibody, murine portions are represented in blue, while human portions are represented in orange.

Five types of mAb are developed for a therapeutic use and are denominated according to the conventions whether they are mouse (-omab), chimeric (-ximab), humanized (-zumab), human (-umab) or artificial recombinant antibodies. The minimal target recognition module of an antibody is composed by two non-covalently associated variable domains (VH+VL). The development of recombinant antibody is based on this concept (Bannas *et al.*, 2017).

Recombinant antibodies are single-domain antibodies that have some unique features like small size, high stability, enhanced binding properties and high penetration in dense tissues (Mir *et al.*, 2019). These properties enhance the efficiency of cancer treatment by targeting tumor environment and favorizing tumor infiltration (Chanier and Chames, 2019). This is a growing field of antibody engineering since their pharmacological and structural properties lead to resist to harsh environments, such as the strong pH of the stomach, or to infiltrate the blood brain barrier and even reach intracellular targets due to their small size. Recombinant antibodies include single chain variable fragments (scFv), diabodies, nanobodies, bispecific antibodies or antibody drug conjugates (ADC) (Deckert, 2009). The fusion of VH and VL domains via a linker peptide into a small single polypeptide binding module is designed as scFv, which can fuse to one another to generate bispecific or multi-specific antibodies (Bannas *et al.*, 2017). Bispecific antibodies refers to a class of constructs in which two antibody-derived antigen specific binding sites are aligned within one molecule by recombinant DNA or cell-fusion technologies (Choi *et al.*, 2011). Indeed, bispecific antibodies used in tumor immunotherapy have one arm specific for a tumor antigen and the other for the effector cells. For example, anti-CD3 x anti-GD2 bispecific antibody 3F8BiAb has been developed for targeting CD3 on T cells and GD2 in NB. 3F8BiAb shows enhance anti-tumoral activity *in vitro* compared to naked 3F8 antibody (Yankelevich *et al.*, 2012). Nanobodies are single domain antibodies devoid of light chains developed by mimicking camelid antibodies. Camelids produce antibodies composed of only heavy chains and a single variable domain (VHH) as a target recognition module (Bannas *et al.*, 2017; Chanier and Chames, 2019; Hamers-Casterman *et al.*, 1993). Three categories of nanobodies exists: naked monomeric, multimerics nanobodies, or nanobodies-peptide fusion (Bannas *et al.*, 2017). ADC could be produced with all generation antibodies by the fusion of cytokines, chemokines, drugs for promoting the cytotoxic effect of the antibody (Govindan and Goldenberg, 2010). ADC aimed to increase the efficiency of cancer treatment by targeting directly cancer cells sparring the surrounding normal tissues.

A large number of different type of antibodies have been developed for cancer immunotherapy. For therapeutic antibody development, key elements are the choice of the

antibody isotype and the production methods which will mainly define its immune effects during patient treatment and allow to optimize antibody properties.

### *3-Anti-cancer therapeutic antibody activities*

Anti-cancer therapeutics antibodies are monoclonal antibodies belonging to IgG isotypes. They are mostly developed to against antigens that are neo-expressed or re-expressed during tumorigenesis, targeting specifically cancer cells but sparing surrounding normal cells. Antigens are preferentially membrane receptors inducing alteration of cell signaling, increasing cell proliferation or migration. The anti-tumor action of developed antibodies can target immune system dependent or independent mechanisms. Immune system independent mechanisms are regrouping neutralizing, agonist and antagonist effects of these antibodies. Immune system dependent mechanisms involve either Complement Dependent Cytotoxicity (CDC) or Antibody Dependent Cell Cytotoxicity (ADCC) through the Fc region. When the therapeutic antibody is fixed on its target, the Fc region which is the carrier of effector function activate ADCC and CDC.

#### **A- Immune system independent mechanisms**

The immune system independent mechanisms consist in the direct effect of the antibody binding. There are three different activities which may be involved: neutralizing effect, agonist or antagonist effect. Neutralizing antibodies are targeting soluble antigens like toxins, virus, or cytokines and block their biological activity by inhibiting their interactions with partners. Antagonist antibodies target membrane receptors and inhibit their activity by competing and interfering with ligand binding, leading to alteration of cell signaling. Agonist antibodies induce similar effects than their target *in fine* exacerbating their activity. Furthermore, conjugated antibodies which can carry cytotoxic immune-based payloads like radioisotopes, toxins or enzymes can enhance the effect of antibody. Finally, anti-idiotypic network is another mechanism contributing to anti-tumor effect. The humoral response of the host generates an anti-idiotypic antibody against the therapeutic antibody. This anti-idiotypic antibody represents an internal image of the therapeutic antibody. The host system subsequently generates a second anti-idiotypic

antibody presenting the antigen expressed on the surface of cancer cells. In that way, therapeutic antibodies contribute to the activation of host immune system (Cheung *et al.*, 2000).

## **B- Immune system dependent mechanisms**

### *1- Complement Dependent cytotoxicity*

CDC occurs when the Fc region of IgG binds to C1q complement molecule and activates the complement cascade, activating in turn the membrane attack complex composed by C5b, C6, C7, C8 and C9. The membrane attack complex form membrane pores inducing the permeabilization of cell membrane resulting in cytotoxicity (Gelderman *et al.*, 2004). Alternatively, complement dependent cell cytotoxicity (CDCC) is activated when iC3b complement molecule recruits effector cells through CR3 receptor binding (Chan and Carter, 2010).

### *2- Antibody Dependent Cell cytotoxicity*

ADCC activation requires the activation of Fc receptors (FcγR) on immune effector cells by binding to the Fc region on IgG of target cells. This activation induces cytotoxic effects on target cell. FcR for For IgG, FcR links the humoral immune part to the cellular immune part. This FcγR family is composed by 6 receptors in human and 4 in mice. These receptors are classified according to their affinity for IgG, their activator or inhibitor function, and their expression in hematopoietic and endothelial cells (Nimmerjahn and Ravetch, 2007). The human IgG receptor family consists in several activating receptors (hFcγRI, hFcγRIIA, hFcγRIIC, hFcγRIIIA), one low-affinity inhibitory receptor (hFcγRIIB), one receptor with unclear functions (hFcγRIIIB) and one receptor involved in recycling function (FcRn) and transport of IgG (Clynes *et al.*, 2000; Wang *et al.*, 2015). Basically, all Fc receptors can be linked to all IgG, except hFcγRI and hFcγRIIB which are linked to IgG1, IgG3, and IgG4 (Shields *et al.*, 2001). hFcγRI expression is restricted to monocytes, macrophages and dendritic cells and is inducibly expressed on neutrophils and mast cells. hFcγRIIA (CD32A) is expressed on myeloid cells except lymphocytes. hFcγRIIB (CD32B) is highly expressed on circulating myeloid cells and basophils, monocytes and neutrophils, macrophages, and dendritic cells. hFcγIIC is expressed on NK cells, monocytes and neutrophils. hFcγRIIIA (CD16)

is expressed in NK cells, monocytes and macrophages. hFcγRIIIB is expressed on neutrophils and basophils (Bruhns, 2012; Magnusson *et al.*, 2007; Meknache *et al.*, 2009; Veri *et al.*, 2007). ADCC is mainly mediated by hFcγRIIIA activating NK cells, inducing the secretion of cytotoxic molecules such perforins or granzymes, which leads to the apoptosis of the target cell (Sulica *et al.*, 2001). Antibody dependent cellular phagocytosis (ADCP), is mainly induced by hFcγRIIA and hFcγRIIIA and corresponds to the macrophage phagocytosis after opsonization of the antigen (Manches *et al.*, 2003). Activated macrophages can also participate in tumoral cell lysis by secreting inflammatory molecules such as cytokines, or interferons. Phagocytosis of opsonized tumor cells can also contribute to the activation of immune system. It has been suggested that dendritic cells can present tumor-associated antigen to immune cells after ingestion of apoptotic tumor-cells (Hoffmann *et al.*, 2000).

The stimulation and the activation of the immune system is triggered by therapeutic antibodies inducing an effective protection of patient against pathologies like cancers. Anti-GD2 antibodies have been engineered since 1980 in order to stimulate patient's immune system against neuroectoderm-derived tumors.

#### *4- Anti-GD2 therapeutic mAb against Neuroblastoma*

##### **A- Neuroblastoma**

NB is the most common extracranial solid tumor in children, it represents 7% of the total childhood cancer diagnosed each year, and 15% of cancer deaths in children. Most of children with NB are below 5, although some can develop the disease later, up to 26 years. The primary lesion is mostly located on adrenal medulla or paraspinal sympathetic ganglia. NB is a highly metastatic cancer spreading to liver, cortical bones, regional lymph nodes, bone marrow, and subcutaneous tissues. Around 40% of localized NB tumors detected in children present a tumor of grade I or II of neuroblastome according to the International NB Staging system (INSS). Localized tumors are chemotherapy responsive and subject to surgery excision. About 60% of children are diagnosed for NB when the disease has already reached its disseminated form (Maris

*et al.*, 2007). Most recently, the international NB risk group staging system (INRGSS) classified NB into very-low risk, low-risk, intermediate-risk and high-risk NB stage following the clinical, pathological, and genetic status. Therapy against NB will be tailored according to the risk staging system. For patients belonging to very low and low risk, surgery for excision of tumors will be performed. For the intermediate risk NB surgery and chemotherapy will be preconized. The high-risk NB patients can be treated using different strategies like chemotherapy, surgery, radiotherapy or even megatherapy by autologous peripheral blood stem cell transplantation or bone marrow transplantation. The risk status predicts the clinical behavior of tumors and how they will respond to therapy. The 5-year event-free survival of patients is near 40% (Dhillon, 2015). Despite the tailored therapeutic combination for the treatment of NB, complete remission is hard to achieve especially for high-risk NB patients which are relapsing in 50% of cases. Dose-intensive chemotherapy improves tumor resectability and post-surgical irradiation reduces the risk of relapse in primary site to less than 10%. Despite a high clinical response seen after the first line of treatment, residual cancerous cells are mainly responsible for the short overall survival of patients (Castel *et al.*, 2010). The standard care for NB is the use of intense chemotherapy to achieve clinical remission and results in lymphopenia and immunosuppression rendering the patients more responsive to therapeutic antibodies treatment (Kushner *et al.*, 2007). Immunotherapy targeting specifically markers of NB cell are required to ensure the proper eradication of tumors cells in patients' organisms. NB cell lines are known for overexpressing of ganglioside GD2. The use of anti-GD2 therapeutic antibodies for relapsing NB has shown promising results in patients.

## **B- Anti-GD2 antibodies**

Therapeutic antibodies against GD2 have been first developed in mice using hybridoma, then chimerized and even humanized to increase their efficiency to treat neuroectoderm-derived cancers. The use of several anti-GD2 antibodies has been approved by the Food Drug Administration and European Medicines Agency respectively in 2015 and 2017 for the treatment



of high-risk pediatric NB patients. Among them, we can distinguish 10B8, 3F8, 14G2a, 14.18 targeting GD2 and 8B6 targeting the *O*-acetylated form of GD2: OAcGD2 (Table 6).

**Table 6: List of anti-GD2 and OAcGD2 antibodies.**

<b>mAb</b>	<b>Target</b>	<b>Isotype</b>	<b>KD</b>	<b>Ref</b>
<b>14.18</b>	Anti-GD2	IgG3, $\kappa$		Schulz et al. 1984
<b>3F8</b>	Anti-GD2	IgG3, $\kappa$	5 nM	Cheung et al., 1985
<b>14G2a</b>	Anti-GD2	IgG2a, $\kappa$	77 nM	Mujoo et al., 1989
<b>10B8</b>	Anti-GD2	IgG3, $\kappa$		Cerrato et al. 1997
<b>60C3</b>	Anti-GD2 Anti-OAcGD2	IgG3, $\kappa$		Cerrato et al. 1997
<b>8B6</b>	Anti-OAcGD2	IgG3, $\kappa$	32 nM	Cerrato et al. 1997

### 1- 3F8 antibody

3F8 was the first anti-GD2 antibody used in phase I study in patients with NB and melanoma (Cheung *et al.*, 1987). This is a murine IgG3 mAb produced in immunized BALB/C mice using hybridoma technology (Cheung *et al.*, 1985). 3F8 has a binding affinity of 5 nM for GD2, which is the best KD among all anti-GD2 mAbs available (Cheung *et al.*, 2012). The murine 3F8 mAb is known for anti-OAcGD2 and GD1b cross-reactivity. This antibody has been shown to be effective against NB and melanoma cell lines. 3F8 induces cell death, and mediates ADCC, and CDC. Granulocytes macrophages-colony stimulating factor (GM-CSF) injection in patients before 3F8 inoculation enhances 3F8-mediated ADCC on GD2 expressing NB and melanoma cell lines (Kushner and Cheung, 1989).

Most patients who have received 3F8 treatment in early clinical trials developed a HAMA response. HAMA response competes for the binding site of the antibody, decreases binding to GD2 and accelerates the clearance of the antibody from the circulation (Klee, 2000).

### 2- 14.18 antibody

14.18 is the murine IgG3 mAb specifically recognizing GD2 on human NB, melanoma, glioblastoma and SCLC cell lines. This antibody was produced against LAN-1 cell by hybridoma technology on BALB/C mice. The 14.18 mAb also reacts with normal adult cerebellum and fetal brain. The m14.18 antibody induced CDC and ADCC in NB cell lines, and suppressed NB tumors growth in athymic mice (Mujoo *et al.*, 1987). The binding affinity of m14.18 mAb is 77 nM for GD2 (Cheung *et al.*, 2012). Isotypes switch variant antibodies were generated using 14.18 hybridoma in order to increase the effector function of m14.18 mAb. The IgG1, IgG2a and IgG2b were produced respectively by hybridoma 14G1, 14G2a, and 14G2b antibodies, and exhibit the same binding activity than 14.18. All antibodies can suppress NB tumor growth in athymic mice. These antibodies exhibit different effector functions. 14.18, 14G2a and 14G2b but not 14G1 activates CDC on NB cells. However, only 14.18 and 14G2a can activate ADCC on tumor cells (Mujoo *et al.*, 1989). Furthermore, 14G2a antibody targeting GD2 induces a mitochondrial-induced cell death on NB and melanoma cell line in an immune system independent manner featuring the common marker for apoptosis and necroptosis (Doronin *et al.*, 2014; Horwacik *et al.*, 2013; Kowalczyk *et al.*, 2009). The combination of chemotherapeutic agents such as doxorubicine, topotecan or carboplatin with 14G2a mAb shows a synergistic effect for killing IMR32 NB cell line *in vitro* (Kowalczyk *et al.*, 2009).

### 3- 8B6 antibody

60C3, 10B8 and 8B6 mAbs were obtained by immunizing A/J mice with hybridoma technology against NB cell lines (Cerato *et al.*, 1997). Thin Layer Chromatography experiments (TLC) showed that 10B8 is specific to GD2 with no cross-reaction with its *O*-acetylated form, whereas 60C3 antibody can react either with GD2 and *O*AcGD2. Interestingly, 8B6 mAb antibody is specific for *O*AcGD2 (Cerato *et al.*, 1997). In NB treatment, GD2 expression on healthy tissue especially on nerve fibers induces severe side toxicity effects due to 14.18 mAb antibody fixation on GD2. The specificity of 8B6 antibody against *O*AcGD2 offers an interesting alternative to limit side toxicity since *O*AcGD2 expression is exclusively expressed on cancer cells. Murine 8B6 mAb shows the same efficacy than 14G2a antibody for tumor growth suppression *in vitro* and *in vivo*

(Alvarez-Rueda *et al.*, 2011; Cochonneau *et al.*, 2013). 8B6 induces mitochondrial induced cell death by activation of caspase 3, leading to apoptosis of NB cell line (Cochonneau *et al.*, 2013). The chimerization of 8B6 was performed by switching murine IgG3 to human IgG1. This process induced the loss of apoptotic properties of 8B6 mAb due to the variation on the whole structure of the antibody, especially the Fc domain. Chimerization of 60C3 showed identical binding, affinity and specificity against GD2 but also induced the loss of the effector function, inducing apoptosis through ADCC and CDC. Tumor growth was not suppressed with the same efficiency when mice were treated with chimeric 60C3 compared to the murine parental version of antibody.

## **C- Dinutuximab/ Qarziba**

### *1- Dinutuximab*

Dinutuximab, (Unituxin™) has been developed by United Therapeutics Corporation and the National Cancer Institute and approved by the Food Drug Administration. This antibody has been approved in combination interleukin 2 and isotretinoin for the treatment of high-risk pediatric NB patients who achieve at least partial response to prior first-line multiagent, multimodality therapy (Dhillon, 2015). The combinatorial use of Dinutuximab with GM-CSF, interleukin 2 and isotretinoin (13-cis retinoic acid) was based on results obtained in phase III open-label randomized trial conducted by the Children's Oncology Group (NCT00026312; ANBL0032). The recommended dosage is 17.5 mg/m<sup>2</sup>/day administrated as an intravenous injection over 10-20h for 4 consecutive days for 5 cycles maximum. The half-life of Dinutuximab in patients' serum is about 66.6 h  $\pm$  27.4 h (Ladenstein *et al.*, 2018). The combinatorial use of Dinutuximab with GM-CSF, interleukin 2 and isotretinoin improved outcomes in patients with high-risk NB who had a response to induction therapy, autologous stem cell transplantation and radiotherapy (Yu *et al.*, 2010). The Children's Oncology group randomized trial on the combination of Dinutuximab, temozolomide and irinotecan demonstrated a high response rate into NB patients with progressive disease. Dinutuximab, ch14.18 is a human/mouse chimeric (IgG1,  $\kappa$ ) switch variant of murine mAb 14G2a produced in murine myeloma cell line SP2/O. Dinutuximab binds to GD2 and induces ADCC and CDC, and subsequent NB cell death (Mueller *et*

*al.*, 2018) in a more effective manner than 14G2a by recruiting granulocytes and natural killer cells from peripheral blood mononuclear population (Barker *et al.*, 1991). The adverse effect of immunotherapy by the combination dinutuximab-isotretinoin-interleukine-2 compared with standard chemotherapy is neuropathic pain 52% vs 6%; hypokalaemia (low potassium level in the blood serum) 35 vs 2%; hypersensitivity reactions 25 vs 1%; hyponatraemia (low sodium level in the blood serum) 23 vs 4%; elevation of alanine transferase level 23 vs 3% and hypotension 18 vs 0% (Yu *et al.*, 2010). Furthermore, approximately 18% of patients developed an anti-dinutuximab antibody response.

## 2- Qarziba

Dinutuximab antibody is produced in a non-secreting murine myeloma cell SP2/0 which contains murine retroviruses. Thus, this antibody is unavailable in Europe. The Society of Paediatric Oncology European NB Group (SIOPEN) has commissioned the production of 14.18 in CHO (Chinese Hamster Ovary) cell lines mostly used for the production of recombinant proteins. This antibody is produced in the same plasmid and has the same sequence than ch14.18 produced in SP2/0 (ch14.18/SP2/0) with the absence of murine xenotropic retroviruses contamination (Shepherd *et al.*, 2003). The chimeric 14.18 produced in CHO (ch14.18/CHO) also exhibits a favorable glycosylation pattern with minor expression of N-glycolylneuraminic acid (Neu5Gc) mainly found in mice, preventing the rapid clearance of the antibody developed against Neu5Gc in early childhood. The European HR-NBL-1/ESIOP studied the benefit of using ch14.18/CHO for immunotherapy to treat high-risk NB patients. The binding specificity of ch14.18/CHO to GD2 is the same than ch14.18/SP2/0. Concerning the effector function of ch14.18/CHO, while the CDC activity exhibited remains the same, ADCC activity is enhanced *in vitro* and *in vivo* at lower concentrations of antibody on NB and melanoma cells. Indeed, ch14.18/CHO is effective in the suppression of NB and liver metastasis *in vivo* by a natural killer cell dependent ADCC (Zeng *et al.*, 2005). The European Medicines Agency approved ch14.18/CHO developed by Apeiron in May 2017 as Qarziba (Dinutuximab beta) then out licensed to EUSA pharma. The EMA recommended Qarziba dosage is 20 mg/m<sup>2</sup>/day administrated as intravenous injection over 8h for 5

consecutives days at 5 cycles maximum and the half-life in patients' serum is  $76.9\text{h} \pm 52.5\text{h}$ . The adverse effects of ch14.18/CHO compared to ch14.18/SP2/0 remains mostly the same (Ladenstein *et al.*, 2018).

## Part II- Gangliosides chemistry and biology

This part is divided in three main axes from (1) the biological role and expression of gangliosides to (2) their structure and (3) metabolism aiming the proper understanding of gangliosides expression and functions in cells.

### *1- Expression and Roles*

In this part, we will focus on ganglioside expression and their roles in physiological and pathological conditions in order to underline gangliosides as antigens of interest for immunotherapy. This part of the work has been published in *Biomolecules* as a review named “Gangliosides: The Double edge-sword of neuroectoderm derived tumors.”

Review

# Gangliosides: The Double-Edge Sword of Neuro-Ectodermal Derived Tumors

Sumeyye Cavdarli, Sophie Groux-Degroote and Philippe Delannoy \* 

Université de Lille, CNRS, UMR8576-UGSF-Unité de Glycobiologie Structurale et Fonctionnelle, F59000 Lille, France

\* Correspondence: philippe.delannoy@univ-lille.fr

Received: 25 June 2019; Accepted: 26 July 2019; Published: 27 July 2019

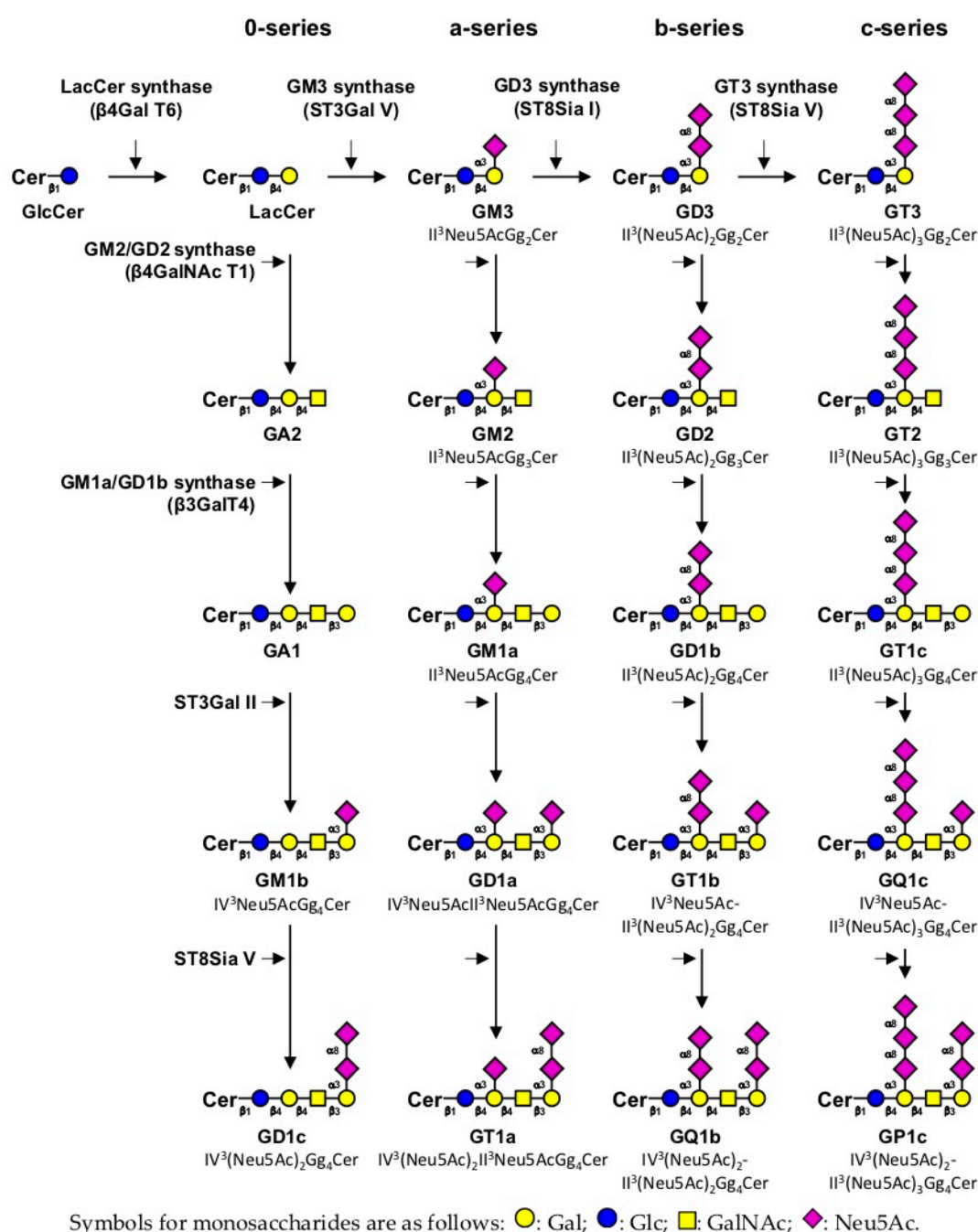


**Abstract:** Gangliosides, the glycosphingolipids carrying one or several sialic acid residues, are mostly localized at the plasma membrane in lipid raft domains and implicated in many cellular signaling pathways mostly by interacting with tyrosine kinase receptors. Gangliosides are divided into four series according to the number of sialic acid residues, which can be also modified by *O*-acetylation. Both ganglioside expression and sialic acid modifications can be modified in pathological conditions such as cancer, which can induce either pro-cancerous or anti-cancerous effects. In this review, we summarize the specific functions of gangliosides in neuro-ectodermal derived tumors, and their roles in reprogramming the lipidomic profile of cell membrane occurring with the induction of epithelial-mesenchymal transition.

**Keywords:** gangliosides; cancer; signal transduction; epithelial-mesenchymal transition; therapy

## 1. Introduction

Gangliosides are acidic glycosphingolipids (GSL) carrying one or more sialic acid residues on their carbohydrate moieties that are mainly located in glycolipid-enriched domains, also called lipid rafts, on the outer leaflet of the plasma membrane bilayer. Raft domains are composed of cholesterol, phospholipids, and glycosphingolipids and enriched in specific proteins [1]. They engage in major cellular pathways and are involved in cell biological properties under physiological conditions. The carbohydrate part of gangliosides is constituted by glucose, galactose, *N*-acetylgalactosamine and sialic acid residues, which could exhibit numerous structural modifications such as *O*-acetylation, *N*-acetylation or sulfation. Irrespective of the elongation status of their core structure (Gal $\beta$ 1-3GalNAc $\beta$ 1-4Gal $\beta$ 1-4Glc $\beta$ 1-1Cer), gangliosides are classified in four series (0-, a-, b- and c-series) according to Svennerholm classification [2] in function of the number of sialic acid residues (from 0 to 3) linked to lactosylceramide. Monosialogangliosides from the a-series such as GM1, GM2 or GM3 are usually considered as simple gangliosides, whereas GD3, GD2 and GD1b (b-series gangliosides) are more complex gangliosides characterized by two sialic acid residues on their carbohydrate moieties (Figure 1). Cancer development is generally associated with glycosylation changes of glycolipids and glycoproteins expressed at the cell surface [3]. These modified carbohydrate epitopes are then defined as tumor associated carbohydrate antigens (TACA), such as GD2 or GD3 ganglioside in neuro-ectodermal derived (ND) cancers [4,5]. In this study, we review the changes in ganglioside content that are associated with tumorigenesis, their roles, and the potential therapeutic approaches that target abnormal ganglioside expression.



**Figure 1.** Simplified representation of ganglioside biosynthesis. Gangliosides are classified in four series according to the number of sialic acid residues linked to lactosylceramide (LacCer) [2]. The 0-series gangliosides are directly synthesized from LacCer and the precursors of other series are synthesized by specific sialyltransferases: ST3Gal V (GM3 synthase), ST8Sia I (GD3 synthase) and ST8Sia V (GT3 synthase), respectively. The elongation of precursors is performed by the sequential action of *N*-acetyl-galactosaminyltransferase (β4GalNAc T1), galactosyltransferase (β3Gal T4) and sialyltransferases (ST3Gal II and ST8Sia V). Cer, ceramide. Adapted from [6].

## 2. Expression of Gangliosides in Human Tissues

### 2.1. Monosialogangliosides Expression

Monosialogangliosides are GSL carrying only one sialic acid residue and they mainly constitute a-series gangliosides in the Svennerholm classification [2], essentially composed by GM3, GM2, and



GM1. Their expression has been extensively studied during development and in different diseases, such as neurodegenerative diseases and cancers. Although there are major differences in gangliosides expression and composition between human tissues, it is widely agreed that non-neural healthy tissues mostly express monosialogangliosides, mainly GM1 [7,8]. In the central nervous system (CNS), which contains as much as 20 to 500 times more gangliosides than other tissues [9], monosialogangliosides are expressed together with more sialylated gangliosides and there is an increase in the content of gangliosides and degree of sialylation during brain development. For example, GM1, GD1a, GT1b and GQ1b were described as the major gangliosides in rat CNS [10], whereas GM3 and GD3 are the major ganglioside species described in healthy mammalian cerebral cortex [7,11].

Although the expression of monosialogangliosides is a characteristic feature of healthy tissues, they are also expressed and not necessarily down-regulated in cancer tissues and cells. Indeed, Dewald et al. showed high GM3, GM2, GM1a/b, and GD1a/b expression in MCF-7 and Hs 578T breast cancer cell lines [12]. Similarly, GM3 and GM1, which are expressed in normal CNS, are also expressed in astrocytoma and glioma cells [13–15]. Interestingly, GM3, which is not expressed in normal melanocytes, is detected in 60% of primary melanoma and 75% in metastatic melanoma [16]. These changes in monosialoganglioside composition seem to be highly dependent on the tumor-type and could reflect essential roles in the biology of a given cell type, contrary to disialogangliosides expression.

## 2.2. Disialogangliosides Expression

Disialogangliosides (alternatively named complex gangliosides) carry two sialic acid residues linked to lactosylceramide and constitute b-series gangliosides. Highly expressed during developmental stages, complex gangliosides are not or slightly expressed in non-neural healthy adult tissues. GD3 and GD2 are essentially expressed in CNS, peripheral nerve tissues and lymphocytes [16]. By immunohistochemical staining, Hersey et al. showed GD2 expression on T cells, B lymphocytes and dendritic reticular cells, whereas GD3 was mainly expressed on T cells [16]. In parallel, GD2 and GD3 are considered as TACA. The tumorigenesis process leads to the over-expression of GD3 and GD2 on neuroectoderm-derived cancers and sarcoma where they are considered as oncofetal markers. GD3 and GD2 are over-expressed in osteosarcoma (OS) cell lines and biopsies from patients [17,18], in leiomyosarcoma [19], in melanoma [20], in small cell lung cancer (SCLC) [21], in glioma [22] and in breast cancer (BC) [23]. GD2 is also expressed at various rates depending on the cancer type: 25% in rhabdomyosarcoma [24,25], 59% in BC [26] and 96% in neuroblastoma (NB) tumors [27].

O-acetylated gangliosides are expressed in healthy tissues during developmental stages and reappear with tumorigenesis. Interestingly, O-acetylated GD3 (OAcGD3) is expressed in acute lymphoblastic leukemia [28] and in regenerating peripheral nerve fibers in adult rats [29]. Furthermore, OAcGD3 is expressed in benign proliferative breast lesions, and its expression increased in invasive ductal and lobular breast carcinomas [23,30], in acute lymphoblastic leukemia [31,32], in SCLC [33] and in glioblastoma (GB) [34]. O-acetylated GD2 (OAcGD2) expression is extensively studied in ND tumors. Alvarez-Rueda and coworkers detected OAcGD2 expression in 100% of NB, 75% of SCLC, 50% of melanoma, and 33% of renal carcinoma tissues [35]. OAcGD2 expression was established in NB, glioma, SCLC, and BC cell lines [36–39] whether OAcGD2 was absent in peripheral nerve fibers and healthy tissues [35,39].

## 3. Gangliosides Involved in Cell Fate

### 3.1. Gangliosides as Essential Components for The Maintenance of Cell Signaling

Specific glycosyltransferases (GT) are involved in the transfer of monosaccharides residues in a stepwise manner on ceramide moieties for the biosynthesis of gangliosides. GT are important tools to identify the function of specific gangliosides. Many strategies have been employed to decipher the role of gangliosides in physiology and pathologies, such as exogenous treatment by gangliosides, or over-expression or depletion of specific glycosyltransferases. The complete depletion of gangliosides



was performed in the *b4galnt1/St3gal5* double knockout mice for GM2 and GM3 synthase. CNS degeneration occurred in these mice exhibiting axonal degeneration, vacuolated oligodendrocytes and abnormal axon-glia interactions [40].

In addition, gangliosides are enriched in lipid rafts, where they can modulate intrinsic and extrinsic cell signaling processes by *cis*- and *trans*- interactions with receptors tyrosine kinase (RTK) and/or the microenvironment [6]. These interactions, which are part of the biology of normal cells, can be modified in cancer cells, in which alterations of ganglioside pattern activate or inhibit modulate RTK-associated downstream signaling pathways. In that way, GM1 and GM3 expression are associated with a protective role against cancer [16,41], whereas GD3 and GD2 have a pro-tumoral role [6,42,43]. These data highlight the role of gangliosides as double-edge sword for the maintenance of cell homeostasis and for the positive or negative regulation of malignant properties of cancer cells.

### 3.2. The Anti-Tumoral Role of Monosialogangliosides in ND Tumors

Hanahan and Weinberg defined the hallmarks of cancer cells, which have to be negatively regulated for the inhibition of malignant properties [44], especially through the inhibition of proliferation, migration and invading capacities of cells. GM3 and GM1 induced the inhibition of cell proliferation in glioma [15], epidermoid carcinoma [45], NB [46] and astrocytoma [14]. Cell growth inhibition takes place in concert with GFR inactivation and apoptosis induction. Mirkin et al. showed that GD1a treatment had a tendency to inhibit NB cell proliferation, while GT1b treatment was more efficient on suppressing the phosphorylation of EGFR, and GM3 treatment had effects on both parameters [46]. EGFR binds to GM3 through carbohydrate-carbohydrate interactions with N-linked glycans having multiple GlcNAc termini of EGFR [47]. Besides, exogenous addition of GM1 to high-density BC cells inhibits proliferation through delocalization of EGFR from raft domains to caveolae [48,49]. GM1 interacts with platelet derived growth receptor (PDGFR), decreasing its activation in raft domains and reducing Swiss 3T3 cell line proliferation [50]. GM3 enhanced the expression of the cyclin-dependent kinase (Cdk) inhibitor p27<sup>kip1</sup> [14] and CDK inhibitor p21<sup>WAF1</sup> expression through phosphatase and tensin homolog deleted on chromosome 10 (PTEN), which inactivate PI3K/Akt signaling [37]. GM3 treatment also blocked dimerization of Vascular Endothelial Growth Factor Receptor-2 (VEGFR2) and its activation in vitro and neovascularization in vivo including in chick chorioallantoic membrane or matrigel plus assay [51] (Figure 2A).

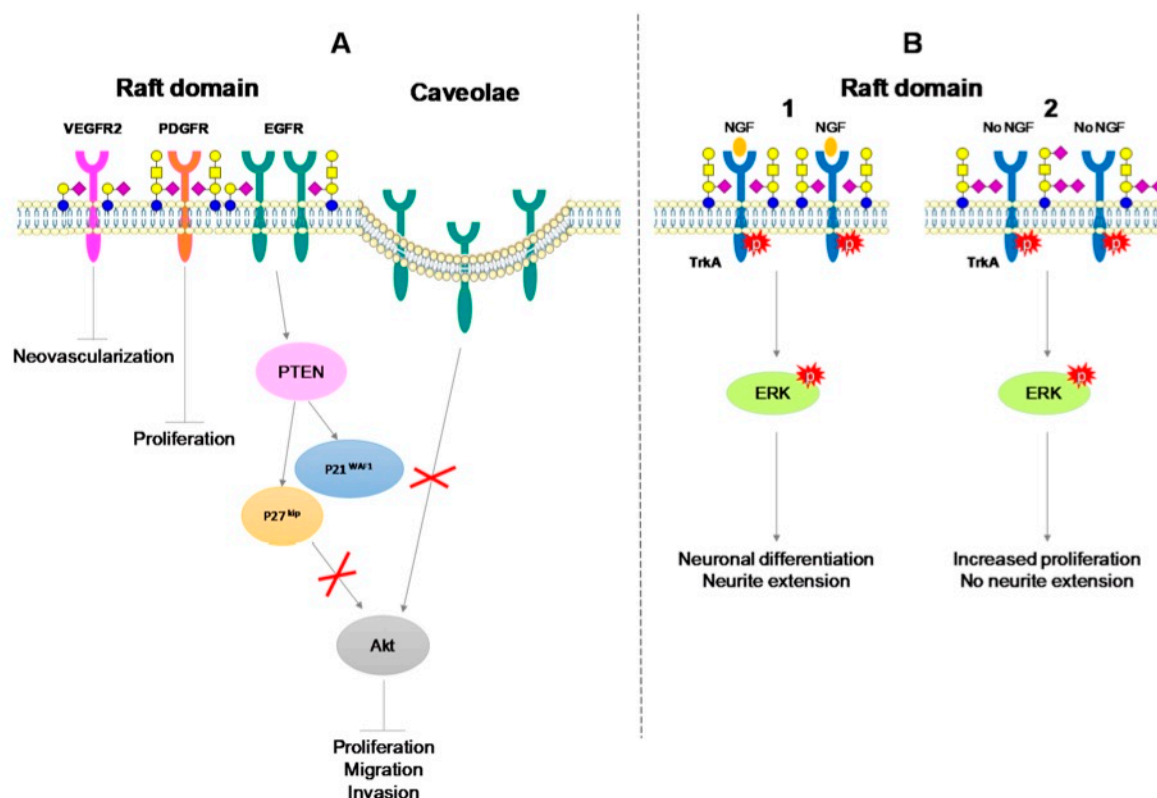
### 3.3. Monosialogangliosides as Enhancers of Tumorigenesis

Monosialogangliosides do not exhibit a unique anti-tumor role in cancer development. In NB or GB, neuronal differentiation and growth are the major properties acquired during the tumorigenic process. The rat pheochromocytoma PC12 cell line is widely used as a differentiation model of neuronal cells after NGF stimulation. GM1 treatment enhanced the NGF effect on neuronal differentiation by directly interacting with TrkA and activating its autophosphorylation [52]. In that case, added GM1 did not change signal transduction or the fate of PC12 cells but just regulated the reactivity of Trk receptor to NGF.

PC12 cells transfected with GD3 synthase (PC12 GD3S+) expressed complex gangliosides GD1b and GT1b rather than GM1. In PC12 GD3S+ cells, TrkA dimerized and was constitutively activated without NGF stimulation, activating in turn the phosphorylation of ERK1/ERK2. PC12 GD3S+ cells exhibited enhanced growth but showed unresponsiveness to NGF regarding neuronal differentiation [53]. PC12 GD3S+ cells recovered neurite extension and TrkA autophosphorylation after GM1 treatment, showing the regulatory role of gangliosides in cell differentiation and proliferation [53] (Figure 2B).

The modulation of GM3 synthase expression has been performed in murine BC cell lines 4T1 or 67NR. The over-expression of GM3 synthase in 67NR induces higher GM3 and GD3 expression, which promoted migration, invasion, anchorage independent growth in vitro and lung metastasis in vivo. The silencing of GM3 synthase in 4T1 inhibited all these acquired properties without affecting cell growth [54]. In conclusion, GM1 and GM3 have been associated either with pro- or

anti-cancerous properties, depending on the cell or tissue of interest. Nevertheless, it seems clear that the pro-tumorigenic effect of monosialogangliosides is essentially due to the co-expression of more complex gangliosides.



Symbols for monosaccharides are as follows: ●: Gal; ●: Glc; ■: GalNAc; ◆: Neu5Ac.

**Figure 2.** Interactions of gangliosides with growth factor receptors in neuro-ectodermal derived (ND) cancers. (A) Negative regulation of malignant properties of cancers cells through GM1 and GM3 interaction with growth factor receptor. (B) Positive regulation of malignant properties of neuronal cells through interactions of TrkA receptor with GM1 in the presence of NGF (1) or with GD1b and GT1b in the absence of NGF (2) [53].

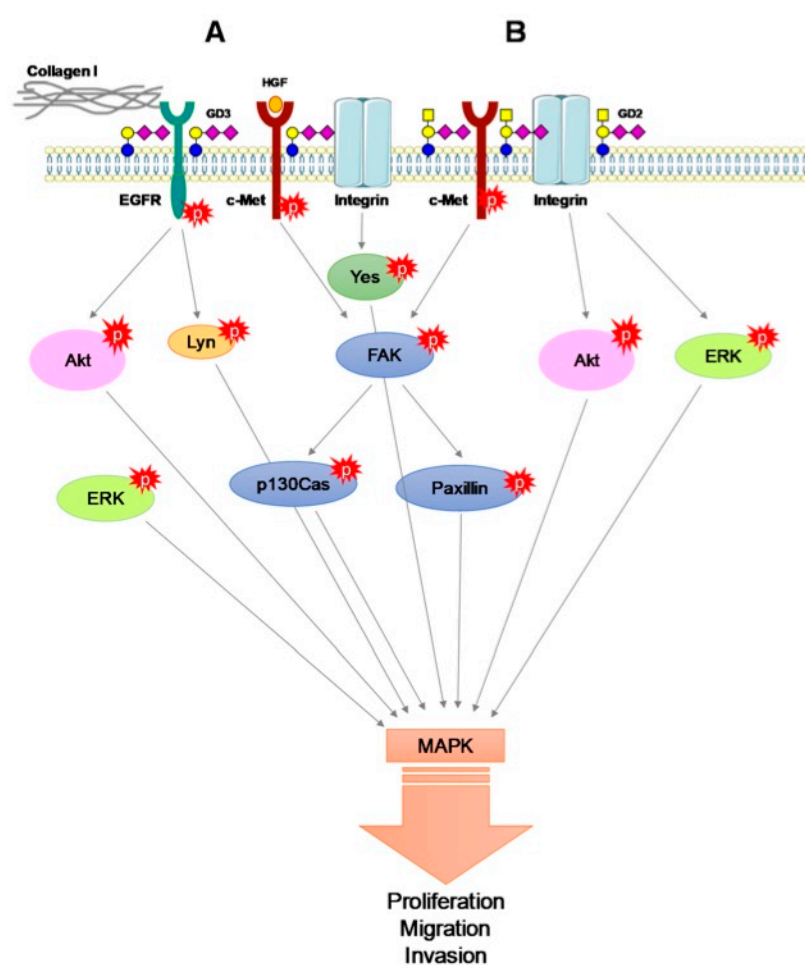
### 3.4. The Pro-Tumoral Role of Cell Membrane GD2 and GD3

On the contrary, GD3 and GD2 were shown to have mainly a pro-tumoral role in ND cancers. GD3 expression and self-renewal capacities in mice neural stem cells or in GB neurospheres have been demonstrated [55,56]. Wang et al. showed maintained EGFR activation by GD3, leading to the promotion EGF/ERK signaling and enhancing self-renewal capacity in mice neural stem cells [55]. In a similar manner, in neurospheres, high GD3 expression correlated with EGFR activation, increased stemness genes expression and self-renewal ability in glioblastoma multiforme [56]. In breast cancer, co-immunoprecipitation and proximity ligation assay showed colocalization of EGFR and GD3 [57], as well as EGFR activation by GD3 in cell membrane, avoiding the EGFR lysosomal degradation process [55]. In that way, GD3 seems to have an opposite role compared to GM3 regarding EGFR activation.

GD3 synthase over-expression in tumor cell lines with low expression of b-series gangliosides leads to GD2 over-expression, which increases cell proliferation in SCLC [21]. GD2 was associated with integrin- $\beta$ 1 and c-Met receptor [57]. Carbohydrate-carbohydrate interactions between GD2 and c-Met induced its constitutive activation even in the absence of HGF [58]. In a starved medium, c-Met constitutive activation enhanced proliferation and migration of BC cell lines over-expressing



GD3 synthase [59,60]. GD3 can also activate c-Met in melanoma cells. c-Met activation by GD3 depends on HGF and collagen type-I co-stimulation in GD3 synthase over-expressing SK-MEL-28 cell lines. The activation of c-Met by the tripartite GD3-HGF-collagen type I activated in turn PI3K/Akt and MEK-ERK signaling pathway, proliferation and invasion [61]. High expression of GD3 in SK-MEL-28 GD3+ cell line enhanced phosphorylation of adaptor molecules such focal adhesion kinase (FAK) and paxillin after serum treatment [42]. Integrin- $\beta$ 1 was essential in the maintenance of the malignant effect induced by GD3 in melanoma. Indeed, GD3 expression induced integrin clustering, enhancing phosphorylation of adaptor molecules such FAK, Paxillin and Yes, enforcing in turn invasion, motility and proliferation [62–64]. GD2 formed a trimeric complex with integrin- $\beta$ 1 and FAK and activated MAPK signaling [43]. In OS, GD2 and GD3 expression correlated with increased invasion and motility signals, with no modification in cell proliferation. GD3 synthase over-expressing OS cells exhibited strong phosphorylation of FAK and Lyn among Src family kinases enforcing paxillin activation [17], which is the key structure forming the linkage between ECM and actin skeleton. Co-immunoprecipitation experiments conducted on rat brain tissue or engineered CHO cell line over-expressing GD3 synthase demonstrated direct interactions between GD3 and Lyn, activating Lyn and the downstream MAPK signaling pathway [65]. GD3 and GD2 enforced proliferation, motility, invasion of ND tumors in vitro and in vivo (Figure 3). In that way, GD3 and GD2 confer resistance to apoptosis.



**Figure 3.** GD2- and GD3-associated MAPK signaling activation. (A) GD3-associated c-Met, EGFR and collagen I activation of MAPK signaling. (B) GD2-associated c-Met constitutive activation and integrin activation induce downstream activation of MAPK signaling.

### 3.5. Alternative Roles of O-acetylated Derivatives of GD3 and GD2 in ND Tumors

Depletion of b-series gangliosides in GD3 synthase null mice showed reduced regeneration after hypoglossal nerve lesions. Complex gangliosides are essential for lesion regeneration [66–68]. Indeed, OAcGD3 was re-expressed for a short time period after sciatic nerve crush in adult rats. OAcGD3 expression was spatio-temporally correlated to axon regrowth through the lesion site. These results suggest that OAcGD3 plays a role in the regeneration of axon fibers after peripheral nerve lesions [29]. We can assume that b-series gangliosides are critical in the repair of damaged neural tissues in vivo [65]. After *de novo* synthesis, GD3 could relocate to the mitochondrial membrane and contribute with intracellular calcium to the opening of mitochondrial pore complex and induce the release of apoptogenic factors such as reactive oxygen species (ROS), cytochrome c, and caspase 9 [69,70]. Endogenous GD3 sustains an apoptotic role in contrast to OAcGD3 or raft domain-localized GD3. In GM2/GD2 synthase KO mice, GM3, GD3 and OAcGD3 accumulate in the brain [71]. In the same manner, HEK-293 cells over-expressing GD3 synthase exhibit higher levels of OAcGD3. Both GB primary tissues and U811 GB cells accumulate OAcGD3, which promotes the survival of GB cells, protecting them from GD3 induced mitochondrial apoptosis [34,72,73].

To date, the mechanisms of ganglioside O-acetylation remain obscure. However, Arming et al. identified human *CASD1* gene (Cas 1 domain containing 1) sharing sequence similarity to *Cas1p* (Capsule Synthesis 1) in *Cryptococcus neoformans* encoding for a sialate O-acetyltransferase (SOAT). *CASD1* transfected COS7 cells exhibit high expression of OAcGD3 [74]. Baumann et al. suggest that *CASD1* acts on the activated sialic acid donor, CMP-Neu5Ac, and not on the ganglioside itself [75]. Yet, the involvement of specific SOAT in ganglioside O-acetylation remains unclear. O-acetylated GD2 is barely studied among ganglioside species. Recently, Cochonneau et al. showed a proliferative role of O-acetylated GD2 in NB and melanoma cell lines and in SCID mice using anti-OAcGD2 monoclonal antibody [36].

### 3.6. Gangliosides Are EMT Modulators

The Epithelial Mesenchymal transition (EMT) is a natural process by which an epithelial cell is subjected to several morphological changes leading to the acquisition of mesenchymal phenotype with the ability to metastasize. The loss of epithelial polarity is therefore one of the main characteristics of EMT. In that sense, Gocht et al. have shown a link between abnormal OAcGD3 localization and the loss of epithelial polarity in BC [30]. Moreover, EMT and metastasis are regulated by several signaling molecules in the microenvironment such as TGF $\beta$  or TNF. TGF $\beta$  induces GM3 synthase expression in human epithelial lens cell HLE-B3, which exhibit higher GM3 expression. GM3 interacts with TGF $\beta$ R and promotes HLE-B3 migration and EMT [76]. Furthermore, cells undergoing EMT acquired self-renewal capabilities and stem cell properties exhibiting markers such CD44<sup>high</sup> CD24<sup>low</sup> [77]. Battula et al. demonstrated that a small proportion of BC cells that exhibit co-expression of GD3 synthase, ganglioside GD2 and CD44<sup>high</sup> CD24<sup>low</sup> were capable of mammosphere formation and tumor initiation [78]. GD2 is considered as a BC stem cell marker and promotes tumorigenesis. GD2 expression is also linked to EMT induction. In EMT-induced HMLE cells, GD3 synthase and GD2 expression increase [78]. In addition, EMT is regulated by FOXC2 transcription factor, which binds directly to GD3 synthase promoter region [57]. There is therefore a feedback loop between EMT and GD3 synthase, which regulates each other's expression and promote tumorigenesis. The intrinsic properties of cancer stem cells with enhanced self-renewal capacities lead to chemotherapy resistance.

## 4. Immune System Reactivity against Ganglioside Expression

### 4.1. Chemoresistance Supported by Gangliosides

Tumors display changes of ganglioside expression on cell membranes. These modifications lead to modulation of cell signaling pathways and to the acquisition of chemoresistant properties. Doxorubicin resistant SCLC cell line expressed higher levels of GM2, and cisplatin resistant SCLC cell



line exhibited a greater amount of both GM3 and GM2 compared to the parental cell line, suggesting that the alteration of ganglioside composition may be involved in the acquisition of drug resistance [79]. GM3 over-expression by transfection on murine 3LL Lewis lung carcinoma cell line also correlated with apoptosis resistance and tumor growth [80].

The immune system plays an important role in chemotherapy response. Deactivation of the immune system is targeted by cancer cells through the inhibition of immune surveillance. The blockade of anti-tumor response in tumor microenvironment results from the combinatory effects on regulatory T-cells, myeloid derived suppressor cells, immunosuppressive dendritic cells and immune inhibitory checkpoint molecules. Tumor infiltrating lymphocytes (TILs) are mononuclear immune cells that infiltrate especially solid tumor tissues. The presence of TILs in and around the tumor is associated with improved outcome to the therapy and a better patient survival. The relationship between TILs and chemotherapy is linear, with a correlation between increasing percentage of tumor infiltration and increased sensitivity and response to therapy, improving overall patients' survival [81,82]. Genetic or transcriptomic alteration of Ras/MAPK signaling was correlated to reduced TILs count in triple negative breast cancer (TNBC) promoting immune evasion. Additionally, GD2 and GD3 expression was demonstrated in TNBC [23]. This expression contributed to the activation of Ras-MAPK signaling pathways in ND cancers. Interestingly Loi et al. demonstrated that Ras-MAPK activity could suppress the expression of MHC-I and MHC-II in TNBC to circumvent the antigen presentation pathway. Thus, ganglioside expression activates mechanisms for cancer cell immune escape, especially GD2, which is characterized as a BC stem cell marker [81,82].

Gangliosides could be shed from tumor cells into the plasma, the serum or could be secreted via exosomes, bind to the surface of normal cells and change the lipid composition of raft domains. They often integrate cells surrounding tumors microenvironment such as fibroblasts, endothelial or immune cells. Gangliosides are involved in tumor associated T-cell activation [83]. Exosome-associated GD3 leads to the functional arrest of T-cells through their TCR in ascites fluids of ovarian cancer [84]. Purified GD3 internalization by activated T-cells initiates apoptosis by induction of ROS, accumulation of p53 and Bax, and cytochrome c release and activation of caspase-9 [65]. GD3 is also known to inhibit innate natural killer T-cells (NKT) activation through binding to CD1d presented antigens in mice and human [85].

#### 4.2. Gangliosides as Therapeutic Targets for Cancer

The effect of gangliosides on cancer cells is highly dependent on the cancer type and the ganglioside of interest. Indeed, exogenous treatment of cells by purified gangliosides was extensively performed, with various results. GM3 treatment of primary cultures of high-grade human GB multiforme drastically reduced the cell number in vitro and also in a murine xenograft model, as well as in tumors from multiple ND origin such as ependymomas, astrocytomas, gliomas, oligodendrogliomas, and gangliogliomas [13]. Besides, exogenous treatment of glioma by OAcGD1b or its derivative O-butryryl GD1b reduced tumor cell proliferation and cell cycle progression, potentiating the antitumoral response in xenotransplants in nude mice and intracranial allotransplants in rats [86]. Increasing the levels of GD1b by exogenous treatment or using transfection on BC cell lines induced caspase-3 and -7 mediated apoptosis. Taxane is an anti-microtubule agent inducing cell apoptosis and causing also damage to the peripheral nerves called "taxane-induced neuropathy" in BC. This adverse effect of chemotherapy is dose limiting and decreases with decreased taxane doses. A recent clinical trial has shown reduced incidence of taxane-induced neuropathy in BC patient after GM1 treatment [87].

#### 4.3. Anti-Ganglioside Immunotherapy

Cancer immunotherapy is a treatment with monoclonal antibody targeting tumor-associated markers, such as GD2 and GD3. A phase I clinical trial of 80 mg/m<sup>2</sup> murine IgG3 R24 anti-GD3 antibody demonstrated tumor regression, Antibody-Dependant-Cell-Cytotoxicity (ADCC), Complement Dependent Cytotoxicity (CDC), and T-cell activation, in patients with malignant melanoma [88].

Recently an anti-GD2 antibody Dinutuximab (Unituxin™) mAb has been approved by Food Drug Administration (FDA) and European Medicines Agency (EMA) for the treatment of high-risk NB patients [89]. A randomized clinical trial demonstrated a significant improvement of patient outcome by therapeutic combination of chimeric antibody targeting GD2 ch14.18, interleukin-2, 13-*cis* retinoic acid and granulocytes and macrophage colony stimulating factor (GM-CSF) [90].

In SCLC, the use of monoclonal anti-GD2 antibody 14G2a induces either anoikis by dephosphorylation of FAK, or apoptosis by p38, c-Jun terminal kinase (JNK) and caspase-3 activation [21,43,91]. In similar manner, anti-GD2 antibody induces apoptosis by alteration of mitochondrial membrane potential, cell membrane permeability, and cell volume decrease in NB [92]. Therapeutic combination of anti-GD2 14G2a antibody with several inhibitors showed enhanced cytotoxicity efficiency. In OS, this antibody combined to endothelin A receptor antagonist (ETAR) had a greater inhibition efficiency of cell growth, invasiveness and MMP-2 activation than individual treatment [93]. In the same manner, the combination of 14G2a with either PI3K/Akt/mTOR inhibitor or aurora kinase A enhanced the cytotoxicity effect by decreasing MYCN amplification and activation of pleckstrin homology like-domain family member 1 (PHLDA1) and p53 in LAN-1, CHP-132 and IMR-32 NBL cell lines [90,94]. The synergistic effect of 14G2a anti-GD2 antibody and cisplatin has been demonstrated in SCLC and OS. This therapeutic combination strongly activated Jun Kinase (JNK), inducing cytotoxicity and apoptosis in SCLC [95] whereas it leads to the endoplasmic reticulum stress associated to apoptosis in MG-63 and Saos-2 OS cells [96].

Nevertheless, the use of anti-GD2 antibody in therapy causes several side toxicity effects such as allodynia in treated patients because of GD2 expression on healthy peripheral nerve fibers. The absence of OAcGD2 expression in healthy tissues suggests that it could be a more specific target for immunotherapy. Indeed, Terme et al., have shown that ch8B6, a chimeric antibody targeting OAcGD2 has the same effect on neuroblastoma as ch14.18 without antibody induced side effects [39].

## 5. Conclusions

Whether monosialogangliosides should be targeted would depend strongly on the tumor type, while disialogangliosides remain good targets for immunotherapy, especially in combination with drugs. Nevertheless, ganglioside composition has a great impact on the effectiveness and efficiency of treatment, which has to be adapted to the specific molecular pattern of the tumor.

**Funding:** This research received no external funding.

**Acknowledgments:** This work was supported by the University of Lille and the CNRS.

**Conflicts of Interest:** The authors declare no conflict of interest.

## References

1. Lingwood, D.; Simons, K. Lipid rafts as a membrane-organizing principle. *Science* **2010**, *327*, 46–50. [[CrossRef](#)] [[PubMed](#)]
2. Svennerholm, L. Ganglioside designation. *Adv. Exp. Med. Biol.* **1980**, *125*, 11. [[CrossRef](#)] [[PubMed](#)]
3. Rodrigues, J.G.; Balmaña, M.; Macedo, J.A.; Poças, J.; Fernandes, Â.; de-Freitas-Junior, J.C.M.; Pinho, S.S.; Gomes, J.; Magalhães, A.; Gomes, C.; et al. Glycosylation in cancer: Selected roles in tumour progression, immune modulation and metastasis. *Cell Immunol.* **2018**, *333*, 46–57. [[CrossRef](#)] [[PubMed](#)]
4. Groux-Degroote, S.; Rodríguez-Walker, M.; Dewald, J.H.; Daniotti, J.L.; Delannoy, P. Gangliosides in Cancer Cell Signaling. *Prog. Mol. Biol. Transl. Sci.* **2018**, *156*, 197–227. [[CrossRef](#)] [[PubMed](#)]
5. Liu, J.; Zheng, X.; Pang, X.; Li, L.; Wang, J.; Yang, C.; Du, G. Ganglioside GD3 synthase (GD3S), a novel cancer drug target. *Acta. Pharm. Sin. B* **2018**, *8*, 713–720. [[CrossRef](#)] [[PubMed](#)]
6. Julien, S.; Bobowski, M.; Steenackers, A.; Le Bourhis, X.; Delannoy, P. How Do Gangliosides Regulate RTKs Signaling? *Cells* **2013**, *2*, 751–767. [[CrossRef](#)] [[PubMed](#)]
7. Ledeen, R.W.; Yu, R.K. Gangliosides: Structure, isolation, and analysis. *Methods Enzymol.* **1982**, *83*, 139–191. [[CrossRef](#)] [[PubMed](#)]



8. Ledeen, R.W.; Wu, G. The multi-tasked life of GM1 ganglioside, a true factotum of nature. *Trends Biochem. Sci.* **2015**, *40*, 407–418. [[CrossRef](#)] [[PubMed](#)]
9. Ledeen, R.W.; Wu, G. Gangliosides of the nervous system. In *Gangliosides, Methods and Protocols*; Sonnino, S., Prinetti, A., Eds.; Humana Press: New York, NY, USA, 2018; pp. 19–56.
10. Kotani, M.; Kawashima, I.; Ozawa, H.; Terashima, T.; Tai, T. Differential distribution of major gangliosides in rat central nervous system detected by specific monoclonal antibodies. *Glycobiology* **1993**, *3*, 137–146. [[CrossRef](#)]
11. Bolot, G.; David, M.J.; Taki, T.; Handa, S.; Kasama, T.; Richard, M.; Pignat, J.C.; Thomas, L.; Portoukalian, J. Analysis of glycosphingolipids of human head and neck carcinomas with comparison to normal tissue. *Biochem. Mol. Biol. Int.* **1998**, *46*, 125–135. [[CrossRef](#)]
12. Dewald, J.H.; Cavdarli, S.; Steenackers, A.; Delannoy, C.P.; Mortuaire, M.; Spriet, C.; Noël, M.; Groux-Degroote, S.; Delannoy, P. TNF differentially regulates ganglioside biosynthesis and expression in breast cancer cell lines. *PLoS ONE* **2018**, *13*, e0196369. [[CrossRef](#)] [[PubMed](#)]
13. Noll, E.N.; Lin, J.; Nakatsuji, Y.; Miller, R.H.; Black, P.M. GM3 as a novel growth regulator for human gliomas. *Exp. Neurol.* **2001**, *168*, 300–309. [[CrossRef](#)] [[PubMed](#)]
14. Nakatsuji, Y.; Miller, R.H. Selective cell-cycle arrest and induction of apoptosis in proliferating neural cells by ganglioside GM3. *Exp. Neurol.* **2001**, *168*, 290–299. [[CrossRef](#)] [[PubMed](#)]
15. Fujimoto, Y.; Izumoto, S.; Suzuki, T.; Kinoshita, M.; Kagawa, N.; Wada, K.; Hashimoto, N.; Maruno, M.; Nakatsuji, Y.; Yoshimine, T. Ganglioside GM3 inhibits proliferation and invasion of glioma. *J. Neurooncol.* **2005**, *71*, 99–106. [[CrossRef](#)] [[PubMed](#)]
16. Hersey, P.; Jamal, O. Expression of the gangliosides GD3 and GD2 on lymphocytes in tissue sections of melanoma. *Pathology* **1989**, *21*, 51–58. [[CrossRef](#)]
17. Shibuya, H.; Hamamura, K.; Hotta, H.; Matsumoto, Y.; Nishida, Y.; Hattori, H.; Furukawa, K.; Ueda, M.; Furukawa, K. Enhancement of malignant properties of human osteosarcoma cells with disialyl gangliosides GD2/GD3. *Cancer Sci.* **2012**, *103*, 1656–1664. [[CrossRef](#)]
18. Roth, M.; Linkowski, M.; Tarim, J.; Piperdi, S.; Sowers, R.; Geller, D.; Gill, J.; Gorlick, R. Ganglioside GD2 as a therapeutic target for antibody-mediated therapy in patients with osteosarcoma. *Cancer* **2014**, *120*, 548–554. [[CrossRef](#)]
19. Ziebarth, A.J.; Felder, M.A.; Harter, J.; Connor, J.P. Uterine leiomyosarcoma diffusely express disialoganglioside GD2 and bind the therapeutic immunocytokine 14.18-IL2: Implications for immunotherapy. *Cancer Immunol. Immunother.* **2012**, *61*, 1149–1153. [[CrossRef](#)]
20. Cheresch, D.A.; Klier, F.G. Disialoganglioside GD2 distributes preferentially into substrate-associated microprocesses on human melanoma cells during their attachment to fibronectin. *J. Cell Biol.* **1986**, *102*, 1887–1897. [[CrossRef](#)]
21. Yoshida, S.; Fukumoto, S.; Kawaguchi, H.; Sato, S.; Ueda, R.; Furukawa, K. Ganglioside G(D2) in small cell lung cancer cell lines: Enhancement of cell proliferation and mediation of apoptosis. *Cancer Res.* **2001**, *61*, 4244–4252.
22. Schulz, G.; Cheresch, D.A.; Varki, N.M.; Yu, A.; Staffileno, L.K.; Reisfeld, R.A. Detection of ganglioside GD2 in tumor tissues and sera of neuroblastoma patients. *Cancer Res.* **1984**, *44*, 5914–5920. [[PubMed](#)]
23. Marquina, G.; Waki, H.; Fernandez, L.E.; Kon, K.; Carr, A.; Valiente, O.; Perez, R.; Ando, S. Gangliosides expressed in human breast cancer. *Cancer Res.* **1996**, *56*, 5165–5171. [[PubMed](#)]
24. Dobrenkov, K.; Ostrovnaya, I.; Gu, J.; Cheung, I.Y.; Cheung, N.K. Oncotargets GD2 and GD3 are highly expressed in sarcomas of children, adolescents, and young adults. *Pediatr. Blood Cancer* **2016**, *63*, 1780–1785. [[CrossRef](#)] [[PubMed](#)]
25. Saraf, A.J.; Dickman, P.S.; Hingorani, P. Disialoganglioside GD2 expression in pediatric rhabdomyosarcoma: A case series and review of the literature. *J. Pediatr. Hematol. Oncol.* **2019**, *41*, 118–120. [[CrossRef](#)] [[PubMed](#)]
26. Orsi, G.; Barbolini, M.; Ficarra, G.; Tazzioli, G.; Manni, P.; Petrachi, T.; Mastrolia, I.; Orvieto, E.; Spano, C.; Prapa, M.; et al. GD2 expression in breast cancer. *Oncotarget* **2017**, *8*, 31592–31600. [[CrossRef](#)] [[PubMed](#)]
27. Terzic, T.; Cordeau, M.; Herblot, S.; Teira, P.; Cournoyer, S.; Beaunoyer, M.; Peuchmaur, M.; Duval, M.; Sartelet, H. Expression of Disialoganglioside (GD2) in Neuroblastic Tumors: A Prognostic Value for Patients Treated With Anti-GD2 Immunotherapy. *Pediatr. Dev. Pathol.* **2018**, *21*, 355–362. [[CrossRef](#)]



28. Sinha, D.; Mandal, C.; Bhattacharya, D.K. Identification of 9-O Acetyl sialoglycoconjugates (9-OAcSGs) as biomarkers in childhood acute lymphoblastic leukemia using a lectin, aconitine, as a probe. *Leukemia* **1999**, *13*, 119–125. [\[CrossRef\]](#)
29. Ribeiro-Resende, V.T.; Oliveira-Silva, A.; Ouverney-Brandão, S.; Santiago, M.F.; Hedin-Pereira, C.; Mendez-Otero, R. Ganglioside 9-O-acetyl GD3 expression is upregulated in the regenerating peripheral nerve. *Neuroscience* **2007**, *147*, 97–105. [\[CrossRef\]](#)
30. Gocht, A.; Rutter, G.; Kniep, B. Changed expression of 9-O-acetyl GD3 (CDw60) in benign and atypical proliferative lesions and carcinomas of the human breast. *Histochem. Cell Biol.* **1998**, *110*, 217–229. [\[CrossRef\]](#)
31. Parameswaran, R.; Lim, M.; Arutyunyan, A.; Abdel-Azim, H.; Hurtz, C.; Lau, K.; Müschen, M.; Yu, R.K.; von Itzstein, M.; Heisterkamp, N.; et al. O-acetylated N-acetylneuraminic acid as a novel target for therapy in human pre-B acute lymphoblastic leukemia. *J. Exp. Med.* **2013**, *210*, 805–819. [\[CrossRef\]](#)
32. Merritt, W.D.; Sztein, M.B.; Reaman, G.H. Detection of GD3 ganglioside in childhood acute lymphoblastic leukemia with monoclonal antibody to GD3: Restriction to immunophenotypically defined T-cell disease. *J. Cell. Biochem.* **1988**, *37*, 11–19. [\[CrossRef\]](#) [\[PubMed\]](#)
33. Fuentes, R.; Allman, R.; Mason, M.D. Ganglioside expression in lung cancer cell lines. *Lung Cancer* **1997**, *18*, 21–33. [\[CrossRef\]](#)
34. Birks, S.M.; Danquah, J.O.; King, L.; Vlasak, R.; Gorecki, D.C.; Pilkington, G.J. Targeting the GD3 acetylation pathway selectively induces apoptosis in glioblastoma. *Neuro. Oncol.* **2011**, *13*, 950–960. [\[CrossRef\]](#) [\[PubMed\]](#)
35. Alvarez-Rueda, N.; Desselle, A.; Cochonneau, D.; Chaumette, T.; Clemenceau, B.; Leprieux, S.; Bougras, G.; Supiot, S.; Mussini, J.M.; Barbet, J.; et al. A monoclonal antibody to O-acetyl-GD2 ganglioside and not to GD2 shows potent anti-tumor activity without peripheral nervous system cross-reactivity. *PLoS ONE* **2011**, *6*, e25220. [\[CrossRef\]](#) [\[PubMed\]](#)
36. Cochonneau, D.; Terme, M.; Michaud, A.; Dorvillius, M.; Gautier, N.; Frikeche, J.; Alvarez-Rueda, N.; Bougras, G.; Aubry, J.; Paris, F.; et al. Cell cycle arrest and apoptosis induced by O-acetyl-GD2-specific monoclonal antibody 8B6 inhibits tumor growth in vitro and in vivo. *Cancer Lett.* **2013**, *333*, 194–204. [\[CrossRef\]](#) [\[PubMed\]](#)
37. Fleurence, J.; Cochonneau, D.; Fougeray, S.; Oliver, L.; Geraldo, F.; Terme, M.; Dorvillius, M.; Loussouarn, D.; Vallette, F.; Paris, F.; et al. Targeting and killing glioblastoma with monoclonal antibody to O-acetyl GD2 ganglioside. *Oncotarget* **2016**, *7*, 41172–41185. [\[CrossRef\]](#) [\[PubMed\]](#)
38. Cavdarli, S.; Dewald, J.H.; Yamakawa, N.; Guérardel, Y.; Terme, M.; Le Doussal, J.M.; Delannoy, P.; Groux-Degroote, S. Identification of 9-O-acetyl-N-acetylneuraminic acid (Neu5,9Ac2) as main O-acetylated sialic acid species of GD2 in breast cancer cells. *Glycoconj. J.* **2019**, *36*, 79–90. [\[CrossRef\]](#)
39. Terme, M.; Dorvillius, M.; Cochonneau, D.; Chaumette, T.; Xiao, W.; Diccianni, M.B.; Barbet, J.; Yu, A.L.; Paris, F.; Sorkin, L.S.; et al. Chimeric antibody c8B6 to O-acetyl-GD2 mediates the same efficient anti-neuroblastoma effects as therapeutic ch14.18 antibody to GD2 without antibody induced allodynia. *PLoS ONE* **2014**, *9*, e87210. [\[CrossRef\]](#)
40. Yamashita, T.; Wu, Y.P.; Sandhoff, R.; Werth, N.; Mizukami, H.; Ellis, J.M.; Dupree, J.L.; Geyer, R.; Sandhoff, K.; Proia, R.L. Interruption of ganglioside synthesis produces central nervous system degeneration and altered axon-glial interactions. *Proc. Natl. Acad. Sci. USA* **2005**, *102*, 2725–2730. [\[CrossRef\]](#)
41. Choi, H.J.; Chung, T.W.; Kang, S.K.; Lee, Y.C.; Ko, J.H.; Kim, J.G.; Kim, C.H. Ganglioside GM3 modulates tumor suppressor PTEN-mediated cell cycle progression—transcriptional induction of p21(WAF1) and p27(kip1) by inhibition of PI-3K/AKT pathway. *Glycobiology* **2006**, *16*, 573–583. [\[CrossRef\]](#)
42. Hamamura, K.; Furukawa, K.; Hayashi, T.; Hattori, T.; Nakano, J.; Nakashima, H.; Okuda, T.; Mizutani, H.; Hattori, H.; Ueda, M.; et al. Ganglioside GD3 promotes cell growth and invasion through p130Cas and paxillin in malignant melanoma cells. *Proc. Natl. Acad. Sci. USA* **2005**, *102*, 11041–11046. [\[CrossRef\]](#) [\[PubMed\]](#)
43. Aixinjueluo, W.; Furukawa, K.; Zhang, Q.; Hamamura, K.; Tokuda, N.; Yoshida, S.; Ueda, R.; Furukawa, K. Mechanisms for the apoptosis of small cell lung cancer cells induced by anti-GD2 monoclonal antibodies: Roles of anoikis. *J. Biol. Chem.* **2005**, *280*, 29828–29836. [\[CrossRef\]](#) [\[PubMed\]](#)
44. Hanahan, D.; Weinberg, R.A. The hallmarks of cancer. *Cell* **2000**, *100*, 57–70. [\[CrossRef\]](#)
45. Bremer, E.G.; Schlessinger, J.; Hakomori, S. Ganglioside-mediated modulation of cell growth. Specific effects of GM3 on tyrosine phosphorylation of the epidermal growth factor receptor. *J. Biol. Chem.* **1986**, *261*, 2434–2440. [\[PubMed\]](#)

46. Mirkin, B.L.; Clark, S.H.; Zhang, C. Inhibition of human neuroblastoma cell proliferation and EGF receptor phosphorylation by gangliosides GM1, GM3, GD1a and GT1b. *Cell Prolif.* **2002**, *35*, 105–115. [[CrossRef](#)] [[PubMed](#)]
47. Yoon, S.J.; Nakayama, K.; Hikita, T.; Handa, K.; Hakomori, S.I. Epidermal growth factor receptor tyrosine kinase is modulated by GM3 interaction with N-linked GlcNAc termini of the receptor. *Proc. Natl. Acad. Sci. USA* **2006**, *103*, 18987–18991. [[CrossRef](#)]
48. Martinez-Outschoorn, U.E.; Sotgia, F.; Lisanti, M.P. Caveolae and signalling in cancer. *Nat. Rev. Cancer* **2015**, *15*, 225–237. [[CrossRef](#)]
49. Zhuo, D.; Guan, F. Ganglioside GM1 promotes contact inhibition of growth by regulating the localization of epidermal growth factor receptor from glycosphingolipid-enriched microdomain to caveolae. *Cell Prolif.* **2019**, e12639. [[CrossRef](#)]
50. Mitsuda, T.; Furukawa, K.; Fukumoto, S.; Miyazaki, H.; Urano, T.; Furukawa, K. Overexpression of ganglioside GM1 results in the dispersion of platelet-derived growth factor receptor from glycolipid-enriched microdomains and in the suppression of cell growth signals. *J. Biol. Chem.* **2002**, *277*, 11239–11246. [[CrossRef](#)]
51. Chung, T.W.; Kim, S.J.; Choi, H.J.; Kim, K.J.; Kim, M.J.; Kim, S.H.; Lee, H.J.; Ko, J.H.; Lee, Y.C.; Suzuki, A.; et al. Ganglioside GM3 inhibits VEGF/VEGFR-2-mediated angiogenesis: Direct interaction of GM3 with VEGFR-2. *Glycobiology* **2009**, *19*, 229–239. [[CrossRef](#)]
52. Mutoh, T.; Tokuda, A.; Miyadai, T.; Hamaguchi, M.; Fujiki, N. Ganglioside GM1 binds to the Trk protein and regulates receptor function. *Proc. Natl. Acad. Sci. USA* **1995**, *92*, 5087–5091. [[CrossRef](#)] [[PubMed](#)]
53. Fukumoto, S.; Mutoh, T.; Hasegawa, T.; Miyazaki, H.; Okada, M.; Goto, G.; Furukawa, K.; Urano, T. GD3 synthase gene expression in PC12 cells results in the continuous activation of TrkA and ERK1/2 and enhanced proliferation. *J. Biol. Chem.* **2000**, *275*, 5832–5838. [[CrossRef](#)] [[PubMed](#)]
54. Gu, Y.; Zhang, J.; Mi, W.; Yang, J.; Han, F.; Lu, X.; Yu, W. Silencing of GM3 synthase suppresses lung metastasis of murine breast cancer cells. *Breast Cancer Res.* **2008**, *10*, R1. [[CrossRef](#)] [[PubMed](#)]
55. Wang, J.; Yu, R.K. Interaction of ganglioside GD3 with an EGF receptor sustains the self-renewal ability of mouse neural stem cells in vitro. *Proc. Natl. Acad. Sci. USA* **2013**, *110*, 19137–19142. [[CrossRef](#)] [[PubMed](#)]
56. Yeh, S.C.; Wang, P.Y.; Lou, Y.W.; Khoo, K.H.; Hsiao, M.; Hsu, T.L.; Wong, C.H. Glycolipid GD3 and GD3 synthase are key drivers for glioblastoma stem cells and tumorigenicity. *Proc. Natl. Acad. Sci. USA* **2016**, *113*, 5592–5597. [[CrossRef](#)]
57. Liang, Y.J.; Wang, C.Y.; Wang, I.A.; Chen, Y.W.; Li, L.T.; Lin, C.Y.; Ho, M.Y.; Chou, T.L.; Wang, Y.H.; Chiou, S.P.; et al. Interaction of glycosphingolipids GD3 and GD2 with growth factor receptors maintains breast cancer stem cell phenotype. *Oncotarget* **2017**, *8*, 47454–47473. [[CrossRef](#)]
58. Cazet, A.; Groux-Degroote, S.; Teylaert, B.; Kwon, K.M.; Lehoux, S.; Slomianny, C.; Kim, C.H.; Le Bourhis, X.; Delannoy, P. GD3 synthase overexpression enhances proliferation and migration of MDA-MB-231 breast cancer cells. *Biol. Chem.* **2009**, *390*, 601–609. [[CrossRef](#)]
59. Cazet, A.; Lefebvre, J.; Adriaenssens, E.; Julien, S.; Bobowski, M.; Grigoriadis, A.; Tutt, A.; Tulasne, D.; Le Bourhis, X.; Delannoy, P. GD<sub>3</sub> synthase expression enhances proliferation and tumor growth of MDA-MB-231 breast cancer cells through c-Met activation. *Mol. Cancer. Res.* **2010**, *8*, 1526–1535. [[CrossRef](#)]
60. Cazet, A.; Bobowski, M.; Rombouts, Y.; Lefebvre, J.; Steenackers, A.; Popa, I.; Guérardel, Y.; Le Bourhis, X.; Tulasne, D.; Delannoy, P. The ganglioside G(D2) induces the constitutive activation of c-Met in MDA-MB-231 breast cancer cells expressing the G(D3) synthase. *Glycobiology* **2012**, *22*, 806–816. [[CrossRef](#)]
61. Furukawa, K.; Kambe, M.; Miyata, M.; Ohkawa, Y.; Tajima, O.; Furukawa, K. Ganglioside GD3 induces convergence and synergism of adhesion and hepatocyte growth factor/Met signals in melanomas. *Cancer Sci.* **2014**, *105*, 52–63. [[CrossRef](#)]
62. Ohkawa, Y.; Miyazaki, S.; Miyata, M.; Hamamura, K.; Furukawa, K.; Furukawa, K. Essential roles of integrin-mediated signaling for the enhancement of malignant properties of melanomas based on the expression of GD3. *Biochem. Biophys. Res. Commun.* **2008**, *373*, 14–19. [[CrossRef](#)]
63. Ohkawa, Y.; Miyazaki, S.; Hamamura, K.; Kambe, M.; Miyata, M.; Tajima, O.; Ohmi, Y.; Yamauchi, Y.; Furukawa, K.; Furukawa, K. Ganglioside GD3 enhances adhesion signals and augments malignant properties of melanoma cells by recruiting integrins to glycolipid-enriched microdomains. *J. Biol. Chem.* **2010**, *285*, 27213–27223. [[CrossRef](#)] [[PubMed](#)]



64. Hamamura, K.; Tsuji, M.; Hotta, H.; Ohkawa, Y.; Takahashi, M.; Shibuya, H.; Nakashima, H.; Yamauchi, Y.; Hashimoto, N.; Hattori, H.; et al. Functional activation of Src family kinase Yes protein is essential for the enhanced malignant properties of human melanoma cells expressing ganglioside GD3. *J. Biol. Chem.* **2011**, *286*, 18526–18537. [[CrossRef](#)] [[PubMed](#)]
65. Okada, M.; Itoh, M.I.; Haraguchi, M.; Okajima, T.; Inoue, M.; Oishi, H.; Matsuda, Y.; Iwamoto, T.; Kawano, T.; Fukumoto, S.; et al. b-series Ganglioside deficiency exhibits no definite changes in the neurogenesis and the sensitivity to Fas-mediated apoptosis but impairs regeneration of the lesioned hypoglossal nerve. *J. Biol. Chem.* **2002**, *277*, 1633–1636. [[CrossRef](#)] [[PubMed](#)]
66. Schnaar, R.L.; Gerardy-Schahn, R.; Hildebrandt, H. Sialic acids in the brain: Gangliosides and polysialic acid in nervous system development, stability, disease, and regeneration. *Physiol. Rev.* **2014**, *94*, 461–518. [[CrossRef](#)] [[PubMed](#)]
67. Furukawa, K.; Yuhstake, O.; Orie, T.; Yuji, K.; Ji, S.; Noboru, H.; Furukawa, K. Gangliosides in Inflammation and Neurodegeneration. *Prog. Mol. Biol. Transl. Sci.* **2018**, *156*, 265–287. [[CrossRef](#)]
68. Kasahara, K.; Watanabe, Y.; Yamamoto, T.; Sanai, Y. Association of Src family tyrosine kinase Lyn with ganglioside GD3 in rat brain. Possible regulation of Lyn by glycosphingolipid in caveolae-like domains. *J. Biol. Chem.* **1997**, *272*, 29947–29953. [[CrossRef](#)] [[PubMed](#)]
69. Kristal, B.S.; Brown, A.M. Apoptogenic ganglioside GD3 Directly induces the mitochondrial permeability transition. *J. Biol. Chem.* **1999**, *274*, 23169–23175. [[CrossRef](#)] [[PubMed](#)]
70. Sa, G.; Das, T.; Moon, C.; Hilston, C.M.; Rayman, P.A.; Rini, B.I.; Tannenbaum, C.S.; Finke, J.H. GD3, an overexpressed tumor-derived ganglioside, mediates the apoptosis of activated but not resting T cells. *Cancer Res.* **2009**, *69*, 3095–3104. [[CrossRef](#)]
71. Furukawa, K.; Aixinjueluo, W.; Kasama, T.; Ohkawa, Y.; Yoshihara, M.; Ohmi, Y.; Tajima, O.; Suzumura, A.; Kittaka, D.; Furukawa, K. Disruption of GM2/GD2 synthase gene resulted in overt expression of 9-O-acetyl GD3 irrespective of Tis21. *J. Neurochem.* **2008**, *105*, 1057–1066. [[CrossRef](#)]
72. Malisan, F.; Franchi, L.; Tomassini, B.; Ventura, N.; Condò, I.; Rippo, M.R.; Rufini, A.; Liberati, L.; Nachtigall, C.; Kniep, B.; et al. Acetylation suppresses the proapoptotic activity of GD3 ganglioside. *J. Exp. Med.* **2002**, *196*, 1535–1541. [[CrossRef](#)] [[PubMed](#)]
73. Kniep, B.; Kniep, E.; Ozkucur, N.; Barz, S.; Bachmann, M.; Malisan, F.; Testi, R.; Rieber, E.P. 9-O-acetyl GD3 protects tumor cells from apoptosis. *Int. J. Cancer* **2006**, *119*, 67–73. [[CrossRef](#)] [[PubMed](#)]
74. Arming, S.; Wipfler, D.; Mayr, J.; Merling, A.; Vilas, U.; Schauer, R.; Schwartz-Albiez, R.; Vlasak, R. The human Cas1 protein: A sialic acid-specific O-acetyltransferase? *Glycobiology* **2011**, *21*, 553–564. [[CrossRef](#)] [[PubMed](#)]
75. Baumann, A.M.; Bakkers, M.J.; Buettner, F.F.; Hartmann, M.; Grove, M.; Langereis, M.A.; de Groot, R.J.; Mühlhoff, M. 9-O-Acetylation of sialic acids is catalysed by CASD1 via a covalent acetyl-enzyme intermediate. *Nat. Commun.* **2015**, *6*, 7673. [[CrossRef](#)] [[PubMed](#)]
76. Kim, S.J.; Chung, T.W.; Choi, H.J.; Kwak, C.H.; Song, K.H.; Suh, S.J.; Kwon, K.M.; Chang, Y.C.; Park, Y.G.; Chang, H.W.; et al. Ganglioside GM3 participates in the TGF- $\beta$ 1-induced epithelial-mesenchymal transition of human lens epithelial cells. *Biochem. J.* **2013**, *449*, 241–251. [[CrossRef](#)] [[PubMed](#)]
77. Mani, S.A.; Guo, W.; Liao, M.J.; Eaton, E.N.; Ayyanan, A.; Zhou, A.Y.; Brooks, M.; Reinhard, F.; Zhang, C.C.; Shipitsin, M.; et al. The epithelial-mesenchymal transition generates cells with properties of stem cells. *Cell* **2008**, *133*, 704–715. [[CrossRef](#)] [[PubMed](#)]
78. Battula, V.L.; Shi, Y.; Evans, K.W.; Wang, R.Y.; Spaeth, E.L.; Jacamo, R.O.; Guerra, R.; Sahin, A.A.; Marini, F.C.; Hortobagyi, G.; et al. Ganglioside GD2 identifies breast cancer stem cells and promotes tumorigenesis. *J. Clin. Invest.* **2012**, *122*, 2066–2078. [[CrossRef](#)]
79. Kiura, K.; Watarai, S.; Ueoka, H.; Tabata, M.; Gemba, K.; Aoe, K.; Yamane, H.; Yasuda, T.; Harada, M. An alteration of ganglioside composition in cisplatin-resistant lung cancer cell line. *Anticancer Res.* **1998**, *18*, 2957–2960.
80. Noguchi, M.; Kabayama, K.; Uemura, S.; Kang, B.W.; Saito, M.; Igarashi, Y.; Inokuchi, J. Endogenously produced ganglioside GM3 endows etoposide and doxorubicin resistance by up-regulating Bcl-2 expression in 3LL Lewis lung carcinoma cells. *Glycobiology* **2006**, *16*, 641–650. [[CrossRef](#)]
81. Luen, S.J.; Savas, P.; Fox, S.B.; Salgado, R.; Loi, S. Tumour-infiltrating lymphocytes and the emerging role of immunotherapy in breast cancer. *Pathology* **2017**, *49*, 141–155. [[CrossRef](#)]

82. Salgado, R.; Denkert, C.; Campbell, C.; Savas, P.; Nuciforo, P.; Aura, C.; de Azambuja, E.; Eidtmann, H.; Ellis, C.E.; Baselga, J.; et al. Tumor-Infiltrating Lymphocytes and Associations With Pathological Complete Response and Event-Free Survival in HER2-Positive Early-Stage Breast Cancer Treated With Lapatinib and Trastuzumab: A Secondary Analysis of the NeoALTTO Trial. *JAMA Oncol.* **2015**, *1*, 448–454. [[CrossRef](#)] [[PubMed](#)]
83. Kudo, D.; Rayman, P.; Horton, C.; Cathcart, M.K.; Bukowski, R.M.; Thornton, M.; Tannenbaum, C.; Finke, J.H. Gangliosides expressed by the renal cell carcinoma cell line SK-RC-45 are involved in tumor-induced apoptosis of T cells. *Cancer Res.* **2003**, *63*, 1676–1683. [[PubMed](#)]
84. Shenoy, G.N.; Loyall, J.; Berenson, C.S.; Kelleher, R.J., Jr.; Iyer, V.; Balu-Iyer, S.V.; Odunsi, K.; Bankert, R.B. Sialic Acid-Dependent Inhibition of T Cells by Exosomal Ganglioside GD3 in Ovarian Tumor Microenvironments. *J. Immunol.* **2018**, *201*, 3750–3758. [[CrossRef](#)] [[PubMed](#)]
85. Webb, T.J.; Li, X.; Giuntoli, R.L., 2nd; Lopez, P.H.; Heuser, C.; Schnaar, R.L.; Tsuji, M.; Kurts, C.; Oelke, M.; Schneck, J.P. Molecular identification of GD3 as a suppressor of the innate immune response in ovarian cancer. *Cancer Res.* **2012**, *72*, 3744–3752. [[CrossRef](#)] [[PubMed](#)]
86. Valle-Argos, B.; Gómez-Nicola, D.; Nieto-Sampedro, M. Glioma growth inhibition by neurostatin and O-But GD1b. *Neuro Oncol.* **2010**, *12*, 1135–1146. [[CrossRef](#)] [[PubMed](#)]
87. Su, Y.; Huang, J.; Wang, S.; Unger, J.M.; Arias-Fuenzalida, J.; Shi, Y.; Li, J.; Gao, Y.; Shi, W.; Wang, X.; et al. The Effects of Ganglioside-Monosialic Acid in Taxane-induced Peripheral Neurotoxicity in Patients with Breast Cancer: A Randomized Trial. *J. Natl. Cancer Inst.* **2019**. [[CrossRef](#)] [[PubMed](#)]
88. Houghton, A.N.; Mintzer, D.; Cordon-Cardo, C.; Welt, S.; Fliegel, B.; Vadhan, S.; Carswell, E.; Melamed, M.R.; Oettgen, H.F.; Old, L.J. Mouse monoclonal IgG3 antibody detecting GD3 ganglioside: A phase I trial in patients with malignant melanoma. *Proc. Natl. Acad. Sci. USA* **1985**, *82*, 1242–1246. [[CrossRef](#)] [[PubMed](#)]
89. Dhillon, S. Dinutuximab: First Global Approval. *Drugs* **2015**, *75*, 923–927. [[CrossRef](#)]
90. Yu, A.L.; Gilman, A.L.; Ozkaynak, M.F.; London, W.B.; Kreissman, S.G.; Chen, H.X.; Smith, M.; Anderson, B.; Villablanca, J.G.; Matthay, K.K.; et al. Anti-GD2 antibody with GM-CSF, interleukin-2, and isotretinoin for neuroblastoma. *N. Engl. J. Med.* **2010**, *363*, 1324–1334. [[CrossRef](#)]
91. Durbas, M.; Horwacik, I.; Boratyn, E.; Kamycka, E.; Rokita, H. GD2 ganglioside specific antibody treatment downregulates PI3K/Akt/mTOR signaling network in human neuroblastoma cell lines. *Int. J. Oncol.* **2015**, *47*, 1143–1159. [[CrossRef](#)]
92. Doronin, I.I.; Vishnyakova, P.A.; Kholodenko, I.V.; Ponomarev, E.D.; Ryazantsev, D.Y.; Molotkovskaya, I.M.; Kholodenko, R.V. Ganglioside GD2 in reception and transduction of cell death signal in tumor cells. *BMC Cancer* **2014**, *14*, 295. [[CrossRef](#)] [[PubMed](#)]
93. Liu, B.; Wu, Y.; Zhou, Y.; Peng, D. Endothelin A receptor antagonism enhances inhibitory effects of anti-ganglioside GD2 monoclonal antibody on invasiveness and viability of human osteosarcoma cells. *PLoS ONE* **2014**, *9*, e93576. [[CrossRef](#)] [[PubMed](#)]
94. Horwacik, I.; Durbas, M.; Boratyn, E.; Węgrzyn, P.; Rokita, H. Targeting GD2 ganglioside and aurora A kinase as a dual strategy leading to cell death in cultures of human neuroblastoma cells. *Cancer Lett.* **2013**, *341*, 248–264. [[CrossRef](#)] [[PubMed](#)]
95. Yoshida, S.; Kawaguchi, H.; Sato, S.; Ueda, R.; Furukawa, K. An anti-GD2 monoclonal antibody enhances apoptotic effects of anti-cancer drugs against small cell lung cancer cells via JNK (c-Jun terminal kinase) activation. *Jpn. J. Cancer Res.* **2002**, *93*, 816–824. [[CrossRef](#)] [[PubMed](#)]
96. Zhu, W.; Mao, X.; Wang, W.; Chen, Y.; Li, D.; Li, H.; Dou, P. Anti-ganglioside GD2 monoclonal antibody synergizes with cisplatin to induce endoplasmic reticulum-associated apoptosis in osteosarcoma cells. *Pharmazie* **2018**, *73*, 80–86. [[CrossRef](#)] [[PubMed](#)]



## 2- Structure

In this part, we will focus on the chemical structure of gangliosides from the monosaccharide building block to the whole ganglioside structure.

### A- Glycosphingolipids

Glycosphingolipids are a heterogeneous class of lipids composed by a ceramide backbone and sugar headgroup. The hydrophobic ceramide part consists of a sphingoid base and a fatty acid inserted in cellular membrane while the sugar head group faces the extracellular space (Figure 4). Glycosphingolipids exhibit a huge heterogeneity in backbone and headgroup structure. In the ceramide backbone, the sphingoid base may vary in length, saturation, hydroxylation, and branching. The fatty acid is amid-linked to amino group of the sphingoid base and can vary in length, saturation and hydroxylation. In human, the fatty acid chain varies in length mostly between 16 and 24 Carbone residues and is often saturated. Complex GSL are made by the stepwise addition of monosaccharide residues from their activated nucleotide precursor onto GlcCer. The oligosaccharidic moiety is usually composed by Glc, Gal, GalNAc and Neu5Ac which allows the classification of GSL into 5 main series: lacto, neolacto, globo, isoglobo and ganglio-series, depending on their core structure composition (Degroote *et al.*, 2004) (Table 7).

**Table 7: Oligosaccharidic cores of GSL-series.**

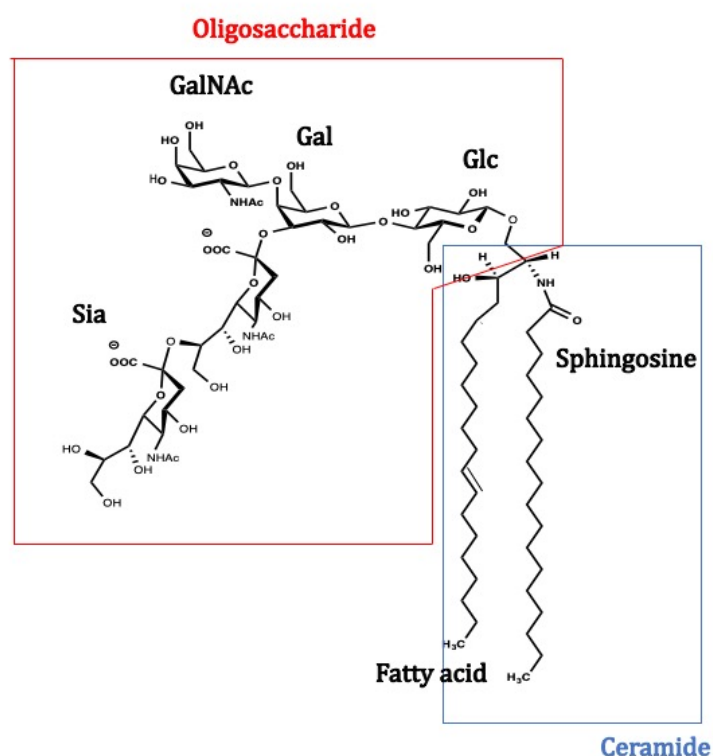
Cer: ceramide; Glc: glucose; Gal: galactose; GalNAc: N-acetylgalactosamine.

Name	Symbol	Structure
<b>Ganglio</b>	Gg	Gal $\beta$ 1-3GalNAc $\beta$ 1-4Gal $\beta$ 1-4Glc $\beta$ 1-Cer
<b>Lacto</b>	Lac	Gal $\beta$ 1-3GlcNAc $\beta$ 1-4Gal $\beta$ 1-4Glc $\beta$ 1-Cer
<b>Neo-Lacto</b>	nLac	Gal $\beta$ 1-4GlcNAc $\beta$ 1-4Gal $\beta$ 1-4Glc $\beta$ 1-Cer
<b>Globo</b>	Gb	GalNAc $\beta$ 1-3Gal $\alpha$ 1-3Gal $\beta$ 1-4Glc $\beta$ 1-Cer
<b>Iso-Globo</b>	iGb	GalNAc $\beta$ 1-3Gal $\alpha$ 1-4Gal $\beta$ 1-4Glc $\beta$ 1-Cer

Glycosphingolipids can also be classified as neutral, sulfated, and acidic glycosphingolipids. Neutral glycosphingolipids are exclusively composed by neutral monosaccharide residues and



composed by globo- and lacto-series glycosphingolipids. They are mainly expressed in skin fibroblasts and blood cells. Sulfated glycosphingolipids contain a sulfate group and the main species are lactosylceramide-sulfate and galactosylceramide-sulfate. Sulfated GSL are expressed in myelin producing oligodendrocytes. Acidic glycosphingolipids are gangliosides carrying one or several N-acetylneuraminic residues and have been primarily characterized in neuronal cells.

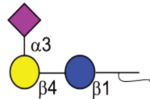
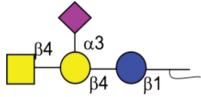
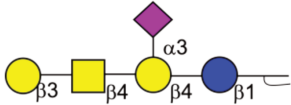
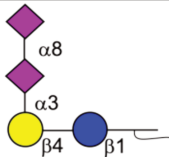
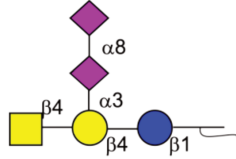
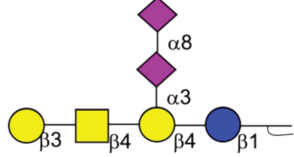
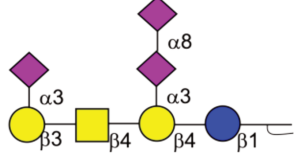
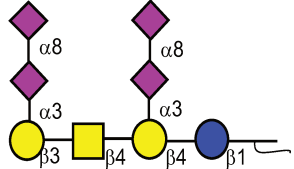






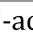
**Figure 4: Structure of a GSL composed of a ceramide backbone and a carbohydrate moiety: the example of GD2 ganglioside.**

## B- Gangliosides

Gangliosides are ganglio-series (GgCer) based glycosphingolipids containing the tetrasaccharidic core (GalNAcβ1-4Galβ1-4Glcβ1-1Cer) and they are highly conserved among vertebrates (Table 7). They carry one or several sialic acid residues in their carbohydrate moieties and are mainly located in glycolipid-enriched microdomains, also called rafts, on the outer leaflet of the membrane bilayer. They are found in different cell types and tissues as a mixture of di-, tri-, tetra-saccharides structures which confers to this subclass a high heterogeneity.

**Table 8: Nomenclature of gangliosides.**

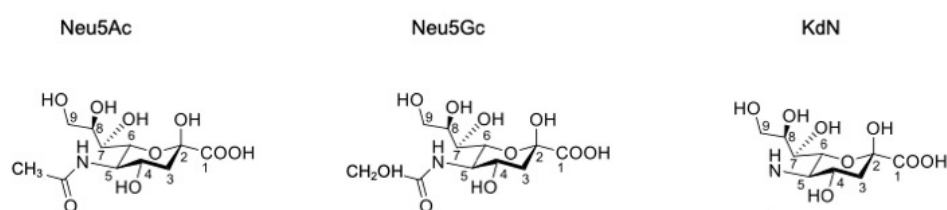
Name	Structure	Representation <sup>1</sup>
GM3	Neu5Ac $\alpha$ 2-3Gal $\beta$ 1-4Glc $\beta$ 1Cer (II <sup>3</sup> Neu5Ac-Gg <sub>2</sub> Cer)	
GM2	GalNAc $\beta$ 1-4(Neu5Ac $\alpha$ 2-3)Gal $\beta$ 1-4Glc $\beta$ 1Cer (II <sup>3</sup> Neu5Ac-Gg <sub>3</sub> Cer)	
GM1a	Gal $\beta$ 1-3GalNAc $\beta$ 1-4(Neu5Ac $\alpha$ 2-3)Gal $\beta$ 1-4Glc $\beta$ 1Cer (II <sup>3</sup> Neu5Ac-Gg <sub>4</sub> Cer)	
GD3	Neu5Ac $\alpha$ 2-8Neu5Ac $\alpha$ 2-3Gal $\beta$ 1-4Glc $\beta$ 1Cer (II <sup>3</sup> Neu5Ac <sub>2</sub> -Gg <sub>2</sub> Cer)	
GD2	GalNAc $\beta$ 1-4(Neu5Ac $\alpha$ 2-8Neu5Ac $\alpha$ 2-3)Gal $\beta$ 1-4Glc $\beta$ 1Cer (II <sup>3</sup> Neu5Ac <sub>2</sub> -Gg <sub>3</sub> Cer)	
GD1b	Gal $\beta$ 1-3GalNAc $\beta$ 1-4(Neu5Ac $\alpha$ 2-8Neu5Ac $\alpha$ 2-3)Gal $\beta$ 1-4Glc $\beta$ 1Cer (II <sup>3</sup> Neu5Ac <sub>2</sub> -Gg <sub>4</sub> Cer)	
GT1b	Neu5Ac $\alpha$ 2-3Gal $\beta$ 1-3GalNAc $\beta$ 1-4(Neu5Ac $\alpha$ 2-8Neu5Ac $\alpha$ 2-3)Gal $\beta$ 1-4Glc $\beta$ 1Cer (IV <sup>3</sup> Neu5AcII <sup>3</sup> Neu5Ac <sub>2</sub> -Gg <sub>4</sub> Cer)	
GQ1b	Neu5Ac $\alpha$ 2-8Neu5Ac $\alpha$ 2-3Gal $\beta$ 1-3GalNAc $\beta$ 1-4(Neu5Ac $\alpha$ 2-8Neu5Ac $\alpha$ 2-3)Gal $\beta$ 1-4Glc $\beta$ 1Cer (IV <sup>3</sup> Neu5Ac <sub>2</sub> II <sup>3</sup> Neu5Ac <sub>2</sub> -Gg <sub>4</sub> Cer)	

<sup>1</sup>  Ceramide;  Galactose;  Glucose;  N-acetyl-galactosamine;  N-acetyl-neuraminic acid.

Irrespective of the elongation status of core structures, gangliosides are characterized by the number and the position of Sia residues that define their classification. In ganglioside nomenclature, the prefix G refers to ganglio: M, D, T, Q and P refer to the number of sialic acid

residues (1 to 5); the Arabic numerals and lower-case letters refers to the order of migration of the gangliosides on thin layer chromatograms. In that way, a-series gangliosides are monosialogangliosides also named simple gangliosides, mainly composed by GM1, GM2, GM3. In contrast, b- and c-series are di- and tri-series gangliosides also named complex gangliosides, and the major species are GD3, GD3, GD1, GT1, GQ1 (Table 8).

### C- Sialic Acids



**Figure 5: Major sialic acid species: Neu5Ac, Neu5Gc, KdN.**

Ganglioside classification is based on the presence of Sia residues. Sia are 9-carbon monosaccharides derived from neuraminic acid: 5-amino, 3,5-dideoxy-D-glycero-D-galactononulosonic acid) containing either acetylated, hydroxylated or glycolated groups. The major groups are N-acetylneuraminic acid (Neu5Ac), and 3-deoxy-non-2-ulosonic acid (KdN), N-glycolylneuraminic acid (Neu5Gc) (Figure 5). The second level of diversity results from the diversity of  $\alpha$ -linkages between the C2 of the sialic acid residue and underlying sugars by specific sialyltransferases. The third level of diversity results from the additional substitutions of *O*-acetyl, *O*-methyl, *O*-sulfate, *O*-lactyl and phosphate groups. Despite this high diversity of structures, a simple nomenclature for Sia has been defined. The core neuraminic structure is defined as Neu for neuraminic acid, and KdN for 2-keto-3-deoxynononic acid. The other substitutions are defined by letter codes Ac for Acetylated, Gc for Glycolyl, Me for Methyl, Lt for Lactyl, and S for Sulfate. For example, 9-*O*-acetylneuraminic acid is defined as Neu5,9OAc<sub>2</sub>. Although KdN is prominently expressed in fish, whereas mammals are known to express Neu5Ac and Neu5Gc (Davies and Varki, 2015). However, humans are deficient in Neu5Gc due to the inactivation of the enzyme CMP-N-acetylneuraminic acid hydroxylase responsible for converting Neu5Ac to Neu5Gc. Accordingly, Neu5Ac is the major sialic acid species in human (Varki, 2001).



### 3- Metabolism

Ganglioside turnover results from the combination of *de novo* biosynthesis, direct glycosylation processes, ganglioside catabolism and salvage pathways which tightly combine to ensure ganglioside turnover on cellular membranes.

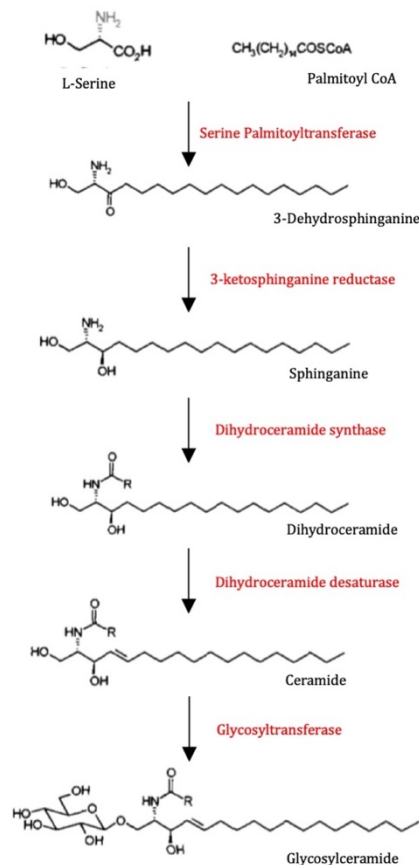
#### A- De novo biosynthesis

Biosynthesis process of gangliosides occurs mainly in ER and Golgi apparatus by the sequential action of membrane bound glycosyltransferases before their transport to the cell surface membrane by exocytic membrane flow. Gangliosides segregate spontaneously together with cholesterol and specific transmembrane proteins into lipid raft domains also called glycolipid enriched microdomains, where they fulfill numerous biological functions.

#### A-1 Ceramide backbone biosynthesis

In mammalian cancer cells, ceramide backbone biosynthesis occurs *de novo* on the cytosolic side of the endoplasmic reticulum (ER). L-serine is condensed to palmitoyl CoA by the action of serine-palmitoyl CoA transferase forming 3-ketodihydrosphingosine. This lipid is reduced to sphinganine also named dihydrosphingosine by 3-ketosphinganine reductase. Dihydroceramide synthase subsequently condenses sphinganine with a fatty acid by an amide bond, forming dihydroceramide. Finally, dihydroceramide desaturase leads to ceramide formation (Figure 6).

Ceramide molecules follow either the vesicular pathway or the CERT-dependent non-vesicular pathway to early Golgi compartments where they can be converted to glucosylceramide (GlcCer) (Perry and Ridgway, 2005). CERT is a Ceramide ER-transport protein recognizing ER by its Pleckstrin Homology domain and the Golgi by its Phosphatidyl 4-phosphate domain. CERT shuttles ceramide from ER to Golgi via its ceramide binding START domain (Perry and Ridgway, 2005). In mammals, the ubiquitously expressed GlcCer is synthesized by the UDP-Glc: ceramide glucosyltransferase (GlcCerT) on the cytosolic side of Golgi membranes, while galactosylceramide (GalCer) synthesis occurs only on ER luminal side of specialized cells in kidney and brain.



**Figure 6: Glucosylceramide synthesis pathway.** Adapted from Van Echten et Sandhoff, 1993.

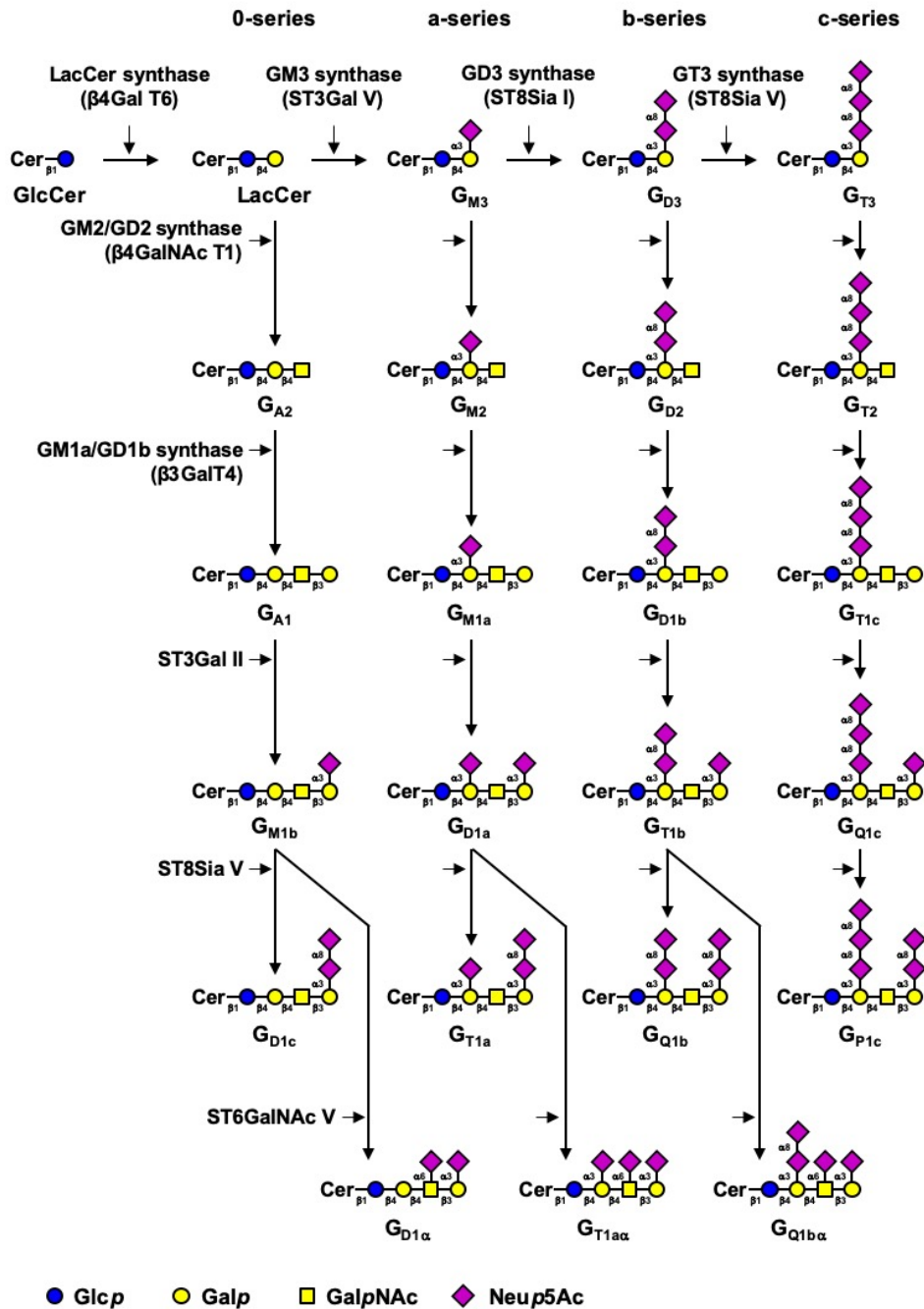
GalCer is the precursor of Gala-series of glycolipids which are expressed exclusively on specialized cells: GalCer and sulfatides are the major lipids of the myelin sheath assembled around the axons on neuronal cells by oligodendrocytes and Schwann cells. The transfer of a Gal residue from UDP-Gal to ceramide occurs in the ER and is catalyzed by a unique UDP-Gal: ceramide galactosyltransferase (Jeckel *et al.*, 1992). GalCer is the precursor of sulfatides which are synthesized by the addition of a sulfate group through an ester linkage to the 3-position of the Gal residue (Huwiler *et al.*, 2000). The sulfation reaction is catalyzed by sulfotransferases in the lumen of the Golgi apparatus (Sundaram and Lev, 1992; Tettamanti, 2004). Among gangliosides, only GM4 ganglioside is synthesized from GalCer rather than from LacCer (Degroote *et al.*, 2004).

### *A-2 Sugar headgroup biosynthesis*

Complex GSL are made by the stepwise addition of monosaccharide residues from their activated nucleotide precursor through the action of specific glycosyltransferases (GT) in the Golgi apparatus. Glycosyltransferases and sialyltransferases are specific for one enzymatic reaction. GlcCer is the precursor of ganglioside biosynthesis and is converted to Lactosylceramide (LacCer) by the action of UDP-Galp-ceramide  $\beta$ -D-glucosyltransferase (or Lactosylceramide synthase, encoded by *B4GALT5* gene) by the transfer of Gal residue (Nomura *et al.*, 1998) in the Golgi lumen (Lannert *et al.*, 1994). Ganglioside synthesis continues in the Golgi lumen (Kolter *et al.*, 2002) by the action of sialyltransferases ST3GalV (GM3 synthase), ST8SiaI (GD3 synthase), and ST8SiaV (GT3 synthase) leading respectively to the biosynthesis of the precursors of a-, b-, and c-series gangliosides. Elongation is performed by the sequential action of  $\beta$ 4GalNAc T1,  $\beta$ 3Gal T4, and of sialyltransferases ST3Gal II, ST8Sia V and ST6GalNAc V. Whereas ST3Gal I, ST3Gal II and ST3Gal V sialyltransferases transfer a Sia residue in  $\alpha$ 2-3 linkage to Gal, ST8Sia I and ST8Sia V sialyltransferases transfer Sia residues in  $\alpha$ 2-8 linkage to Sia (Tettamanti, 2004).

The 0-series gangliosides are directly synthesized from LacCer, producing sequentially GA2, GA1, GM1b, and GD1c. GM3 is the precursor of a-series gangliosides, producing GM2, GM1a, GD1a, GT1a. GD3 is the precursor of b-series gangliosides, notably, GD2, GD1b, GT1b and GQ1b. GT3, the precursor of c-series gangliosides leads to the biosynthesis of GT2, GT1c, GQ1c, and GP1c (Figure 7).

*De novo* produced gangliosides are then transported from the trans-Golgi network to the cell surface by vesicular pathways.

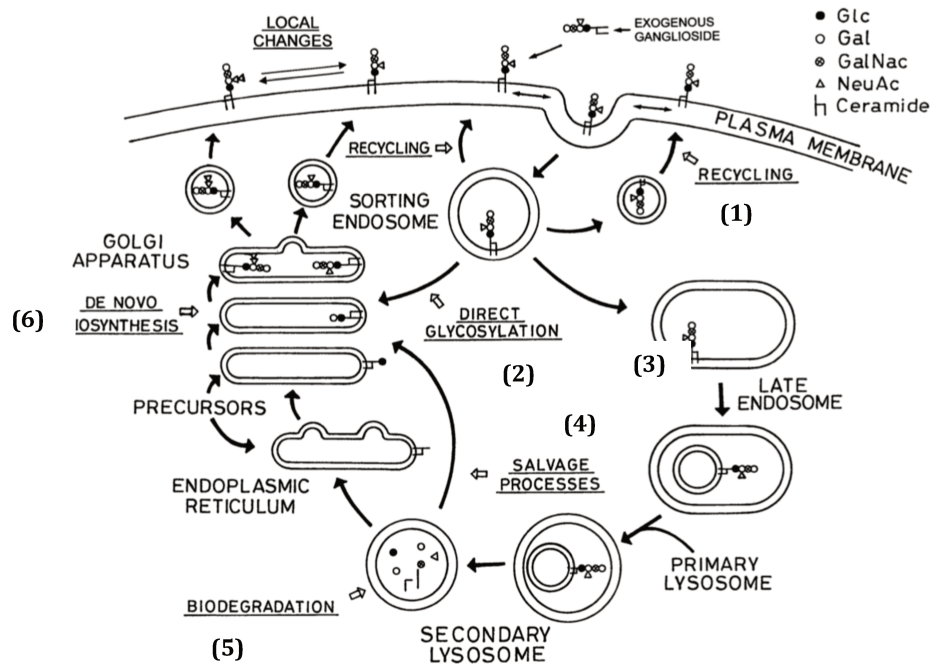


**Figure 7: Biosynthesis pathway for gangliosides.** Adapted from Julien *et al.*, 2013.

## B- Catabolism

Ganglioside degradation occurs sequentially by the removal of sugar residues into acidic compartments of cells. Firstly, fragments of the plasma membrane containing gangliosides are endocytosed as coated pits or through clathrin-independent vesicles mainly through caveolae-mediated endocytosis (Crespo *et al.*, 2008; Daniotti and Iglesias-Bartolomé, 2011; Sharma *et al.*,

2003). Endocytosed gangliosides can either be transported into the Golgi apparatus to serve as substrates for the synthesis of more complex gangliosides or recycled to the plasma membrane, or they can be transported to the late endosomal-lysosomal system for degradation (Figure 8).



**Figure 8: Subcellular traffic and metabolic turnover of gangliosides.**

Adapted from Tettamanti *et al.* 2004. Gangliosides are endocytosed into vesicles from the cell membrane and can be (1) recycled to the cell membrane, (2) be addressed to the Golgi apparatus for direct glycosylation, (3) fused to late endosomes-lysosomes for degradation, (4) escape lysosomes and enter salvage pathway, or (5) be completely degraded and (6) be used for de novo biosynthesis.

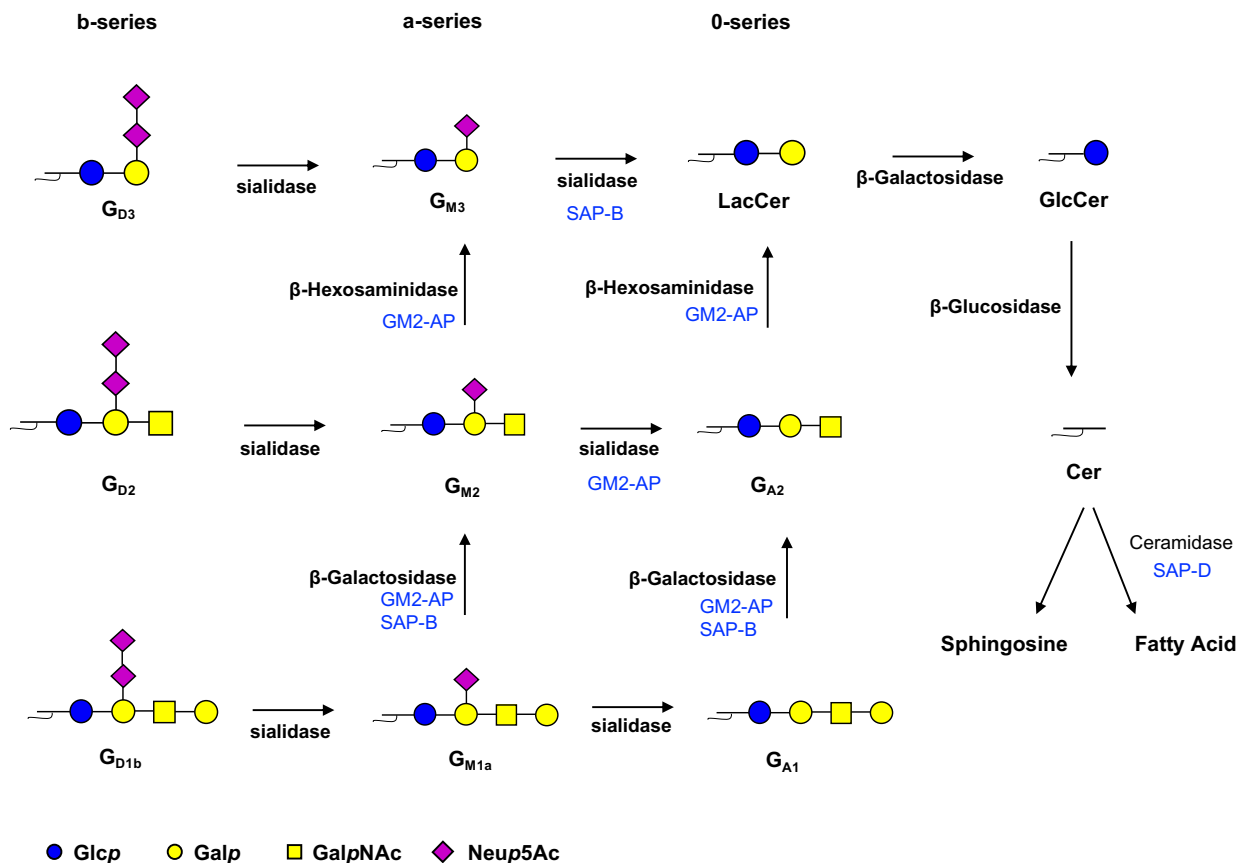
Ganglioside degradation process starts with the fusion of lysosomes with endosomes. This fusion exposes gangliosides into the lysosomal matrix in which they become available for degradation. Then, the glycohydrolases, water-soluble lysosomal enzymes, digest each single residue in a stepwise manner starting from the non-reducing terminal residue. Simple gangliosides composed by one to four residues are not accessible to the water-soluble enzymes. Thus, their hydrolysis requires membrane perturbing activator proteins such as saposins also called Sphingolipid Activator Proteins (SAPs) -A to -D (Morimoto *et al.*, 1990) or GM2-Activator

Protein (GM2-AP) (Wilkening *et al.*, 2000). The complex formed by SAP and gangliosides is recognized and hydrolyzed by exohydrolases. All four SAPs -A to -D derive from a single SAP-precursor which is proteolytically processed to produce individual SAP (Vielhaber *et al.*, 1996). SAPs bear a site of N-glycosylation and three disulfide bridges that render SAP stable to the acidic pH of lysosomes (Kishimoto *et al.*, 1992)(Vaccaro *et al.*, 1995). These non-enzymatical glycoproteins share a lipid binding and a membrane perturbing property. SAP-A and -B bind to GM1 or GM2, whereas SAP-C and SAP-D contribute to ceramide degradation (Klein *et al.*, 1994; Linke *et al.*, 2001) (Kishimoto *et al.*, 1992). GM2-AP is a small non-enzymatic lysosomal glycoprotein bearing N-glycosidically bound oligosaccharide chains and containing four disulfide bridges (Schütte *et al.*, 1998). Thin-layer chromatography experiments showed that GM2-AP binds selectively to GM1, GM2 or GM3 (Hama *et al.*, 1997) and lifts them out of the membrane to render gangliosides accessible to exohydrolases (Wilkening *et al.*, 2000). The resulting degradation products can leave the lysosomes to enter the salvage pathway, or can be further degraded. The salvage pathways consist in integrating catabolism products into a biosynthetic process

Ganglioside degradation occurs in the following way: complex gangliosides from b- and c-series are transformed into simple a- series gangliosides through the removal of sialic acid residues by sialidases. GM2, GM1 or GM3 obtained by this first step of degradation are subsequently digested. GM1 produces GM2 by the removal of Gal residue by a  $\beta$ -galactosidase in the presence of either GM2-AP or SAP-B (Wilkening *et al.*, 2000). GM2 degradation to GM3 requires GM2-AP and occurs by the removal of GalNAc residue through the sequential action of  $\beta$ -N-acetylhexosaminidase and by  $\beta$ -galactosidase (Fürst and Sandhoff, 1992). The removal of the sialic acid residue from GM3 by a sialidase forms LacCer in the presence of SAP-B (Fingerhut *et al.*, 1992). The alternative way of GM2 and GM1 degradation is the removal of sialic acid residue by a sialidase, forming GA2 and GA1 respectively. GA2 and GA1 are then converted to LacCer by the action of  $\beta$ -N-acetylhexosaminidase and by  $\beta$ -galactosidase action. LacCer is digested by  $\beta$ -galactosidase and  $\beta$ -glucosidase to form ceramide. This resulting lipid moiety is digested by

ceramidase to a fatty acid and a sphingoid base in the presence of SAP-D (Linke *et al.*, 2001) (Figure 9).

An alternative pathway for ganglioside catabolism consists in the cleavage of the  $\beta$ -glycosidic linkage between glucose and ceramide by an endoglucoceramidase occurring in bacteria and leeches, but this process still remains controversial in mammals (Tettamanti, 2004) (Ito and Yamagata, 1986). The resulting catabolism products can either be further degraded or can escape the lysosomes to be used in salvage pathways. (Figure 8).



**Figure 9: Ganglioside catabolism pathway.** Adapted from Tettamanti *et al.*, 2004

### C- Regulation of ganglioside metabolism

The metabolic turnover of gangliosides implies as indicated in Figure 5 many different biological processes including (1) membrane recycling of internalized gangliosides, (2) direct

glycosylation of gangliosides in the Golgi apparatus, (3) degradation in lysosomes/late endosomes, (4) salvage processes, (5) complete degradation, or (6) *de novo* biosynthesis (Figure 8). Assuming the complexity of internalized ganglioside metabolism, the determination of ganglioside turnover remains difficult to study, due to the metabolic and functional states of cell and membrane renewal fluxes that are highly dynamic and variable, especially endocytosis and exocytosis. The only acceptable measurements of gangliosides content are the data cumulated from *de novo* biosynthesis, direct glycosylation, and salvage pathways. The contribution of other events remains extremely difficult to take into account (Tettamanti, 2004). The calculation of the half-life of gangliosides has been determined on cultured cells. The values range from 2 to 5 h in CHO cells, to 30 h in NB cells (Medlock and Merrill, 1988; Miller-Podraza and Fishman, 1982). Thus, gangliosides turnover is highly dependent on the cell-type and still remains uneasy to study. Nevertheless, gangliosides metabolic turnover depends highly on membrane turnover and supply, and on the availability of enzymes, carrier proteins, activator proteins and substrates (Tettamanti, 2004).

### *C-1 Spatio-temporal expression and localization of GT*

The pattern of ganglioside expression in tissues highly depends on the spatio-temporal expression of GT involved in the synthesis, their availability, kinetic parameters and enzymatic activities. The major changes described in the literature regarding ganglioside expression patterns during embryogenesis are in agreement with modifications of GT activities. For example, GD3 synthase gene expression is higher during early stages whereas GM2/GD2 synthase expression increases during late stages of brain development in mice, which correlates with changes in ganglioside expression implicated in brain development (Yamamoto *et al.*, 1996). In the same manner, Yu and coworkers have shown a shift between GT expression during fetal development in mice, leading a preferential expression of simple gangliosides, such as GM1, GD1a, and GT1a (Yu *et al.*, 1988). GT are membrane-bound enzymes located in the different cisternae of the Golgi apparatus. The precise subcellular localization of GT in the Golgi apparatus plays an important role in the regulation of ganglioside synthesis. While simple gangliosides synthesis



occurs in the proximal regions of the Golgi apparatus, complex gangliosides synthesis takes place in more distal regions (Giraudo and Maccioni, 2003). In agreement, LacCer synthase and GM3 synthase form an enzymatic complex for the synthesis of GM3 in CHO-K1 cells. This enzymatic complex is located in the cis-Golgi apparatus. GD3 synthase overexpression in these cells lead to the formation of trimeric complexe between LacCer synthase-GM3 synthase-GD3 synthase localized to trans-Golgi network (Giraudo and Maccioni, 2003; Uliana *et al.*, 2006).

GT enzymatic activity is usually very specific, as their activity consists in the transfer of a single monosaccharide residue on a specific acceptor substrate. However, several GT, such as those encoded by *B4GALNT1* and *B3GALT4* genes, can act on different substrates during gangliosides synthesis (Figure 7). Thus, substrate availability, which is linked to the expression level of the different GT genes, regulates by itself ganglioside composition in various tissues and cell-types. For example, GD3 synthase overexpression in PC12 neuronal cell lines leads to the expression of GD1b and GT1b, whereas MDA-MB-231 GD3+ BC cells produce mostly GD3, GD2, GT3 (Cazet *et al.*, 2009; Fukumoto *et al.*, 2000).

### *C-2 Transcriptional and posttranscriptional regulation of GT*

GT are mainly regulated at the transcriptional level, leading to tissue-specific or cell-specific GT expression (Nairn *et al.*, 2008). GD2 synthase mRNA are highly expressed in human brain, lung and testis whereas GM3 synthase transcripts are ubiquitously expressed in adults (Hidari *et al.*, 1994; Ishii *et al.*, 1998). Cytoplasmic phosphorylation/dephosphorylation mechanisms modulate GT expression and Golgi/ER location. In NB cells, the activation of protein kinase C (PKC) and protein kinase A (PKA) induces an increase of  *$\beta$ 4GalNAcT1* activity and reduces ST3Gal I and ST3Gal II activity resulting in GM1 accumulation (Yu and Bieberich, 2001). Besides, PKC induces the phosphorylation of serine and threonine residue in the cytoplasmic tails of  *$\beta$ 4GalNAcT1* and ST3GalII which decreases to half the activity of these enzymes (Gu *et al.*, 1995). Furthermore, the distribution of GT and their trafficking from Golgi to ER is regulated by

their N-glycosylation. For example, N-glycosylation of GD3 synthase is crucial for both its catalytic activity and proper trafficking from the ER to the Golgi apparatus (Martina *et al.*, 1998).

### *C-3 Crosstalk between gangliosides and GT synthesis*

GT synthesis can be modulated by gangliosides expression. GM1, GM2, GT1b and to a major extent GD1a, inhibit GM2/GD2 synthase expression. GQ1b, GT1b and GD1a inhibit GD3 synthase expression in Golgi vesicles isolated from rat liver (Yusuf *et al.*, 1987). The bifunctional enzyme UDP-GlcNAc 2-epimerase/ManNAc 6-kinase controls Sia biosynthesis by converting UDP-GlcNAc to N-acetylmannosamine. Wang and coworkers have shown that overexpression of this enzyme increases GM3 and GD3 synthase mRNA levels and ganglioside synthesis, whereas its repression decreases GM3 and GD3 synthase mRNA levels (Wang *et al.*, 2006). These data suggest the existence of a cross-regulation between the expression of enzymes involved in glycolipid synthesis (GT, or enzymes such as UDP-GlcNAc 2-epimerase/ManNAc 6-kinase that is involved in Sia metabolism) and the expression of gangliosides.

In conclusion, GT activity is highly dependent on their subcellular localization in the different Golgi cisternae, on gangliosides that are already expressed, the possibility to multimerize with surrounding enzymes and the substrate availability which explains the cell-type dependent pattern of gangliosides.

### *C-4 Spatio-temporal localization and function of sialidases*

Sialidases, or neuraminidases are glycosidases that catalyze the removal of Sia from glycoconjugates. Sialidase level and activity is essential for the regulation of gangliosides turnover. Four types of sialidases have been identified and characterized so far. NEU1, a lysosomal sialidase, uses oligosaccharides and glycopeptides as substrates and contributes to immune functions at the cell surface like the activation of Toll like receptor 4 (TLR4), or to the induction of airway inflammation caused by hyposialylation of hyaluronic receptor of CD4+ in T cells, and is also involved in lysosomal catabolism. NEU2 has been characterized as the cytosolic sialidase and is active on oligosaccharides, glycopeptides and gangliosides. NEU2 is involved in muscle cell

differentiation (Monti and Miyagi, 2015). NEU3 is a plasma membrane sialidase using gangliosides as substrates. NEU4 is able to desialylate oligosaccharides, glycoproteins, and gangliosides (Monti and Miyagi, 2015). NEU4 location has been suggested to be the lysosome (Seyrantepe *et al.*, 2004), mitochondria (Yamaguchi *et al.*, 2005), and/or the ER (Bigi *et al.*, 2010). NEU3 and NEU4 regulate neuronal differentiation (Monti and Miyagi, 2015). The last three neuraminidases can use gangliosides as substrates and are potentially implicated in the regulation of ganglioside expression. NEU2 expression is expressed at very low levels in healthy or cancer human cells. Abnormal upregulation of NEU3 is involved in the progression of malignancy in various types of cancers. In human colon cancer, NEU3 mRNA is increased 3- to 100- fold compared to non-tumor mucosa (Kakugawa *et al.*, 2002). In contrast to human colon carcinoma, NEU3 level is downregulated in glioblastoma accelerating cell invasion via the disassembly of focal adhesions (Takahashi *et al.*, 2017). The mRNA level of NEU4 in human colon mucosa is markedly decreased in human colon cancer. The decreased level of NEU4 is related to a significant inhibition of apoptosis and to an increase of invasion and motility (Yamanami *et al.*, 2007). Sawada and coworkers have shown that low metastatic mouse colon adenocarcinoma cell clones express low level of sialidases compared to clones with higher metastatic potential, showing that sialidases levels affects the metastatic ability. Besides, overexpression of NEU2 in N17 highly metastatic lung cells leads to the inhibition of lung metastasis, reduces motility and invasive capability accompanied by a decrease of sialyl Lewis x (sLe<sup>x</sup>) and GM3 amounts. Furthermore, targeting GM3 using a specific antibody decreases metastasis (Sawada *et al.*, 2002). Desialylation by itself is involved in the suppression of tumorigenesis. NEU4 deficiency in mice induces morphological abnormalities and modifies ganglioside relative amounts in brain, with an increase in GD1a and a decrease in GM1 levels. Sialidase levels and activities in cancer is a determining factor for metastatic ability, independently of the cell type.

## **D- *O*-acetylated gangliosides**

### *D-1 Expression of O-acetylated gangliosides*

*O*-acetylated gangliosides are considered as oncofetal markers in cancer. *O*-acetylation is one of the main modifications of gangliosides and *O*-acetylated species are known to be neo-expressed during cancer development. The *O*-acetylation reaction takes place in the Golgi apparatus and is cell type specific and developmentally regulated (Gerardy-Schahn *et al.*, 2015). Their synthesis and degradation of *O*-acetylated glycolipids are finely tuned processes. The *O*-acetylation reaction is highly dependent on the availability of acceptors, substrates, the Golgi-ER transporters, clathrin-dependent internalization of gangliosides and the balance between the Sialyl-*O*-acetyltransferases (SOAT) and the Sialyl-*O*-acetyl esterase (SOAE) activity. SOAT activity and *O*-acetylated gangliosides expression are tightly linked. Reduced SOAT activity decreases *O*-acetylation, whereas enhanced SOAT activity increases *O*-acetylation and decreases hyposialylation by membrane-bound sialidase (Corfield *et al.*, 1999; Shen *et al.*, 2004). These finely regulated processes give rise to a tissue/cell-type specific pattern of *O*-acetylated gangliosides expression (Mandal *et al.*, 2015).

After the translocation of CMP-sialic acid to the lumen of the Golgi apparatus by a nucleotide sugar transporter, sialyltransferases catalyze Sia transfer onto a Gal, GalNAc, GlcNAc or Sia residue in an  $\alpha$ 2-3,  $\alpha$ 2-6,  $\alpha$ 2-8, and  $\alpha$ 2-9 linkages. The *O*-acetylation reactions catalyzed by SOAT correspond to the transfer of an acetyl group from acetyl coenzyme A to the C4/7/8/9 OH-position of the Sia residue. The primary site of *O*-acetyl group transfer on Sia is thought to be C7, from which the *O*-acetyl group can subsequently migrate in acidic pH conditions to the C8 and to the C9 position, considered as the final position (Vandamme-Feldhaus and Schauer, 1998). The *O*-acetyl groups are removed from Sia by Sialyl-*O*-acetyl esterases (SIAE). SIAE can remove C4 or C9-*O*-acetyl groups on Sia-linked to glycoconjugates or on free Sia released from glycoconjugates by sialidases. It is well established that the *O*-acetylation reaction takes place in the Golgi apparatus by a membrane-bound SOAT, whereas de-*O*-acetylation can either take place into the lysosomal compartment by a membrane-bound sialyl *O*-acetyl esterase (Lse) or in the cytoplasm by a soluble

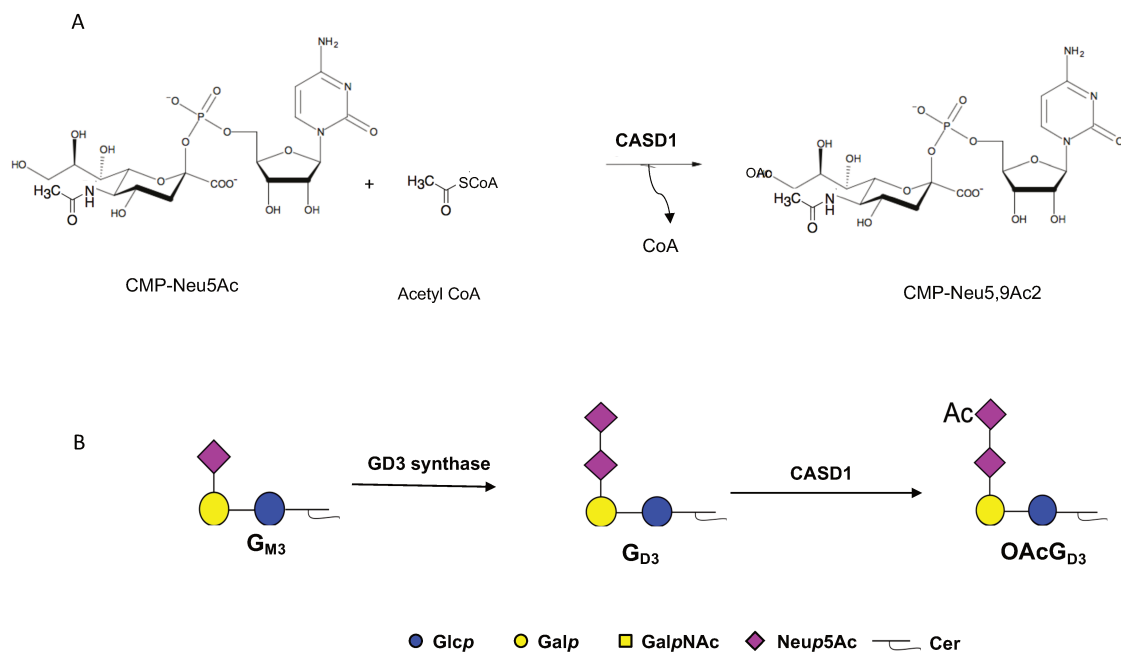
esterase. Takematsu and coworkers' studies suggest that full length Lse goes through the ER-Golgi pathway and localizes primarily in lysosomes, while an alternative splice variant at the 5' end (lacking the signal peptide encoding region) encodes for a cytoplasmic SIAE. SIAE mRNA expression is also differentially regulated among tissues. While mRNA encoding Lse are ubiquitous among tissues, the ones encoding cytoplasmic SIAE are mainly expressed in liver, ovary and brain (Takematsu *et al.*, 1999). Furthermore, neutral to alkaline pH is required for optimal activity of SIAE, which corresponds to the pH of the cytoplasm, but not to the lysosomal one. It has been suggested that either minimum Lse activity could be maintained at acidic pH or that lysosomal pH is increased for Lse (Butor *et al.*, 1993). Despite the limited knowledge concerning SOAT and SIAE enzymes, the diversity of *O*-acetylated gangliosides and their differential expression among tissues and developmental stages suggest a regulation at multiple levels.

#### *D-2 SOATs*

In this project, the main focus concerns the neo expression of *O*-acetylated GD2 ganglioside in neuroectoderm-derived tumors. Different levels of diversity regulate *O*-acetylated ganglioside expression, including the position of the *O*-acetyl group on the carbone residue, the number of *O*-acetylated Sia residues and their position in the carbohydrate chains of glycoconjugates, as well as the cellular SOAT activity. Despite the limited information available on *O*-acetylated gangliosides expression in human tissues or cells, some studies on diverse biological sources are still available. The first level of diversity is due to the transfer of acetyl group from acetyl-coenzyme A to the C4/7/8/9 of the Sia residue, generating different *O*-acetylated gangliosides. The preferential site of insertion of the *O*-acetyl group is the C7 of the Sia residue. It is proposed that from this primary insertion site, the *O*-acetyl group can migrate to C8 and C9 due to acidic pH, leaving C7 available for a new transfer (Vandamme-Feldhaus and Schauer, 1998). Mono-*O*-acetylation of the C4 residue seems to be unusual, whereas di-*O*-acetylation is commonly found on C4-7, C4-8 or C4-9 in horse serum hydrolysates (Klein *et al.*, 1997). *In vitro* studies have demonstrated that SOAT isolated from different sources have preferential acceptors for the *O*-

acetylation reaction. Several acceptors including free Sia, CMP-Sia, gangliosides, glycoprotein bound-Sia could be acetylated by SOAT. The transfer of Sia on glycoconjugates is achieved by specific sialyltransferases that use CMP-Sia transported into the lumen of the Golgi apparatus by the CMP-Sia transporter. The isolation of SOAT by biochemical procedures has led to the identification of different SOAT activities. On the one hand, SOAT isolated from microsomes prepared from bovine submaxillary glands preferentially transfers *O*-acetylated groups to the C7 of the Sia residue, these *O*-acetyl groups subsequently migrate spontaneously to C8 and then to C9 due to the acidic pH (Vandamme-Feldhaus and Schauer, 1998). On the other hand, SOAT isolated from Golgi-enriched fractions from the Guinea pig liver transfers *O*-acetyl groups to the C4 of the Sia residue (Iwersen *et al.*, 1998, 2003). Furthermore, some observations support the possibility that distinct SOAT activities may exist in cells, due to a preferential specificity towards  $\alpha$ 2-8 rather than  $\alpha$ 2-3 linked Sia (Chen *et al.*, 2006). All the attempts made for the biochemical isolation of SOAT enzymes were unsuccessful since a purified enzyme has not been obtained yet. However, expression cloning lead to the identification of SOAT in cell lines overexpressing GD3 synthase. In that way, Kanamori *et al.* first characterized by expression cloning in the ER of COS cells a multimembrane spanning protein which is an *O*-acetyl coenzyme A transporter (AT-1 or SLC33A1) (Kanamori *et al.*, 1997). AT-1 overexpression in Hela cells exacerbates the *O*-acetylation of GD3 and GT3 (Kanamori *et al.*, 1997). In a CHO cell line overexpressing GD3 synthase (CHO-GD3S+), the cell cycle regulator expression Tis21 is reduced compared to control cells. The overexpression of Tis 21 in CHO-GD3S+ increases OAcGD3 expression. These studies suggest that *O*-acetylation of GD3 is enhanced by Tis21 induction (Satake *et al.*, 2003). The role of Tis21 in GD3-*O*acetylation has been controversial in GM2/GD2 synthase knock-out mice lacking all complex gangliosides. These mutant mice exhibit high expression of OAcGD3 in nerve tissues despite a downregulated Tis21 expression (Furukawa *et al.*, 2008). *CASD1* has been described as encoding the only human SOAT up-to-now. *CASD1* expression is upregulated in human primary cell lines, melanoma and liver-derived cells. The overexpression of *CASD1* and *GD3 synthase* genes correlated with an increase in 7-*O*AcGD3 biosynthesis in COS cells (Arming *et al.*, 2011), and in 9-

*O*AcGD3 in near human haploid HAP-1 cells (Baumann *et al.*, 2015). Moreover, inactivated *CASD1* using CRISPR/Cas9 in HAP-1 cells resulted in the loss of 9-*O* acetylated GD3 (Figure 10B). Baumann and coworkers' *in vitro* experiments suggest that *CASD1* would act on the activated sialic acid donor, CMP-Neu5Ac and not on the sialylated glycolipid itself (Figure 10A). On the contrary, *CASD1*-deficient mice exhibit a complete loss of *O*-acetylation of Sia on the surface of hematopoietic lineage cells such as myeloid, erythroid and CD4<sup>+</sup> T cells (Mahajan *et al.*, 2019). The biosynthesis pathways for ganglioside *O*-acetylation remain unclear, but *CASD1* seems to have a role in the *O*-acetylation process.



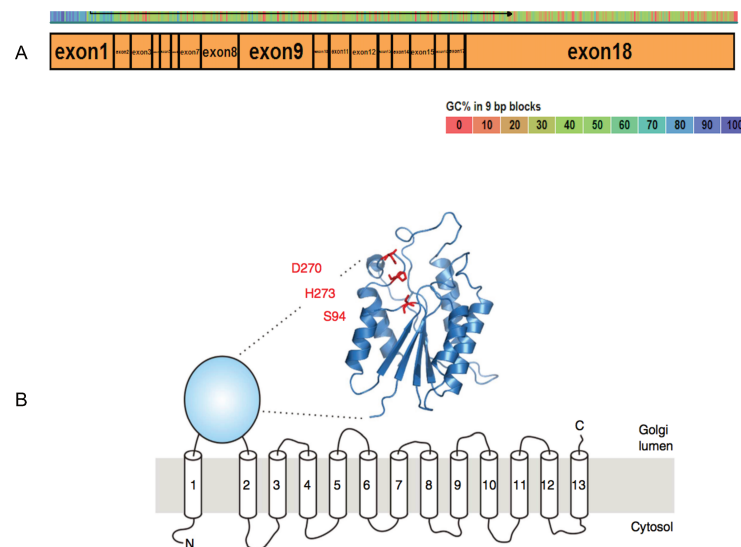
**Figure 10: Proposed *CASD1* acetyltransferase activity.**

A- *CASD1* SOAT activity on CMP-Neu5Ac. B- Biosynthesis pathway for OAcGD3 ganglioside by directly acetylation of GD3.

### D-3 *CASD1*

In 2011, Cas 1 domain 1 containing (*CASD1*) gene has been identified by data mining of the human genome for encoding a potential *O*-acetyltransferase. *CASD1* is similar to the gene of the yeast strain *Cryptococcus neoformans* (Arming *et al.*, 2011). Yeast Cas1p adds *O*-acetyl groups at the C6 position of a mannose residue in a capsid structure composed of glucuronoxylomannans.

The deletion of the fungal gene resulted in the loss of *O*-acetylation on Man residues of glucuronoxylomannans (Janbon *et al.*, 2001).



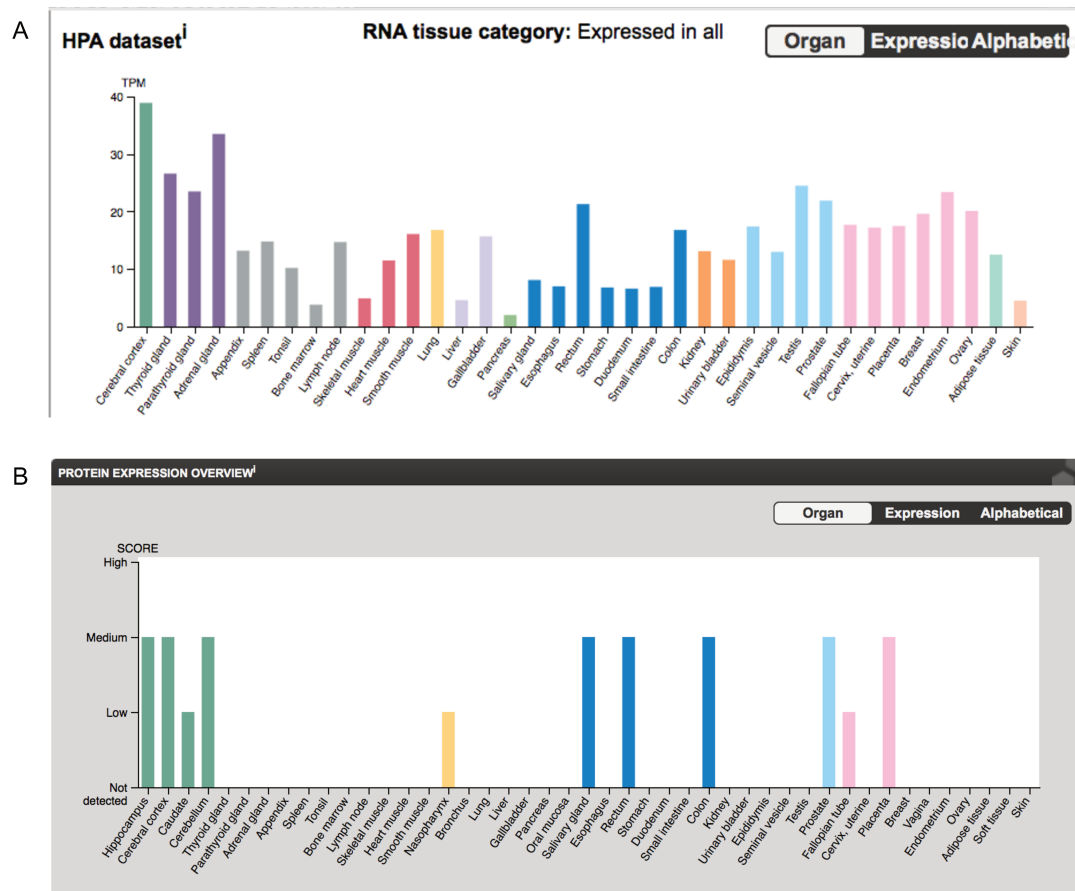
**Figure 11: Organization of *CASD1* gene and protein.**

A- *CASD1* gene organization. *CASD1* is composed by 18 exons on chromosome 7q21.3. B- Homology modeling of *CASD1*. Adapted from Baumann *et al.*, 2015. The overall architecture of the catalytic domain encompassing residues 83-290 AA is represented. The predicted catalytic triad of SNGH domain is highlighted in red in the Golgi lumen.

The human *CASD1* gene consists of 18 exons on chromosome 7q21.3, encoding for 5 transcripts (Figure 11A). The full-length transcripts of 3942 nucleotides encodes for a protein of 792 amino acid (AA) residues composed by a N-terminal serine-glycine-asparagine-histidine (SNGH) hydrolase domain and a transmembrane C-terminal domain. *CASD1* belongs to PFAM family PF13839 : GDSL/SNGH-like acyl-esterase family found in Pmr5 and Cas1p (Anantharaman and Aravind, 2010). Initially described as a protein belonging to SIAE family, *CASD1* engineering experiments on HAP cells suggest that *CASD1* is an *O*-acetyltransferase. In this SGNH-like domain, the predicted catalytical triad corresponds to residues D270, H273 and S94; site-directed mutagenesis experiments have shown that S94 by itself carries the catalytic activity of *CASD1* (Baumann *et al.*, 2015). The homology modeling predicts a multimembrane spanning protein composed by 8 to 13 transmembrane domains located in the Golgi apparatus (Figure 11B). The 4



other transcripts variants encode for truncated and non-functional proteins of 125 AA, 103 AA and 45 AA. CASD1 is the unique potential human SOAT identified so far.

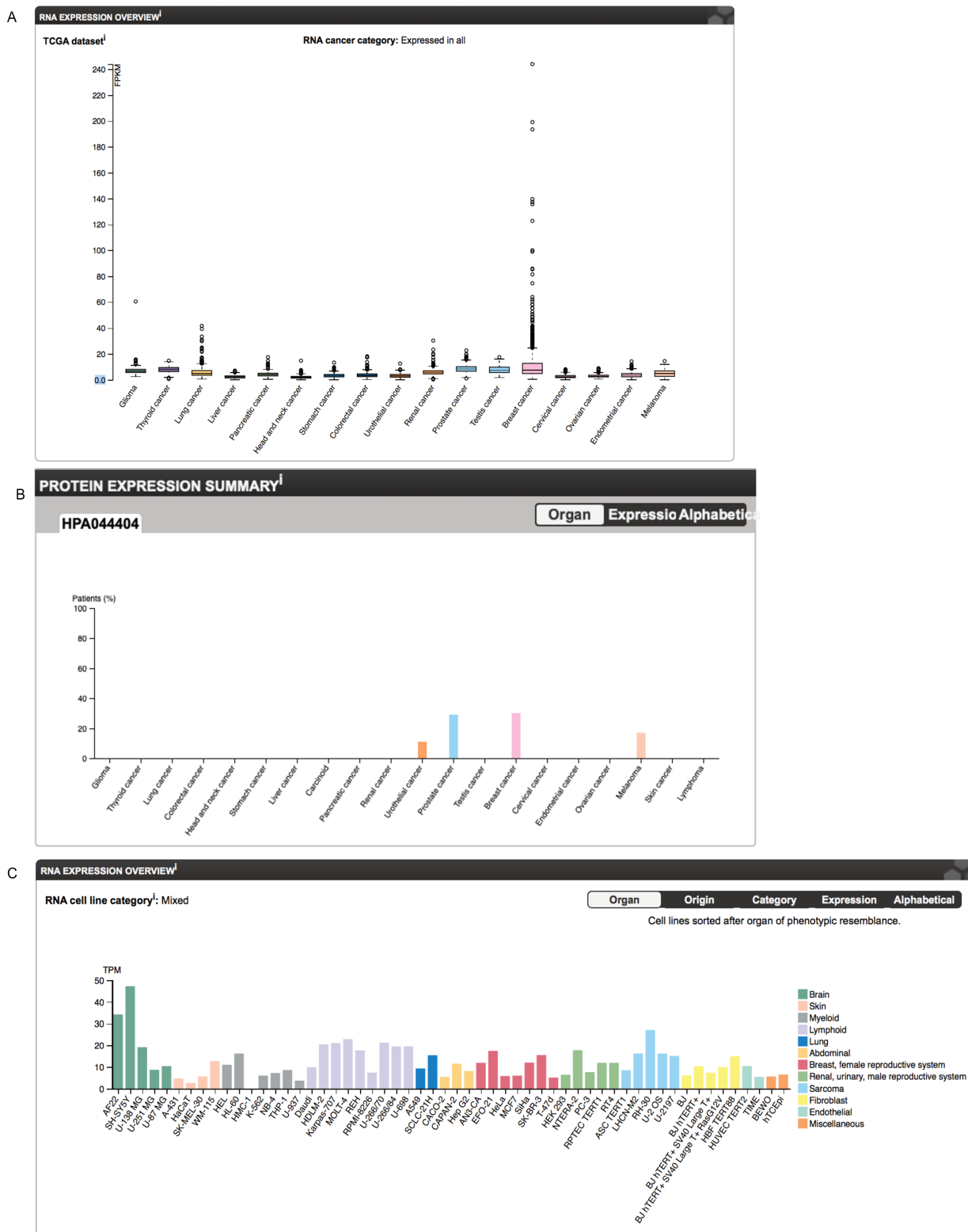


**Figure 12: CASD1 gene expression in healthy tissues according to the Human Protein Atlas.**

A- CASD1 mRNA expression in healthy tissues using HPA dataset. B- CASD1 protein expression analysis in healthy tissues.

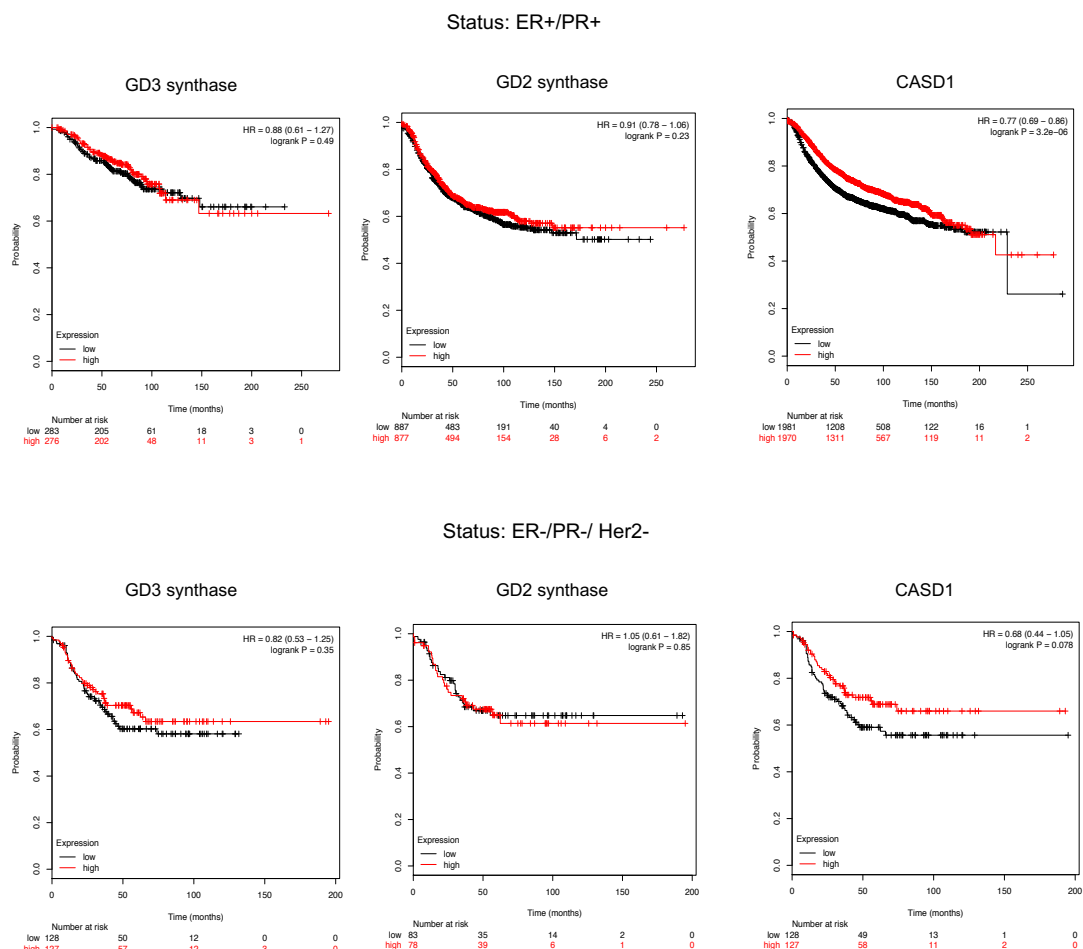
The human protein atlas reveals that *CASD1* is expressed in almost all tissues. The RNA expression dataset shows a ubiquitous expression of *CASD1* in healthy tissues (Figure 12A). The protein expression dataset shows *CASD1* expression in the nervous system, nasopharynx, salivary gland, rectum, colon, prostate, fallopian tube and placenta (Figure 12B). In the same manner, *CASD1* mRNA are widely expressed in cancer tissues and cell lines (Figure 13 A, C), but protein expression is restricted to urothelial cancer, prostate, BC, and melanoma (Figure 13B). Because of this broad expression in healthy and cancer tissues and cells, *CASD1* does not appear to be the key regulatory factor for O-acetylation of glycoconjugates. However, its SOAT activity has to be

clarified, since *in vitro* experiment showed an activity on CMP-Sia rather than GD3 itself, whereas in human haploid cells, CASD1 seems to acetylate GD3.



**Figure 13: CASD1 expression in cancer tissues and cell lines on the Human Protein Atlas.**

A- *CASD1* mRNA expression in cancer tissues using HPA dataset. B-*CASD1* protein expression analysis in cancerous tissues. C- *CASD1* expression in cancer cell lines.



**Figure 14: Kaplan Meier survival plotter in BC patients.**

The database integrates gene expression and clinical data simultaneously. The two patient cohorts are compared by a Kaplan-Meier survival plot, and the hazard ratio with 95% confidence intervals and log rank P value are calculated. GD3 synthase, GD2 synthase, and CASD1 expression are assessed in ER+/PR+ BC patients (upper) and ER-/PR-/Her2- BC patients (bottom). The black line represents the overall survival of patient with a low gene expression. The red line represents the overall survival of BC patients with high gene expression.

The effect of CASD1 expression level in BC patients could be assessed by Kaplan Meier plotter database which integrates gene expression and clinical data simultaneously for evaluating the overall survival of patients according to the level of gene expression. While GD2 synthase and GD3 synthase expression levels do not affect BC patients' overall survival regardless of their ER/PR/Her2 status, CASD1 high expression is associated with a better survival of BC patients having ER-/PR-/Her2- status (Figure 14). Although *O*-acetylation of glycoconjugates is clearly related to tumorigenesis promotion, the role of CASD1 remain unclear.

## STATE OF THE ART

BC is the most prevalent cancer among women. Approximatively 1 in 8 women worldwide have a lifetime risk of developing BC (Rojas and Stuckey, 2016). This is one of the most frequent leading cause of women death worldwide. It develops through a multistep process influenced by environmental and genetic factors (Sun *et al.*, 2017). While early stage diagnosis is successful, metastatic spreading of the cancer represents more than 90% of death (Valastyan and Weinberg, 2011). The expression of di-sialylated gangliosides GD2, the well-described oncofetal marker of NB and melanoma, is highly prevalent in a cohort of BC patients, especially in very aggressive BC subtypes bearing patients (Orsi *et al.*, 2017). The treatment of pediatric NB with dinutuximab antibody shows severe side toxicities due to the expression of GD2 in healthy peripheral nerve fibers. However, the *O*-acetylated form of GD2 is exclusively expressed in cancer tissues, and represents a better therapeutic target than GD2 (Alvarez-Rueda *et al.*, 2011). Thus, targeting *O*AcGD2 in aggressive BC subtypes may represent the best therapeutic solution to reduce relapse and improve patient outcomes. The specific expression of *O*AcGD2 in cancer tissues highlights the specificity of *O*-acetylation mechanisms. This is a simple process consisting in the transfer of an *O*-acetyl group onto an acceptor molecule by a SOAT. However, this mechanism remains unclear since only one SOAT, encoded by *CASD1*, has been identified in human up to now. *CASD1* induces *O*-acetylation of either CMP-Sia or GD3 gangliosides depending on the experimental procedures used (Baumann *et al.*, 2015). Although these studies suggest that *CASD1* is involved in ganglioside *O*-acetylation, its precise activity and function remain controversial, as well as the biosynthesis pathways of gangliosides *O*-acetylation. In order to clarify these points, the aim my PhD project was to study the biosynthesis mechanisms underlying GD2 *O*-acetylation in BC.

## THESIS OBJECTIVES

My PhD thesis aimed at studying the expression and biosynthesis mechanisms of *OAcGD2* antigenicity in BC in order to evaluate the potential therapeutic use of a specific anti-*OAcGD2* antibody developed by OGD2 Pharma company to treat BC patients. In order to achieve this goal, my project objectives were splitted according into fundamental and translational research objectives.

In that way, my fundamental goals were to:

- 1- Establish the expression profile of gangliosides in BC cells
- 2- Decipher of the biosynthesis mechanisms of *OAcGD2* in BC cells
- 3- Study *OAcGD2* biological functions in BC cells
- 4- Identify new genes potentially involved in gangliosides *O*-acetylation

My translational objectives were:

- 1- The identification of the *OAcGD2* antigen
- 2- The quantification of *OAcGD2* in tumor cells

## RESULTS

## PART I: Role of CASD1 in GD2 *O*-acetylation in breast cancer cell lines

### *1-Introduction*

In order to assess the potential role of CASD1 in GD2 *O*-acetylation in SUM159PT BC cell line, the modulation of *CASD1* gene expression by transfection has been performed. SUM 159PT is a triple negative BC cell line derived from anaplastic carcinoma (Neve *et al.*, 2006). Previous works in OGD2 Pharma has led to the identification of a higher expression of *O*AcGD2 in SUM159PT compared to MDA-MB-468, MDA-MB-231 and 4T1 cell lines by flow cytometry. Previous works also showed that 9,4% of SUM159PT cells expressing *O*AcGD2 also express CD44<sup>high</sup>/CD24<sup>low</sup> stem cell markers. Finally, anti-*O*AcGD2 8B6 mAb treatment of SUM159PT cells inhibits their growth (data not shown). Following these preliminary data, SUM159PT has been chosen to assess CASD1 involvement in GD2 *O*-acetylation.

The modulation of *CASD1* expression had been performed in order to deplete or increase *CASD1* gene expression in a transient or stable manner. The effect of CASD1 modulated expression has been assessed by using immunofluorescence and confocal microscopy. Further studies of the biological properties exhibited by selected clones stably overexpressing CASD1 have been performed using MTS tetrazolium and Transwell assay.

### *2-Material and methods*

#### *Antibodies*

The anti-GD2 mAb 14.18 mouse IgG3/κ and the anti-*O*AcGD2 mAb 8B6 mouse IgG3/κ were produced in CHO cells by OGD2 Pharma (Nantes, France). The secondary antibodies Alexa Fluor 488 donkey anti-mouse IgG and Alexa Fluor 546 donkey anti-rabbit IgG were purchased from Invitrogen (Cergy Pontoise, France).

#### *Cell culture*

Cell culture reagents were purchased from Lonza (Verviers, Belgium). The human BC cell SUM159PT was obtained by the American Tissue Culture Collection (ATCC, Rockville, MD, USA).



Cells were routinely grown in monolayer culture and maintained at 37°C in an atmosphere of 5% CO<sub>2</sub>. SUM159PT cells were grown in DMEM/F12 (1:1) containing 5% heat-inactivated fetal calf serum (FCS), 2 mM L-glutamine, 1 µg/ml hydrocortisone and 5 µg/ml insulin.

#### *siRNA transfection*

Depletion of *CASD1* was performed using siRNA strategy by a double transfection. The second transfection was performed 48h after the first one using the same conditions. Cells were grown in six-well plates and transfections were performed with 2µM of siRNA-targeting *CASD1* (L-016926-01-0010, Horizon) or a scramble sequence and 8 µL RNAimax (#137781, Thermo fisher Scientific) in 1 ml of UltraMem (Lonza). After 5h, transfection was stopped by adding 1 ml of DMEM Ham's F12 media supplemented with 5% FCS. Cells were collected at 72h for qPCR and immunocytochemistry experiments.

#### *shRNA transfection*

Stable depletion of *CASD1* was performed using shRNA strategy. Cells were grown in six-well plates and transfection was performed in 500 ng shRNA plasmid targeting-*CASD1* (A236.1b) or a scramble sequence in 4 µL lipofectamine 2000 (Invitrogen). The selection of stable transfectants was performed by adding hygromycin at 500 µg/ml 48h after transfection.

#### *Transfection by CASD1-encoding expression vector*

The plasmid pcDNA3.1-V5-tag-CASD1-cMyc used for the transfection experiments was kindly provided by Dr Mühlenhoff (Hannover University, Germany) (Baumann *et al.*, 2015). Transfection of SUM159PT cells was performed with RNAimax transfection reagent (#137781, Thermo Fisher Scientific). Cells were grown in six-well plates, washed twice with UltraMem and transfected with 2 µg of plasmid DNA and 4 µL of RNAimax in 1 ml of UltraMem (Lonza). After 5h, transfection was stopped by adding 1 ml of DMEM Ham's F12 media supplemented with 5% of FCS. For the selection of stable transfectants, 500 µg/ml of hygromycin was added per well 48h post-transfection. Clones were isolated by limited dilution. Positive clones were selected by qPCR and immunocytochemistry-confocal microscopy experiments.

### *RNA extraction, cDNA synthesis and qPCR*

Gene expression was evaluated using real-time qPCR analysis after RNA extraction and cDNA synthesis. All the processes used for the preparation and analysis were previously described (Cavdarli *et al.*, 2019).

### *Immunocytochemistry and confocal microscopy*

Transfected cells were grown on glass coverslips fixed for 15 min in 4% paraformaldehyde in 0.1 M sodium phosphate buffer. Cells were washed thrice with PBS and membrane permeabilization was performed in 5 µg/ml digitonine in PBS for 20 min. After saturation in blocking buffer, cells were incubated with either with the anti-GD2 or anti-OAcGD2, or anti-V5-tag mAbs at 20 µg/ml for 1h followed by the secondary antibody for 1h. Cells were washed and mounted in fluorescent mounting medium (Dako, Carpinteria, CA, USA). Stained slides were analyzed under a Zeiss LSM 700 confocal microscope. The same settings were used for all of the acquisition so as to ensure the comparability of the data obtained.

### *MTS assay*

Cell growth was analyzed using the MTS reagent (Promega, Charbonnières-les-bains) according to the manufacturer's instructions. Briefly, cells were seeded in 96 well plates in 0%, 1% or 5% FCS containing media in which MTS reagents was added. The proliferation rate was measured by the absorbance of MTS reagent at 490 nm at 24h, 48h, 72h, and 96 h after seeding.

### *Transwell assay*

Migration and invasion properties of cells were measured by transwell assay using migration chambers or invasion chambers (Dutscher, Brumath, France). Cells were seeded in 24 well plates containing either migration or invasion chambers in serum-free media. After 24h incubation at 37°C, cells were fixed 4% paraformaldehyde in 0.1 M sodium phosphate buffer and non-migratory/invasive cells were swabbed with cotton swabs. Nuclei were counterstained with DAPI and membrane were mounted on the slide with fluorescent mounting medium (Dako, Carpinteria, CA, USA). Nuclei were counted under Leica microscope.

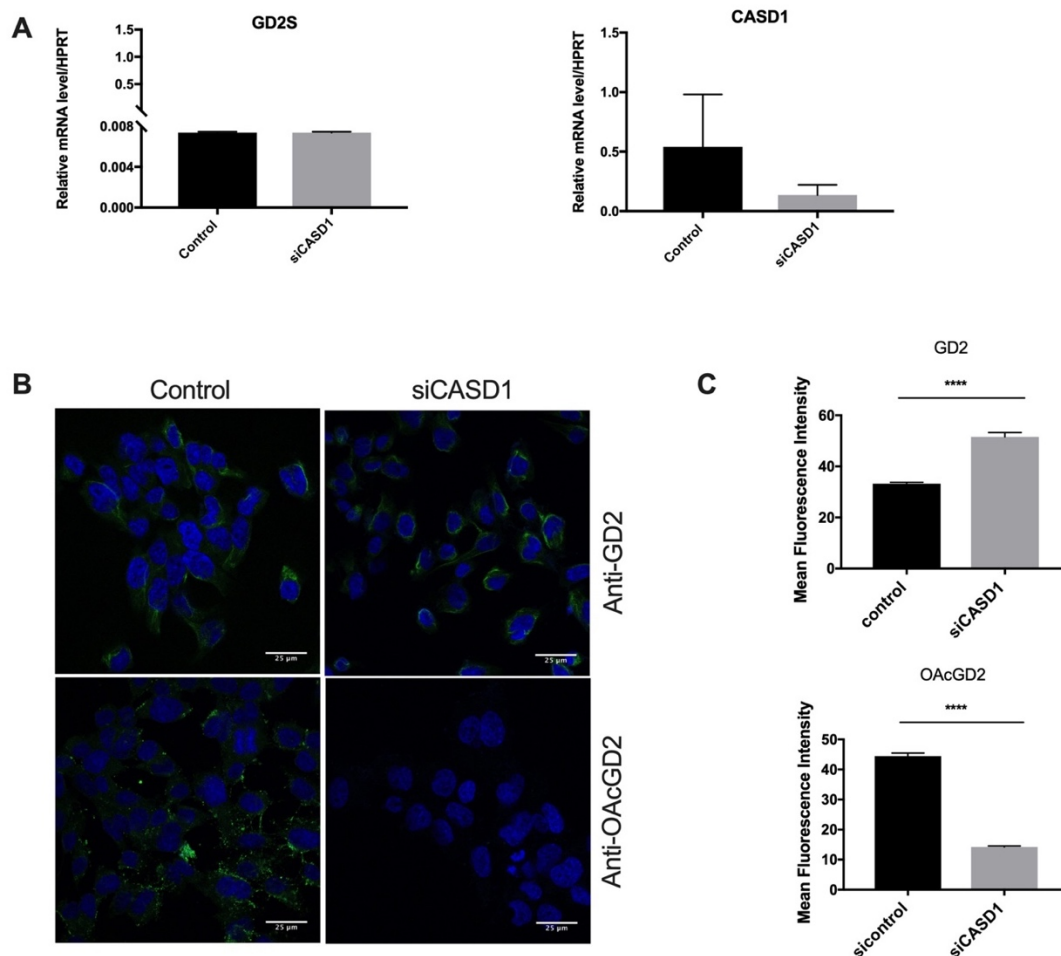
### Statistical analysis

Statistical difference was assessed using unpaired t-test with Welch's correction:

\*\*\*\* $p < 0.0001$ .

## 3-Results

### A-Depletion of *CASD1* expression



**Figure 15: Reduced *OAcGD2* expression in SUM159PT depleted for *CASD1* expression using siRNA strategy.**

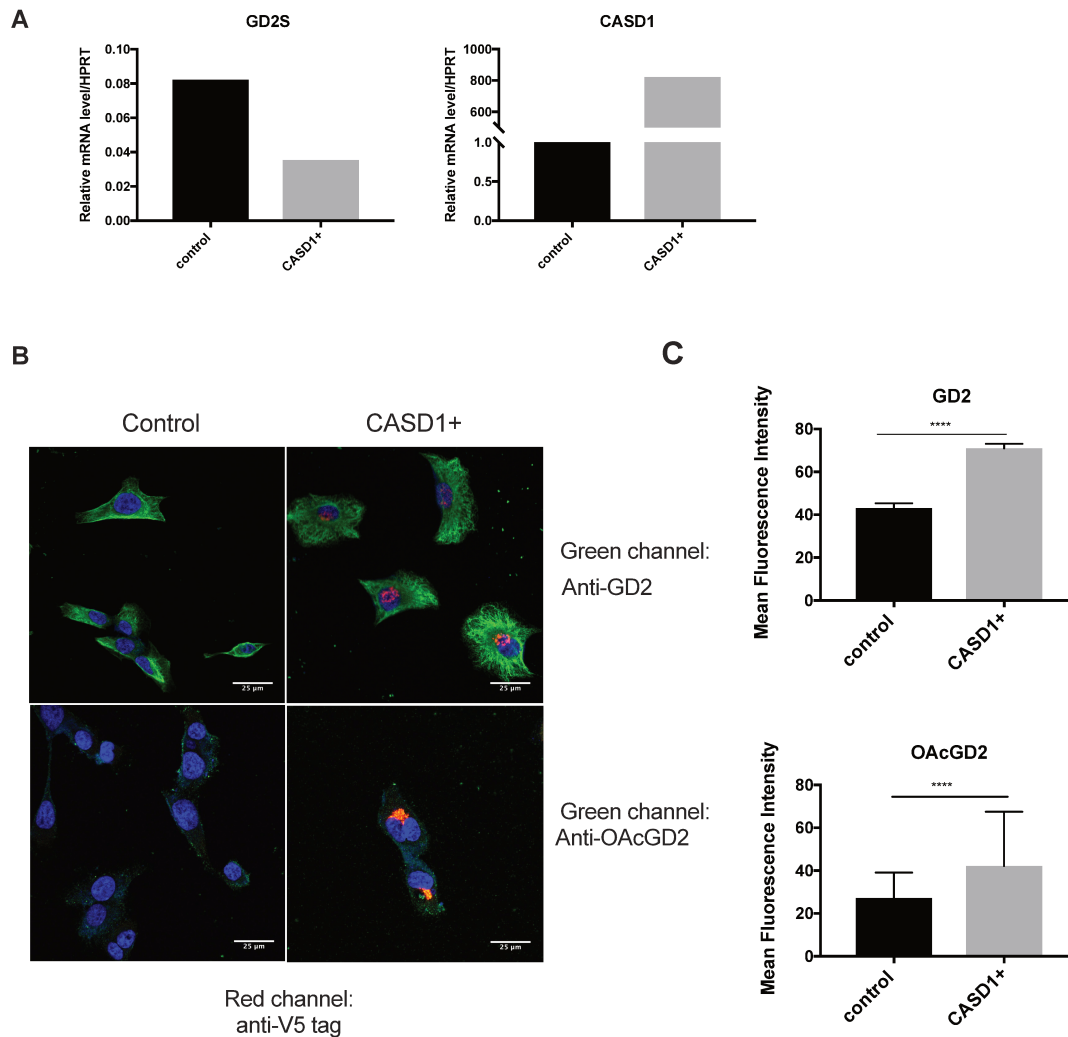
A- qPCR quantification of GD2 synthase and *CASD1* genes in transiently transfected and control SUM159PT cells (n=3). Results were normalized to the expression of *HPRT* mRNA. B-Representative images of the analysis of GD2 and *OAcGD2* expression in BC cells using immunochemistry and confocal microscopy (n=3). Cells were incubated with an anti-GD2 and anti-*OAcGD2* mAbs and gangliosides were visualized using IgG conjugate Alexa Fluor 488. The nuclei were counterstained with DAPI. All images were taken in the same settings. C- Quantification of mean fluorescence intensity of GD2 and *OAcGD2*. \*\*\*\* $p < 0.0001$  Statistical difference using unpaired t-test with Welch's correction.

The depletion of *CASD1* expression in SUM159PT has been performed by transient transfection using siRNA strategy. The expression levels of GD2 synthase (*B4GALNT1*) and *CASD1* genes were determined by qPCR experiments and normalization to hypoxanthine phosphoribosyltransferase (HPRT) gene expression. Transfected cells exhibit a decrease of *CASD1* gene expression up to 50% while *GD2 synthase* gene expression is unchanged compared to control cells (Figure 15A). The effect of *CASD1* depletion on *OAcGD2* expression has been evaluated by immunofluorescence and confocal microscopy experiments and suggest that *OAcGD2* expression is reduced in *CASD1* depleted cells compared to control cells (Figure 15B). The mean fluorescence intensity calculated based on multiple images shows that transfected cells exhibit a 75% of reduced *OAcGD2* expression compared to control cells (Figure 15C). We conclude that a 50% depletion of *CASD1* gene expression leads to a 75% decrease of *OAcGD2* expression in transfected cells compared to SUM159PT control cells. The stable depletion of *CASD1* expression using shRNA strategy has been performed. Nevertheless, transfected cells did not grow after antibiotic passage. Therefore, *CASD1* role in *OAcGD2* expression remains unclear. We next performed overexpression of *CASD1* in SUM159PT cells.

## **B- Transient overexpression of *CASD1* in SUM159PT cells**

Overexpression of *CASD1* in SUM159PT cell has been performed using pcDNA3.1 V5-tag-*CASD1*-cMyc plasmid kindly provided by Dr Mühlenhoff (Medical School Hannover, Germany). In the same way as the siRNA strategy, *CASD1* and *B4GALNT1* (GD2 synthase) gene expression was assessed by qPCR experiments and the effect on *OAcGD2* expression was assessed by immunocytochemistry and confocal microscopy. *CASD1* mRNA expression level increased up to 3000 folds in transfected cells compared to control cell. *B4GALNT1* expression remains unchanged between control and transfected cells (Figure 16A). Representatives images from immunocytochemistry analysis shows the efficiency of transfection using anti-V5-tag antibody in the red channel (to visualize tagged-*CASD1*) and gangliosides expression with either anti-GD2 or anti-*OAcGD2* antibodies in the green channel. *CASD1* transfected cells exhibit an increase of *OAcGD2* and GD2 expression compared to control cells (Figure 16B). Mean fluorescence intensity

quantified for each condition shows that overexpression of *CASD1* increases GD2 and *OAcGD2* expression of 60 % and 55%, respectively (Figure 16C). Similarly to the transient inhibition of *CASD1* gene expression, the transient overexpression of *CASD1* in SUM159PT shows an effect on *OAcGD2* expression. Stable depletion of *CASD1* by shRNA in this cell line remaining unsuccessful, stable overexpression had been considered.

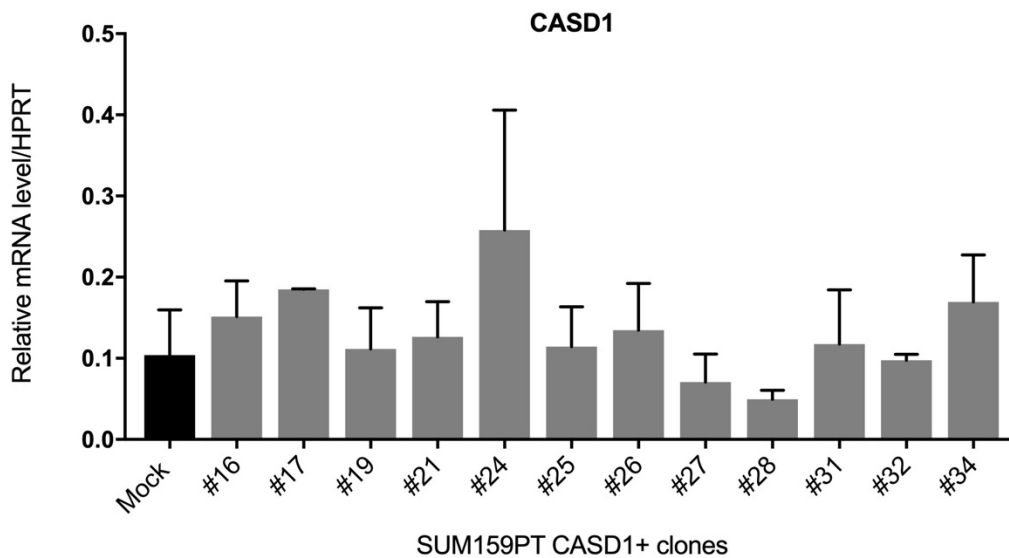


**Figure 16: Increased OAcGD2 expression in CASD1 overexpressing SUM159PT cells using plasmid transfection.**

A-qPCR quantification of *B4GALNT1* (GD2 synthase) and *CASD1* genes in transiently transfected SUM159PT cells (n=3). Results were normalized to the expression of HPRT mRNA. B-Representative images of the analysis of GD2, *OAcGD2* and V5-tag expression in BC cells by immunochemistry and confocal microscopy (n=3). Cells were incubated with anti-V5-tag and either anti-GD2 or anti-*OAcGD2* mAbs. Gangliosides were visualized using IgG conjugated-Alexa Fluor 488 and V5-tag using IgG conjugated-Alexa Fluor 546. The nuclei were counterstained with DAPI. All images were taken in the same settings. C- Quantification of mean fluorescence intensity of GD2 and *OAcGD2*. \*\*\*\*p<0.0001 Statistical difference using unpaired t-test with Welch's correction.

### C- Effect of stable CASD1 overexpression in SUM159PT cells

Stable transfectants overexpressing *CASD1* (SUM159PT CASD1+) have been produced using the plasmid pcDNA3.1 V5-tag-CASD1-cMyc and clones were isolated after antibiotic passage and limited dilutions. From the 28 clones pre-selected, 12 clones were maintained during proliferation monitoring. *CASD1* expression level in these isolated clones was assessed by qPCR experiments showing up to 2-fold overexpression of *CASD1* in CASD1+ clones compare to controls (Figure 17).



**Figure 17: *CASD1* expression in SUM159PT CASD1+ clones after stable transfection.**

qPCR quantification of *CASD1* gene expression in stably transfected and control SUM159PT cells (n=3). Results were normalized to HPRT mRNA expression.

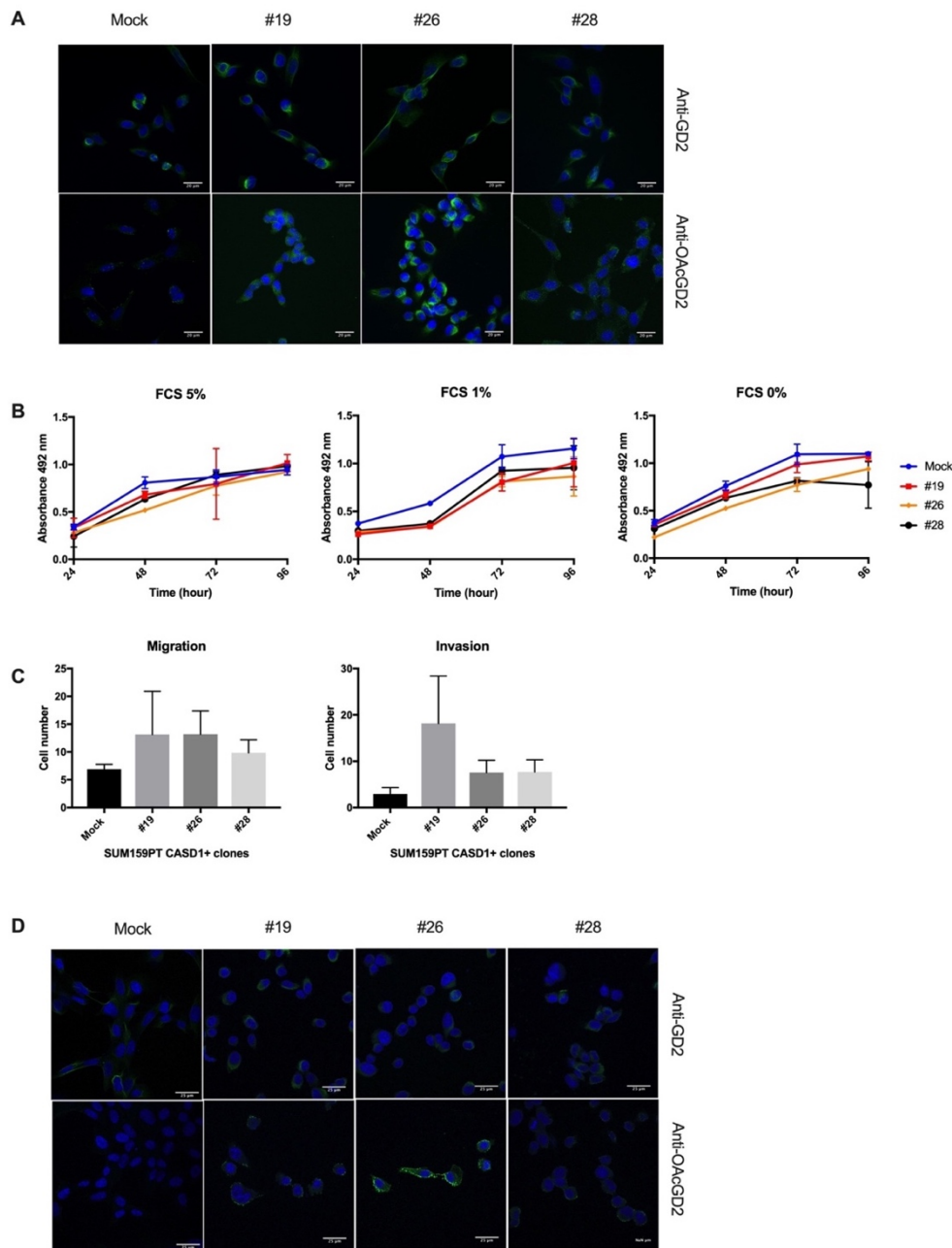
Selection of CASD1+ clones among the 12 clones isolated has been performed by the analysis of GD2 and *O*AcGD2 expression using immunocytochemistry and confocal microscopy. CASD1+ clones exhibiting higher *CASD1* gene expression and *O*AcGD2 ganglioside expression have been chosen. Thus, the following 3 clones have been selected for further analysis: #19, #26, and #28 (Figure 17 & 18A). Biological properties of these clones were studied by MTS and Transwell assays, so as to respectively assess their proliferation and migration/invasion capabilities. While CASD1+ clones did not exhibit differential growth properties compared to their control

counterpart regardless of FCS composition in media (Figure 18B), they had increased migration and invasion capabilities in serum free media (Figure 18C). The migration capabilities of CASD1+ clones increased twice compared to their control counterpart. The invasion activity of clones #26 and #28 was doubled compared to control while this activity increased up to 10 folds in clone #19 compared to control (Figure 18C). Nevertheless, CASD1+ clones maintained in culture lost the expression of GD2 and OAcGD2 two months after selection and did not allow further experiments (Figure 18D).

#### *4-Discussion & Conclusion*

The modulation of *CASD1* expression using transfection strategies provides interesting results concerning the potential role of *CASD1* in *O*-acetylated gangliosides synthesis. Indeed, transient depletion or overexpression of *CASD1* induces variations of *OAcGD2* expression in SUM159PT cells compared to their control counterpart. However, stable inhibition of *CASD1* by shRNA strategy or stable overexpression have not been as informative as transient transfections. In the first case, cells transfected with shRNA targeting-*CASD1* did not proliferate and underwent apoptosis. In the second case of stable overexpression, the expression of *CASD1* measured in transfected cells was slightly increased and led to the selection of 3 clones with increased migration and invasion capabilities. Nevertheless, *OAcGD2*, GD2 and *CASD1* expression were lost in these selected clones maintained after 2 months of culture. Since the expression of *CASD1* in transfected SUM159PT clones is not stable, their biological properties are debatable, and still the role of *CASD1* in GD2 *O*-acetylation remains obscure. As a consequence, the structural characterization of *OAcGD2* expressed by other BC cell lines is required and constitutes the next part of this project.





**Figure 18: Biological properties of selected SUM159PT CASD1+ clones.**

A and D- Representatives images from the analysis of GD2 and OAcGD2 expression by immunocytochemistry and confocal microscopy in stably transfected and control SUM159PT cells selected by limited dilution. Cells were incubated either with anti-GD2 or anti-OAcGD2 mAbs and gangliosides were visualized using IgG-conjugated Alexa 488. The nuclei were counterstained with DAPI. All images were taken in the same settings. A- Images were taken right after the selection of clones by limited dilution. D- Images were taken 2 months after the selection of clones by limited dilution. B- Control, SUM159PT CASD1+ #19, #26, #28 clones growth was assessed after 0, 24h, 48h, 72h and 96h using MTS reagent (Promega) in media containing 0%, 1% or 5% of fetal calf serum (FCS). C- The migration and invasion capabilities of control and SUM159PT CASD1+ clones #19, #26, #28 clones migration and invasion capabilities were assessed after 48h by Transwell assay in serum free media.

## PART II: Identification of 9-*O*-Acetyl-N-Acetylneuraminic acid as the main *O*-acetylated sialic acid species of GD2 in breast cancer cells.

In this part, we focused on the characterization and expression of disialogangliosides GD3, GD2 and their *O*-acetylated forms expression in BC cell lines. We used SUM159PT, Hs 578T native cell lines, MDA-MB-231, MCF-7 and their GD3 synthase overexpressing clones. The expression of glycosyltransferases genes involved in gangliosides biosynthesis has been studied by qPCR experiments. Immunodetection experiments allowed the identification of gangliosides of interest by FACS or immunocytochemistry and confocal microscopy. The identification and quantification of *O*-acetylated gangliosides remaining challenging due to the lability of the *O*-acetyl modification, we used of DMB labeled sialic acid and LC-MS to bypass these difficulties. Sialic acids have been released from total gangliosides extracted by cells and then derivatized to DMB before being injected to LC-MS for DMB-Sia derivatives analyses. This approach allows the identification of 9-*O*-acetylated sialic acid as the main acetylated species express among gangliosides extracted from BC cells. Results obtained have been published in January 2019 in *Glycoconjugate Journal*.



# Identification of 9-O-acetyl-N-acetylneuraminic acid (Neu5,9Ac<sub>2</sub>) as main O-acetylated sialic acid species of GD2 in breast cancer cells

Sumeyye Cavdarli<sup>1,2</sup> · Justine H. Dewald<sup>1</sup> · Nao Yamakawa<sup>1</sup> · Yann Guérardel<sup>1</sup> · Mickaël Terme<sup>2</sup> · Jean-Marc Le Doussal<sup>2</sup> · Philippe Delannoy<sup>1</sup> · Sophie Groux-Degroote<sup>1</sup>

Received: 4 September 2018 / Revised: 18 December 2018 / Accepted: 20 December 2018  
© Springer Science+Business Media, LLC, part of Springer Nature 2019

## Abstract

Mainly restricted to the nervous system in healthy adults, complex gangliosides such as GD3 and GD2 have been shown to be involved in aggressiveness and metastasis of neuro-ectoderm derived tumors such as melanoma and neuroblastoma. Interestingly, *O*-acetylated forms of GD2, not expressed in human peripheral nerve fibers, are highly expressed in GD2+ tumor cells. Very little information is known regarding the expression of *O*-acetylated disialogangliosides in breast cancer (BC) cell lines. Here, we analyzed the expression of GD2, GD3 and their *O*-acetylated forms *O*-acetyl-GD2 (*O*AcGD2) and *O*-acetyl-GD3 (*O*AcGD3) in BC cells. We used Hs 578T and SUM159PT cell lines, as well as cell clones over-expressing GD3 synthase derived from MDA-MB-231 and MCF-7. Using flow cytometry and immunocytochemistry/confocal microscopy, we report that BC cells express b-series gangliosides GD3 and GD2, as well as significant amounts of *O*AcGD2. However, *O*AcGD3 expression was not detected in these cells. *O*-acetylation of gangliosides isolated from BC cells was examined by LC-MS analysis of sialic acid DMB-derivatives. We report that the main acetylated form of sialic acid expressed in BC gangliosides is 9-*O*-acetyl-N-acetylneuraminic acid (Neu5,9Ac<sub>2</sub>). These results highlight a close interrelationship between Neu5,9Ac<sub>2</sub> and *O*AcGD2 expression, and suggest that *O*AcGD2 is synthesized from GD2 and not from *O*AcGD3 in BC cells.

**Keywords** Breast Cancer · Gangliosides · Antibody · GD2 · *O*-acetyl-GD2 · Sialic acid

## Introduction

Gangliosides are glycosphingolipids carrying one or several sialic acid residues, and are essential compounds of the plasma membrane with their sialylated sugar chains protruding out of cells. They are enriched together with phospholipids and cholesterol in lipid microdomains named “glycosynapses”, where they can modulate cell signaling, leading to changes in cellular phenotypes [1]. The pattern of gangliosides expression depends on numerous genes encoding glycosyltransferases (GT), transporters or even degradation enzymes such as sialidases. Gangliosides are synthesized from lactosylceramide (LacCer), and four series have been defined

(0-, a-, b- and c-) depending on the number of sialic acid (N-acetylneuraminic acid, Neu5Ac) residues (0 to 3) linked on the LacCer backbone. The precursor structures of each series can be further elongated by the sequential addition of other sugar residues such as N-acetylgalactosamine (GalNAc), galactose (Gal), and sialic acid, by specific GT (Fig. 1). Normal adult tissues usually express 0- and a-series gangliosides, whereas the expression of gangliosides from b- and c-series plays important roles during embryogenesis and is restricted to the central nervous system in healthy adults. Hakomori and coworkers demonstrated that the expression of gangliosides is affected in various ways by malignant transformation [1]. Complex gangliosides are over-expressed and considered as tumor-associated carbohydrate antigens (TACAs) in human neuro-ectodermal tumors such as melanoma, glioblastoma and neuroblastoma, promoting tumor aggressiveness [1, 2]. As a consequence, disialogangliosides have been used as target molecules for cancer immunotherapy, such as GD2 in neuroblastoma [3]. Recently, dinutuximab (Unituxin<sup>TM</sup>), an anti-GD2 antibody, has been approved by the Food Drug Administration and the European Medicines Agency for

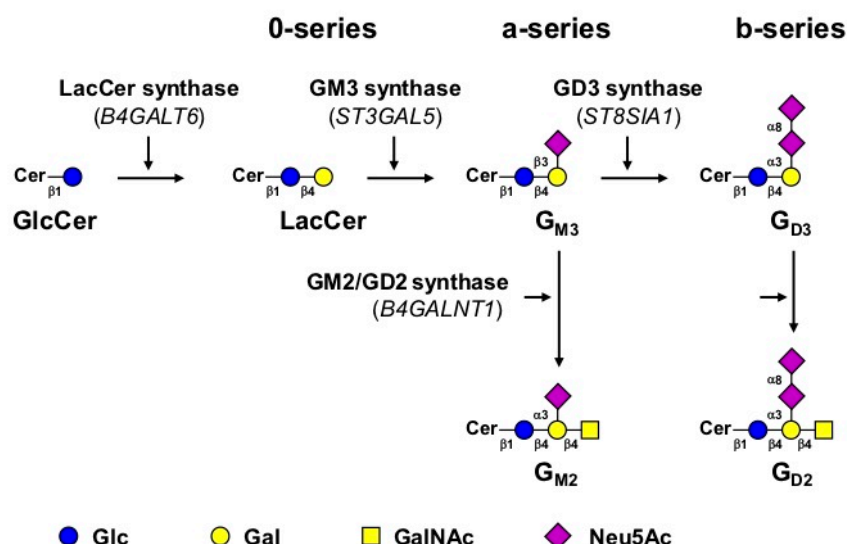
✉ Sophie Groux-Degroote  
sophie.groux-degroote@univ-lille.fr

<sup>1</sup> CNRS, UMR 8576 - UGSF - Unité de Glycobiologie Structurale et Fonctionnelle, University Lille, F-59000 Lille, France

<sup>2</sup> OGD2 Pharma, Institut de Recherche en Santé de l'Université de Nantes, 44007 Nantes, France



**Fig. 1** Biosynthesis pathways for b-series GD2 and GD3 gangliosides. Gangliosides are synthesized by stepwise addition of monosaccharides to lactosylceramide (LacCer). The action of the GM3 synthase (encoded by *ST3GAL5*) and GD3 synthase (*ST8SIA1*) leads to the biosynthesis of the precursors of a-, b-series gangliosides, respectively. Elongation is performed by the sequential action of GM2/GD2 synthase (*B4GALNT1*) to make GM2 from GM3 or GD2 from GD3. The names of corresponding genes are indicated into brackets



neuroblastoma therapy but complement activation on GD2 expressing nerves limits the use of this immunotherapy [4]. Interestingly, unlike GD2, *O*-acetylated derivatives of GD2 are highly expressed by GD2 positive tumor cells but are not found in human peripheral nerve fibers [5]. *O*-acetylated gangliosides are expressed in fetal tissues, especially in central nervous system but decreased in healthy adult tissues. They are also found in tumor tissues and are often associated with tumor aggressiveness. For example, 9-*O*-acetylation of GD3 blocks the pro-apoptotic activity of GD3 and promotes the survival of tumor cells [6]. In the same manner, in acute lymphoblastic leukemia, survival and resistance to treatment of malignant lymphoblasts depends on GD3 *O*-acetylation [7]. We have a long time interest in studying the mechanisms involved in sialylated TACAs over-expression in breast cancer, as well as their pathological consequences [8]. In normal breast tissues, complex gangliosides are absent or expressed at very low levels. However, total amount of lipid-bound sialic acid is significantly higher in breast tumor tissues than in normal mammary tissues, and GD3 and 9-*O*-acetylated GD3 were proposed as oncofetal markers in invasive ductal breast carcinoma [9]. Clinical studies have also shown that high expression of the gene encoding GD3 synthase (GD3S, encoded by *ST8SIA1*) is associated with Estrogen Receptor (ER) negativity and high histological grade of breast tumors [10]. The expression of the GD3S and complex gangliosides in BC cells results in the acquisition of higher proliferative capacity of tumor cells in the absence of growth factors [11]. GD3S expressing cells bypass the need of growth factors by a specific and constitutive activation of c-Met receptor and activation of PI3K/Akt and Erk/MAPK pathways [11, 12]. GD3S expression also enhanced tumor growth in SCID mice, and a higher expression of *ST8SIA1* in “basal-like” subtype of human breast tumors is also observed [12]. The decrease of GD2 expression by silencing of the GM2/GD2 synthase or

competition assays using anti-GD2 mAbs reversed the proliferative phenotype as well as c-Met phosphorylation [13] demonstrating the involvement of GD2 in breast cancer cell proliferation via the constitutive activation of c-Met. However, the expression and the role of ganglioside acetylation have never been analyzed in breast cancer. Sialic acid *O*-acetylation on gangliosides can occur at the hydroxyl groups of C4, C7, C8 and C9, although C9 seems to be the preferential position. The *O*-acetylation of sialic acids further increases their complexity, and are involved in the fine regulation of their multiple biological functions [14]. Sialic acid *O*-acetylation on gangliosides could therefore modulate the malignant properties of breast cancer cells.

The biosynthesis of *O*-acetylated sialic acids involves sialate *O*-acetyltransferases (SOAT) that transfer an acetyl group from acetyl-coenzyme A onto the C4/C7/C8/C9 positions of sialic acids at the terminal position of sialylated glycoconjugates. However, a recent study by Baumann and co-workers suggests that the potential and unique SOAT characterized so far, CASD1, would act on the activated sialic acid donor, CMP-Neu5Ac, and not on the sialylated glycolipid itself [15]. The detection and analysis of *O*-acetylated gangliosides are challenging and difficult to achieve using classical purification or immunological procedures. Preparation of gangliosides involves a mild alkaline hydrolysis of glycerophospholipids, but this procedure will also result in the loss of all *O*-acetyl groups on sialic acids. Lectins have been also used for detection of *O*-acetylated sialic acids on glycoconjugates [16–20]. For the study of acetylated gangliosides, several monoclonal antibodies (mAb) are available and can be used for their immunodetection, using techniques such as flow cytometry, immuno-high performance thin layer chromatography, and immunocytochemistry/microscopy [21]. However, the fine specificity of these antibodies is not well-defined and does not allow to precisely determine the



position(s) of the acetyl group(s) on sialic acids. MAbs 8B6 and 7H2 were reported to specifically recognize *O*AcGD2 and *O*AcGD3, respectively, but the complete structural analysis required to define the *O*-acetylation position(s) on these sialylated antigens is not achieved yet [22].

In this study, we analyzed the *O*-acetylation of sialic acids on glycolipids, using mAbs 8B6 and 7H2, in two breast cancer (BC) cells known to express high levels of disialogangliosides GD2 or GD3. We used Hs 578T and SUM159PT BC cells. We also used MDA-MB-231 and MCF-7 clones stably transfected with GD3S and expressing high levels of both GD2 and GD3 [11, 23]. In parallel, we analyzed the *O*-acetylated sialic acids using DMB-derivation and Liquid Chromatography/Mass spectrometry (LC/ESI-MS) present in gangliosides from BC cells. Our results indicate that 9-*O*-acetyl-N-acetylneuraminic acid (Neu5,9Ac<sub>2</sub>) is the main form of glycolipid-linked acetylated sialic acid in BC cells, in connection with *O*AcGD2 expression.

## Material and methods

### Antibodies

Anti-GD3 R24 mouse IgG3 was purchased from Abcam (Cambridge, MA, USA). The anti-*O*AcGD3 7H2 mouse IgG3 was purchased from Santa-Cruz biotechnology (Dallas, Texas, USA). The anti-GD2 14.18 mouse IgG3 and the anti-*O*AcGD2 8B6 mouse IgG3 were produced in CHO cells by OGD2 Pharma (Nantes, France). The secondary antibody Alexa Fluor 488<sup>®</sup> donkey anti-mouse IgG was purchased from Invitrogen (Cergy Pontoise, France).

### Cell culture

Cell culture reagents were purchased from Lonza (Verviers, Belgium). The human melanoma cells SK-MEL-28, the human breast cancer cell line Hs578T and SUM159PT were obtained by the American Tissue Culture Collection (ATCC, Rockville, MD, USA). MDA-MB-231 GD3S+ clone, as well as MCF-7 GD3S+ clone were obtained as previously described [11]. Cells were routinely grown in monolayer culture and maintained at 37 °C in an atmosphere of 5% CO<sub>2</sub>. SK-MEL-28, Hs 578T, MDA-MB-231 and MCF-7 cells were grown in Dulbecco's modified Eagle's medium (DMEM) supplemented with 10% heat-inactivated fetal calf serum, 2 mmol/L L-glutamine and 100 units/mL penicillin-streptomycin. SUM159PT cells were grown in DMEM/F12 (1:1) containing 5% heat-inactivated fetal calf serum, 2 mM L-glutamine, 100 units/mL penicillin-streptomycin, 1 µg/ml hydrocortisone and 5 µg/ml insulin.

### RNA extraction, cDNA synthesis and quantitative real-time polymerase chain reaction (qPCR)

Total RNA was extracted from the different cell lines using the Nucleospin RNA II kit (Macherey-Nagel, Düren, Germany). The amount of extracted RNA was quantified using a DeNovix DS-11 spectrophotometer (DeNovix Inc., Wilmington, DE, USA) and the purity of the RNA was checked by the ratio of the absorbance at 260 and at 280 nm. Total RNA was subjected to reverse transcription using the Maxima First Strand cDNA Synthesis Kit (ThermoFisher Scientific, Villeneuve d'Ascq, France) according to the protocol provided by the manufacturer. The oligonucleotide sequences (Eurogentec, Seraing, Belgium) used as primers for the PCR reactions are given in Table 1. qPCR and subsequent data analysis were performed using the Mx3005p Quantitative System (Stratagene, La Jolla, CA, USA). PCR reaction (25 µL) contained 12.5 µL of the 2X Brilliant SYBR Green qPCR Mastermix (Thermo Fischer Scientific, Rockford, USA), 300 nM of primers and 4 µL of cDNA (1:40). DNA amplification was performed with the following thermal cycling profile: initial denaturation at 94 °C for 10 min, 40 cycles of amplification (denaturation at 94 °C for 30 s, annealing at T<sub>m</sub> for 30 s, and extension at 72 °C for 30 s) and a final extension at 72 °C for 5 min. Hypoxanthine-guanine PhosphoRibosylTransferase (HPRT) gene was used to normalize the expression of genes of interest [13]. The fluorescence monitoring occurred at the end of each cycle. The analysis of amplification was performed using the Mx3005p software. For each primer pair, the specificity of the amplification was checked by recording the dissociation curves. The efficiency of amplification was checked by serial dilutions of cDNA from SK-MEL-28 cells and was between 97 and 102%. All experiments were performed in triplicate. The quantification was performed by the method described by Pfaffl [24].

**Table 1** Primer pairs used for qPCR experiments

Genes	Probes 5' 3'	T <sub>m</sub>	Slope
<i>HPRT</i>	GCC AGA CTT TGT TGG ATT TG CTC TCA TCT TAG GCT TTG TAT TTT	58 °C	-3343
<i>CASDI</i>	GTG GAT TTT CTG TGG CAT CC AAG CGC TTC ACT GCT ACC AT	60 °C	-3304
<i>B4GALT6</i>	GCG ATT ACG GAA AGG AAT GA TCA TTG GAG GCC AAA AGA CT	60 °C	-3503
<i>ST3GAL5</i>	TTC ATA GCA GCC ATG CAT TGA ATC GGT GTC ATT GCC GCC GTT GT	60 °C	-3312
<i>ST8SIAI</i>	GCG ATG CAA TCT CCC TCC T TTC CCG AAT TATGCT GGG AT	60 °C	-3440
<i>B4GALNT1</i>	CAG CGC TCT AGT CACGAT TGC CCA CGG TAA CCG TTG GGT AG	51 °C	-3371



## Flow cytometry analysis

Analysis of cell surface gangliosides was performed by indirect immunofluorescence measured by flow cytometry. Cells were incubated with either anti-OAcGD2 8B6 (20 µg/mL), or anti-GD2 14.18 (20 µg/mL), or anti-GD3 R24 (4 µg/mL) or anti-OAcGD3 7H2 (10 µg/mL) mAbs for 30 min at 4 °C. Antibody binding was detected by incubation with secondary antibody for 30 min at 4 °C. Cell fluorescence was analyzed using a FACScalibur flow cytometer from Beckton Dickinson (Le Pont-de-Claix, France) and Cell QuestPro Software (BD Biosciences). Relative fluorescence intensities of 10,000 cells were recorded as histograms. The mean fluorescence value was calculated for each histogram. Results were expressed as the mean fluorescence intensity, which was calculated by dividing the mean fluorescence value for cells stained with antigen specific antibody by the mean fluorescence value of cells stained with secondary antibody.

## Immunocytochemistry and confocal microscopy

Cells were grown on glass coverslips, washed once with PBS, and fixed by incubation in 4% paraformaldehyde in 0.1 M sodium phosphate buffer for 15 min at room temperature. The coverslips were washed with PBS. Membrane permeabilization was performed with 0.1% (v/v) Triton X-100 in PBS for 20 min at room temperature. The cells were incubated with either anti-OAcGD2 8B6 mAb or anti-GD2 14.18 mAb at 20 µg/mL for 1 h followed by the incubation with secondary antibody for 1 h. Cells were then washed under PBS and mounted in Fluorescent Mounting medium (Dako, Carpinteria, CA, USA). Stained slides were examined under a Zeiss LSM 700 confocal microscope. The image acquisition characteristics were the same throughout the different experiments and conditions to ensure the comparability of the results and fluorescence levels.

## Extraction of glycoconjugates

Cells were suspended in PBS and centrifuged 15 min at 4000 rpm. Pellets were sequentially extracted twice by 1 volume of CHCl<sub>3</sub>/CH<sub>3</sub>OH mixture 2:1 (v/v) and 1 volume of CHCl<sub>3</sub>/CH<sub>3</sub>OH/H<sub>2</sub>O mixture 1:2:0.8 (v/v/v). Supernatants were collected and dried gently under N<sub>2</sub> stream.

## DMB derivatization of sialic acids

Dried glycoconjugate extracted from BC cell lines were hydrolyzed at 80 °C for 4 h in 4 M propionic acid. Hydrolyzed sialic acids were subsequently coupled to 1,2-diamino-4,5-methylene-dioxybenzene dihydrochloride (DMB). Samples were heated at 50 °C for 2 h in the dark in 7 mM DMB, 1 M β-mercaptoethanol, 18 mM sodium hydrosulfite in

5 mM acetic acid [25]. Sialic acids coupled to DMB (DMB-Sia) were then analyzed by LC/ESI-MS.

## Quantitation analysis of DMB-Sia on micro-LC/ESI-MS3

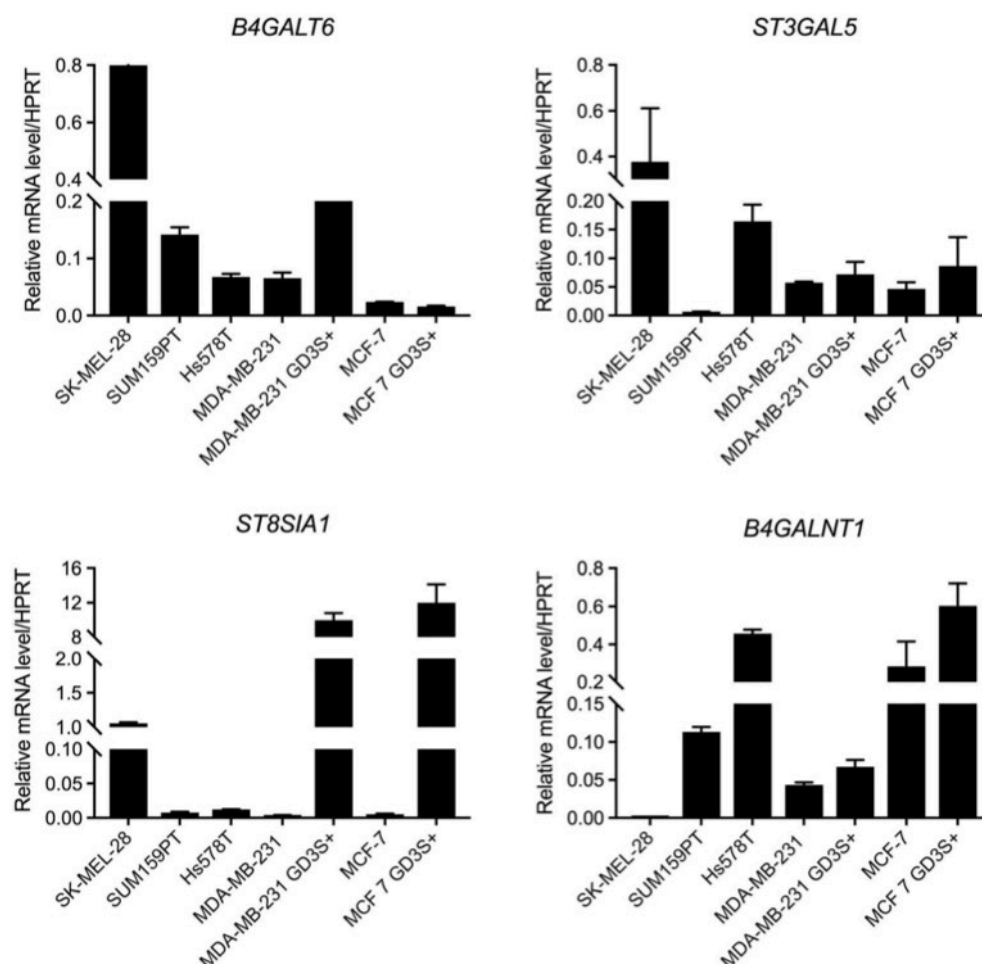
Quantitative analyses were performed in positive ion mode on an amaZon speed ETD ion trap mass spectrometer equipped with the standard electrospray ionization (ESI) ion source and controlled by Hystar 3.2 software (Bruker Daltonics). DMB-coupled sialic acid separation was achieved on micro LC system (Prominence LC-20AB, Shimadzu, Kyoto, Japan). 5 µL of samples were applied to the reversed-phase Luna C18-2 column (150 × 1.00 mm, 3 µm particles, Phenomenex) with an isocratic elution of CH<sub>3</sub>CN/CH<sub>3</sub>OH/H<sub>2</sub>O (6:4:90, v/v/v) at a flow rate of 70 µL/min. The targeted MS3 scans for DMB-coupled sialic acid were performed using an ultrascan mode (26,000 amu/s). Data obtained for external standards run on the same time were used for estimation of DMB-Sia amounts in our BC cell lines samples. Sialic acid species were identified by referring to elution positions and MS3 fragmentation of Neu5Ac and Neu5,9Ac<sub>2</sub> standards. The reported values were based on signal area of the single ion chromatogram at the appropriate retention time [26].

## Results

### GM2/GD2S expression is ubiquitous among breast cancer cells

We performed qPCR experiments in order to determine the expression of the glycosyltransferase genes involved in GD3 and GD2 biosynthesis: *B4GALT6* (encoding LacCer synthase), *ST3GAL5* (encoding GM3 synthase), *ST8SIA1* (encoding GD3 synthase) and *B4GALNT1* (encoding GM2-GD2 synthase), in different breast cancer cells (SUM159PT, Hs 578T, MDA-MB-231 and MCF-7 cells) described to express various amounts of b-series gangliosides. In particular, we used 2 cell clones deriving from MDA-MB-231 (MDA-MB-231 GD3S+) and MCF-7 (MCF-7 GD3S+) that express high level of b-series gangliosides [11, 23]. SK-MEL-28 melanoma cells were also used as control. The mRNA levels for each glycosyltransferase were normalized to the expression of hypoxanthine phosphoribosyltransferase (HPRT) mRNA. The results presented in Fig. 2 indicate that LacCer synthase and GM3 synthase exhibit a low level expression in BC cell lines compared to SK-MEL-28. The highest expression of LacCer synthase was observed in MDA-MB-231 and the lowest in MCF-7 cells. The highest GM3 synthase mRNA level was detected in Hs 578T and the lowest to SUM159PT. In the other hand, we confirmed a high expression level of GD3S in MDA-MB-231 and MCF-7 clones over-expressing GD3S. A

**Fig. 2** Quantitative real-time PCR quantification of glycosyltransferase involved in GD2 biosynthesis. *B4GALT6*, *ST3GAL5*, *ST8SIA1*, and *B4GALNT1* mRNA expression was determined by RT-qPCR in BC cell lines. Results were normalized to the expression of *HPRT* mRNA. The quantification was performed by the method described by Pfaffl [24]. SK-MEL-28 were used as a control. Each bar represents the mean  $\pm$  SD of  $n = 3$  experiments



lower expression level of GD3S was detected in SK-MEL-28, and GD3S expression was not detected in SUM159PT and Hs 578T. In contrast to GD3S, GM2-GD2S expression was detected in all BC cell lines but not in SK-MEL-28. The expression level was high in Hs 578T and MCF-7, and lower in SUM159PT and MDA-MB-231 (Fig. 2).

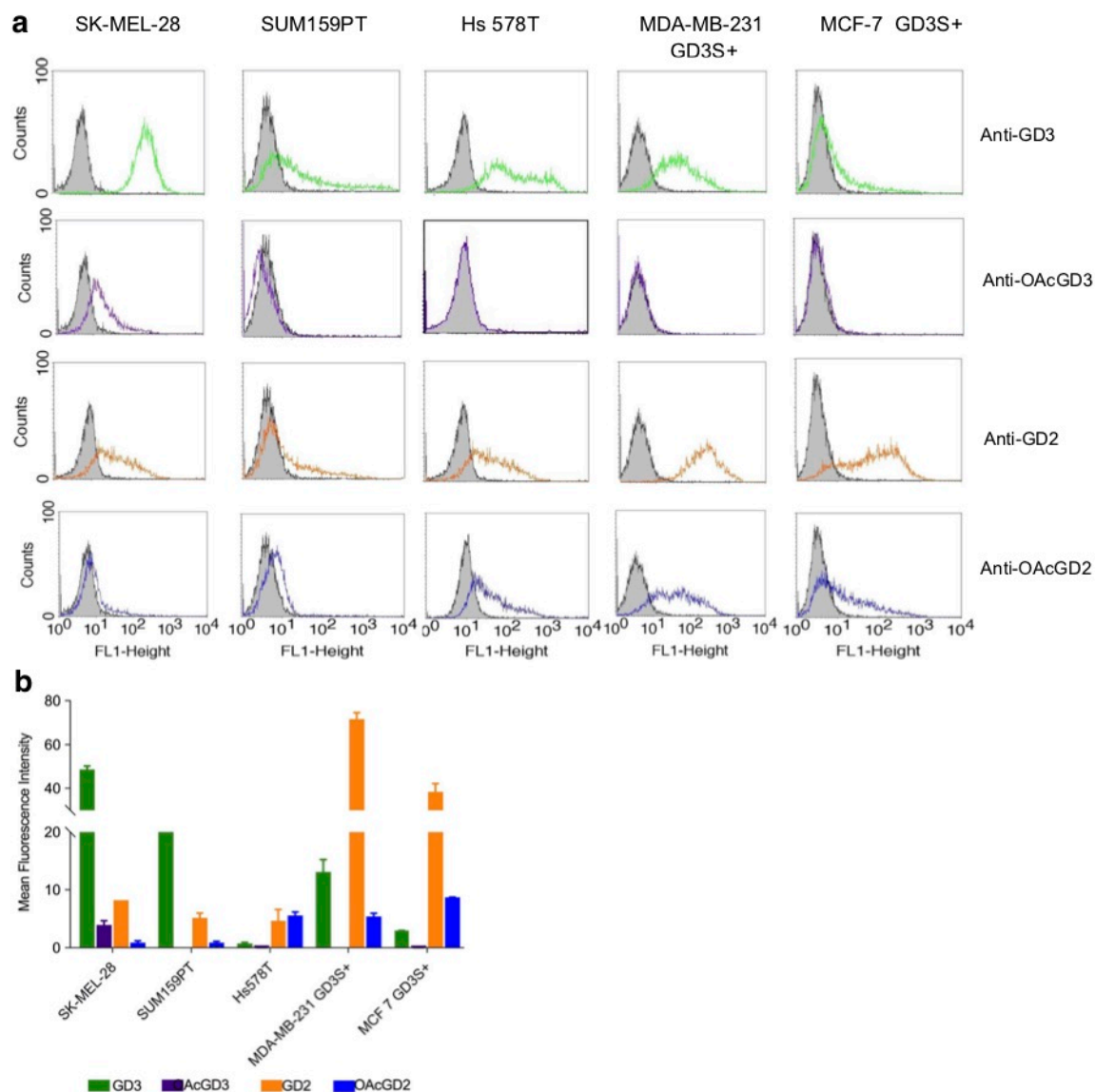
### BC cells express OAcGD2, but no OAcGD3

Biosynthesis of GD2 and GD3 gangliosides and their *O*-acetylated counterparts was analyzed using flow cytometry and confocal microscopy in two BC cells and two recombinant clones known to express b-series gangliosides: Hs 578T and SUM159PT cells, as well as MDA-MB-231 GD3S+ and MCF-7 GD3S+ clones over-expressing GD3S. The human melanoma cell line SK-MEL-28 was used as positive control. Flow cytometry analysis indicate that all these BC cells expressed GD3, GD2 and *O*AcGD2 even if SUM159PT expressed lower amount of *O*AcGD2 and Hs 578T mainly very low amount of GD3 (Fig. 3). Interestingly the expression of *O*AcGD3 was limited to SK-MEL-28 melanoma cell line, whereas *O*AcGD2 was not expressed in these cells (Fig. 3). The mean fluorescence

intensity (MFI) was determined for each diagram to compare the intensity of ganglioside staining (Fig. 3b). Although MFI value for GD3 and GD2 are ranging from 5 to 80, *O*AcGD3 and *O*AcGD2 MFI values are between 1 to 10 depending on the cells. The MFI value of GD3 is 5-fold higher to GD2 staining in SK-MEL-28 and SUM159PT cell lines. Interestingly, an opposite trend is observed in the other BC cells. The MFI value of GD2 is 5-fold higher than GD3 MFI in MDA-MB-231 GD3S+ and 10-fold higher in MCF-7 GD3S+ and Hs 578T. Although similar MFI values for GD2 and *O*AcGD2 are observed in Hs 578T, a 5-fold change is observed between GD2 and *O*AcGD2 MFI values in SUM159PT and MCF-7 GD3S+ and a 10-fold change is observed in SK-MEL-28 and MDA-MB-231 GD3S+ (Fig. 3b).

Immunocytochemistry followed by confocal microscopy experiments were performed to confirm the expression of GD2 and *O*AcGD2 in BC cells. In agreement with FACS analysis, GD2 and *O*AcGD2 were detected at the cell surface and in punctuated structures in the different BC cells (Fig. 4). These results allowed us to confirm using two different immunochemistry approaches the expression of GD2 and *O*AcGD2, and the absence of *O*AcGD3 in BC cells.





**Fig. 3** Analysis of GD2 and GD3 gangliosides and their O-acetylated counterparts expression in breast cancer cells using flow cytometry. **a:** Representative flow cytometry histograms for GD2, OAcGD2, GD3 and OAcGD3 expression at the cell surface of Hs 578T, SUM159PT, MDA-MB-231 GD3S+, MCF-7 GD3S+ cells using 14.18, 8B6, R24, 7H2

antibodies, respectively ( $n=3$ ). The grey peak corresponds to the signal observed after incubation of cells with the secondary antibody alone. SK-MEL-28 cells were used as a positive control for disialoganglioside expression. **b:** Mean fluorescence intensity corresponding to histograms obtained by flow cytometry ( $n=3$ )

Furthermore, the expression levels of GD3S (*ST8SIA1*) and GM2/GD2 synthase (*B4GALNT1*) correlated with the pattern of disialogangliosides detected by flow cytometry and confocal microscopy analysis, with a major expression of GM2/GD2 synthase compared to GD3S in BC cell lines (Fig. 2).

### Neu5,9Ac<sub>2</sub> is the main O-acetylated sialic acid species among gangliosides isolated from BC cells

Sialic acid is the carrier of O-acetylated groups on gangliosides, and sialic acid residues can be acetylated at the 4, 7, 8

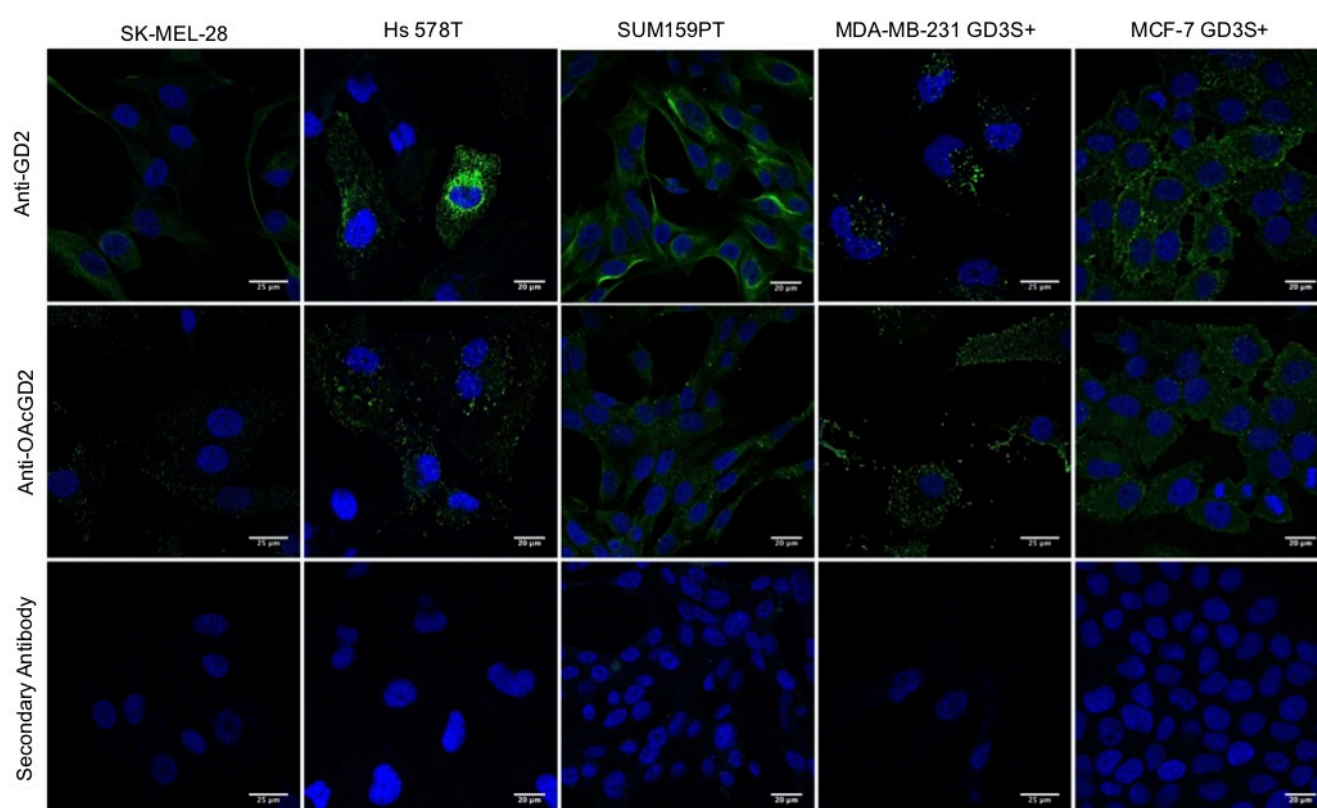
and/or 9 positions. Therefore, we analysed the different O-acetylated sialic acid species expressed in BC cells. Sialic acids were released from gangliosides extracted from BC cells by acidic hydrolysis and derivatize with 1,2-diamino-4,5-methylenedioxybenzene (DMB) at the free reducing end. The obtained fluorescent DMB-derivatives were analysed by micro-Liquid Chromatography system coupled to Mass Spectrometry (LC-MS) set to separate only the mono-O-acetylated DMB Sia derivatives. Sialic acids released from bovine submaxillary mucin (BSM) were used as a control. N-acetylneuraminic acid (Neu5Ac) and 9-O-acetyl-N-

acetylneuraminic acid (Neu5,9Ac<sub>2</sub>) were used as external standards for the identification and quantification of sialic acid species based on the retention time on liquid chromatography column. Among Neu5Ac species, we identified Neu5,9Ac<sub>2</sub> as the main *O*-acetylated form of sialic acid in all BC cells tested (Fig. 5). We also detected low amounts of Neu5,8Ac<sub>2</sub> in SUM159PT, MDA-MB-231 GD3S+, and MCF-7 GD3S+ cells (Fig. 5). Glycolipids from SK-MEL-28 melanoma cells contained both Neu5,9Ac<sub>2</sub> and Neu5,8Ac<sub>2</sub> derivatives. To confirm the nature of the peak assigned to Neu5Ac and Neu5,9Ac<sub>2</sub>, MS3 fragmentation was performed on DMB-Sia derivatives. We obtained a typical fragmentation of DMB-Neu5Ac (Fig. 6a) and DMB-Neu5,9Ac<sub>2</sub> (Fig. 6b) with an *m/z* value respectively based on 450 and 408 [M + Na]<sup>+</sup>. Peaks corresponding to Neu5Ac and Neu5,9Ac<sub>2</sub> were then quantified and both sialic acid species were expressed as fg/cell in the different cells. The amount of Neu5Ac was higher in SUM159PT and Hs 578T than in MDA-MB-231 GD3S+ and MCF-7 GD3S+ (Table 2). Neu5,9Ac<sub>2</sub> was expressed at lower levels than Neu5Ac in all cells. The highest amount of Neu5,9Ac<sub>2</sub> was detected in Hs 578T cells. MDA-MB-231 GD3S+ and MCF-7 GD3S+ contained lower amounts of

Neu5,9Ac<sub>2</sub> and the lowest amounts were detected for SUM159PT cells (Table 2).

### The fraction of Neu5,9Ac<sub>2</sub> detected is linked to OAcGD2 expression in BC cells

Based on LC/ESI-MS data, the ratio of Neu5,9Ac<sub>2</sub> / Neu5Ac was determined in each sample (Table 2), which allowed us to determine the percentage of Neu5,9Ac<sub>2</sub> in the ganglioside fraction of BC cells. We detected the highest Neu5,9Ac<sub>2</sub> / Neu5Ac ratios in MDA-MB-231 GD3S+ (0.09) and MCF-7 GD3S+ (0.07). The Neu5,9Ac<sub>2</sub> fraction was increased 3-fold in MDA-MB-231 GD3S+ and in MCF-7 GD3S+, as compared to their Mock counterpart. The fraction of Neu5,9Ac<sub>2</sub> species was lower in gangliosides from Hs 578T cells (0.02) and in SUM159PT cells (0.005) (Table 2). Interestingly, the mean fluorescence intensity (MFI) obtained for OAcGD2 staining by flow cytometry followed the same distribution as the Neu5,9Ac<sub>2</sub> fraction in glycolipids, except for Hs 578 T cell line. (Fig. 3b and Table 2). The absence of OAcGD3 expression in BC cells allows us to observe that Neu5,9Ac<sub>2</sub> amount is consistent with OAcGD2 expression. In contrast, in SK-



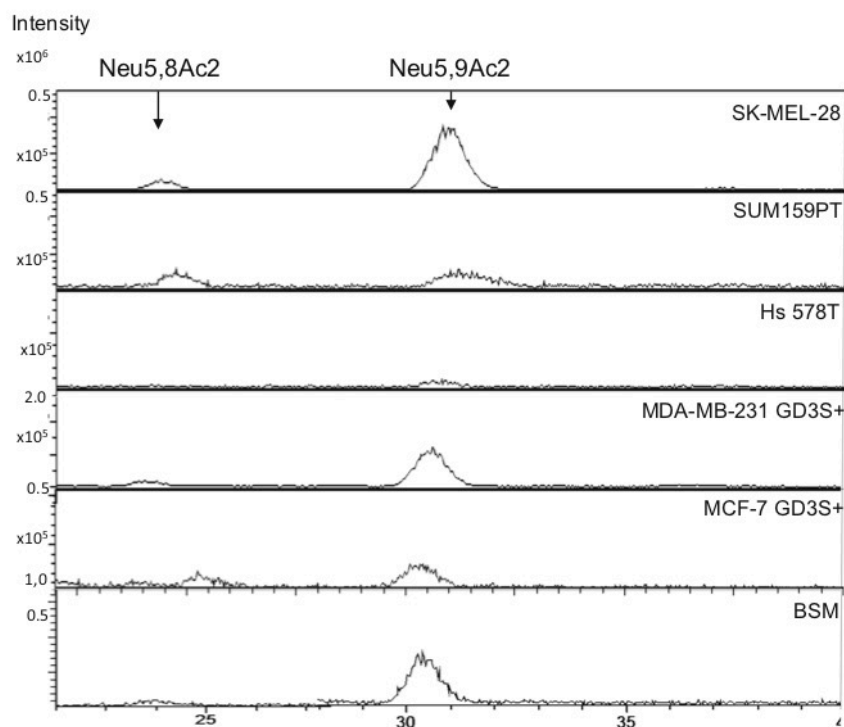
**Fig. 4** Analysis of GD2 and OAcGD2 expression in breast cancer cells using immunocytochemistry and confocal microscopy. SK-MEL-28, Hs 578T, SUM159PT cells, MDA-MB-231 GD3S+ and MCF-7 GD3S+ grown on coverslips were incubated with anti-GD2 or anti-OAcGD2

mAbs and gangliosides were visualized using IgG-conjugated Alexa Fluor 488, using confocal microscopy. The nuclei were counter stained with DAPI. All images were taken using the same settings



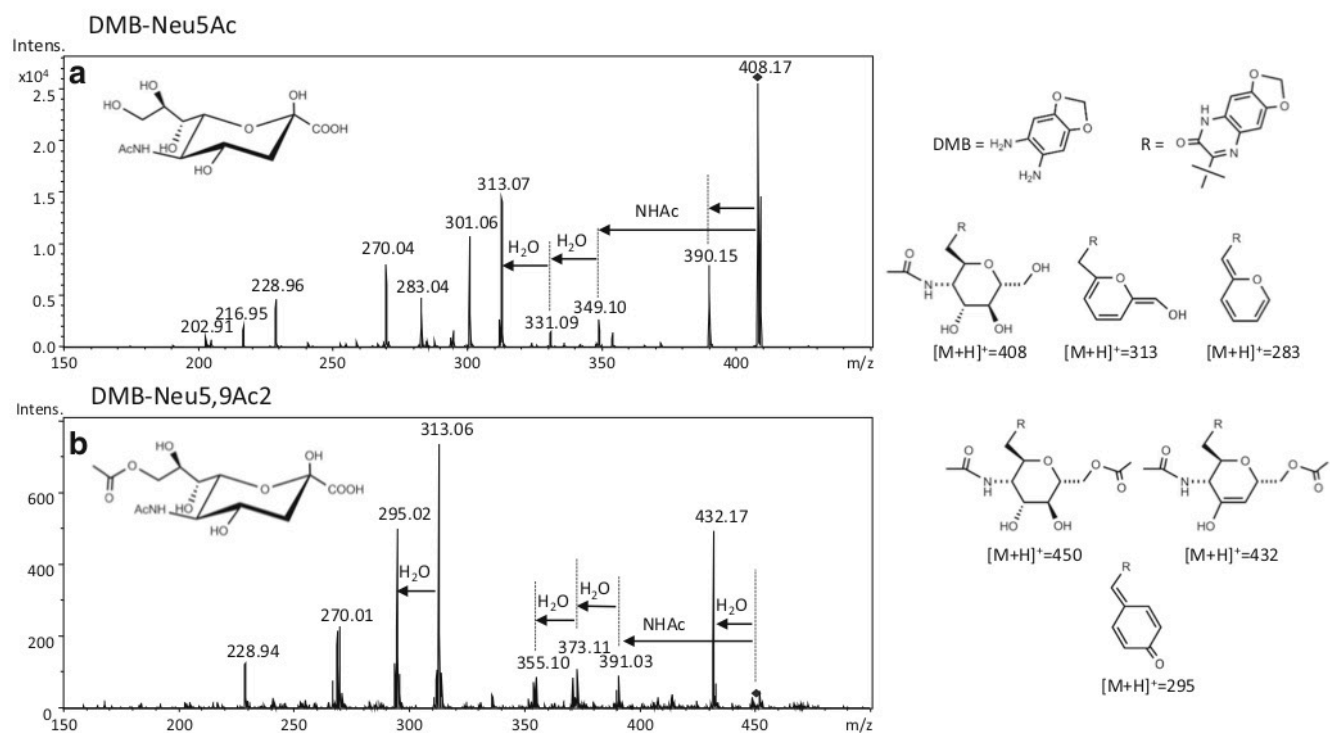
**Fig. 5** Identification of 9-O-acetylated N-acetylneuraminic acid as the main sialic acid species in breast cancer gangliosides by DMB-LC/ESI-MS.

Representative extracted ion chromatogram of DMB-derivatives samples of SK-MEL-28, SUM159PT, Hs 578T, MDA-MB-231 GD3S+, MCF-7 GD3S+ glycolipids. Bovine submaxillary mucin (BSM) was used as a control. The peaks corresponding to Neu5,9Ac<sub>2</sub> and Neu5,8Ac<sub>2</sub> were identified by referring elution time (min) for of their counterpart liberated from BSM



MEL-28 melanoma cells, which express GD2, GD3, OAcGD3 but no acetylated GD2, the Neu5,9Ac<sub>2</sub> fraction

(0,04) is likely present on GD3 and potentially on more complex gangliosides (Table 2).



**Fig. 6** Identification by LC/ESI-MS<sup>3</sup> of DMB-Neu5Ac (a) and DMB-Neu5,9Ac<sub>2</sub> (b). Representative MS<sup>3</sup> spectra of DMB-Neu5Ac (a) and DMB-Neu5,9Ac<sub>2</sub> (b), [M + H]<sup>+</sup> at m/z 426 and at m/z 468, respectively. The ion [M + H - 18]<sup>+</sup> at m/z 408 and at m/z 450 are indicated by the blue

colored diamond. The peaks corresponding to Neu5,9Ac<sub>2</sub> and Neu5,8Ac<sub>2</sub> were identified by referring elution time (min) for of their counterpart liberated from BSM. The major structure fragments were illustrated

**Table 2** Quantification of Neu5Ac and Neu5,9Ac<sub>2</sub> in BC cells and SK-MEL-28

Sample	Neu5Ac (fg/cell)		Neu5,9Ac <sub>2</sub> (fg/cell)		Ratio Neu5,9Ac <sub>2</sub> /Neu5Ac
	Mean	SEM	Mean	SEM	
SK-Mel-28	53.17	10.32	2.16	0.28	0.04
SUM159PT	12.64	3.62	0.07	0.04	0.005
Hs 578T	18.89	13.71	0.42	0.13	0.02
MDA-MB-231	3.17	1.84	0.10	0.05	0.03
MDA-MB-231 GD3S+	2.38	0.80	0.21	0.07	0.09
MCF-7	0.45	0.16	0.01	0.00	0.02
MCF-7 GD3S+	2.01	0.69	0.15	0.18	0.07

## Discussion

### Expression of complex gangliosides and their acetylated forms in BC cells

A large number of reports have underlined the role of disialogangliosides, especially GD3 and GD2, in cancers from neuro-ectoderm origin such as melanoma or neuroblastoma, demonstrating the implication of complex gangliosides in cell proliferation, migration, tumor growth and angiogenesis [27, 28]. The effects mainly result from the interaction of complex gangliosides with signaling molecules as it was clearly demonstrated in melanoma where GD3 expression results in a high level of phosphorylation and activation of the major adaptor proteins paxillin, p130Cas and FAK [29]. In BC cells, the expression of the GD3S and complex gangliosides results in the acquisition of higher proliferative capacity of tumor cells. GD3S expressing MDA-MB-231 cells bypass the need of growth factors by a specific and constitutive activation of c-Met receptor and activation of PI3K/Akt and Erk/MAPK pathways. Moreover, GD3S expression MDA-MB-231 cells also enhanced tumor growth in SCID mice [12]. The decrease of GD2 expression by silencing of the GM2/GD2 synthase or competition assays using anti-GD2 mAbs reversed the proliferative phenotype as well as c-Met phosphorylation, demonstrating the involvement of GD2 in BC cell proliferation via the constitutive activation of c-Met [30].

Here, we examined the *O*-acetylation of GD3 and GD2 in two BC cells and two recombinant clones. The role of ganglioside *O*-acetylation in cancer cell aggressiveness has not been widely studied, mostly because of the lack of suitable analytical tools. The expression of *O*AcGD2 was analyzed by immunohistochemistry in neuroblastoma, and in glioblastoma cells and tissues, using anti-*O*AcGD2 mAb 8B6 [31, 32]. In glioblastoma, *O*AcGD2 expression was higher in tumor tissues when compared to cultured cells derived from the tumor [31]. In addition, *O*AcGD2 was shown to exhibit a differential expression pattern compared to GD2. Alvarez Rueda and co-workers described the absence of *O*AcGD2 expression in healthy adult tissues [5]. It was also demonstrated that the

anti-*O*AcGD2 mAb 8B6 could either activate Antibody Dependent Cell Death (ADCC) and Complement Dependent Cytotoxicity (CDC) [32], or could induce cell death by the activation of mitochondrial mediated apoptotic pathway by increasing BAX in cytoplasm, and cytochrome-c at mitochondria, resulting in the activation of caspase-3 [33]. 8B6 mAb appears therefore a good candidate for cancer immunotherapy. Of note, the fact that *O*AcGD2 is absent from peripheral nerves could represent a real advantage compared to dinutuximab targeting GD2. Anti-GD2 immunotherapy has been shown highly promising, but unfortunately also quite toxic (dose-limiting pain and neuropathies) since GD2 is also expressed on the surface of normal nerves and brain cells.

*O*-acetylated gangliosides could be also molecules of major biological relevance in BC, modulating the malignant properties of BC cells as well as interesting targets for immunotherapy. According to the fact that *O*-acetylated gangliosides were poorly characterized in BC tissues or cell lines, we investigated *O*AcGD2 expression and characterized *O*-acetylated sialic acid species in four BC cells that express b-series gangliosides either naturally (SUM159PT and Hs 578T), or by ectopic expression of GD3S (MDA-MB-231-GD3S+ and MCF-7 GD3S+). By flow cytometry and immunocytochemistry/confocal microscopy, we confirmed that few selected BC cells expressed b-series gangliosides GD3 and GD2, and showed expression of *O*AcGD2, while the majority of BC cells does not express b-series gangliosides.

The expression of *O*AcGD3 was previously detected by immunohistochemistry in melanoma [34], neuroblastoma [35], glioblastoma [31] and also in BC tissues [9]. Interestingly, GM2/GD2S KO mice exhibit an accumulation of GM3 and GD3, as well as an increase of *O*AcGD3 in the nervous tissues of mice irrespective of sialate-*O*-acetyltransferase Tis 21 accumulation [36]. We could speculate that the accumulation of GD3 (not converted into GD2) is responsible for *O*AcGD3 expression in these mice. In a similar manner, our results suggest that the absence of *O*AcGD3 in BC cell lines is due to the high expression of GM2/GD2S compared to GD3S. The biosynthesis of *O*-acetylated gangliosides is still controversial: data from



Baumann and co-workers obtained in vitro using recombinant SOAT CASD1 suggest that *O*AcGD3 is synthesized by addition of activated CMP-*O*-acetyl-Neu5Ac on monosialylated ganglioside GM3 [15]. Our results, which highlight a link between GD2 and *O*AcGD2 expression, rather suggest that *O*AcGD2 is synthesized by direct acetylation of GD2 in BC cells.

### Identification of *O*-acetylated Sia species in BC cells

Our results clearly identify *O*AcGD2 in BC cells using immunological approaches, but the determination of the position of *O*-acetyl group(s) on the sialic acid residues was a challenging issue. The use of specific mAbs is the most common way to study against ganglioside *O*-acetylation. Importantly, the anti-GD2 antibody 14.18 that we used in our experiments also recognizes to some extent *O*-acetylated species of GD2, although with a much lower affinity compared to its preferential target GD2. The specificity of 8B6 mAb for *O*AcGD2 developed by Cerrato and collaborators has been demonstrated by several thin layer chromatography- immunostaining experiments by the loss of *O*AcGD2 staining after alkali-based treatment [5, 22, 32]. However, these experiments do not allow to determine the position of *O*-acetylated groups on GD2 sialic acid residues. This antibody was used for the screening of *O*AcGD2 expression among neuroblastoma, and glioblastoma cells and tissues, but the precise identity of its *O*-acetylated ligands remains unknown.

Several methods have been used for the identification and quantification of gangliosides. Reverse phase HPLC coupled to LC-ESI-MS-MS has been used for the quantification of GM2 ganglioside in complex biological mixtures (serum, blood, tissue) from GM2 gangliosidosis patients [37]. Recently, Barrientos and collaborators used RPLC-MS-MS analysis for identification and quantification of ganglioside after chemoselective oxidation of the sialic acid side chain and ligation with a carbonyl-reactive isobaric tandem mass tag reagent. This approach conducts to the loss of C8 and C9 and is therefore not an appropriate for our studies [38]. Despite all recent improvements in the identification and quantification of gangliosides, the methods frequently used induce the loss of the *O*-acetyl groups. In this study, our aim was to identify the different *O*-acetylated sialic acid species from BC cells ganglioside fraction, to study the link between ganglioside expression and *O*-acetylated Sia species. We analyzed DMB-labeled Sia derivatives using LC/ESI-MS to detect and quantify mono-*O*-acetylated sialic acid residues. We identified Neu5,9Ac<sub>2</sub> as the main *O*-acetylated form of Neu5Ac among gangliosides, mostly GD2, expressed by BC cells, and a lower expression of Neu5,8Ac<sub>2</sub>. Surprisingly, in our experiments, only trace amounts of Neu5,7Ac<sub>2</sub> were detected. Differences have been observed in studies on *O*-acetylation positions on sialic acid residues of gangliosides. Several studies identified the *O*-acetyl group at the C9 position of the outer sialic acid of *O*AcGD3 and *O*AcGD2 [39].

Conversely, Ren and co-workers identified an *O*-acetyl group on the C7 position of *O*AcGD3 in melanoma cells [40]. These discrepancies may be linked to the property of *O*-acetyl groups of migrating spontaneously from position 7 to position 9 of sialic acids when exposed to mild alkaline conditions. Therefore, controlling experimental conditions during experiments is critical to avoid the loss and the migration of the *O*-acetyl group.

Malisan and coworkers observed that *O*-acetylated sialic acid suppress the proapoptotic activity of GD3 reducing malignant property of glioblastoma [6]. In contrast to *O*AcGD3, the biological role of *O*AcGD2 remains mostly unknown. Cochonneau and co-workers showed that targeting *O*AcGD2 using 8B6 mAb promotes cell cycle arrest and apoptosis in tumor cells, as well as inhibition of tumor cell growth in vitro and in vivo. The precise mechanisms involved in apoptosis induced by anti-*O*AcGD2 antibody binding to tumor cells require further investigations.

**Acknowledgements** We thank Christian Slomianny of the BICeL-Campus Lille1 (Univ. Lille, Bio Imaging Center Lille, F-59000 Lille, France) facility for access to instruments and technical advices. We are indebted to the PAGés plateforme (Plateforme d'Analyses des Glycoconjugués, CNRS, UMR 8576, UGSF, Université de Lille), F-59000 Lille, France for the use of the mass spectrometer.

### Compliance with ethical standards

**Conflicts of interest** The authors declare that they have no conflicts of interest.

**Ethical approval** This article does not contain any studies with human participants or animals performed by any of the authors.

**Abbreviations** BC, Breast Cancer; BSM, Bovine Submaxillary Mucin; CMP Neu5Ac, cytidine-monophosphate N-acetylneuraminic acid; DMB, 1,2-diamino-4,5-methylenedioxybenzene; ER, Estrogen Receptor; Gal, Galactose; GalNAc, N-acetylgalactosamine; GD2S, GD2 synthase; GD3S, GD3 synthase; GT, Glycosyltransferase; HPRT, Hypoxanthine-guanine PhosphoRibosylTransferase; LacCer, Lactosyl-ceramide; LC/ESI-MS, Liquid Chromatography/ Electrospray ionization coupled to Mass Spectrometry; mAb, monoclonal antibody; MFI, Mean Fluorescence Intensity; Neu5Ac, N-acetylneuraminic acid; Neu5,8Ac<sub>2</sub>, 8-*O*-acetyl-N-acetylneuraminic acid; Neu5,9Ac<sub>2</sub>, 9-*O*-acetyl-N-acetylneuraminic acid; *O*AcGD2, *O*-acetyl-GD2; *O*AcGD3, *O*-acetyl-GD3.; TACA, Tumor-Associated Carbohydrate Antigens; TNBC, Triple Negative Breast Cancer

**Publisher's Note** Springer Nature remains neutral with regard to jurisdictional claims in published maps and institutional affiliations.

### References

1. Hakomori, S.: Aberrant glycosylation in cancer cell membranes as focused on glycolipids: overview and perspectives. *Cancer Res.* **45**(6), 2405–2414 (1985)
2. Yoshida, S., Fukumoto, S., Kawaguchi, H., Sato, S., Ueda, R., Furukawa, K., Ganglioside, G.: (D2) in small cell lung cancer cell lines: enhancement of cell proliferation and mediation of apoptosis. *Cancer Res.* **61**(10), 4244–4252 (2001)



3. Yu, A.L., Gilman, A.L., Ozkaynak, M.F., London, W.B., Kreissman, S.G., Chen, H.X., Smith, M., Anderson, B., Villablanca, J.G., Matthay, K.K., Shimada, H., Grupp, S.A., Seeger, R., Reynolds, C.P., Buxton, A., Reisfeld, R.A., Gillies, S.D., Cohn, S.L., Maris, J.M., Sondel, P.M., Children's Oncology, G.: Anti-GD2 antibody with GM-CSF, interleukin-2, and isotretinoin for neuroblastoma. *N. Engl. J. Med.* **363**(14), 1324–1334 (2010). <https://doi.org/10.1056/NEJMoa0911123>
4. Dhillon, S.: Dinutuximab: first global approval. *Drugs*. **75**(8), 923–927 (2015). <https://doi.org/10.1007/s40265-015-0399-5>
5. Alvarez-Rueda, N., Desselle, A., Cochonneau, D., Chaumette, T., Clemenceau, B., Leprieux, S., Bougras, G., Supiot, S., Mussini, J.M., Barbet, J., Saba, J., Paris, F., Aubry, J., Birkle, S.: A monoclonal antibody to O-acetyl-GD2 ganglioside and not to GD2 shows potent anti-tumor activity without peripheral nervous system cross-reactivity. *PLoS One*. **6**(9), e25220 (2011). <https://doi.org/10.1371/journal.pone.0025220>
6. Malisan, F., Franchi, L., Tomassini, B., Ventura, N., Condo, I., Rippo, M.R., Rufini, A., Liberati, L., Nachtigall, C., Kniep, B., Testi, R.: Acetylation suppresses the proapoptotic activity of GD3 ganglioside. *J. Exp. Med.* **196**(12), 1535–1541 (2002)
7. Mukherjee, K., Chava, A.K., Mandal, C., Dey, S.N., Kniep, B., Chandra, S., Mandal, C.: O-acetylation of GD3 prevents its apoptotic effect and promotes survival of lymphoblasts in childhood acute lymphoblastic leukaemia. *J. Cell. Biochem.* **105**(3), 724–734 (2008). <https://doi.org/10.1002/jcb.21867>
8. Recchi, M.A., Hebbar, M., Homez, L., Harduin-Lepers, A., Peyrat, J.P., Delannoy, P.: Multiplex reverse transcription polymerase chain reaction assessment of sialyltransferase expression in human breast cancer. *Cancer Res.* **58**(18), 4066–4070 (1998)
9. Marquina, G., Waki, H., Fernandez, L.E., Kon, K., Carr, A., Valiente, O., Perez, R., Ando, S.: Gangliosides expressed in human breast cancer. *Cancer Res.* **56**(22), 5165–5171 (1996)
10. Ruckhaberle, E., Kam, T., Rody, A., Hanker, L., Gatje, R., Metzler, D., Holtrich, U., Kaufmann, M.: Gene expression of ceramide kinase, galactosyl ceramide synthase and ganglioside GD3 synthase is associated with prognosis in breast cancer. *J. Cancer Res. Clin. Oncol.* **135**(8), 1005–1013 (2009). <https://doi.org/10.1007/s00432-008-0536-6>
11. Cazet, A., Groux-Degroote, S., Teylaert, B., Kwon, K.M., Lehoux, S., Slomianny, C., Kim, C.H., Le Bourhis, X., Delannoy, P.: GD3 synthase overexpression enhances proliferation and migration of MDA-MB-231 breast cancer cells. *Biol. Chem.* **390**(7), 601–609 (2009). <https://doi.org/10.1515/BC.2009.054>
12. Cazet, A., Julien, S., Bobowski, M., Krzewinski-Recchi, M.A., Harduin-Lepers, A., Groux-Degroote, S., Delannoy, P.: Consequences of the expression of sialylated antigens in breast cancer. *Carbohydr. Res.* **345**(10), 1377–1383 (2010). <https://doi.org/10.1016/j.carres.2010.01.024>
13. Steenackers, A., Vanbeselaere, J., Cazet, A., Bobowski, M., Rombouts, Y., Colomb, F., Le Bourhis, X., Guerardel, Y., Delannoy, P.: Accumulation of unusual gangliosides G(Q3) and G(P3) in breast cancer cells expressing the G(D3) synthase. *Molecules*. **17**(8), 9559–9572 (2012). <https://doi.org/10.3390/molecules17089559>
14. Mandal, C., Schwartz-Albiez, R., Vlasak, R.: Functions and biosynthesis of O-acetylated sialic acids. *Top. Curr. Chem.* **366**, 1–30 (2015). [https://doi.org/10.1007/128\\_2011\\_310](https://doi.org/10.1007/128_2011_310)
15. Baumann, A.M., Bakkers, M.J., Buettner, F.F., Hartmann, M., Grove, M., Langereis, M.A., de Groot, R.J., Muhlenhoff, M.: 9-O-acetylation of sialic acids is catalysed by CASD1 via a covalent acetyl-enzyme intermediate. *Nat. Commun.* **6**(7673), (2015). <https://doi.org/10.1038/ncomms8673>
16. Mandal, C., Srinivasan, G.V., Chowdhury, S., Chandra, S., Mandal, C., Schauer, R., Mandal, C.: High level of sialate-O-acetyltransferase activity in lymphoblasts of childhood acute lymphoblastic leukaemia (ALL): enzyme characterization and correlation with disease status. *Glycoconj. J.* **26**(1), 57–73 (2009). <https://doi.org/10.1007/s10719-008-9163-3>
17. Ravindranath, M.H., Higa, H.H., Cooper, E.L., Paulson, J.C.: Purification and characterization of an O-acetylsialic acid-specific lectin from a marine crab *Cancer antennarius*. *J. Biol. Chem.* **260**(15), 8850–8856 (1985)
18. Shama, V., Chatterjee, M., Mandal, C., Sen, S., Basu, D.: Rapid diagnosis of Indian visceral leishmaniasis using alectinH, a 9-O-acetylated sialic acid binding lectin. *Am J Trop Med Hyg.* **58**(5), 551–554 (1998)
19. Zimmer, G., Suguri, T., Reuter, G., Yu, R.K., Schauer, R., Herler, G.: Modification of sialic acids by 9-O-acetylation is detected in human leucocytes using the lectin property of influenza C virus. *Glycobiology*. **4**(3), 343–349 (1994)
20. Ravindranath, M.H., Paulson, J.C., Irie, R.F.: Human melanoma antigen O-acetylated ganglioside GD3 is recognized by *Cancer antennarius* lectin. *J. Biol. Chem.* **263**(4), 2079–2086 (1988)
21. Saito, M., Kasai, N.: Yu, R.K.: in situ immunological determination of basic carbohydrate structures of gangliosides on thin-layer plates. *Anal. Biochem.* **148**(1), 54–58 (1985)
22. Cerato, E., Birkle, S., Portoukalian, J., Mezazigh, A., Chatal, J.F., Aubry, J.: Variable region gene segments of nine monoclonal antibodies specific to disialogangliosides (GD2, GD3) and their O-acetylated derivatives. *Hybridoma*. **16**(4), 307–316 (1997). <https://doi.org/10.1089/hyb.1997.16.307>
23. Steenackers, A., Cazet, A., Bobowski, M., Rombouts, Y., Lefebvre, J., Guérardel, Y., Tulasne, D., Le Bourhis, X., Delannoy, P.: Expression of GD3 synthase modifies ganglioside profile and increases migration of MCF-7 breast cancer cells. *C.R. Chimie*. **15**, 3–14 (2012)
24. Pfaffl, M.W.: A new mathematical model for relative quantification in real-time RT-PCR. *Nucleic Acids Res.* **29**(9), e45 (2001)
25. Klein, A., Diaz, S., Ferreira, I., Lamblin, G., Roussel, P., Manzi, A.E.: New sialic acids from biological sources identified by a comprehensive and sensitive approach: liquid chromatography-electrospray ionization-mass spectrometry (LC-ESI-MS) of SIA quinoxalinones. *Glycobiology*. **7**(3), 421–432 (1997)
26. Sommer, U., Herscovitz, H., Welty, F.K., Costello, C.E.: LC-MS-based method for the qualitative and quantitative analysis of complex lipid mixtures. *J. Lipid Res.* **47**(4), 804–814 (2006). <https://doi.org/10.1194/jlr.M500506-JLR200>
27. Bobowski, M., Vincent, A., Steenackers, A., Colomb, F., Van Seuningen, I., Julien, S., Delannoy, P.: Estradiol represses the G(D3) synthase gene ST8SIA1 expression in human breast cancer cells by preventing NFκB binding to ST8SIA1 promoter. *PLoS One*. **8**(4), e62559 (2013). <https://doi.org/10.1371/journal.pone.0062559>
28. Groux-Degroote, S., Guerardel, Y., Delannoy, P.: Gangliosides: structures, biosynthesis, analysis, and roles in Cancer. *Chembiochem.* **18**(13), 1146–1154 (2017). <https://doi.org/10.1002/cbic.201600705>
29. Hamamura, K., Furukawa, K., Hayashi, T., Hattori, T., Nakano, J., Nakashima, H., Okuda, T., Mizutani, H., Hattori, H., Ueda, M., Urano, T., Lloyd, K.O., Furukawa, K.: Ganglioside GD3 promotes cell growth and invasion through p130Cas and paxillin in malignant melanoma cells. *Proc. Natl. Acad. Sci. U. S. A.* **102**(31), 11041–11046 (2005). <https://doi.org/10.1073/pnas.0503658102>
30. Cazet, A., Bobowski, M., Rombouts, Y., Lefebvre, J., Steenackers, A., Popa, I., Guerardel, Y., Le Bourhis, X., Tulasne, D., Delannoy, P.: The ganglioside G(D2) induces the constitutive activation of c-met in MDA-MB-231 breast cancer cells expressing the G(D3) synthase. *Glycobiology*. **22**(6), 806–816 (2012). <https://doi.org/10.1093/glycob/cws049>
31. Fleurence, J., Cochonneau, D., Fougeray, S., Oliver, L., Geraldo, F., Terme, M., Dorvillius, M., Loussouam, D., Vallette, F., Paris, F., Birkle, S.: Targeting and killing glioblastoma with monoclonal



- antibody to O-acetyl GD2 ganglioside. *Oncotarget*. **7**(27), 41172–41185 (2016). <https://doi.org/10.18632/oncotarget.9226>
32. Terme, M., Dorvillius, M., Cochonneau, D., Chaumette, T., Xiao, W., Diccianni, M.B., Barbet, J., Yu, A.L., Paris, F., Sorkin, L.S., Birkle, S.: Chimeric antibody c.8B6 to O-acetyl-GD2 mediates the same efficient anti-neuroblastoma effects as therapeutic ch14.18 antibody to GD2 without antibody induced allodynia. *PLoS One*. **9**(2), e87210 (2014). <https://doi.org/10.1371/journal.pone.0087210>
  33. Cochonneau, D., Terme, M., Michaud, A., Dorvillius, M., Gautier, N., Frikeche, J., Alvarez-Rueda, N., Bougras, G., Aubry, J., Paris, F., Birkle, S.: Cell cycle arrest and apoptosis induced by O-acetyl-GD2-specific monoclonal antibody 8B6 inhibits tumor growth in vitro and in vivo. *Cancer Lett*. **333**(2), 194–204 (2013). <https://doi.org/10.1016/j.canlet.2013.01.032>
  34. Cheresch, D.A., Pierschbacher, M.D., Herzig, M.A., Mujoo, K.: Disialogangliosides GD2 and GD3 are involved in the attachment of human melanoma and neuroblastoma cells to extracellular matrix proteins. *J. Cell Biol*. **102**(3), 688–696 (1986)
  35. Kohla, G., Stockfleth, E., Schauer, R.: Gangliosides with O-acetylated sialic acids in tumors of neuroectodermal origin. *Neurochem. Res*. **27**(7–8), 583–592 (2002)
  36. Furukawa, K., Aixinjueluo, W., Kasama, T., Ohkawa, Y., Yoshihara, M., Ohmi, Y., Tajima, O., Suzumura, A., Kittaka, D., Furukawa, K.: Disruption of GM2/GD2 synthase gene resulted in overt expression of 9-O-acetyl GD3 irrespective of Tis21. *J. Neurochem*. **105**(3), 1057–1066 (2008). <https://doi.org/10.1111/j.1471-4159.2008.05232.x>
  37. Fuller, M., Duplock, S., Hein, L.K., Rigat, B.A., Mahuran, D.J.: Liquid chromatography/electrospray ionisation-tandem mass spectrometry quantification of GM2 gangliosides in human peripheral cells and plasma. *Anal. Biochem*. **458**, 20–26 (2014). <https://doi.org/10.1016/j.ab.2014.04.018>
  38. Barrientos, R.C., Zhang, Q.: Isobaric labeling of intact gangliosides toward multiplexed LC-MS/MS-based quantitative analysis. *Anal. Chem*. **90**(4), 2578–2586 (2018). <https://doi.org/10.1021/acs.analchem.7b04044>
  39. Sjoberg, E.R., Manzi, A.E., Khoo, K.H., Dell, A., Varki, A.: Structural and immunological characterization of O-acetylated GD2. Evidence that GD2 is an acceptor for ganglioside O-acetyltransferase in human melanoma cells. *J. Biol. Chem*. **267**(23), 16200–16211 (1992)
  40. Ren, S., Ariga, T., Scarsdale, J.N., Zhang, Y., Slominski, A., Livingston, P.O., Ritter, G., Kushi, Y.: Yu, R.K.: characterization of a hamster melanoma-associated ganglioside antigen as 7-O-acetylated disialoganglioside GD3. *J. Lipid Res*. **34**(9), 1565–1572 (1993)

### PART III: *O*-acetylated gangliosides profiling in breast cancer cell lines by mass spectrometry

This part apprehends the characterization of *O*-acetylated gangliosides diversity in neuroectoderm derived tumor cells. Native gangliosides extracted from dried cell pellets have been analyzed on MALDI-QIT-TOF. GM1, GM2, GM3, GD1b, GD2, GD3 and GT3 have been identified in SK-Mel28 (melanoma), LAN-1 (NB), Hs 578T, SUM 159PT, MDA-MB-231, MCF-7, and BC cell lines overexpressing GD3 synthase. *O*AcGM1, *O*AcGD3, *O*AcGD2, *O*AcGT2 and *O*AcGT3 expression have been identified in these cell lines. This method allows us to identify the sialic acid residue that carries the *O*-acetyl group on gangliosides by MS/MS fragmentation, and to determine whether *O*-acetylation occurs on the subterminal and/or the terminal sialic acid residue. These results highlight the limitation of immuno-detection for the complete identification of *O*-acetylated ganglioside profiles in cancer cells and showed that ganglioside *O*-acetylation can occur on the first and/or the second sialic acid residue in a cell type-dependent manner, suggesting different *O*-acetylation pathways for glycolipids. Results obtained have been submitted for publication in November 2019 in the *International Journal of Molecular Science*.



Article

# Profiling of O-acetylated Gangliosides Expressed in Neuroectoderm Derived Cells

Sumeyye Cavdarli <sup>1,2</sup>, Nao Yamakawa <sup>1</sup>, Charlotte Clarisse <sup>1</sup>, Kazuhiro Aoki <sup>3</sup>,  
Guillaume Brysbaert <sup>1</sup>, Jean-Marc Le Doussal <sup>2</sup>, Philippe Delannoy <sup>1</sup>, Yann Guérardel <sup>1</sup>  
and Sophie Groux-Degroote <sup>1,\*</sup>

<sup>1</sup> Univ. Lille, CNRS, UMR 8576-UGSF-Unité de Glycobiologie Structurale et Fonctionnelle, F-59000 Lille, France; sumeyye.cavdarli@univ-lille.fr (S.C.); nao.yamakawa@univ-lille.fr (N.Y.); charlotte.clarisse@univ-lille.fr (C.C.); guillaume.brysbaert@univ-lille.fr (G.B.); philippe.delannoy@univ-lille.fr (P.D.); yann.guerardel@univ-lille.fr (Y.G.)

<sup>2</sup> OGD2 Pharma, Institut de Recherche en Santé de l'Université de Nantes, 44007 Nantes, France; ledoussal@ogd2pharma.com

<sup>3</sup> Complex Carbohydrate Research Center, University of Georgia, Athens, GA 30602, USA; kaoki@ccrc.uga.edu

\* Correspondence: sophie.groux-degroote@univ-lille.fr

Received: 22 November 2019; Accepted: 31 December 2019; Published: 6 January 2020

**Abstract:** The expression and biological functions of oncofetal markers GD2 and GD3 were extensively studied in neuroectoderm-derived cancers in order to characterize their potential as therapeutic targets. Using immunological approaches, we previously identified GD3, GD2, and OAcGD2 expression in breast cancer (BC) cell lines. However, antibodies specific for O-acetylated gangliosides are not exempt of limitations, as they only provide information on the expression of a limited set of O-acetylated ganglioside species. Consequently, the aim of the present study was to use structural approaches in order to apprehend ganglioside diversity in melanoma, neuroblastoma, and breast cancer cells, focusing on O-acetylated species that are usually lost under alkaline conditions and require specific analytical procedures. We used purification and extraction methods that preserve the O-acetyl modification for the analysis of native gangliosides by MALDI-TOF. We identified the expression of GM1, GM2, GM3, GD2, GD3, GT2, and GT3 in SK-Mel28 (melanoma), LAN-1 (neuroblastoma), Hs 578T, SUM 159PT, MDA-MB-231, MCF-7 (BC), and BC cell lines over-expressing GD3 synthase. Among O-acetylated gangliosides, we characterized the expression of OAcGM1, OAcGD3, OAcGD2, OAcGT2, and OAcGT3. Furthermore, the experimental procedure allowed us to clearly identify the position of the sialic acid residue that carries the O-acetyl group on b- and c-series gangliosides by MS/MS fragmentation. These results show that ganglioside O-acetylation occurs on both inner and terminal sialic acid residue in a cell type-dependent manner, suggesting different O-acetylation pathways for gangliosides. They also highlight the limitation of immuno-detection for the complete identification of O-acetylated ganglioside profiles in cancer cells.

**Keywords:** gangliosides; O-acetylation; mass spectrometry; neuroectoderm-derived cancer; sialic acid

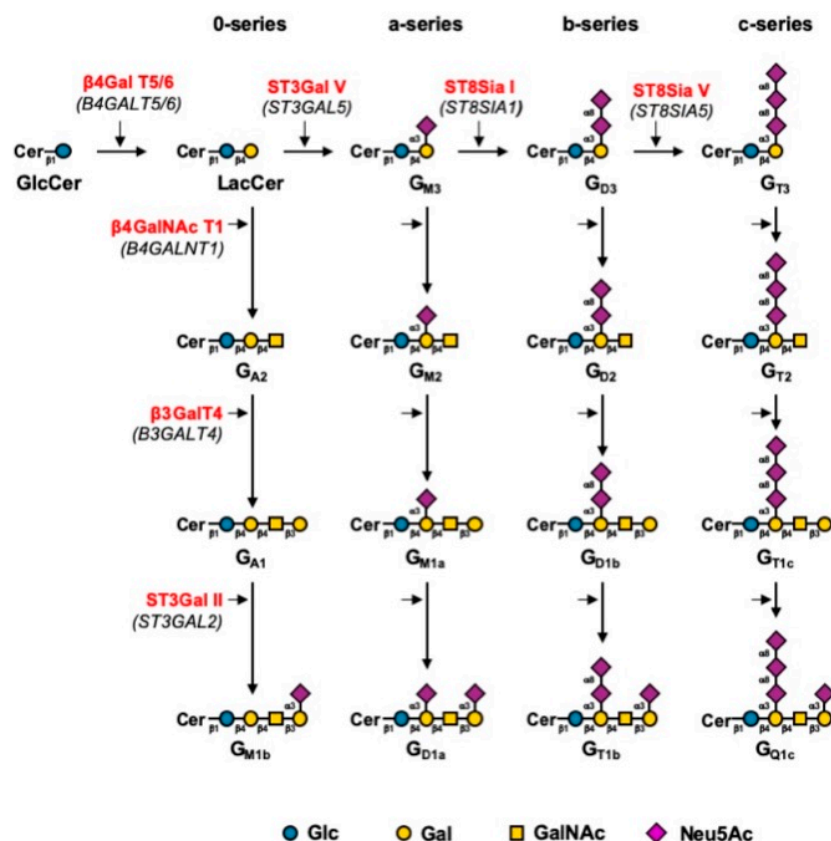
## 1. Introduction

Gangliosides are acidic glycosphingolipid carrying one or several sialic acid residues located in lipid raft in which they play an important role in the regulation of cell signaling [1]. Their biosynthesis process has been well established as depicted in Figure 1 [2]. Indeed, lipid raft domains

are microdomains from which major cellular pathways are engaged, not only in normal physiological conditions, but also under pathological conditions, such as neurodegenerative diseases or cancer. In neuroectoderm-derived cancers, gangliosides over-expression participates to tumor aggressiveness. For example, in MDA-MB-231 breast cancer cell line, GD2 over-expression increases tumorigenesis by activating c-Met receptor [3]. These properties led to the characterization of gangliosides as tumor associated carbohydrate antigens (TACA). GD3 and GD2 have been described as TACA and also oncofetal markers in melanoma, small cell lung carcinoma (SCLC), and neuroblastoma [4,5], and are potent targets for immunotherapy, especially GD2. Therapeutic antibodies developed against GD2 have been approved by the Food Drug Administration (FDA) as dinutuximab and European Medicine Agency (EMA) as qarziba for the treatment of high-risk pediatric neuroblastoma [6]. The standard care for neuroblastoma is the use of intense chemotherapy to achieve clinical remission. However, the complete remission of patients is hard to achieve and relapse occurs in 50% of cases. The use of anti-GD2 therapeutic antibodies for relapsing neuroblastoma has shown promising results in patients, but also severe side toxicities such as allodynia [6]. Indeed, GD2 expression is not exclusive to cancer cells, and peripheral nerve fibers are expressing GD2, which explains the downside effects. Interestingly, the use of an antibody targeting specifically the *O*-acetylated form of GD2 (OAcGD2) suggested that OAcGD2 expression is exclusive to cancer cells and tissues [7]. Terme et al. have shown that 8B6 antibody targeting OAcGD2 exhibits the same efficiency as anti-GD2 antibody without inducing allodynia [8]. Besides, *O*-acetylated GD2 has been shown to promote neuroblastoma growth *in vitro*, and *in vivo* [8,9]. Similarly, *O*-acetylated GD3 (OAcGD3) protects glioblastoma cells from GD3 induced mitochondrial apoptosis [10,11]. These properties exhibited by the *O*-acetylated forms of GD3 and GD2 pose them as valuable alternative therapeutic targets compared to their non-*O*-acetylated forms. However, there is very limited knowledge about ganglioside *O*-acetylation mechanisms. Previous studies using immunodetection analysis established that breast cancer cell lines displayed major expression of GD3, GD2, and OAcGD2, but not OAcGD3 [12]. Baumann and coworkers have previously reported that CASD1 was the only human sialyl-*O*-acetyltransferase (SOAT), and suggested it would act on the sialic acid donor CMP-Neu5Ac rather than on glycolipid itself [13]. The *O*-acetylation of gangliosides catalyzed by SOAT may occur on the hydroxyl residues of C4, C7, C8, or C9. In contrast, our work suggests that the OAcGD2 is generated directly from GD2 in breast cancer cells [12]. In order to get insights into the biosynthesis mechanisms underlying ganglioside *O*-acetylation process, we decided to establish the pattern of *O*-acetylated gangliosides of neuroectoderm-derived cell lines that express tumor-associated GD2 and GD3, with a special interest for OAcGD3 and OAcGD2.

Indeed, despite the biological relevance of *O*-acetylated GSL in cancer, very little is known about their distributions in cells and tissues and about their fine chemical structure, i.e., the position of the *O*-acetyl group(s), and which sialic acid residue is *O*-acetylated in di- or tri-sialylated ganglioside species. This is partly related to the fact that detection and analysis of *O*-acetylated gangliosides remain challenging due to the lability of the *O*-acetyl group using classical procedures and to the lack of specific antibodies that show minimal cross-reactivity with non-acetylated glycan moieties [14–16]. In this context, we established the expression patterns of gangliosides in neuroectoderm-derived cancers cells using mass spectrometry. To this end, we combined a purification and extraction procedure for native gangliosides analysis by MALDI-TOF, avoiding the loss of the *O*-acetyl modifications. GM1, GM2, GM3, GD2, GT2, and GT3 gangliosides have been identified in SK-Mel-28 melanoma cells, in LAN-1 neuroblastoma cells, in Hs 578T, SUM159PT, MDA-MB-231, MCF-7 BC cells, and in BC cell lines over-expressing GD3 synthase. Among *O*-acetylated gangliosides, we characterized the expression of OAcGM1, OAcGD3, OAcGD2, OAcGT3, OAcGT2. This method allowed us to identify the sialic acid residues carrying the *O*-acetyl groups on b- and c-series gangliosides by MS/MS fragmentation, giving us insights into the cellular *O*-acetylation mechanisms.



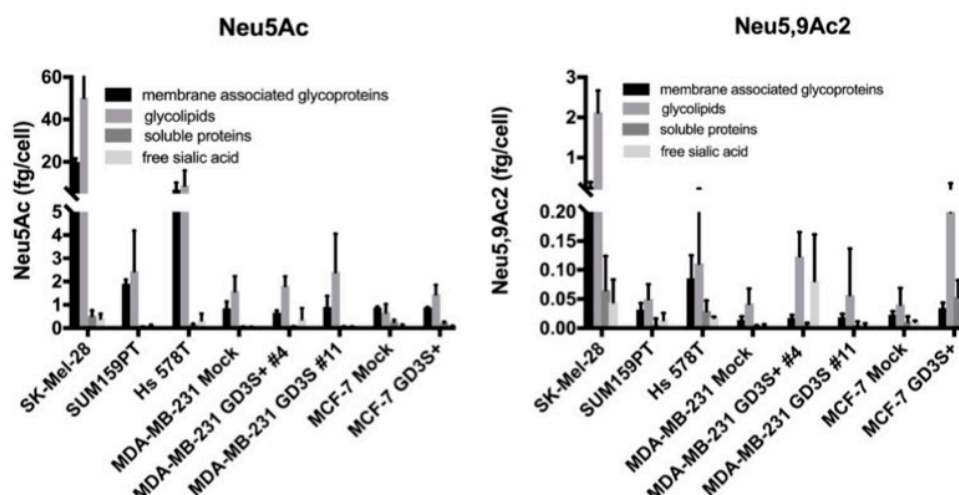


**Figure 1.** Biosynthesis pathway for gangliosides [2]. Gangliosides are synthesized by stepwise addition of monosaccharides to GlcCer. Extension of GlcCer occurs through the action of the UDP-Gal: GlcCer  $\beta 1,4$ -galactosyltransferase to make lactosylceramide (LacCer). The action of the GM3 synthase, GD3 synthase, and GT3 synthase leads to the biosynthesis of the precursors of a-, b-, and c-series gangliosides, respectively. The 0-series gangliosides are directly synthesized from LacCer. Elongation is performed by the sequential action of  $\beta 4$ GalNAc T1,  $\beta 3$ Gal T4, and the sialyltransferases ST3Gal II and ST6Sia V. Genes encoding the different glycosyltransferases involved are indicated in italics between brackets.

## 2. Results

### 2.1. O-acetylated Sialic Acid Species Are Highly Expressed on Glycolipids in Cancer Cells

As previously described, we performed the quantification of sialic acid species in cancer cells using LC-ESI/MS analysis of DMB-Sia derivatives [12]. Our results suggest that the main O-acetylated sialic acid species expressed by these cells is Neu5,9Ac<sub>2</sub>. Here, we quantified the amounts of total sialic acid (Neu5Ac) and acetylated sialic acid (Neu5,9Ac<sub>2</sub>) in different cell fractions. Dried pellets were fractionated into membrane associated glycoproteins, soluble proteins, glycolipids, and free sialic acid before sialic acid extraction and DMB derivatization. As depicted in Figure 2, the amounts of Neu5Ac remain higher in all fractions compared to Neu5,9Ac<sub>2</sub> levels, reaching 60 fg/cell and 3 fg/cell, respectively.



**Figure 2.** Neu5Ac and Neu5,9Ac2 DMB-Sia derivatives quantification by LC-ESI/MS in different cell fractions. Cell pellets were fractionated into membrane associated glycoproteins, glycolipids, soluble proteins, and free sialic acid fractions and hydrolyzed by propionic acid. The extracted sialic acids were derivatized using DMB and injected into LC-ESI/MS for identification and quantification. The amounts of Neu5Ac and Neu5,9Ac2 were quantified by integrating the corresponding areas obtained using extracted ion chromatogram on DMB-Sia derivatives. Each bar represents the mean of three independent experiments.

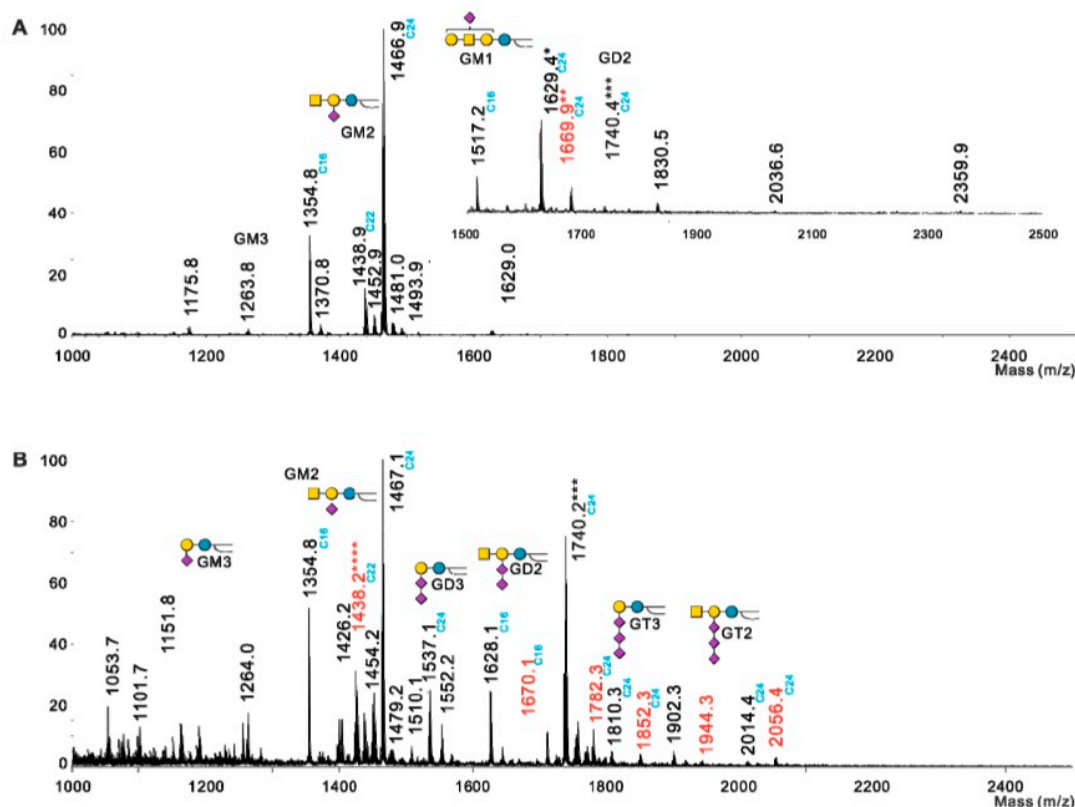
While the amounts of Neu5Ac and Neu5,9Ac2 were markedly cell-type dependent, the highest amount of sialic acid was quantified in the glycolipid fraction, except for the MDA-MB-231 GD3S+ clone #4, which exhibited high expression of Neu5,9Ac2 in the free sialic acid fraction. Besides the glycolipid fraction, the highest expression of Neu5,9Ac2 was detected in the membrane associated glycoprotein fraction for SK-MEL-28, MDA-MB-231 GD3S+ clones #4 and #11, MCF-7 GD3S+, progressively decreasing in Hs 578T, SUM159PT, MDA-MB-231, and MCF-7 (Figure 2). These results complete our previous study, confirming that GD3 synthase over-expression increases sialic acid *O*-acetylation. In order to supplement this approach and to identify the *O*-acetylated ganglioside species, native gangliosides extracted from all cell lines were analyzed by MALDI-QIT-TOF.

## 2.2. Profiling of *O*-acetylated Gangliosides in Breast Cancer, Melanoma, and Neuroblastoma Cell Lines

The detection of *O*-acetylated gangliosides by mass spectrometry is a challenging issue due to the loss of *O*-acetyl groups following chemical treatments usually performed to improve purification (mild saponification of non-ceramide lipids) or detection sensibility in mass spectrometry analysis (permethylation). Here, we used extraction and purification methods designed to preserve *O*-acetylation of GSL. Potentially *O*-acetylated GSL were extracted from dried pellets on eight different neuroectoderm-derived cell lines and analyzed in native forms by MALDI-QIT-TOF. Ganglioside expression patterns were established based on the calculated compositions of individual signals and further confirmed by MS/MS analyses. It is noteworthy that most di- and tri-sialylated GSL were observed mostly at  $m/z$   $[M-H_2O-H]^-$  and  $[M-2H_2O-H]^-$  adducts, respectively (Table 1). MS/MS fragmentation analyses showed that dehydration of GSL resulted from the lactonization of oligosialic acids [17]. Examples of spectra obtained in Hs 578T and MDA-MB-231 GD3S+ clone #4 are presented in Figure 3. Mass spectra obtained for Hs 578T BC cell line led to the identification of GM3, GM2, GM1, OAcGM1, OAcGD2, and of trace amounts of GD2, OAcGD3, and OAcGT3 (Figure 3A). In MDA-MB-231 GD3S+ clone #4, GM3, GM2, GM1, GD3, GD2, GD1b, GT3, GT2, OAcGD3, OAcGD2, and OAcGT3 were detected (Figure 3B). These two cell lines exhibit similar expression patterns of gangliosides, but a cell-type dependent pattern of *O*-acetylated



gangliosides species (Figure 3). These two cell lines exhibit similar expression patterns of gangliosides, but a cell-type dependent pattern of *O*-acetylated gangliosides species (Figure 3).

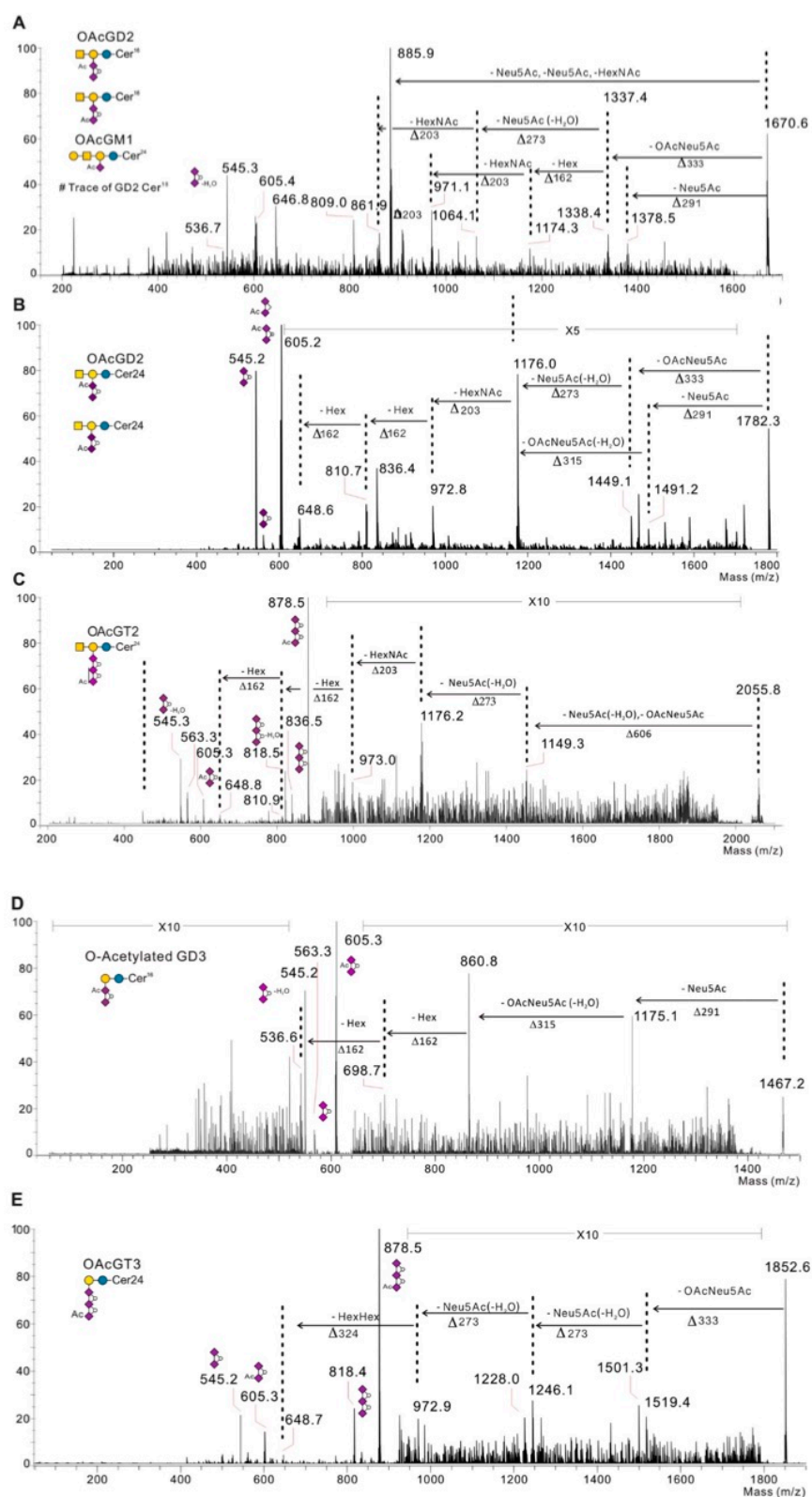


**Figure 3.** Gangliosides profiling by representative MS spectra in Hs 578T (A) and MDA-MB-231 GD3S+4 (B). Ceramide consists mainly of d18:1 long chain base and C16, C18, C24 either/both saturated or/and saturated fatty acids. Red signals identify acetylated gangliosides species and black signals non-acetylated forms of gangliosides species. The nature of long fatty acid chain is indicated in blue on the spectra. \* and \*\*\* indicates that GD2 Cer<sup>16</sup> and OAcGT3Cer<sup>16</sup> are respectively present in traces amount; \*\* indicates that signal corresponds to a mixture of OAcGM1Cer<sup>24</sup> with OAcGD2Cer<sup>18</sup>; \*\*\*\* indicates that signal corresponds to a mixture of GM2 with OAcGD3. Gangliosides are depicted according to the following: □, Ceramide; ●, Galactose; ●, Glucose; ■, N-acetyl-galactosamine; ◆, N-acetyl-neuraminic acid.


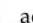
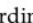
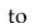
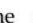
As depicted in Figure 4, MS/MS fragmentation has been performed for *O*-acetylated gangliosides so as to confirm signal identification, especially when one signal might correspond to two isobaric structures. Moreover, in the case of the identification of two species separately for one molecular ion by MS/MS fragmentation, the fragmentation allows the comparison of the relative amount of the two species characterized. For example, the fragmentation of the signal at *m/z* 1670 in Hs 578T confirmed the identification of the following two species: OAcGD2 (d18:1 Cer16:0) and OAcGM1 (d18:1 Cer24:0) (Figure 4A).

**Table 1.** List of identified gangliosides in neuroectoderm derived cells. Monosylalylated GSL are observed at  $[M-H]^-$ . Di- and trisialylated GSL were mainly observed at  $m/z$   $[M-H_2O-H]^-$  and  $[M-2H_2O-H]^-$ .  $\checkmark$  indicates the presence of GSL, and  $\checkmark$  T indicates that GSL is present in traces amount.

GSL	Fatty Acids	Monoisotopic Mass $[M-H]^-m/z$	Lactonization	SK-Mel-28	LAN-1	SUM 159 PT	Hs 578T	MDA-MB-231	MDA-MB-231 GD3S+ Clone #4	MDA-MB-231 GD3S+ Clone #11	MCF-7	MCF-7 GD3S+
GM3	C16	1151.7		$\checkmark$	$\checkmark$			$\checkmark$	$\checkmark$	$\checkmark$		
	C18	1179.7		$\checkmark$								
	C22	1235.8		$\checkmark$				$\checkmark$		$\checkmark$		
	C24	1263.8		$\checkmark$			$\checkmark$	$\checkmark$	$\checkmark$	$\checkmark$		
GM2	C16	1354.8		$\checkmark$	$\checkmark$	$\checkmark$	$\checkmark$	$\checkmark$	$\checkmark$	$\checkmark$	$\checkmark$	$\checkmark$
	C18	1382.8			$\checkmark$							
	C22	1438.9			$\checkmark$	$\checkmark$	$\checkmark$	$\checkmark$	$\checkmark$	$\checkmark$	$\checkmark$	$\checkmark$
	C24	1466.9			$\checkmark$	$\checkmark$	$\checkmark$	$\checkmark$	$\checkmark$	$\checkmark$		
GM1	C16	1516.8			$\checkmark$	$\checkmark$	$\checkmark$	$\checkmark$	$\checkmark$	$\checkmark$	$\checkmark$	
	C24	1629.0		$\checkmark$	$\checkmark$	$\checkmark$	$\checkmark$	$\checkmark$		$\checkmark$	$\checkmark$	$\checkmark$
LacNAcGM1	C16	1882.0			$\checkmark$							
GD3	C16	1424.8	-H <sub>2</sub> O	$\checkmark$	$\checkmark$							
	C16	1442.8		$\checkmark$								
	C18	1452.8	-H <sub>2</sub> O	$\checkmark$								
	C22	1508.9	-H <sub>2</sub> O	$\checkmark$						$\checkmark$		
	C24	1536.9	-H <sub>2</sub> O	$\checkmark$					$\checkmark$	$\checkmark$		
	C24	1554.9		$\checkmark$					$\checkmark$	$\checkmark$		
GD2	C16	1628.9	-H <sub>2</sub> O		$\checkmark$	$\checkmark$	$\checkmark$	$\checkmark$ T	$\checkmark$	$\checkmark$		$\checkmark$ T
	C18	1671.9		$\checkmark$	$\checkmark$				$\checkmark$	$\checkmark$		
	C24	1740.0	-H <sub>2</sub> O			$\checkmark$	$\checkmark$		$\checkmark$	$\checkmark$		
GD1b	C24	1902.1	-H <sub>2</sub> O						$\checkmark$	$\checkmark$		
GT3	C24	1810.0	-2H <sub>2</sub> O						$\checkmark$	$\checkmark$		
GT2	C24	2013.1	-2H <sub>2</sub> O						$\checkmark$	$\checkmark$		
OAcGM1	C24	1671					$\checkmark$		$\checkmark$			
OAcGD3	C14	1438.8	-H <sub>2</sub> O			$\checkmark$	$\checkmark$ T		$\checkmark$	$\checkmark$		
	C16	1466.8	-H <sub>2</sub> O	$\checkmark$		$\checkmark$	$\checkmark$ T					
	C24	1578.9	-H <sub>2</sub> O	$\checkmark$						$\checkmark$		
OAcGD2	C16	1670	-2H <sub>2</sub> O		$\checkmark$	$\checkmark$	$\checkmark$			$\checkmark$		$\checkmark$
	C24	1782	-H <sub>2</sub> O						$\checkmark$	$\checkmark$		
OAcGT3	C16	1740.0	-2H <sub>2</sub> O						$\checkmark$ T	$\checkmark$		$\checkmark$
	C24	1852.0	-2H <sub>2</sub> O						$\checkmark$	$\checkmark$		
OAcGT2	C24	2055.1							$\checkmark$	$\checkmark$		



**Figure 4.** Representative MS/MS fragmentation of the molecular ion corresponding to OAcGM1, OAcGD3, OAcGD2, OAcGT3, and OAcGT2. (A) MS/MS fragmentation of the molecular ion  $m/z$  1670 in Hs 578T corresponding to OAcGM1 and OAcGD2 ganglioside. MS/MS fragmentation of the

molecular ion  $m/z$  1782 (B)  $m/z$  2055 (C) respectively corresponding to OAcGD2 and OAcGT2 gangliosides in MDA-MB-231 GD3S + clone #4. (D) MS/MS fragmentation of the molecular ion  $m/z$  1467 corresponding to OAcGD3 identified in SK-Mel-28. (E) MS/MS fragmentation of the molecular ion  $m/z$  1852 corresponding to OAcGT3 identified in MDA-MB-231 GD3S+ clone #11. Gangliosides are indicated according to the following  Ceramide;  Galactose;  Glucose;  N-acetyl-galactosamine;  N-acetyl-neuraminic acid, ° dehydration Ac: O-acetyl group.

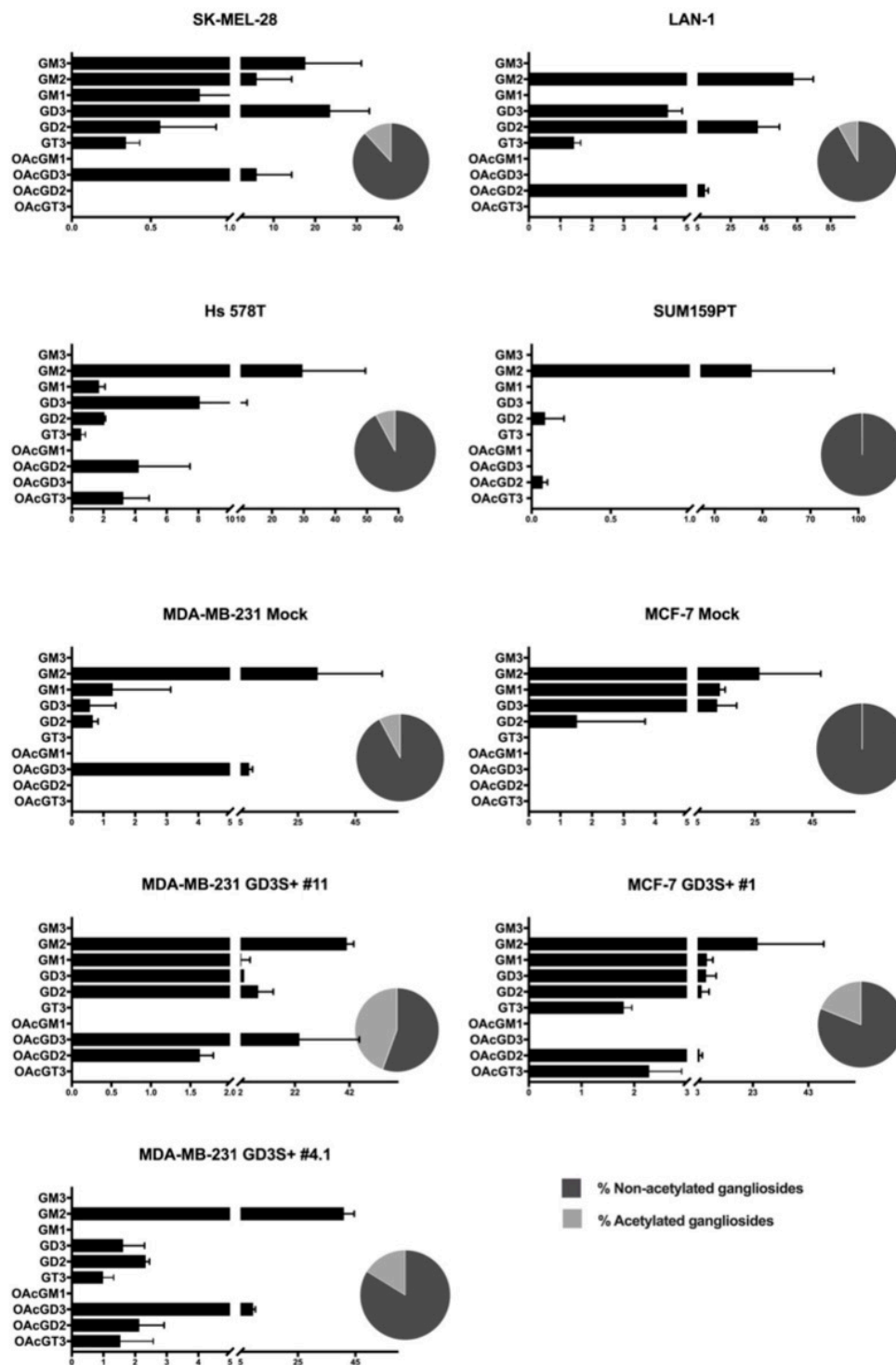
As depicted in Table I, our results indicate that the pattern of ganglioside O-acetylation is not representative of neuroectoderm derived cancer cells, but is cell type-dependent, while the representative pattern of expressed gangliosides is similar between the different cell lines. Basically, GM1, GM2, GM3, and GD2 are expressed in all cell lines tested. GD3 is expressed in SK-Mel-28, LAN1, MDA-MB-231 GD3S+ clone #4 and #11. GT3 and GT2 are expressed in MDA-MB-231 GD3S+ clone #4 and #11. Regarding O-acetylated gangliosides species pattern in cancer cell lines, OAcGD2 is expressed in all cell lines except SK-Mel-28, MDA-MB-231, and MCF-7. OAcGD3 is expressed in SK-Mel-28, LAN-1, Hs 578T, MDA-MB-231 GD3S+ clone #11, and MCF-7 GD3S+ clone #1. OAcGT3 and OAcGT2 are in turn expressed in MDA-MB-231 GD3 synthase overexpressing clones (Figure 5). The method used here led us to estimate the structure of sphingoid base and fatty acid chain according to the  $m/z$  detected for all ganglioside species identified. Most gangliosides exhibit a ceramide moiety corresponding to the combination of a long chain base sphingosine d18:1 and a fatty acid chain composed mainly by C16 or C24. C14, C18, and C22 are detected as minor components in cells. MCF-7 cell line displays variations on ceramide moiety as mixture of different combinations of the sphingosine base d18:1 and a highly hydroxylated ceramide (Supplementary Figure S1). Besides, C16 and C18 fatty acids are saturated, whereas C24 is always present in its saturated and unsaturated form (data not shown).

### 2.3. O-acetylated Ganglioside Species Expression Increases in GD3 Synthase Overexpressing Clones

The relative amounts of the different ganglioside species were calculated by integrating the intensity of individual signals detected on MALDI-QIT-TOF mass spectra. The proportion of O-acetylated gangliosides was 1% in SUM159PT, 9% in MDA-MB-231 and MCF-7, 10% in LAN-1 and Hs 578T, and 12% in SK-Mel-28 (Figure 5). The highest amounts of O-acetylated gangliosides were observed in clones over-expressing GD3 synthase in a cell dependent manner: 18% in MDA-MB-231 GD3S+ clone #4, 22% in MCF-7 GD3S+, and 50% in MDA-MB-231 GD3S+ clone #11. In parallel, we observed that OAcGD3 was the most expressed O-acetylated ganglioside species compared to OAcGD2 and OAcGT3. OAcGD3 expression was quantified as 23.6% of total gangliosides in MDA-MB-231 GD3S+ clone #11, 9.5% in MDA-MB-231 GD3S+ clone #4, 9% in MDA-MB-231 mock, 5.9% in SK-MEL-28. OAcGD2 expression remains lower than OAcGD3 content in all cell lines.

Besides the diversity observed for the position of the O-acetyl group on sialic acid, the O-acetylated ganglioside species expressed is cell line-dependent. OAcGD3 is the only O-acetylated ganglioside expressed by SK-Mel-28, MDA-MB-231, while OAcGD2 is solely expressed in LAN-1 and SUM159PT cells. In the other cancer cell lines, different combinations of O-acetylated gangliosides species are detected: OAcGD2 and OAcGT3 are detected in Hs 578T and MCF-7 GD3S+. MDA-MB-231 clone #11 express both OAcGD3 and OAcGD2, whereas MDA-MB-231 clone #4 shows the additional expression of OAcGD3, OAcGD2, and OAcGT3. Interestingly, GD3 synthase over-expression in MDA-MB-231 does not result in the expression of the same O-acetylated species expressed by the two clones. Moreover, OAcGD2 was not detected in MDA-MB-231 and MCF-7, but only in their clones over-expressing GD3 synthase, with a respective 2 and 3 fold increase, confirming our previous results [12]. OAcGT3 was the O-acetylated ganglioside species present in lowest amounts and was mostly present in Hs 578T (3.2%) and MDA-MB-231 clone #4 (1.5%) (Figure 5). OAcGT2 expression was confirmed using MS/MS fragmentation in MDA-MB-231 GD3S+ clone #4. However, signals assigned for OAcGT2 were too weak and could not be included in the relative quantification process.

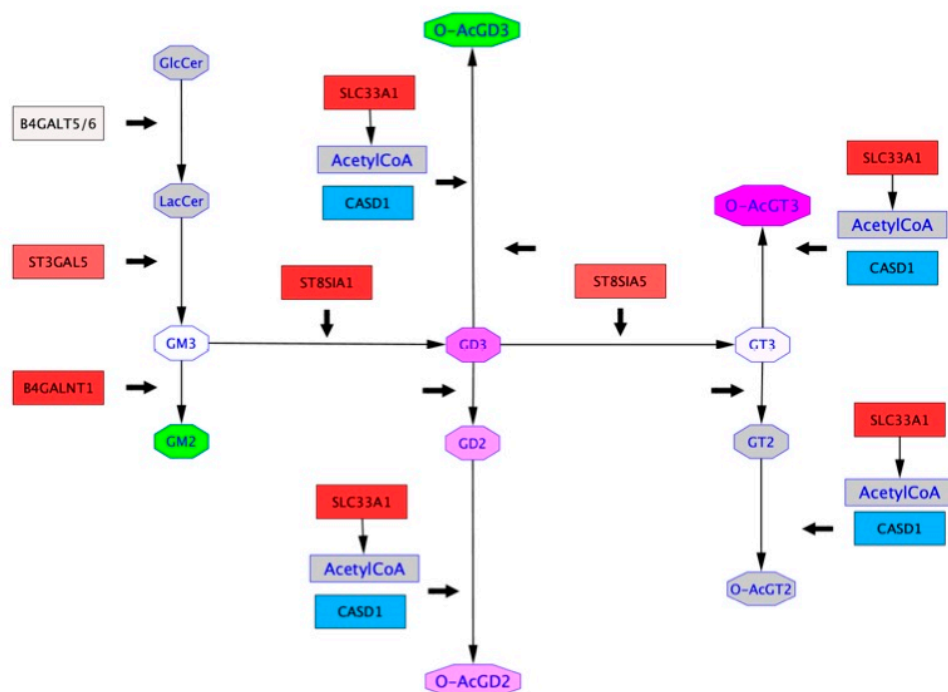




**Figure 5.** Relative quantification of the global content of main ganglioside species by MALDI-QIT-TOF. Relative quantification of ganglioside content of the apex intensities (mV) of the peak assigned on MALDI-QIT-TOF spectra ( $n = 3$ ). Total ganglioside content was normalized to 100 for each cell line. The relative amount of each species is calculated as the percentage of the total ganglioside content. The pie charts represent the percentage of total acetylated gangliosides (light grey) vs. non-acetylated (dark grey).

#### 2.4. Mapping of GTs Gene Expression and Gangliosides Content on a Ganglioside Metabolism Pathway

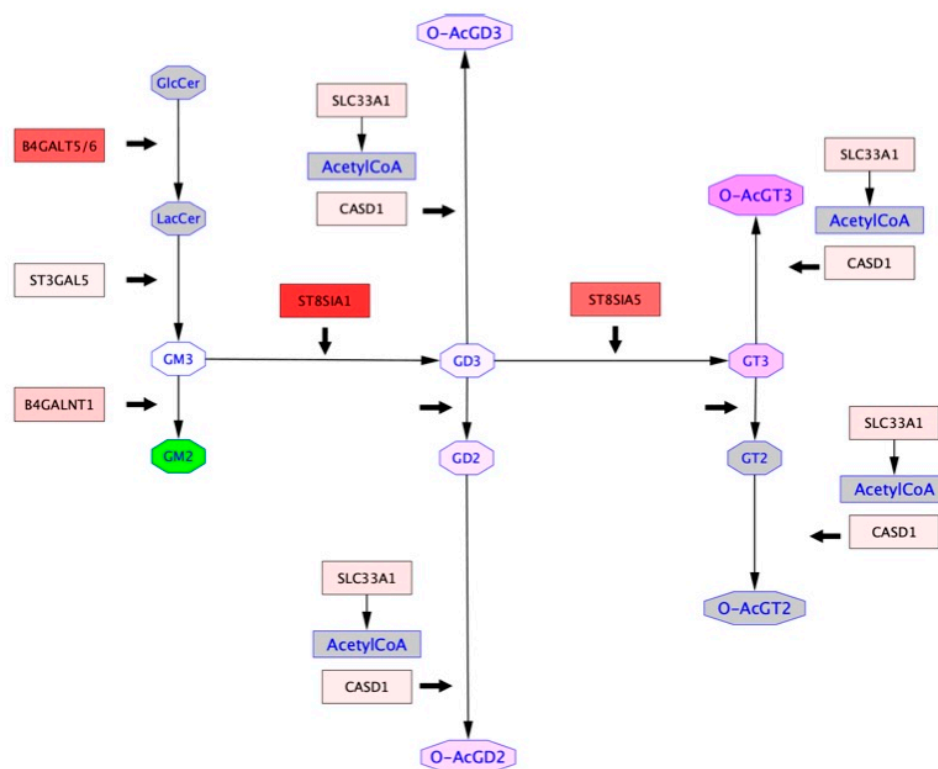
In order to get an insight on ganglioside expression and biosynthesis mechanisms in cancer cells, we performed *in silico* analysis. Differential expression of genes encoding GTs and gangliosides were mapped onto a subpart of “Ganglio-sphingolipid metabolism” pathway retrieved from WikiPathway in Hs 578T vs. MDA-MB-231 cells (Figure 6) and in MDA-MB-231 vs. MDA-MB-231 GD3S+ cells (Figure 7). These representations ensure the combination of GTs gene expression and ganglioside content obtained respectively by qPCR and MALDI-QIT-TOF in one biosynthetic scheme. Thus, gene expression of *B4GALT6*, *ST3GAL5*, *ST8SIA1*, *B4GALNT1*, and *ST8SIA5* encoding GTs involved in gangliosides biosynthesis assessed by qPCR experiments in each cell line. Besides, *SCL33A1* and *CASD1* gene expression were analyzed by qPCR. These two genes were selected for their potential implication in ganglioside *O*-acetylation, respectively encoding the acetyl coenzyme 1 Golgi transporter and the only known human SOAT (Supplementary Figure S3). Our results highlight the upregulation of *ST3GAL5*, *B4GALNT1*, *ST8SIA1*, *ST8SIA5*, and *SCL33A1*, and the downregulation of *CASD1* in Hs 578T compared to MDA-MB-231 (Figure 6). All genes assessed by qPCR were up-regulated in MDA-MB-231 GD3S+ vs. MDA-MB-231 (Figure 7). These results highlight the repression of *CASD1* in Hs 578T compared to MDA-MB-231 cells, but the upregulation of *CASD1* in MDA-MB-231 GD3S+ compared to MDA-MB-231 cells.



**Figure 6.** Differential ganglioside metabolism pathways between Hs 578T and MDA-MB-231 breast cancer cells. Glycosyltransferase gene expression profile obtained by qPCR were mapped onto a subpart of the “Ganglio-sphingolipid metabolism” pathway from WikiPathways [18,19] based on the differential expression between two cell lines. In the squared nodes, colors vary from blue ( $\leq -2$ ) to white ( $= 0$ ) and red ( $\geq 2$ ) to indicate the repression to the over-expression of the glycosyltransferase gene in Hs 578T compared to MDA-MB-231 cells (thick black arrows). Quantitative data concerning the relative amounts of gangliosides obtained by MALDI-QIT-TOF mass spectrometry were added to the pathway based on the comparison between Hs 578T and MDA-MB-231 cells. In the octagonal nodes, colors vary from green ( $\leq -8$ ) to white ( $= 0$ ) and fuchsia ( $\geq 8$ ) to indicate a restraint to a rise of the amount of a given ganglioside based on the differences observed between the two cell lines. Grey color indicates the absence of any available quantitative data about the expression.



Ganglioside proportions defined by MALDI-QIT-TOF analysis were also mapped onto these pathways to represent the differential ganglioside expression in Hs 578T vs. MDA-MB-231, and in MDA-MB-231 GD3S+ vs. MDA-MB-231. The differential ganglioside expression analysis brings out the upregulation of OAcGD2 and OAcGT3 and the downregulation of OAcGD3 in Hs578T compared to MDA-MB-231. In contrast, the same analysis highlights the upregulation of OAcGT3, OAcGD3, and OAcGD2 in MDA-MB-231 GD3S+ vs. MDA-MB-231 (Figure 7). These analyses reveal the upregulation of GD3, GD2, and GT3 in both pathways. The levels of gangliosides upregulation in Hs578T vs. MDA-MB-231 are higher than those identified in MDA-MB-231 GD3S+ vs. MDA-MB-231 (Figures 6 and 7). The combinatorial approach that we used allows to perceive the relationships between gangliosides expressed and GTs gene expression between two cell lines. In both cases (Hs 578T vs. MDA-MB-231, and MDA-MB-231 GD3S+ vs. MDA-MB-231), O-acetylated gangliosides appear to be upregulated independently of CASD1 expression variations between two cell lines, and in a substrate-dependent manner. O-acetylated ganglioside expression appears not only dependent on the expression level of enzymes involved in the biosynthesis of gangliosides, but also on substrate availability.



**Figure 7.** Differential ganglioside metabolism pathways between MDA-MB-231 GD3S+ clone #4 and MDA-MB-231 breast cancer cells. Glycosyltransferase gene expression profile obtained by qPCR were mapped onto a subpart of the “Ganglio-sphingolipid metabolism” pathway from WikiPathways [18,19] based on the differential expression between two cell lines. In the squared nodes, colors vary from blue ( $\leq -2$ ) to white ( $= 0$ ) and red ( $\geq 2$ ) to indicate the repression to the over-expression of the glycosyltransferase gene in MDA-MB-231 GD3S+ clone #4 compared to MDA-MB-231 cells (thick black arrows). Quantitative data concerning the relative amounts of gangliosides obtained by MALDI-QIT-TOF mass spectrometry were added to the pathway based on the comparison between MDA-MB-231 GD3S+ clone #4 and MDA-MB-231 cells. In the octagonal nodes, colors vary from green ( $\leq -8$ ) to white ( $= 0$ ) and fuchsia ( $\geq 8$ ) to indicate a restraint to a rise of the amount of a given ganglioside based on the differences observed between the two cell lines. Grey color indicates the absence of any available quantitative data about the expression.

### 3. Discussion

For almost 50 years, profiling gangliosides expression in developmental and pathological conditions has been of high interest for their remarkable roles in oncogenesis and neurodegenerative diseases, in which gangliosides are considered as useful and promising diagnostic and prognostic tools, as well as targets for immunotherapy, especially in the field of neuroectoderm-related cancers (melanoma, neuroblastoma, small cell lung cancer) [20,21]. As an example, anti-GD2 clinical trials for neuroblastoma have confirmed the efficacy of anti-GD2 antibody immunotherapy for this rare but often lethal childhood cancer [22]. Different experimental approaches were developed to get more precise information about the structure of gangliosides from various biological samples. Basically, immunodetection methods and mass spectrometry are currently the major tools for ganglioside analysis. While immunodetection is based on in situ detection, mass spectrometry requires the extraction of gangliosides from biological samples before the analysis. Recently, the combination of these two detection methods has allowed a lot of progress regarding ganglioside profiling in sera [23,24], tissues [25], or cellular extracts [26]. Besides, *O*-acetylation of the sialic acid residues is one of the most common modifications of gangliosides and is sufficient to induce dramatic changes of physiopathological properties carried by the native non-*O*-acetylated gangliosides. For example, *O*-acetylation relocates GD3 from the mitochondria to the cell membrane, inducing the suppression of GD3 apoptotic effect in cancer cells [11,27,28]. Interestingly, targeting OAcGD2 rather than GD2 in cancer therapy seems to be a better option since OAcGD2 is exclusively expressed in cancer tissues [7].

The *O*-acetyl group is alkali labile, rendering it very difficult to handle for mass spectrometry analysis. Thus, immunodetection methods such as TLC, FACS, or immunocytochemistry followed by confocal microscopy were mainly used for the identification and quantification of *O*-acetylated gangliosides species [14]. Using the immunodetection methods mentioned above, we previously identified the expression of OAcGD2, but not OAcGD3 in BC cells [12]. However, the absence of OAcGD3 in BC cells was not confirmed in this work [12]. Indeed, native gangliosides extracted from the same cell lines were positive for OAcGD3 expression, indicating that the anti-OAcGD3 7H2 mouse IgG3 (Santa-Cruz biotechnology, Dallas, TX, USA) used in our previous study was not suitable for the identification of OAcGD3 by FACS as well as immunocytochemistry procedures. Besides the properties and specificity of anti-ganglioside antibodies, the accessibility of the target is also a major limitation since gangliosides are located in lipid rafts, surrounded by cholesterol and glycoproteins enhancing the steric hindrance, and the accessibility of gangliosides at the surface of BC cells may be an issue. Furthermore, antibodies targeting *O*-acetylated species may cross react and detect more than one species at a time like 493D4 [25], Jones antibody [29], A2B5 [30] targeting either OAcGD3/OAcGT3 either OAcGT2.

Brain tissue is the major biological material used for the analysis of *O*-acetylated ganglioside species. For example, OAcGT2 has been detected in cod brain by TLC and mass spectrometry combining mild alkaline treatment [31]. In bovine brain, OAcGD3 and OAcGT3 were identified as major acetylated species [25], and enhanced OAcGT3 was also identified in cultured glial cells [30]. OAcGD3 is also considered as an oncofetal marker in human melanoma [32]. The presence of OAcGD3 was also reported in tumors from neuroectodermal origin [33], childhood lymphoblastic leukemia [34], and glioblastoma [35]. The expression of *O*-acetylated gangliosides was poorly studied in breast cancer; a single article reports OAcGD3 and OAcGT3 expression in BC tissues using GMR2 and 493D4 mouse antibodies and TLC analysis [36]. However, some ambiguity remains because *O*-acetylated gangliosides analysis in cells and tissues was mostly performed using antibodies more or less specific of *O*-acetylated forms, some of them cross reacting with *O*-acetylated and non-*O*-acetylated ganglioside species. Here, OAcGM1, OAcGD3, OAcGD2, OAcGT2, OAcGT3 were identified as native gangliosides by mass spectrometry in neuroectoderm derived-cell lines. Besides, MS/MS fragmentation defined that *O*-acetylation occurs on both inner or terminal sialic acid residues. Furthermore, Neu5,9Ac was the main sialic acid species expressed among glycolipids, confirming our previous study [12]. *O*-acetylated gangliosides species were fully characterized in terms of ganglioside species and position of *O*-acetylated group on the sialic acid residues, revealing

a cell-type dependent profile. Interestingly, clones over-expressing GD3 synthase showed an increased expression of complex non-acetylated and *O*-acetylated gangliosides, highlighting again the key role of GD3 synthase for b- and c-series gangliosides expression. Substrate availability is the second parameter, which drives *O*-acetylated gangliosides expression. If high amounts of precursor gangliosides are expressed, they can potentially serve for the biosynthesis of *O*-acetylated gangliosides.

*O*-acetylation of sialic acid is highly dependent on the balance between SOAT and Sialyl-*O*-acetyl-esterase (SIAE) activity. These activities are finely tuned processes, resulting in a cell type dependent pattern of *O*-acetylated gangliosides species. Recently, Mlinac et al. suggested that SIAE-induced deacetylation of GD3 increases medulloblastoma sensitivity to etoposide. The concept used in the paper was based on recovering the pro-apoptotic role of mitochondrial GD3 by deacetylation of OAcGD3. Besides, they showed a higher expression of SIAE in medulloblastoma compared to normal cerebellum [37]. These data seem contradictory, but they give an important insight on the complexity of the processes regulating the expression and the role of OAcGD3 and GD3 in cancer tissues. SOAT activity was closely related to *O*-acetylated gangliosides expression. Indeed, reduced SOAT activity decreased *O*-acetylated gangliosides, while increased SOAT activity upregulated *O*-acetylated gangliosides expression [38,39]. Despite all the attempts made for the purification of SOAT, a single human SOAT encoded by *CASD1* has been identified [40]. *CASD1* is Golgi spanning multimembrane protein, which induces the *O*-acetylation of CMP-sialic acid and is involved in GD3 *O*-acetylation [13]. Here, we show that *O*-acetylation of gangliosides is not dependent on the level of *CASD1*, but much more dependent on the availability of ganglioside substrate and acetyl-CoA availability as underlined by the acetyl-CoA transporter SLC33A1 upregulation, regardless of the BC cell lines. However, the validation of this concept would require transfection experiments to modulate the expression of SLC33A1 or *CASD1* in these cell lines.

This work highlights the cell-type dependent pattern of *O*-acetylated gangliosides species expressed by neuroectoderm-derived cell lines. Performing similar analyses in normal and cancer tissues is the next essential step to determine to what extent specific *O*-acetylated gangliosides are tumor-specific antigens and promising targets for neuroectoderm-derived tumors immunotherapy.

#### 4. Materials and Methods

##### 4.1. Cell Culture

The human breast cancer cells Hs 578T, MDA-MB-231, MCF-7, SUM159PT, and the melanoma cell line SK-MEL-28 were obtained from the American Tissue Culture Collection (ATCC, Rockville, MD, USA). The neuroblastoma cell line LAN-1 was obtained by Deutsche Sammlung von Mikroorganismen und Zellkulturen GmbH (DSMZ, Leibniz Institute, Braunschweig, Germany). LAN-1 cells were cultured and maintained in Rosewall Park Memorial Institute medium 1640 (RPMI) containing 10% heat-inactivated fetal calf serum, 2 mmol/L L-glutamine, and 100 units/mL penicillin-streptomycin. MCF-7 and MDA-MB-231 clones over-expressing GD3 synthase were obtained as described [41]. All BC cell lines and the melanoma cell line SK-MEL-28 were cultured as previously described [12].

##### 4.2. RNA Extraction and Quantitative Real Time Polymerase Chain Reaction

The extraction of total RNA from different cell lines was performed using Nucleospin RNA II kit (Macherey-Nagel, Düren, Germany). Extracted RNA was quantified using DeNovix DS-11 spectrophotometer (DeNovix Inc., Wilmington, DE, USA). Reverse transcription of purified RNA was performed using the Maxima First Strand cDNA Synthesis Kit (Thermo Fisher Scientific, Villeneuve d'Ascq, France) according to the protocol provided by the manufacturer. The oligonucleotide sequences (Eurogentec, Seraing, Belgium) used for PCR reactions are the following primer pairs: 5'-ctg-gga-gga-aac-tgg-cct-tc-3' and 5'-agg-gct-gta-aca-cat-gag-cc-3' (*SLC33A1*), 5'-gtg-gat-ttt-ctg-tgg-atc-c-3' and 5'-aag-cgc-ttc-act-gct-acc-at-3' (*CASD1*), 5'-tat-gtg-ctg-tca-gcg-tct-gct-3' and 5'-aca-aag-aca-tcc-tct-aat-ggg-aga-a-3' (*B3GALT4*),

5'-gtg-gat-ttt-ctg-tgg-cat-cc-3' and 5'-aag-gcg-ttc-act-gct-acc-at-3'(ST8SIA5). PCR reactions were processed using Mx3005p Quantitative System (Stratagene, La Jolla, CA, USA) using 2X Brilliant SYBR Green qPCR Mastermix (Thermo Fisher Scientific, Villeneuve d'Ascq, France) in 300 nM of primers and 4 µL cDNA as previously described [12]. All experiments were performed in triplicate.

#### 4.3. DMB Derivatization of Sialic Acids

Cells were suspended in PBS and centrifuged 15 min at 4000 rpm. Pellets were sequentially extracted by CHCl<sub>3</sub>/CH<sub>3</sub>OH (2/1; v/v) and CHCl<sub>3</sub>/CH<sub>3</sub>OH/H<sub>2</sub>O (1/2/0.8; v/v/v). Pellets contained membrane associated glycoproteins, whereas supernatants contained the ganglioside fractions. Supernatants were precipitated with ice cold 100% ethanol overnight and centrifuged 5 min at 10,000× g. Supernatants contained free sialic acids, whereas pellets contained soluble proteins [42]. Dried pellets of BC cell lines were hydrolyzed at 80 °C for 4 h in 4 M propionic acid and then precipitated in 4 volumes of 100% ethanol. Hydrolyzed sialic acids were subsequently coupled to 1,2-diamino-4,5-methylenedioxybenzene dihydrochloride (DMB). Samples were heated at 50 °C for 2 h in the dark in 7 mM DMB, 1 M β-mercaptoethanol, 18 mM sodium hydrosulfite in 5 mM acetic acid [43]. Sialic acids coupled to DMB (DMB-Sia) were then analyzed by LC-MS.

#### 4.4. Quantitation Analysis of DMB-Sia on Micro-LC/ESI-MS3

Quantitative analyses were performed in positive ion mode on an amaZon speed ETD ion trap mass spectrometer equipped with the standard electrospray ionization (ESI) ion source and controlled by Hystar 3.2 software (Bruker Daltonics, Billerica, MA, USA). DMB-coupled sialic acid separation was achieved on micro LC system (Prominence LC-20AB, Shimadzu, Kyoto, Japan). 5 µL of samples were applied to the reversed-phase Luna C18-2 column (150 × 1.00 mm, 3 µm particles, Phenomenex, Torrance, CA, USA) with an isocratic elution of CH<sub>3</sub>CN/CH<sub>3</sub>OH/H<sub>2</sub>O (6/4/90; v/v/v) at a flow rate of 70 µL/min. The targeted MS3 scans for DMB-coupled sialic acid were performed using an ultrascan mode (26,000 amu/s). Data obtained for external standards run on the same time were used for estimation of DMB-Sia amounts in BC cell line our BC cell lines samples. Sialic acid species were identified by referring to elution positions and MS<sub>3</sub> fragmentation of Neu5Ac and Neu5,9Ac<sub>2</sub> standards. The reported values were based on signal area of the single ion chromatogram at the appropriate retention time [44].

#### 4.5. Extraction of Native Gangliosides

Cell were suspended in PBS and centrifuged at 4,000 rpm during 15 min. Pellets were extracted thrice by 2 volumes of CHCl<sub>3</sub>/CH<sub>3</sub>OH (2/1; v/v) and 1 volume CHCl<sub>3</sub>/CH<sub>3</sub>OH/H<sub>2</sub>O (1/2/0.8; v/v/v). Supernatants were collected and dried gently under N<sub>2</sub> stream. Glycosphingolipids were separated from other lipids and from hydrophilic components on a tC<sub>18</sub> cartridge Sep-Pak connected to QMA Sep-Pak cartridge (Waters, St Quentin Yvelines, France) equilibrated in CH<sub>3</sub>OH/CF<sub>3</sub>COOH/H<sub>2</sub>O (1/0.1/1; v/v/v) by extensive washing. Neutral glycosphingolipids were eluted in 2 volumes of CH<sub>3</sub>OH. Acidic glycosphingolipids were eluted twice in CH<sub>3</sub>OH/CH<sub>3</sub>COONH<sub>4</sub> (1/1; v/v) within 0.05 M, 0.15 M, and 0.45 M CH<sub>3</sub>COONH<sub>4</sub> sequentially in 1 volume each. Neutral and acidic glycosphingolipids were dried gently under N<sub>2</sub> stream. Acidic glycosphingolipids were separated from ammonium acetate on a tC<sub>18</sub> cartridges Sep-pack (Waters, St Quentin Yvelines, France) equilibrated in CH<sub>3</sub>OH/CF<sub>3</sub>COOH/H<sub>2</sub>O mixture (1/0.1/1; v/v/v) by extensive washing. Acidic glycosphingolipids were eluted in 2 volumes of CH<sub>3</sub>OH and dried under N<sub>2</sub> stream before reconstitution in CHCl<sub>3</sub>/CH<sub>3</sub>OH (1/2; v/v) and analysis on MALDI-QIT-TOF.

#### 4.6. Mass Spectrometry Analysis

Acidic glycosphingolipids were analyzed by an MALDI-QIT-TOF Shimadzu AXIMA Resonance mass spectrometer (Shimadzu Europe, Manchester, UK) in the negative mode. Samples were prepared by mixing directly on the target 0.5 µL of acidic glycosphingolipid sample with 0.5 µL 2'-4'-6'-trihydroxyacetophenone monohydrate matrix solution (0.5 M in EtOH) containing by 0.1



M hydrated di-ammonium hydrogen citrate mixture (2/1; v/v). The mid mode for a mass range  $m/z$  1500–3000 was used and laser power was set to 100 2 shots each in 200 locations per spot.

#### 4.7. In Silico Mapping of Glycosyltransferase Gene Expression and Ganglioside Species Quantification

The pathway was retrieved from WikiPathways [18] using the WikiPathways app [19] for Cytoscape [45], the “Ganglio Sphingolipid Metabolism” pathway for *Homo sapiens* was used as a basis. Only a subpart was conserved and enriched with some metabolites and genes. For each figure, qPCR data were mapped onto the genes of the pathway, calculating the log2 ratio of expression of one condition and a second one; colors vary from blue ( $\leq -2$ ) to white ( $= 0$ ) and red ( $\geq 2$ ). Relative quantity amounts of gangliosides measured in MALDI-QIT-TOF mass spectroscopy were also mapped onto the gangliosides in the pathway, calculating the difference in signals between two conditions; colors vary from green ( $\leq -8$ ) to white ( $= 0$ ) and fuchsia ( $\geq 8$ ).

**Supplementary Materials:** Supplementary Materials can be found at [www.mdpi.com/xxx/s1](http://www.mdpi.com/xxx/s1).

**Author Contributions:** Conceptualization, S.C. and Y.G.; methodology, K.A., Y.G., G.B., and N.Y.; software, N.Y. and G.B.; validation, N.Y., Y.G., and P.D.; formal analysis, S.C. and C.C.; investigation, S.C.; resources, S.C. and C.C.; data curation, S.C.; writing—original draft preparation, S.C.; writing—review and editing, S.C., Y.G., S.G.-D., and P.D.; visualization, S.C. and N.Y.; supervision, S.G.-D. and P.D.; project administration, S.C.; funding acquisition, J.-M.L.D. All authors have read and agreed to the published version of the manuscript.

**Funding:** This research received no external funding.

**Acknowledgments:** We are indebted to the PAGés platform (Plateforme d’ Analyses des Glycoconjugués, CNRS, UMR 8576, UGSF, Université de Lille), F-59000 Lille, France for the use of mass spectrometry facilities.

**Conflicts of Interest:** The authors declare no conflict of interest.

#### Abbreviations

BC	Breast Cancer
GlcCer	Glucosylceramide
LacCer	Lactosylceramide
LC-ESI/MS	Liquid Chromatography Electrospray Ionisation/Mass Spectrometry
Neu5,9Ac <sub>2</sub>	9-O-acetyl-N-acetylneuraminic acid
OAcGD2	O-acetylated GD2
OAcGD3	O-acetylated GD3
RPLC-MS	Reverse-Phase Liquid Chromatography Mass Spectrometry
SCLC	Small Cell Lung Carcinoma
SOAT	Sialyl-O-acetyltransferase
SIAE	Sialyl-O-acetyltransferase
TACA	Tumor Associated Carbohydrate Antigen
TLC	Thin Layer Chromatography

#### References

1. Hakomori, S. Aberrant glycosylation in cancer cell membranes as focused on glycolipids: Overview and perspectives. *Cancer Res.* **1985**, *45*, 2405–2414.
2. Julien, S.; Bobowski, M.; Steenackers, A.; Le Bourhis, X.; Delannoy, P. How Do Gangliosides Regulate RTKs Signaling? *Cells* **2013**, *2*, 751–767.
3. Cazet, A.; Bobowski, M.; Rombouts, Y.; Lefebvre, J.; Steenackers, A.; Popa, I.; Guérardel, Y.; Le Bourhis, X.; Tulasne, D.; Delannoy, P. The ganglioside G(D2) induces the constitutive activation of c-Met in MDA-MB-231 breast cancer cells expressing the G(D3) synthase. *Glycobiology* **2012**, *22*, 806–816.
4. Yoshida, S.; Fukumoto, S.; Kawaguchi, H.; Sato, S.; Ueda, R.; Furukawa, K. Ganglioside G(D2) in small cell lung cancer cell lines: Enhancement of cell proliferation and mediation of apoptosis. *Cancer Res.* **2001**, *61*, 4244–4252.






5. Furukawa, K.; Hamamura, K.; Aixinjueluo, W.; Furukawa, K. Biosignals modulated by tumor-associated carbohydrate antigens: Novel targets for cancer therapy. *Ann. N. Y. Acad. Sci.* **2006**, *1086*, 185–198.
6. Dhillon, S. Dinutuximab: First global approval. *Drugs* **2015**, *75*, 923–927.
7. Alvarez-Rueda, N.; Desselle, A.; Cochonneau, D.; Chaumette, T.; Clemenceau, B.; Leprieur, S.; Bougras, G.; Supiot, S.; Mussini, J.-M.; Barbet, J.; et al. A Monoclonal Antibody to O-Acetyl-GD2 Ganglioside and Not to GD2 Shows Potent Anti-Tumor Activity without Peripheral Nervous System Cross-Reactivity. *PLoS ONE* **2011**, *6*, e25220. doi:10.1371/journal.pone.0025220.
8. Terme, M.; Dorvillius, M.; Cochonneau, D.; Chaumette, T.; Xiao, W.; Diccianni, M.B.; Barbet, J.; Yu, A.L.; Paris, F.; Sorkin, L.S.; et al. Chimeric antibody c8B6 to O-acetyl-GD2 mediates the same efficient anti-neuroblastoma effects as therapeutic ch14.18 antibody to GD2 without antibody induced allodynia. *PLoS ONE* **2014**, *9*, e87210.
9. Cochonneau, D.; Terme, M.; Michaud, A.; Dorvillius, M.; Gautier, N.; Frikeche, J.; Alvarez-Rueda, N.; Bougras, G.; Aubry, J.; Paris, F.; et al. Cell cycle arrest and apoptosis induced by O-acetyl-GD2-specific monoclonal antibody 8B6 inhibits tumor growth in vitro and in vivo. *Cancer Lett.* **2013**, *333*, 194–204.
10. Kniep, B.; Kniep, E.; Ozkucur, N.; Barz, S.; Bachmann, M.; Malisan, F.; Testi, R.; Rieber, E.P. 9-O-acetyl GD3 protects tumor cells from apoptosis. *Int. J. Cancer* **2006**, *119*, 67–73.
11. Malisan, F.; Franchi, L.; Tomassini, B.; Ventura, N.; Condò, I.; Rippo, M.R.; Rufini, A.; Liberati, L.; Nachtigall, C.; Kniep, B.; et al. Acetylation suppresses the proapoptotic activity of GD3 ganglioside. *J. Exp. Med.* **2002**, *196*, 1535–1541.
12. Cavdarli, S.; Dewald, J.H.; Yamakawa, N.; Guérardel, Y.; Terme, M.; Le Doussal, J.-M.; Delannoy, P.; Groux-Degroote, S. Identification of 9-O-acetyl-N-acetylneuraminic acid (Neu5,9Ac2) as main O-acetylated sialic acid species of GD2 in breast cancer cells. *Glycoconj. J.* **2019**, *36*, 79–90.
13. Baumann, A.-M.T.; Bakkers, M.J.G.; Buettner, F.F.R.; Hartmann, M.; Grove, M.; Langereis, M.A.; de Groot, R.J.; Mühlhoff, M. 9-O-Acetylation of sialic acids is catalysed by CASD1 via a covalent acetyl-enzyme intermediate. *Nat. Commun.* **2015**, *6*, 7673.
14. Mandal, C.; Schwartz-Albiez, R.; Vlasak, R. Functions and Biosynthesis of O-Acetylated Sialic Acids. *Top. Curr. Chem.* **2015**, *366*, 1–30.
15. Ravindranath, M.H.; Higa, H.H.; Cooper, E.L.; Paulson, J.C. Purification and characterization of an O-acetylsialic acid-specific lectin from a marine crab *Cancer antennarius*. *J. Biol. Chem.* **1985**, *260*, 8850–8856.
16. Sharma, V.; Chatterjee, M.; Mandal, C.; Sen, S.; Basu, D. Rapid diagnosis of Indian visceral leishmaniasis using alectinH, a 9-O-acetylated sialic acid binding lectin. *Am. J. Trop. Med. Hyg.* **1998**, *58*, 551–554.
17. Sugiyama, E.; Hara, A.; Uemura, K.; Taketomi, T. Application of matrix-assisted laser desorption/ionization time-of-flight mass spectrometry with delayed ion extraction to ganglioside analyses. *Glycobiology* **1997**, *7*, 719–724.
18. Slenter, D.N.; Kutmon, M.; Hanspers, K.; Riutta, A.; Windsor, J.; Nunes, N.; Mélius, J.; Cirillo, E.; Coort, S.L.; Digles, D.; et al. WikiPathways: A multifaceted pathway database bridging metabolomics to other omics research. *Nucleic Acids Res* **2018**, *46*, D661–D667.
19. Kutmon, M.; Lotia, S.; Evelo, C.T.; Pico, A.R. WikiPathways App for Cytoscape: Making biological pathways amenable to network analysis and visualization. *F1000Research* **2014**, *3*, 152.
20. Krenzel, U.; Bousquet, P.A. Molecular recognition of gangliosides and their potential for cancer immunotherapies. *Front. Immunol.* **2014**, *5*, 325.
21. Rabu, C.; McIntosh, R.; Jurasova, Z.; Durrant, L. Glycans as targets for therapeutic antitumor antibodies. *Future Oncol.* **2012**, *8*, 943–960.
22. Modak, S.; Cheung, N.-K.V. Disialoganglioside directed immunotherapy of neuroblastoma. *Cancer Invest.* **2007**, *25*, 67–77.
23. Fuller, M.; Duplock, S.; Hein, L.K.; Rigat, B.A.; Mahuran, D.J. Liquid chromatography/electrospray ionisation-tandem mass spectrometry quantification of GM2 gangliosides in human peripheral cells and plasma. *Anal. Biochem.* **2014**, *458*, 20–26.
24. Busch, C.M.; Desai, A.V.; Moorthy, G.S.; Fox, E.; Balis, F.M. A validated HPLC-MS/MS method for estimating the concentration of the ganglioside, GD2, in human plasma or serum. *J. Chromatogr. B Anal. Technol. Biomed. Life Sci.* **2018**, *1102–1103*, 60–65. doi: 10.1016/j.jchromb.2018.10.010.
25. Zhang, G.; Ji, L.; Kurono, S.; Fujita, S.C.; Furuya, S.; Hirabayashi, Y. Developmentally regulated O-acetylated sialoglycans in the central nervous system revealed by a new monoclonal antibody 493D4 recognizing a wide range of O-acetylated glycoconjugates. *Glycoconj. J.* **1997**, *14*, 847–857.

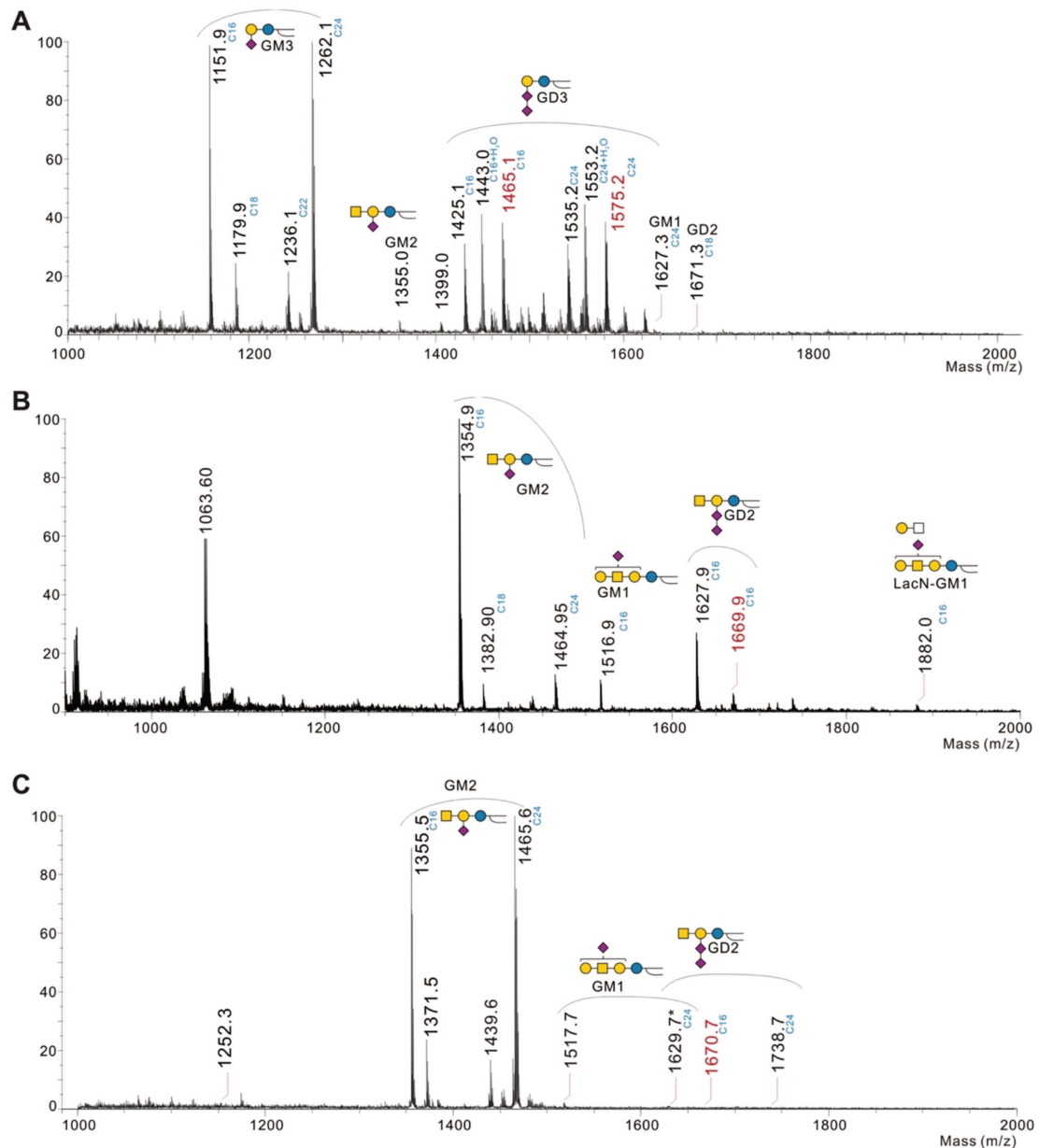


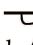

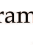
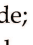

26. Rossdam, C.; Konze, S.A.; Oberbeck, A.; Rapp, E.; Gerardy-Schahn, R.; von Itzstein, M.; Buettner, F.F.R. Approach for Profiling of Glycosphingolipid Glycosylation by Multiplexed Capillary Gel Electrophoresis Coupled to Laser-Induced Fluorescence Detection to Identify Cell-Surface Markers of Human Pluripotent Stem Cells and Derived Cardiomyocytes. *Anal. Chem.* **2019**, *91*, 6413–6418.
27. Kristal, B.S.; Brown, A.M. Apoptogenic ganglioside GD3 directly induces the mitochondrial permeability transition. *J. Biol. Chem.* **1999**, *274*, 23169–23175.
28. Sa, G.; Das, T.; Moon, C.; Hilston, C.M.; Rayman, P.A.; Rini, B.I.; Tannenbaum, C.S.; Finke, J.H. GD3, an overexpressed tumor-derived ganglioside, mediates the apoptosis of activated but not resting T cells. *Cancer Res.* **2009**, *69*, 3095–3104.
29. Constantine-Paton, M.; Blum, A.S.; Mendez-Otero, R.; Barnstable, C.J. A cell surface molecule distributed in a dorsoventral gradient in the perinatal rat retina. *Nature* **1986**, *324*, 459–462.
30. Farrer, R.G.; Quarles, R.H. GT3 and its O-acetylated derivative are the principal A2B5-reactive gangliosides in cultured O2A lineage cells and are down-regulated along with O-acetyl GD3 during differentiation to oligodendrocytes. *J. Neurosci. Res.* **1999**, *57*, 371–380.
31. Waki, H.; Masuzawa, A.; Kon, K.; Ando, S. A new O-acetylated trisialoganglioside, 9-O-acetyl GT2, in cod brain. *J. Biochem.* **1993**, *114*, 459–462.
32. Ravindranaths, M.H.; Paulson, J.C.; Irie, R.F. Human melanoma antigen O-acetylated ganglioside GD3 is recognized by Cancer antennarius lectin. *J. Biol. Chem.* **1988**, *263*, 2079–2086.
33. Fahr, C.; Schauer, R. Detection of sialic acids and gangliosides with special reference to 9-O-acetylated species in basalomas and normal human skin. *J. Investig. Dermatol.* **2001**, *116*, 254–260.
34. Mukherjee, K.; Chava, A.K.; Mandal, C.; Dey, S.N.; Kniep, B.; Chandra, S.; Mandal, C. O-acetylation of GD3 prevents its apoptotic effect and promotes survival of lymphoblasts in childhood acute lymphoblastic leukaemia. *J. Cell. Biochem.* **2008**, *105*, 724–734.
35. Birks, S.M.; Danquah, J.O.; King, L.; Vlasak, R.; Gorecki, D.C.; Pilkington, G.J. Targeting the GD3 acetylation pathway selectively induces apoptosis in glioblastoma. *Neuro Oncol.* **2011**, *13*, 950–960.
36. Marquina, G.; Waki, H.; Fernandez, L.E.; Kon, K.; Carr, A.; Valiente, O.; Perez, R.; Ando, S. Gangliosides expressed in human breast cancer. *Cancer Res.* **1996**, *56*, 5165–5171.
37. Mlinac, K.; Fabris, D.; Vukelić, Z.; Rožman, M.; Heffer, M.; Bogner, S.K. Structural analysis of brain ganglioside acetylation patterns in mice with altered ganglioside biosynthesis. *Carbohydr. Res.* **2013**, *382*, 1–8.
38. Corfield, A.P.; Myerscough, N.; Warren, B.F.; Durley, P.; Paraskeva, C.; Schauer, R. Reduction of sialic acid O-acetylation in human colonic mucins in the adenoma-carcinoma sequence. *Glycoconj. J.* **1999**, *16*, 307–317.
39. Shen, Y.; Kohla, G.; Lrhof, A.L.; Sipos, B.; Kalthoff, H.; Gerwig, G.J.; Kamerling, J.P.; Schauer, R.; Tiralongo, J. O-acetylation and de-O-acetylation of sialic acids in human colorectal carcinoma. *Eur. J. Biochem.* **2004**, *271*, 281–290.
40. Arming, S.; Wipfler, D.; Mayr, J.; Merling, A.; Vilas, U.; Schauer, R.; Schwartz-Albiez, R.; Vlasak, R. The human Cas1 protein: A sialic acid-specific O-acetyltransferase? *Glycobiology* **2011**, *21*, 553–564.
41. Cazet, A.; Groux-Degroote, S.; Teylaert, B.; Kwon, K.-M.; Lehoux, S.; Slomianny, C.; Kim, C.-H.; Le Bourhis, X.; Delannoy, P. GD3 synthase overexpression enhances proliferation and migration of MDA-MB-231 breast cancer cells. *Biol. Chem.* **2009**, *390*, 601–609.
42. Guérardel, Y.; Chang, L.-Y.; Fujita, A.; Coddeville, B.; Maes, E.; Sato, C.; Harduin-Lepers, A.; Kubokawa, K.; Kitajima, K. Sialome analysis of the cephalochordate *Branchiostoma belcheri*, a key organism for vertebrate evolution. *Glycobiology* **2012**, *22*, 479–491.
43. Klein, A.; Diaz, S.; Ferreira, I.; Lamblin, G.; Roussel, P.; Manzi, A.E. New sialic acids from biological sources identified by a comprehensive and sensitive approach: Liquid chromatography-electrospray ionization-mass spectrometry (LC-ESI-MS) of SIA quinoxalinones. *Glycobiology* **1997**, *7*, 421–432.
44. Sommer, U.; Herscovitz, H.; Welty, F.K.; Costello, C.E. LC-MS-based method for the qualitative and quantitative analysis of complex lipid mixtures. *J. Lipid Res.* **2006**, *47*, 804–814.
45. Shannon, P.; Markiel, A.; Ozier, O.; Baliga, N.S.; Wang, J.T.; Ramage, D.; Amin, N.; Schwikowski, B.; Ideker, T. Cytoscape: A software environment for integrated models of biomolecular interaction networks. *Genome Res.* **2003**, *13*, 2498–2504.

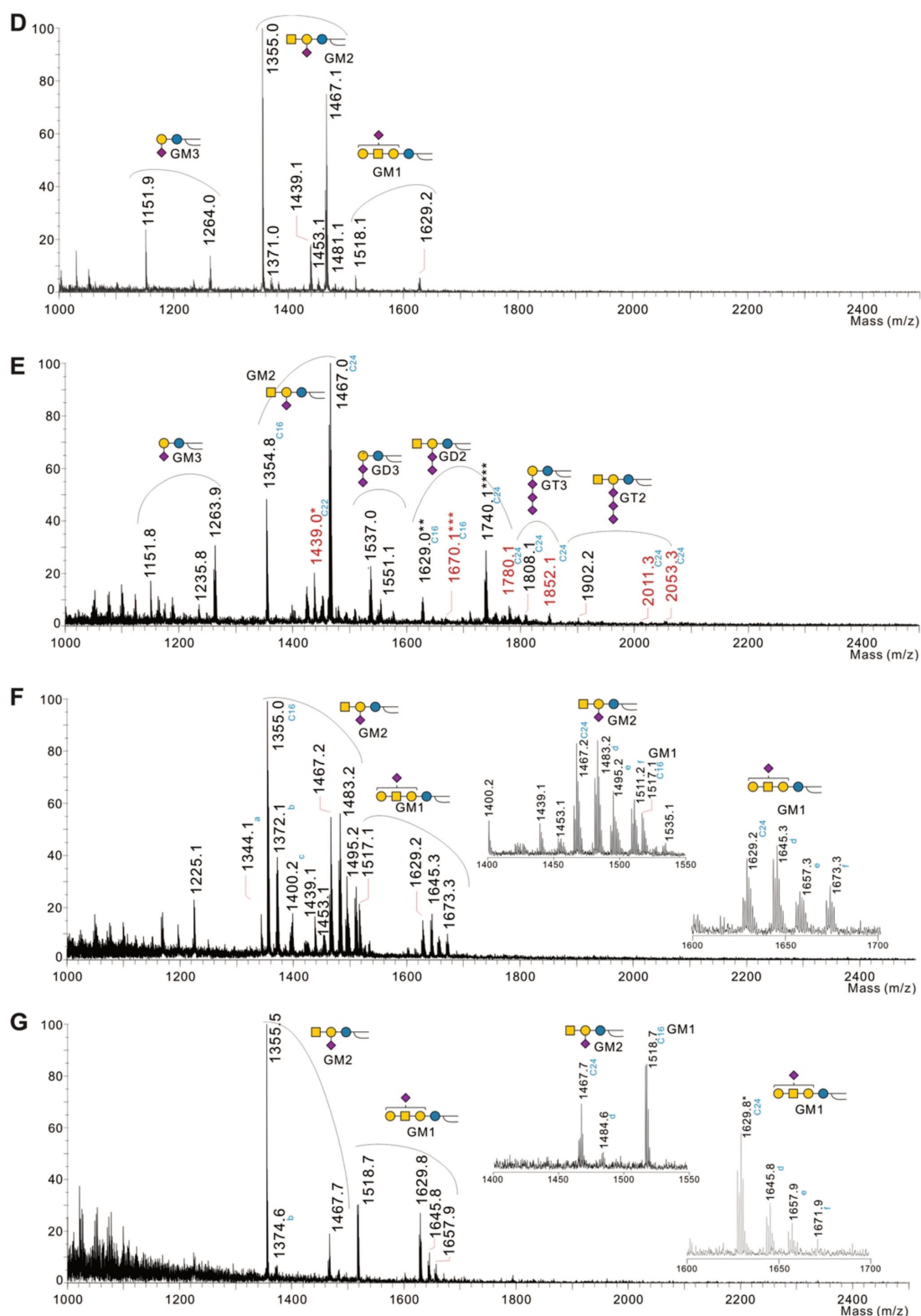


© 2020 by the authors. Licensee MDPI, Basel, Switzerland. This article is an open access article distributed under the terms and conditions of the Creative Commons Attribution (CC BY) license (<http://creativecommons.org/licenses/by/4.0/>).

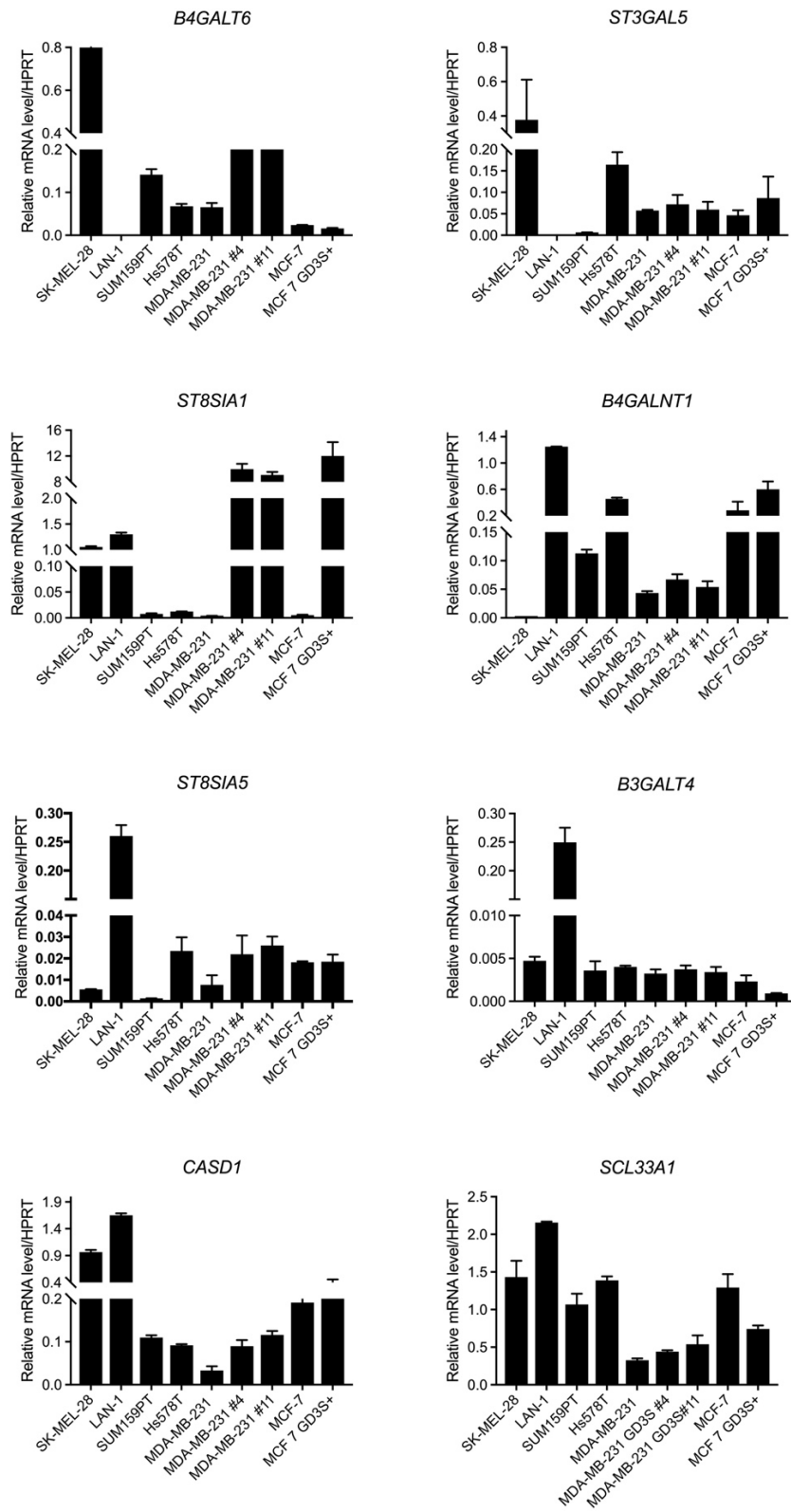
**Supplementary Figure S1: Representative ganglioside profile of SK-Mel-28 (A), LAN-1 (B), SUM 159 PT (C).** Ceramide consists mainly of d18:1 long chain base and C16, C18, C24 either/both saturated or/and saturated fatty acids. The mass number with ceramide length colored in blue means the structure were identified by MS<sub>2</sub> fragmentation. The mass number colored in red indicates the presence of O-Acetylated structures. \* indicates that signal corresponds to a mixture of GM1Cer<sup>24</sup> and GD2Cer<sup>16</sup> (C). Gangliosides are indicated according to the following nomenclature , Ceramide; , Galactose; , Glucose; , N-acetyl-galactosamine; , N-acetyl-neuraminic acid, Ac: O-acetyl group.



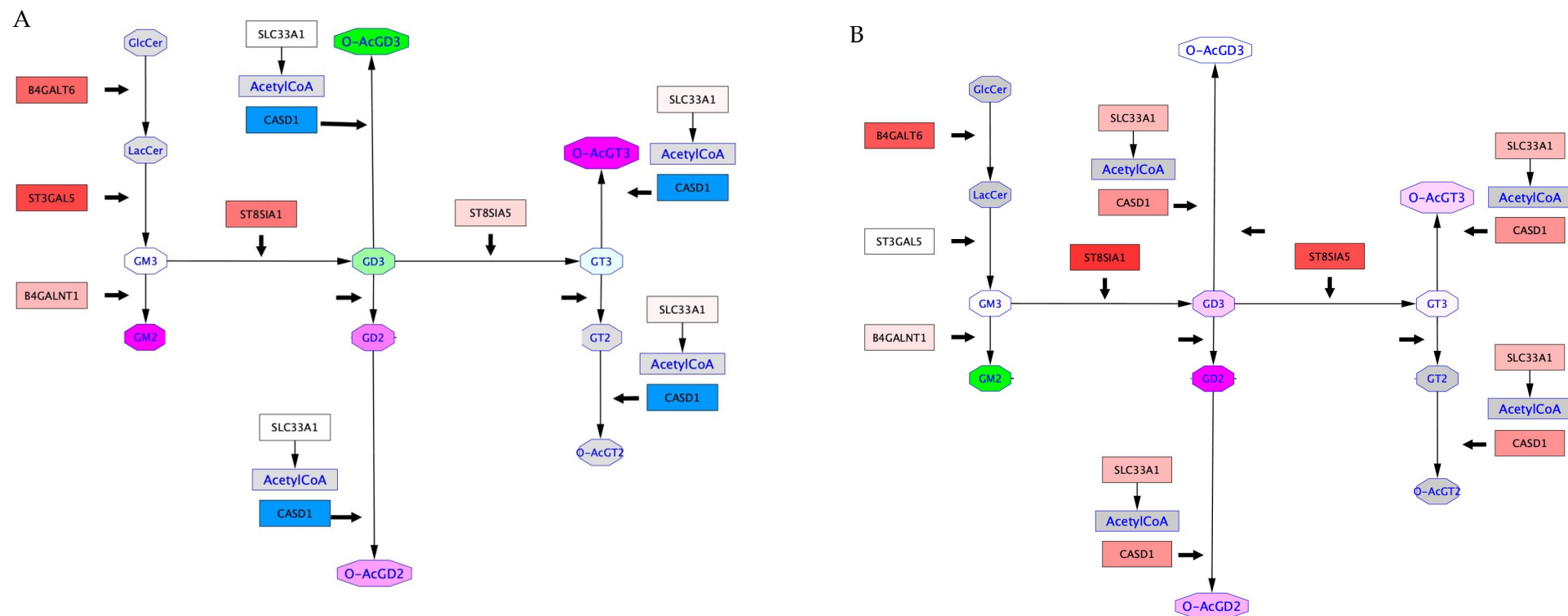
**Supplementary Figure S1 continued: Representative ganglioside profile of MDA-MB-231 (D), MDA-MB-231 GD3S+ clone #11 (E), MCF-7 (F), MCF-7 GD3S+ (G).** Ceramide consists mainly of d18:1 long chain base and C16, C18, C24 either/both saturated or/and saturated fatty acids. The mass number with ceramide length colored in blue means the structure were identified by MS<sub>2</sub> fragmentation. The mass number colored in red indicates the presence of *O*-Acetylated structures. \* indicates that signal corresponds to a mixture of GM2Cer<sup>16</sup> with OAcGM3Cer<sup>14</sup>; \*\* indicates that signal corresponds to a mixture of GM1Cer<sup>24</sup> and GD2Cer<sup>16</sup>; \*\*\* indicates that signal corresponds to a mixture of OAcGD2Cer<sup>16</sup> and GD2Cer<sup>18</sup>; \*\*\*\* indicates that OAcGT3Cer<sup>16</sup> is present in traces amount (E). a, b, c, d, e, f indicates that ceramide is highly hydroxylated (F-G). Gangliosides are indicated according to the following nomenclature , Ceramide; , Galactose; , Glucose; , N-acetyl-galactosamine; , N-acetyl-neuraminic acid, Ac: O-acetyl group.



**Supplementary Figure S2: Glycosyltransferase gene expression profiling in neuroectoderm derived cancer cell lines.** *B4GALT6* (Lactosylceramide synthase), *ST3GAL5* (GM3 synthase), *ST8SIA1* (GD3 synthase), *B4GALNT1* (GD2 synthase), *ST8SIA5* (GT3 synthase) by qPCR. Gene expression analysis of *CASD1* encoding for SOAT, and *SCL33A1* encoding for Acetyl CoA transporter by qPCR on the same cell lines. Each bar represents the mean  $\pm$  SD of n= 3 experiments.



**Supplementary Figure S3: Differential ganglioside metabolism pathway between Hs 578T *vs* MCF-7 (A) and MDA-MB-231 GD3S+ clone #11 *vs* MDA-MB-231 (B).** Glycosyltransferase gene expression data obtained by qPCR were mapped onto Wikipathway [27,28] based on the differential expression between two cell lines. In the squared nodes, colors vary from blue to red for indicating the repression to the over-expression of the glycosyltransferase gene in the first cell line compared to the second which are pointed by the thick black arrow. Quantitative data concerning the amounts of gangliosides obtained by MALDI-QIT-TOF mass spectrometry were added to the pathway based on the comparison between the first and the second cell line. In the octagonal nodes, colors vary from green to fuchsia to indicate a restraint to a rise of the amount of a given ganglioside based on the difference between the two cell lines. Grey color indicates the absence of any available data about the expression





## PART IV: Identification of genes involved in OAcGD2 biosynthesis using phosphatome/ kinome siRNA high throughput screening.

### 1- Introduction

Gangliosides and OAcGD2 are specifically related cancer antigens currently explored for therapeutic exploitation (Terme *et al.*, 2014). However, our understanding of these antigens remains largely incomplete. In particular, we poorly understand how neuroectoderm-derived cancer cells up-regulate the expression of OAcGD2. Using the cutting-edge technology of high throughput RNAi screening coupled to confocal imaging, we have aimed at establishing the genetic network underlying OAcGD2 expression in breast cancer cells in collaboration with Dr X. Le Guezennec and Dr F. Bard. This experiment has been performed in the RNAi screening facility of FB lab in A\*Star Institute (Singapore). The expression of OAcGD2 in a given cell type may be the result of the conjunction of many parameters including the balance between *O*-acetyltransferase and *O*-acetyl esterase activities, the activity of different glycosyltransferases involved in gangliosides expression, but also the subcellular trafficking and organization of the glycosylation machinery. Given the complexity of this biosynthetic model, the clarification of the mechanisms that regulates the expression of tumor specific OAcGD2 remains challenging. This complexity further delays the elucidation of OAcGD2 functional role in tumorigenesis and its potential interest as a prognostic marker or therapeutic target.

In order to identify genes involved in OAcGD2 expression we performed siRNA screening against kinase/phosphatase gene families with arrayed pooled siRNA immunofluorescence followed by confocal microscopy experiments were performed 72h after siRNA transfection to determine the effect of genes silencing on OAcGD2 expression. In this study, we used breast cancer cells MDA-MB-231-GD3S+ which stably express high level of GD2 and OAcGD2 (Cavdarli *et al.*, 2019).

## *2-Material & Methods*

### *Cell culture*

Cell culture reagents were purchased from Lonza (Verviers, Belgium). The human breast cancer cell line MDA-MB-231 GD3S+ clone was obtained as previously described (Cazet *et al.*, 2009). Cells were routinely grown in monolayer culture and maintained at 37°C in an atmosphere of 5% CO<sub>2</sub>. MDA-MB-231 GD3S+ cells were grown in Dulbecco's modified Eagle's medium (DMEM) supplemented with 10% heat-inactivated fetal calf serum, 2 mmol/L L-glutamine and 1 mM sodium pyruvate.

### *SiRNA reverse transfection*

2.5 µL/well of 500 nM siGenome siRNA (Dharmacon/Horizon) was printed into black-walled 384 well cell carrier ultra plates (Perkin Elmer) with Velocity 11 (Agilent) as described before (Chia *et al.*, 2012). Reverse siRNA transfection was performed by pre-mixing 0.1 µL of Dharmafect 1 transfection reagent (#T-2001-03, Horizon) with 7.4 µL of Optimem for 5 minutes. Addition of mixture to the siRNA plate was then performed with small multidrop combi cassette (Thermo-Fisher) and was left for complexation for 20 minutes with shaking. Addition of 2750 cells in 40 µL of DMEM supplemented with 10% FCS per well was then performed with multidrop combi standard cassette at medium speed (Thermo-Fisher). siRNA targeting-GD2S (L-011279-00-0020, Horizon), Polo like kinase 1 (PLK1; L-003290-00-0020, Horizon) and on-targeting pool (D-001810-10-20, Horizon) were used as screen controls.

### *Immunofluorescence staining and automated images acquisition*

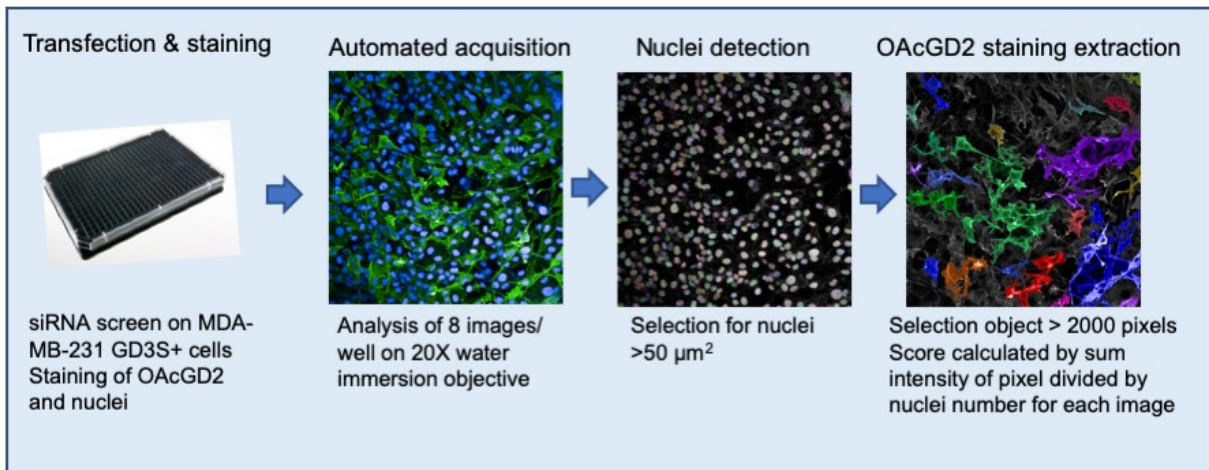
After 72h of incubation transfected cells were fixed with 50µL per well of 4% paraformaldehyde in 2% sucrose and 0.1M sodium phosphate buffer, 15 min at 37°C. Cells were washed once with Hepes buffer 0.2M pH 7.4 and membrane permeabilization was performed in 5µg/ml of digitonine in Hepes buffer for 20 min. Blocking was performed for 1h with blocking buffer containing 0.2% gelatin, 2% BSA and 2% FCS. Aspiration of any liquid was performed with a 384 channels aspiration manifold at constant distance height from bottom of the well (V&P Scientific Inc). Sodium hydroxide treatment at 1 mM was added to selective control non-

transfected well for the deacetylation of sialic acid. Staining of OAcGD2 was performed by incubation of 8B6 mAbs followed by suitable anti-mouse conjugated Alexa Fluor 488 secondary antibody at 1/500 dilution (Thermo Fisher Scientific). Each antibody was incubated successively for 1h each on a 1 cm-span orbital shaker at 150 rpm. Nuclei were counterstained with 1 µg/ml Hoechst Thermo Fisher Scientific. Washings after antibody incubation were performed three times with 0.2M Hepes pH 7.4 and 5 minutes shaking. All dispensing steps were performed with multidrop combi standard cassette. Stained plates were subjected to sequential channel acquisition for Hoechst/Alexa 488 with high content spinning disk confocal imager: phenix Opera (Perkin Elmer). Eight fields per well were acquired with 20X NA 1.0 water immersion objective with default laser power and exposure settings.

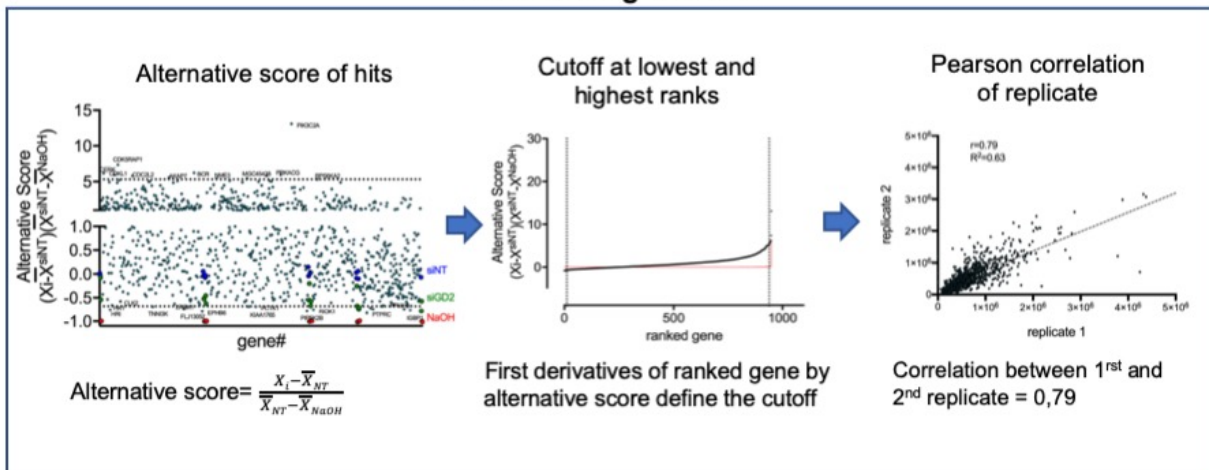
#### *Segmentation pipeline for the selection of the hits*

An OAcGD2 expression metric was derived with total cell thresholded fluorescence intensity obtained by immunodetection with 8B6 mAb in MDA-MB-231 GD3S+ cells and was normalized with Hoechst nuclei counts. The phosphatome/kinome library consist of pools of four siRNAs per gene arrayed in a series of four 384-well plates covered with 973 individual siRNA (Figure 19). The segmentation pipeline applied for analysis of data derived with Columbus (Perkin Elmer) image analysis software and consisted of few module blocks: a basic flatfield correction for each image. Nuclei count detection with method B excluding nuclei object < 50 µm<sup>2</sup> and with a 0.4 common intensity threshold. OAcGD2 signal detection with Image region-based algorithm with a threshold of 0.6 and with multiple objects detection, file hole algorithm on objects and exclusion of object size <2000 square pixel. The calculation of OAcGD2 fluorescent signal metric was then derived with the sum of pixel intensity for all objects over 2000 square pixels size divided by the nuclei number for all 8 fields image per well. The exclusion of objects with area less than 2000 square pixel size was applied to subfilter antibody artefacts.

## I- Image processing



## II- Formatting Results



## III- Selection of hits

### Selection criterion of hits

- Exclusion of wells containing < 1000 nuclei
- Visual confirmation of alternative score
- Reproducibility of hits in 2 replicates.

### Relevance of hits

- Cytoscape
- String network
- Gene Ontology



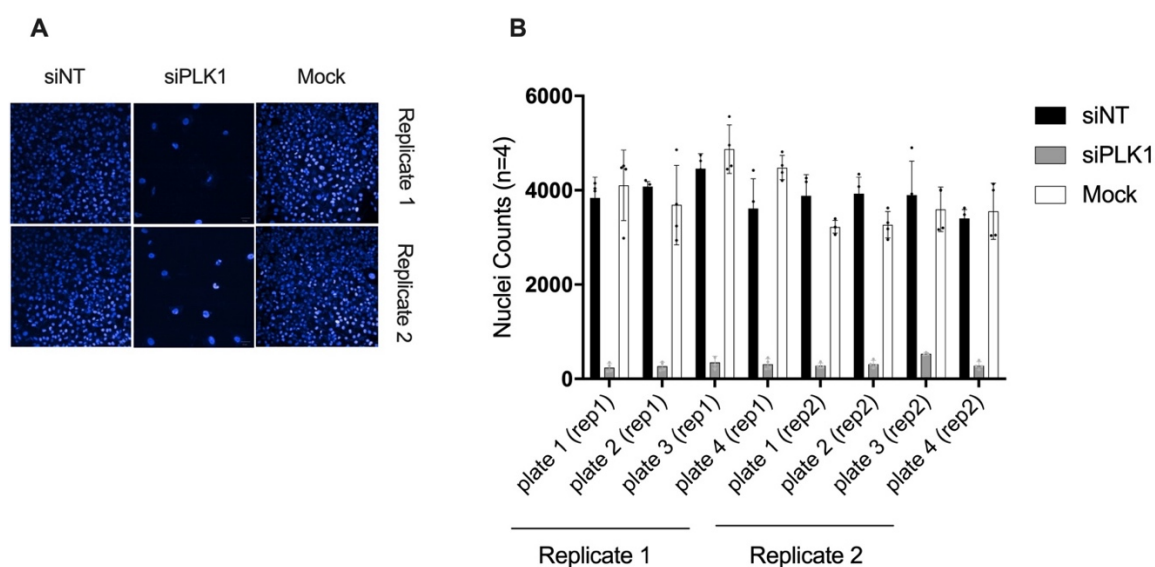
Figure 19: Workflow of phosphatome/kinome screen on OAcGD2 expression in MDA-MB-231 GD3S+ cells.

### 3-Results

#### A- Workflow of phosphatome/kinome siRNA screen

##### A-1 Key controls

Key controls were designed to validate consistency of our workflow and to normalize plate to plate variations. In this screening, siRNA Non-Targeting pool (siNT) was added to empty wells of each 384-well plate as a negative control, siRNA targeting-Polo like kinase 1 (siPLK1) was used as siRNA transfection control. Finally, siRNA targeting GD2 synthase (siGD2S) was used as a modulator of *OAcGD2* staining fluorescent signal. siPLK1 induced over 95% decrease in nuclei count as compared to NT transfected wells and confirmed efficient siRNA transfection in all plates tested (Figure 20). As depicted in Figure 20B, nuclei count between siNT-transfected wells or non-transfected control wells were very similar highlighting the specific siPLK1 killing mediated effect and the very low level of transfection toxicity induces by our transfection reagents (Figure 20).

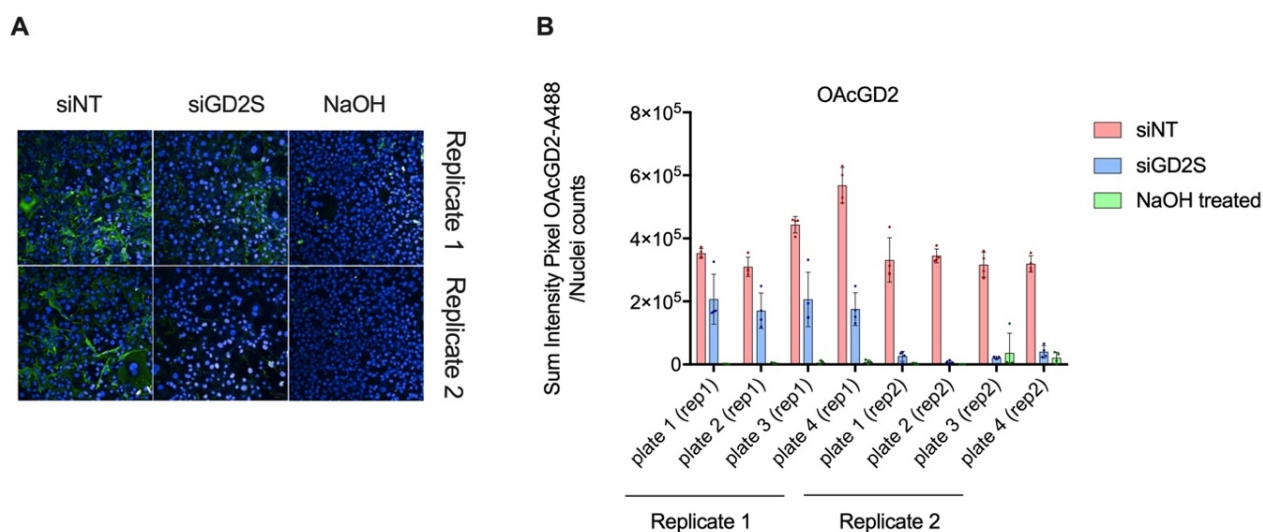


**Figure 20: Identification of the transfection efficiency on both replicates.**

A- Representative images of the nuclei stained with Hoechst of siNT or siPLK1 transfected wells and non-transfected control wells on replicates 1 and 2. B- Quantification of nuclei number in each plate composing the two replicates of siNT and siPLK1 transfected cells or non-transfected control cells. Mean and SD derived from 4 wells are presented.



SiGD2S mediates a reduced intensity of *OAcGD2* fluorescent signal in all plates tested when compared to signal in siNT control wells but showed some changes in silencing performance between the first screen replicate vs the second screen replicate. Due to this variability, the chemical treatment was used to control the modulation of *OAcGD2* fluorescent signal. Sodium hydroxide has been shown previously to deacetylate all acetyl groups present on the cell surface and blocked efficiently antigen recognition by 8B6 mAb. Fixed cells in selected control wells were thus treated with NaOH 0.1M before primary antibody staining. *OAcGD2* staining obtained on NaOH-treated wells was consistently abolished when compared to siNT transfected wells (Figure 21B). The Z factor for siGD2S vs siNT was equal to 0.30 whereas the Z factor for NaOH treated wells vs siNT was around 0.70. Since Z factor readout with siNT and NaOH treated wells showed better consistency, these 2 key controls were used to calibrate screen data for normalization.



**Figure 21: *OAcGD2* staining in control wells.**

A- Representative images of *OAcGD2* staining by 8B6 mAb and IgG-conjugated Alexa Fluor 488 in siNT or siGD2S transfected cells or by sodium hydroxide-treated cells in each plate on both replicates. B- Scoring of *OAcGD2* staining by the sum of intensity of pixels corresponding to immunodetection of 8B6/Alexa Fluor 488 divided by the nuclei number in siNT or siGD2S transfected cells or sodium hydroxide-treated-cells in each plate on both replicates. Mean and SD derived from 4 wells are presented.

## A-2 Formatting results

SiRNA that showed high toxicity in the wells (total nuclei counts<1000) were excluded from the analysis. The number of wells affected by toxicity constituted fewer than 5% of total

siRNA tested. To minimize variations between plate data, each datapoint was normalized with the alternative score dependent on plate mean values of control siNT and plate mean values of NaOH treated controls wells (Moreau *et al.*, 2011) by applying the following formula:

$$\text{Alternative score} = \frac{X_i - \bar{X}_{siNT}}{\bar{X}_{siNT} - \bar{X}_{NaOH}}$$

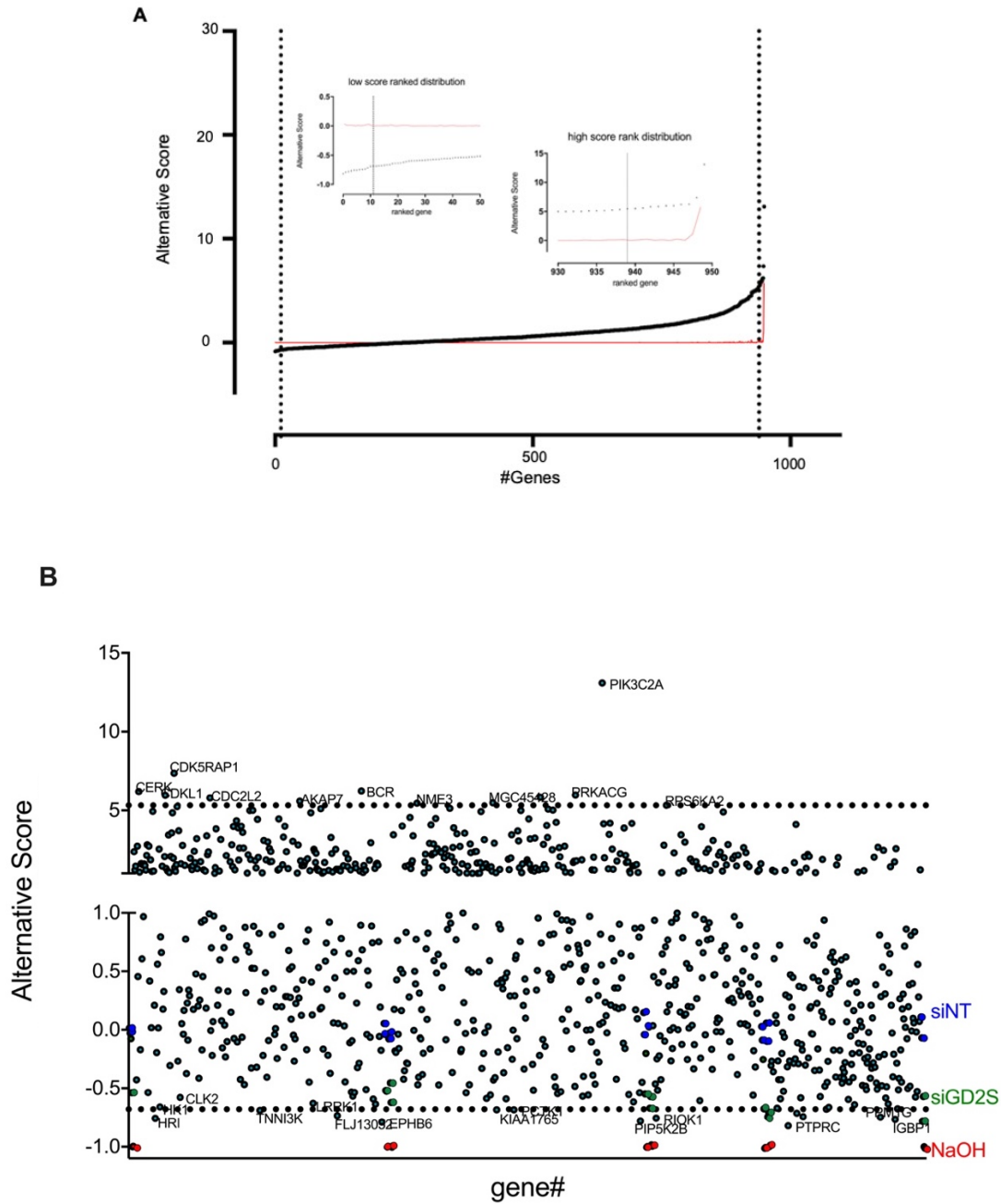
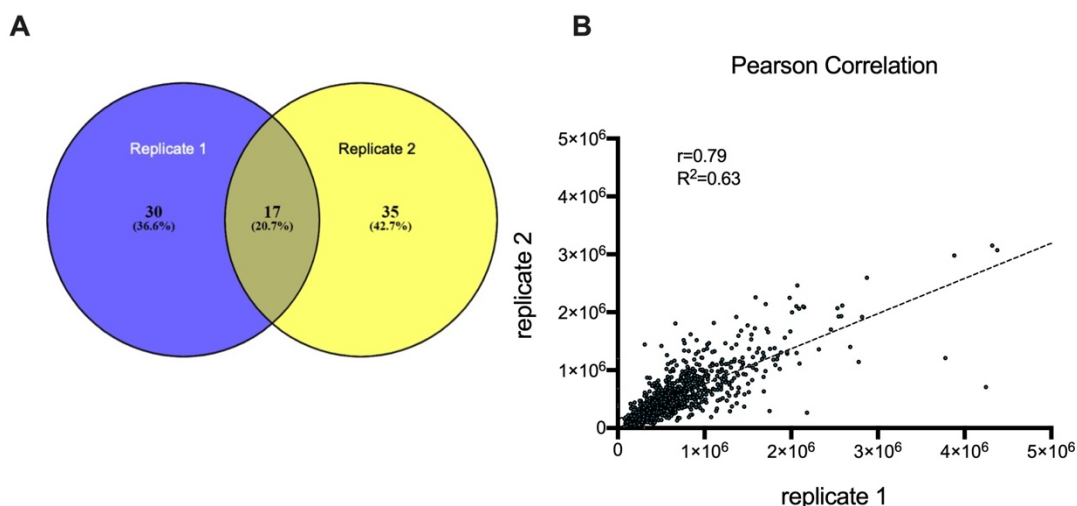


Figure 22: Kinome/phosphatome screening of replicate 1 formatted with Alternative score.

A- First derivative of ranked gene by alternative score respectively represented in red line and ranked alternative score represented in black line. Cutoff before the largest spike at lowest and highest ranks is respectively represented in left side and right side. B- Alternative scoring of all data from replicate 1 reformatted plate by plate. Blue dots represent siNT cells. Green dots represent siGD2S transfected cells. Red dots represent NaOH treated wells. Cyan dots show all siRNA wells tested from the screen. The upper dotted line represents the highest rank cutoff. The lowest dotted line represents the lowest rank cutoff.

The cutoff for the selection of *OAcGD2* up or downregulating hits was defined with the first derivative approach (Moreau *et al.*, 2011). Genes were ranked according to their alternative score value from the minimum to the maximum (Figure 22A). The cutoffs were designed before the largest spike at lowest ranks and highest ranks of the first derivative as described previously (Figure 22B).

## B- Selection of hits



**Figure 23: Correlation of replicates.**

A- Representative diagram of the overlap of top hits from both replicates based on individual replicate first derivative cutoff. B-Pearson correlation of both replicates according to hit alternative score.

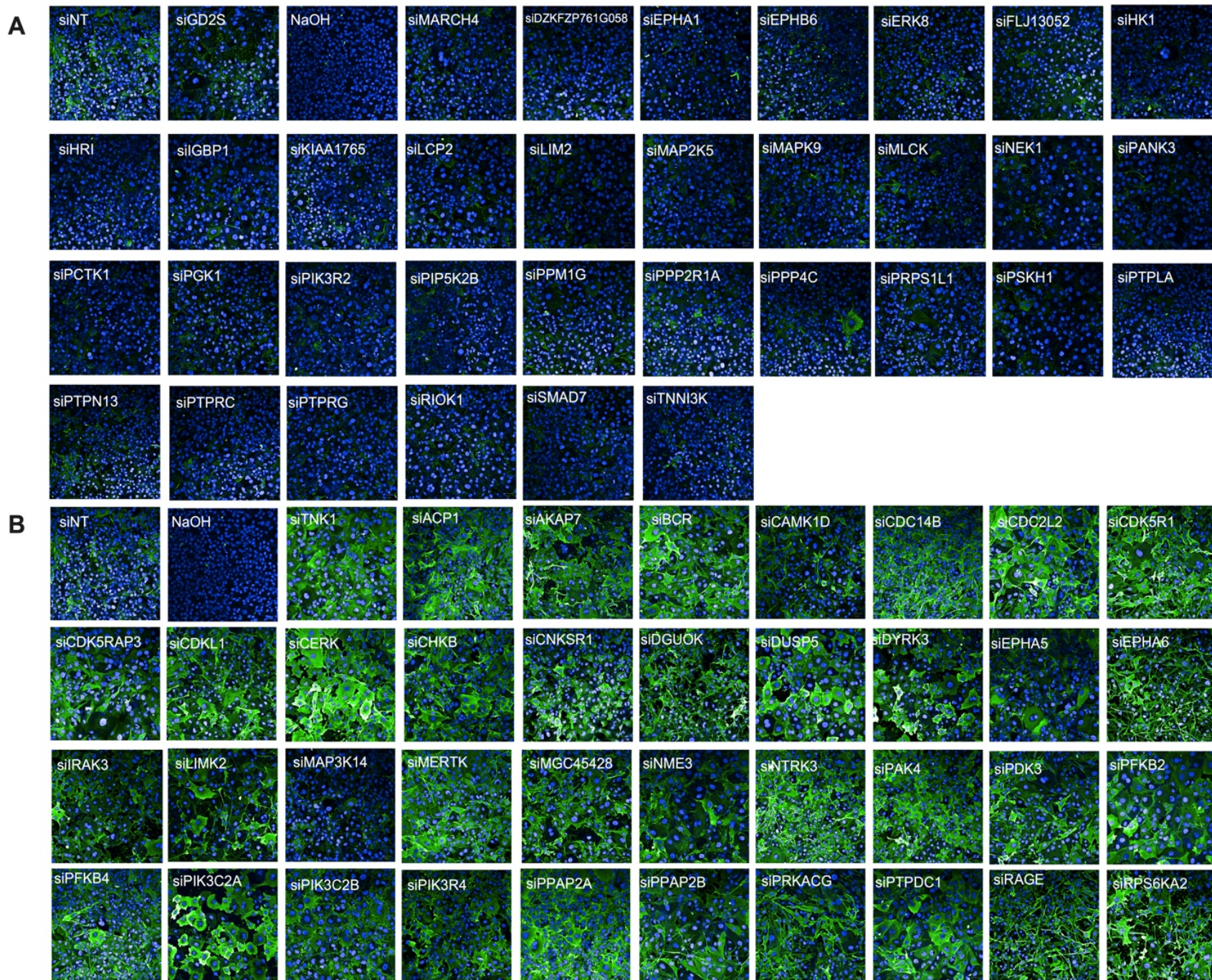
Pearson correlation ( $r$  or  $R^2$ ) factor was calculated on the basis of alternative scores on both replicates datapoints. In this screening experiment, we obtained  $r = 0.79$  and  $R^2 = 0.63$  showing that the linear correlation between the two replicates was acceptable and that the screen outcome was reasonably reproducible (Figure 23B). In the second replicate, on row 3 to 8 abnormally high staining of all wells have been observed and rendered these 6 rows of data are

not suitable for analysis. As a consequence, replicate 1 data was more complete than replicate 2 data. In the first replicate, 20 siRNA have been identified for downregulating and 27 for upregulating *OAcGD2* expression. In the second replicate, *OAcGD2* expression was downregulated by 29 hits and upregulated by 23 hits. With the first derivative approach on both replicates 17 siRNA identified were reproducible among the two replicates with 7 hits for *OAcGD2* expression downregulation and 10 hits for *OAcGD2* upregulation (Figure 23A).

Based on first derivatives approach, 17 siRNA have been identified as hits reproduced on both replicates (Figure 23). However, the final selection of all possible hits was considered by combining hits outputs of both replicates and visual confirmation of acquired images for limiting stringency of cutoff method individually applied on replicates. Considering this limitation, the phosphatome/kinome screening of *OAcGD2* expression allowed the identification of 33 siRNA as downregulating hits (Table 9). Images sampling along with alternative score of each of these siRNA showed from this extended list showed the expected signal change in both replicates and strengthened the validity of these siRNA hit list highlighted by this screen (Figure 24B).

In order to assess the biological relevance of all hits selected, the functional association between genes selected was studied with String interaction network (Szklarczyk *et al.*, 2019). The interaction network of genes upregulating *OAcGD2* expression highlighted reactome pathway to metabolism and lipid metabolism (Figure 24). The interaction network of genes downregulating *OAcGD2* highlighted reactome pathway related to metabolism and carbohydrate metabolism (Figure 25). However, the biological relevance of all genes identified in the assay cannot be based solely on the String interaction network and requires the analysis of the literature for a better understanding of the links between hits and *OAcGD2* expression.





**Figure 24: Representative images of selected genes modulating *OAcGD2* expression.**

A- Hits downregulating *OAcGD2* expression.  
B- Hits upregulating *OAcGD2* expression.



**Table 9: Hit list of genes modulating *O*AcGD2 expression in MDA-MB-231 GD3S+ cells.**

OAcGD2 downregulating hits			
gene	nmid	Replicate 1 alt score	Replicate 2 alt score
MARCH4	NM_020814	-0.92	-0.43
DKFZP761G058	NM_152542	-0.66	-0.74
EPHA1	NM_005232	-0.84	-0.53
EPHB6	NM_004445	-0.789	-0.52
ERK8	NM_139021	-0.79	-0.64
FLJ13052	NM_023018	-0.74	-0.61
HK1	NM_000188	-0.66	-0.52
HRI	NM_014413	-0.75	-0.76
IGBP1	NM_001551	-0.77	-0.74
KIAA1765	XM_047355	-0.84	-0.68
LCP2	NM_005565	-0.85	-0.30
LIM	NM_006457	-0.78	-0.52
MAP2K5	NM_002757	-0.95	-0.47
MAPK9	NM_002752	-0.90	-0.49
MLCK	NM_182493	-0.82	-0.53
NEK1	XM_291107	-0.80	-0.42
PANK3	NM_024594	-0.87	-0.59
PCTK1	NM_006201	-0.89	-0.68
PGK1	NM_000291	-0.81	-0.49
PIK3R2	NM_005027	-0.80	-0.55
PIP5K2B	NM_003559	-0.94	-0.78
PPM1G	NM_002707	-0.85	-0.75
PPP2R1A	NM_014225	-0.64	-0.52
PPP4C	NM_002720	-0.84	-0.68
PRPS1L1	NM_175886	-0.91	-0.54
PSKH1	NM_006742	-0.81	-0.36
PTPLA	NM_014241	-0.74	-0.37
PTPN13	NM_006264	-0.71	-0.54
PTPRC	NM_002838	-0.82	-0.72
PTPRG	NM_002841	-0.82	-0.38
RIOK1	NM_031480	-0.76	-0.68
SMAD7	NM_005904	-0.82	-0.57
TNNI3K	NM_015978	-0.74	-0.69

OAcGD2 upregulating hits			
gene	nmid	Replicate 1 alt score	Replicate 2 alt score
ACP1	NM_004300	3.87	1.20
AKAP7	NM_004842	5.58	3.11
BCR	NM_004327	4.84	6.23
CAMK1D	NM_020397	4.10	3.04
CDC14B	NM_003671	4.52	2.08
CDC2L2	NM_024011	5.79	
CDK5R1	NM_003885	5.23	
CDK5RAP1	NM_016082	7.37	
CDK5RAP3	NM_025197	4.85	
CDKL1	NM_004196	5.96	
CERK	NM_022766	5.24	6.19
CHKB	NM_005198	4.50	2.14
CNKSR1	NM_006314	5.21	4.94
DGUOK	NM_001929	4.99	
DUSP5	NM_004419	5.32	4.85
DYRK3	NM_003582	5.28	5.11
EPHA5	NM_004439	4.48	0.89
EPHA6	XM_496653	5.01	
IRAK3	NM_007199	4.49	0.83
LIMK2	NM_005569	5.01	2.62
MAP3K14	NM_003954	4.15	3.88
MERTK	NM_006343	4.99	2.44
MGC45428	NM_152619	3.833	5.49
NME3	NM_002513	5.52	5.46
NTRK3	NM_002530	5.13	2.78
PAK4	NM_005884	4.93	2.15
PDK3	NM_005391	5.84	2.23
PFKFB2	NM_006212	5.09	1.97
PFKFB4	NM_004567	3.88	0.94
PIK3C2A	NM_002645	13.10	8.13
PIK3C2B	NM_002646	4.00	4.15
PIK3R4	NM_014602	5.54	4.18
PPAP2A	NM_003711	5.67	2.57
PPAP2B	NM_003713	4.37	1.73
PRKACG	NM_002732	5.97	5.08
PTPDC1	NM_152422	4.71	2.05
RAGE	NM_014226	4.85	4.56
RPS6KA2	NM_021135	5.33	2.94
TNK1	NM_003985	6.41	4.90

#### 4-Discussion

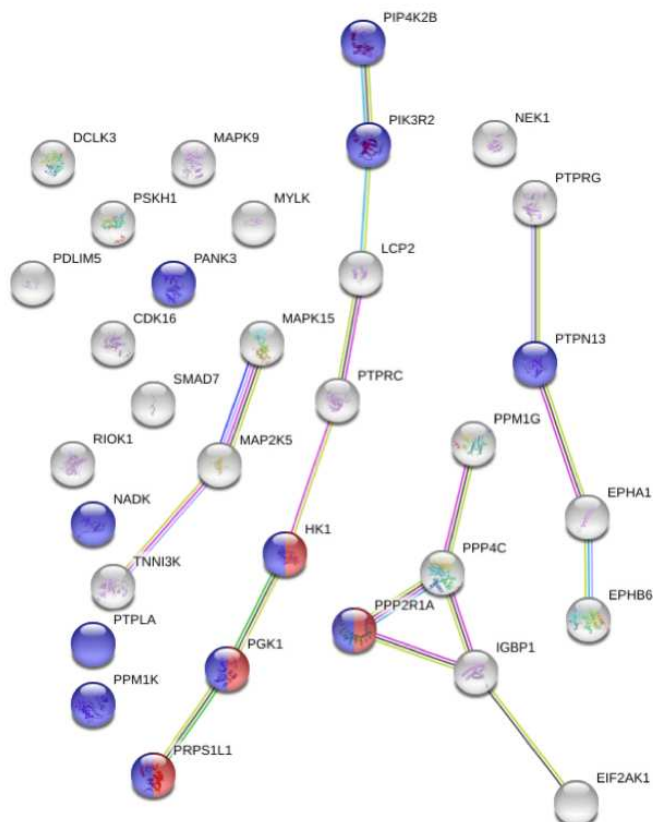
The *OAcGD2* phosphatome/kinome siRNA screen was analyzed based on the fluorescence intensity obtained by immunodetection using 8B6 mAb in MDA-MB-231 GD3S+ cells. Results were replicated and analyzed by combining first derivatives cutoff method and visual confirmation of hits on both replicates leading to the identification of 72 siRNA with 33 hits downregulating *OAcGD2* expression and 39 hits upregulating *OAcGD2* expression. Results obtained can be interpreted based on the identification of hits but also on the images acquired. As indicated in Figure 24, images obtained from the transfection of the MDA-MB-231 GD3S+ using siRNA targeting the different genes selected from our screen revealed significant variations of cellular morphology, especially for the hits upregulating *OAcGD2* with a intracellular and membrane staining pattern. In contrast, several siRNA such as siRAGE, siLIMK2, siEPHA6, siPRKACG, siRPS6KA1, siCDC14B and siCAMK1D induced extension like neurite filipodia and could be possibly associated to a neuronal shape. Cells transfected with SiRNA like siCERK, siPI3KC2A, siPPAP2B, siPTPDC1 and siPFKFB2 showed extended shape (Figure 24B). Modifications of cell morphology after siRNA transfection can occur frequently depending on the depleted gene. The evidence of the direct implication of these identified hits on cytoskeletal organization is not obvious but cannot be completely abrogated. Despite the low level of toxicity of the transfection depicted in Figure 20, some siRNA such as siPLK1, siFNK3RB, or siWEE1 still remained toxic leaving less than 1000 nuclei per images. The depletion of these toxic siRNA upregulates *OAcGD2* staining obtained (Data not shown). In order to avoid confounding toxicity effect with selected genes in our readout, we used a stringent nuclei count cutoff was applied for removing wells exhibiting less than 1000 nuclei counts.

Assessing the biological relevance of hits identified is the main step to evaluate the value of the hits identified according to the literature. String database was used for the query of the reliability of hits found. This database is known for predicting direct or functional protein-protein associations. As depicted in Figure 25, *OAcGD2* upregulating and downregulating genes were

successively queried on String using the lowest cutoff (0.400). Both networks identified exhibit only a few associations among hits related to the synthesis of phosphoinositol phosphates, metabolism, MAPK signaling... However, genes from the metabolism pathways especially lipid metabolism for *OAcGD2* downregulating hits and carbohydrate metabolism for *OAcGD2* upregulating hits retained our attention due to their potential implication in the *O*-acetylation of GD2.

Metabolism is the main field to which belongs the following genes found: CERK, PDK3, PFKFB2, PFKFB4, NADK, PPAP2A and PPAP2B. While CERK, NADK, PPAP2A and PPAP2B, PANK3 are mainly involved in lipid synthesis, PFKF2B, PFKF2A, PDK3, HK1 are known to be involved in glycolysis. Interestingly, CERK encodes for ceramide kinase which uses ceramide as a substrate to produce ceramide-1-phosphate. Knowing that ceramide residue is the common substrate for the synthesis of gangliosides and ceramide-1-phosphate, siRNA targeting CERK depletion leaves more ceramide available for gangliosides synthesis by glucosylceramidase. In the same manner than CERK, siRNA targeting either PPAP2A or PPAP2B induces overexpression of *OAcGD2*. PPAP2A and PPAP2B are encoding for lipid phosphate phosphatases LLP1 and LLP3 respectively. LLP1 and LLP3 catalyzes lipid dephosphorylation of Ceramide-1-phosphate producing ceramide (Y. C. Tang et al. 2018) leaving in turn more substrates available for gangliosides synthesis. Finally, NAD kinase (NADK) catalyzes the phosphorylation of nicotinamide adenine dinucleotide (NAD<sup>+</sup>) on to nicotinamide adenine dinucleotide phosphate (NADP<sup>+</sup>) which is then reduced to NADPH by glucose-6-phosphate dehydrogenase or the malic enzymes (Tedeschi et al. 2016). NADPH is one of the cofactors required for lipid synthesis, including ceramide synthesis. Screening results showed that NADK (FLJ13052) depleted cells are exhibiting a reduced level of *OAcGD2* highlighting that decrease level of NADPH reduces lipid biogenesis. All of these genes mentioned above underlined the role of ceramide for gangliosides synthesis; highlighting a tight regulation especially through enzymes competition for ceramide as a substrate.

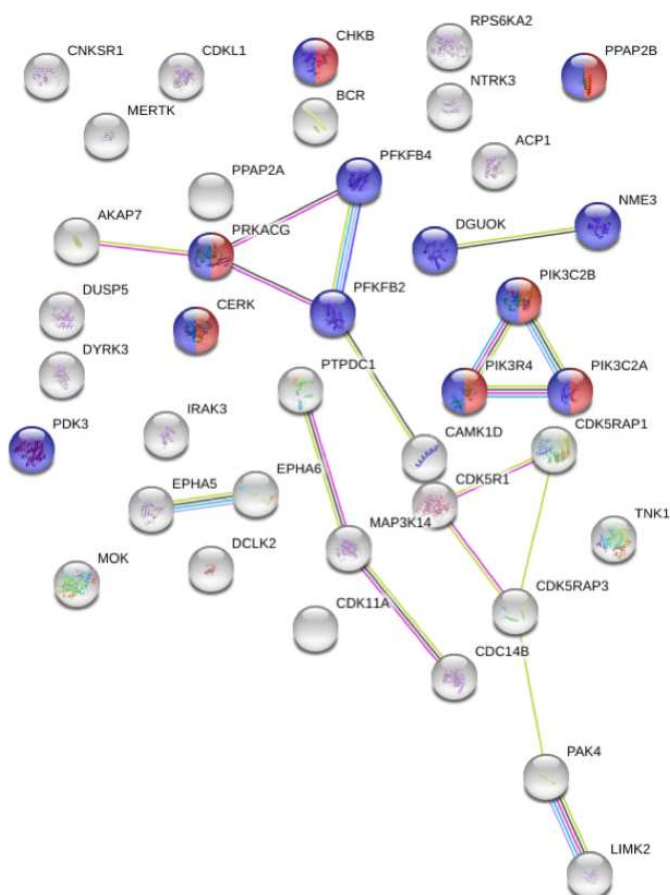
**A**



**Figure 25: String interaction networks of hit list genes identified in systemic siRNA screening experiment.**

A- Interaction network of genes involved in *OAcGD2* upregulation. Genes identified in the screening experiment have been selected as an input. Networks edges indicates the type of interaction evidence on all sources and the cutoff for showing the interaction has been set to the lowest (0.400). Red dots highlights genes involved in metabolism of lipids while blue dots genes belong to metabolism reactome pathways. B- Interaction network of genes involved in *OAcGD2* expression downregulation. Hits associated to *OAcGD2* reduces expression have been selected as an input. Networks edges indicate the type of interaction evidence on all sources and the cutoff for showing carbohydrate metabolism in red while blue dots genes belong to metabolism reactome pathways.

**B**



Altered metabolism is one of the main characteristic of tumor cells (Hanahan and Weinberg, 2000). Besides, it is well known that glucose consumption and absorption is increased in cancer cells involving the activation of the glycolytic degradation pathway. Glycolysis generates degradation products for synthesizing new products. Most enzymatic reactions of glycolysis reaction are reversible, only three steps catalyzed by PFKFB2/PFKFB4, PDK3, and HK1 are irreversibles (Akram, 2013). PFKFB2/PFKFB4 encodes for phosphofructokinases. These are the key enzymes involved in glucose degradation to AcCoA. Pyruvate dehydrogenase 3 is encoded by PDK3 and is involved in the degradation of pyruvate to AcCoA (Klyuyeva *et al.*, 2019). HK1 encodes for hexokinase 1 and is implicated in the degradation of glucose. In this screening assay, the depletion of PDK3, PFKFB2 and PFKFB4 induce the upregulation of *OAcGD2* while *OAcGD2* expression is downregulated in HK1 depleted cells (Table 9). Altering the glycolysis by depleting these enzymes might either increase AcCoA rate in cells or decrease glucose rate. While the increase of AcCoA can potentiate *O*-acetylation of gangliosides, the decrease of glucose might decrease gangliosides synthesis. The possible explanation concerning the role of these enzymes are pointing out the role of metabolism for gangliosides synthesis.

Among kinases and phosphatases identified in the hit list genes, several cyclin dependent kinases (CDK) have been identified such CDC14B, CDC2L2, CDK5R1, CDK5RAP1, CDKL1 and PAK1 (Table 9). CDCL2 (cell division cycle 2 like kinase) also named CDK11A (cyclin dependent kinase 11A) encoded in chromosome 1p36 is frequently altered or deleted in NB with MYCN amplification (Lahti *et al.*, 1994; Nelson *et al.*, 1999). Besides, it is also well known that higher *OAcGD2* expression has been detected in NB among all the cancer classified as neuroectoderm-derived cancers (Alvarez-Rueda *et al.*, 2011). Moreover, the level of 1p36 chromosome alteration remains very low in breast cancer (Titus *et al.*, 2017), in which the level of *OAcGD2* expression remains low compared to the other neuroectoderm derived tumors. In the screening experiment, depletion of CDC2L2 in MDA-MB-231 GD3S+ cells induces *OAcGD2* overexpression (Table 9). The result obtained points out the link between CDC2L2 depletion and *OAcGD2* expression in tumor cells suggesting the therapeutic potentiality of this gene. In the same manner, CDKL1 (CDC2-



related kinase family member) depletion in cells induces *OAcGD2* overexpression (Table 9). However, *CDKL1* is known for promoting tumors development and progression of breast cancer (L. Tang et al. 2012), melanoma (Song et al. 2015), colorectal cancer (Qin et al. 2017) and gastric cancers (Sun et al. 2012). In that case, assessing the biological effect of *CDKL1* depletion on *OAcGD2* expression still has to be investigated. *CDK5R1*, *CDK5RAP1*, and *CDKRAP3* are associated to *CDK5* which is mostly implicated in the cytoarchitecture of central nervous system (Dhavan and Tsai 2001). The individual depletion of all of these genes induces *OAcGD2* upregulation. Interestingly, these genes exert a repressor effect on *OAcGD2* expression highlighting a finely tuned process of *OAcGD2* expression.

Finally, from all selected hits, an important number are implicated in cell signaling pathway such *MAP3K14*, *PIK3C2A*, *PIK3C2B*, *PIK3R4* and *RAGE* identified for inducing the upregulation of *OAcGD2* expression and *ERK8*, *MAP2K5* for *OAcGD2* downregulation. The implication of *MAPK/PI3K* signaling pathways in tumorigenesis promotion is undeniable but interpreting their effect on *OAcGD2* expression is not so obvious. However, they have a great therapeutic potentiality that has to be explored in combination with anti-*OAcGD2* immunotherapy.

## 5-Conclusion

The phosphatome/kinome screening assay was the first pilot study conducted on *OAcGD2* expression leading to the identification of 72 hits involved in up- or down-regulation of its expression. While the potent implication of a certain number of hits was predictable, the direct implication of other hits has to be elucidated. Further studies can be conducted through different approaches. One of the possibilities concerns an *in silico* approach using Cytoscape analysis for building interaction networks. This analysis could be more stringent for the identification of interaction among hits identified and cancer cell metabolism pathways. The second possibility is a low throughput screening on deconvoluted siRNA identified in the pilot study. In this way, false negatives hits can be rejected from the selection keeping all the positive hits. The third one is

performing a targeted approach on selected hits. This approach will require a pre-selection of one or two hits on the basis of the literature. The involvement of these hits in ganglioside *O*-acetylation pathways could be tested in two steps. Firstly, the gene will be depleted either by pharmacological inhibitors or siRNA. Then, the effect on *O*AcGD2 expression will be assessed either by immunocytochemistry followed by confocal microscopy or MALDI-QIT-TOF analysis developed in part III.

Finally, the ultimate perspective of this pilot assay is to perform a genome wide screening on *O*AcGD2. Using the framework of the pilot study, the genome wide assay could provide new genes potentially implicated in *O*-acetylation pathways, leading to the identification of new targets for anti-cancer therapy.

## DISCUSSION & PERSPECTIVES

Intricate relationships exist between the alteration of glycolipid composition of membranes and the development and progression of cancers. Based on this, immunotherapy targeting specific membrane glycolipids was rapidly adopted as an anti-cancer strategy. My thesis project was born and raised on this concept. Because of the side-effects of targeting GD2 using Dinutuximab, the exclusive expression of *O*AcGD2 in cancerous tissues suggests that it could be a better therapeutic target than GD2. Indeed, Alvarez and coworkers analyzed the expression of *O*AcGD2 using an immunoperoxidase assay on 33 different cancer tissues, showing no binding of 8B6 mAb on human healthy tissues. In parallel, *O*AcGD2 expression was detected in NB, melanoma, SCLC and renal carcinoma, whereas *O*AcGD2 was absent in pancreatic and ovarian carcinoma. This distribution pattern of *O*AcGD2 according to the tissue type highlights a marked expression of *O*AcGD2 in neuroectoderm derived tumors. Anti-*O*AcGD2 antibodies represents a therapeutic alternative to anti-GD2 antibodies with reduced side effects (Alvarez-Rueda *et al.*, 2011). Furthermore, the murine anti-*O*AcGD2 antibody 8B6 induces impairment of cell growth, cell cycle arrest and mitochondrial apoptosis on *O*AcGD2 expressing NB tumors (Cochonneau *et al.*, 2013). These preliminary data concerning the effect of murine 8B6 mAb on *O*AcGD2 expressing tumors promoted the further optimization of 8B6 for immunotherapy. Indeed, the chimerization of 8B6 mAb has been established as c8B6 (IgG1,  $\kappa$ ) and produced the same anti-NB effect than ch14.18 antibody without inducing allodynia in syngeneic NB bearing A/J mice (Terme *et al.*, 2014). These preliminary data suggest that chimeric c8B6 mAb could represent a powerful therapeutic and diagnostic tool for immunotherapy. Indeed, the 8B6 mAb represents the best tool to assess the expression and the role of *O*AcGD2 antigen by immunodetection analysis. Besides the translational approach for the use of 8B6, this antibody could have a great impact for basic research. Understanding the mechanisms of ganglioside *O*-acetylation ganglioside and their abnormalities in pathologies such as cancers could be beneficial for the set-up of clinical applications of 8B6 mAb.

Based on this concept, the first step of my project was the assessment of *O*-acetylation of GD2 in breast cancer cells. Basically, *O*-acetylation is produced by the enzymatic action of SOAT

on a sialic acid residue. CASD1 is the only human SOAT known up to date for inducing the *O*-acetylation of GD3 ganglioside (Baumann *et al.*, 2015). Thus, the involvement of CASD1 in GD2 *O*-acetylation is reasonably questionable. The modulation of CASD1 has been adopted as the strategy to assess the potential SOAT activity of CASD1 on GD2 *O*-acetylation in SUM159PT BC cell line. While transient overexpression or depletion of *CASD1* in SUM159PT modulated *O*AcGD2 expression, the effect of stable clones overexpressing or depleted for *CASD1* expression was more difficult to analyze. Indeed, the stable depletion of *CASD1* using shRNA was not successful. No clones were able to grow longer than a month after the administration of the antibiotic for selection. However, 30 clones overexpressing CASD1 have been isolated and assessed for *O*AcGD2 expression. Three clones were selected according to their level of *O*AcGD2/*CASD1* overexpression. These clones exhibited higher migrative and invasive capacities with no modification of their proliferation rates. Nevertheless, during the maintenance of the clones in culture, the expression of *O*AcGD2 has been lost, as well as the expression of CASD1. These results raise many questions concerning the choice of BC cells used for the study, and the methods employed to generate stable clones. Baumann and coworkers demonstrated CASD1 role in GD3 *O*-acetylation in HAP-1 (human haploid cell) and CHO (Chinese Hamster Ovary) cells (Baumann *et al.*, 2015). Natively, cultured cancer cells bear more chromosomic aberrations (especially an increased chromosome copy number) and different metabolic features compared to normal cells. However, cancer cell lines are usually extrapolated to *in vivo* human tumors and their importance as models for drug testing and translational study have been recognized by many biomedical and pharmaceutical companies. Results obtained by transient transfections in SUM159PT cells were an incentive to use the same cell line for the generation of stably transfected clones. Furthermore, the moderate *O*AcGD2 expression rate in SUM159PT cells was adapted to induce both an increase and a decrease of *O*AcGD2 expression, avoiding of the use of two different cell models to study the effect of *CASD1* modulation on *O*AcGD2 expression. On the other side, shRNA used for stable depletion of *CASD1* expression was designed based on siRNA probes which could efficiently induce *CASD1* depletion. In the same manner, the plasmid used for CASD1 overexpression was the



same for the transient and stable transfection. Interestingly, *CASD1* overexpressing clones could be obtained and isolated, whereas *CASD1* depleted clones did not proliferate at all. The absence of growth of cells depleted for *CASD1* can be interpreted as an ineffective shRNA strategy for the depletion which could be replaced by developing gene editing technologies approaches such as CRISPR-Cas9. Importantly, *CASD1* is ubiquitously expressed in all tissues and cells according to the Human Protein Atlas. Besides, Kaplan Meier plotter shows a better survival of BC patients when *CASD1* is highly expressed. These data confer to *CASD1* an essential role in cell maintenance and could explain the absence of cell growth when *CASD1* is depleted in human cancer cell lines. However, *CASD1* knock out cells were edited by CRISPR Cas-9 technology in HAP-1 (human haploid cells) and CHO (Chinese hamster ovary) cells. These clones did not show any disturbance of their proliferative and growth capacities (Baumann *et al.*, 2015). This reflects an issue either in the experimental process used for knocking out *CASD1* or in the choice of cell-type used for this experiment. Moreover, an additional complexity level to understand the role of *CASD1* arises from the results obtained using *CASD1* overexpressing clones. The maintenance of these clones in culture for 10 passages induced both the loss of *CASD1* overexpression and of *OAcGD2* expression suggesting that an inducible overexpression system would be more suitable to study the effect of *CASD1* effect in SUM159PT in a time independent manner. It is commonly admitted that ganglioside expression is versatile and depends on cell confluency and passage number. That is why all the experiments performed for gangliosides analysis have been processed at maximum 80% of cell confluency, using cells maintained in culture for less than 15 passages. The MDA-MB-231 GD3S+ clones overexpressing GD3 synthase previously produced in our lab are different: they maintain their ganglioside expression pattern regardless of the cell confluency and cell passage number. Considering these facts, the loss of *OAcGD2* in SUM159PT could be due to the versatility of gangliosides expression but this did not explain the loss of *CASD1* overexpression in clones. However, the difficulty to modulate *CASD1* expression in SUM159PT cells suggests a highly regulated *CASD1* expression in these cells, and maybe in a more general manner. For now, *CASD1* is mentioned only in 7 publications in Pubmed (NCBI) highlighting the little knowledge available

regarding CASD1 physiological role. The difficulties encountered in the cloning and isolation of SOAT up to now render the deciphering of *O*-acetylated ganglioside biosynthesis mechanisms more complicated. Besides, the effects of CASD1 in GD2 *O*-acetylation are still unclear. Indeed, the transient transfection experiments predict a role of CASD1 in GD2 *O*-acetylation suggesting that CASD1-dependent pathway for ganglioside *O*-acetylation exist. In order to gain further insights into the biosynthesis mechanisms of ganglioside *O*-acetylation, the structural characterization of *O*-acetylated gangliosides was required.

Consequently, in the second part on my project, gangliosides expression have been analyzed on a panel of BC cell lines and a melanoma cell line. Based on immunodetection analysis, GD3, GD2 and *O*AcGD2 expression has been detected in BC cell lines. The absence of *O*AcGD3 expression in BC cell lines was confirmed by flow cytometry and immunocytochemistry followed by confocal microscopy analysis. The absence of *O*AcGD3 expression suggests a direct synthesis of *O*AcGD2 by *O*-acetylation of GD2. Structural analysis of gangliosides by mass spectrometry is a combinatorial approach to *in situ* immunodetection methods. However, the *O*-acetylated group is alkali labile and remains challenging to handle during mass spectrometry analysis. Accordingly, the first approach developed for structural analysis of *O*-acetylated gangliosides was the analysis of DMB-Sia derivatives. Gangliosides were extracted from cell pellets and sialic acids were hydrolyzed before being derivatized with the fluorescent DMB. This study has been performed on six BC cell lines, two native cell lines SUM 159 PT and Hs 578T, two controls cell lines MDA-MB-231 and MCF-7 and two clones overexpressing GD3 synthase MDA-MB-231 GD3S+ and MCF-7 GD3S+. The analysis of DMB-Sia derivatives by LC-MS shows that the main *O*-acetylated sialic acid species expressed by gangliosides is 9-*O*-acetylated sialic acid. A minor expression of 8-*O*-acetylated sialic acid has been also identified in gangliosides extracted from BC cell lines. The ratios Neu5,9Ac<sub>2</sub>/Neu5Ac detected in gangliosides for MDA-MB-231 GD3S+ and MCF-7 GD3S+ are up to 3-fold higher than their control counterpart. Interestingly, the ratio Neu5,9Ac<sub>2</sub>/Neu5Ac detected in other cellular fractions such as soluble proteins and free sialic acids remains the same between GD3S+ clones and their control counterparts. Besides, GD3S+ cell lines exhibit *O*AcGD2

expression while *OAcGD2* expression is absent in their control counterpart using flow cytometry analysis. These results highlight a close interrelationship between *OAcGD2* and Neu5,9Ac<sub>2</sub> expression suggesting that *OAcGD2* is mainly 9-*O*-acetylated.

The analysis of DMB-Sia derivatives by LC-MS gives structural insights by allowing the identification of the carbone residue that carries the *O*-acetyl group but does not provide information regarding the complete structure of *O*-acetylated gangliosides. That is why in a next step, native gangliosides analysis by MALDI-QIT-TOF was optimized to obtain precise and complete structural characterization of the entire ganglioside species. Our experiments allowed the profiling of *O*-acetylated gangliosides species in BC cell lines, with the identification of *OAcGM1*, *OAcGD3*, *OAcGD2*, *OAcGT3* and *OAcGT2* gangliosides. Interestingly, the relative quantification of gangliosides species leads to the same result than the one obtained by LC-MS on DMB Sia derivatives. The quantification of the different ganglioside species showed that the *O*-acetylated gangliosides amounts detected in MDA-MB-231 GD3S+ and MCF-7 GD3S+ are 3-fold higher than in their control counterparts. The role of GD3 synthase as the key enzyme for b-series gangliosides expression is already well documented. Besides this role, results obtained in GD3S+ clones highlight the role of GD3 synthase in *O*-acetylated ganglioside expression which could be due to substrate availability. Indeed, GD3 synthase is the key enzyme for b-series ganglioside expressions leading to the synthesis of precursor gangliosides such as GD3, GT3. The more substrates for *O*-acetyltransferases are available, the more *O*-acetylated gangliosides can be expressed, and further steps are engaged in the biosynthesis pathways. Furthermore, MS/MS fragmentation led to the identification of the sialic acid residues that carry the *O*-acetylated groups on gangliosides. Previous data suggested that *O*-acetylation of gangliosides occurs only on terminal sialic acid residue (Kohla et al., 2002). Our MS/MS fragmentation experiments identified *O*-acetyl groups on the subterminal or the terminal sialic acid residue, in a cell type dependent manner, regardless of the *O*-acetylated ganglioside species. In Hs 578T and MDA-MB-231 GD3S+ clones, GD2 *O*-acetylation can occur on the subterminal or the terminal sialic acid residue, whereas it occurs on the terminal sialic acid residue in LAN-1 cell line. In the same manner, *O*-

acetylation in *O*AcGD3 and *O*AcGT3 can occur on the terminal sialic acid residue in MDA-MB-231 clones overexpressing GD3 synthase. The biological significance of *O*-acetylation on the subterminal or the terminal sialic acid remains unclear. Indeed, there are no data underlining this possibility in the literature. However, the migration of *O*-acetyl group from C7 to C9 of the sialic acid residue has been described (Vandamme-Feldhaus and Schauer, 1998). Considering the carbohydrate moiety of ganglioside as a dynamic entity, a possible suggestion might be the migration of *O*-acetylated group from one sialic acid residue to the other. The absence of specificity of *O*-acetylation position (subterminal or terminal) according to the ganglioside species but rather in a cell-type dependent-manner suggests that SOAT would not act directly on activated CMP-Neu5Ac as reported (Baumann *et al.*, 2015), but rather that *O*-acetylation of sialic acid occur directly on the carbohydrate moiety of gangliosides. This hypothesis could be verified by enzymatic reaction on plate by an *in vitro* assay using GD2 as the acceptor substrate, acetyl CoA as the donor substrate and soluble CASD1 as SOAT. The first step of the experimental procedure consists on coating purified GD2 on 96-well plate. Then soluble CASD1, produced as recombinant enzyme in Sf9 insect cells or p3xflagCMV9 vector, has to be added to the 96-well plates. The reaction mixture will be supplemented by the donor substrate acetyl CoA. The production of *O*AcGD2 will be assessed by immunofluorescence using anti-*O*AcGD2 8B6 mAb. If the product resulting from the enzymatic reaction is *O*AcGD2, it will verify the activity of CASD1 on GD2 itself. If *O*AcGD2 is produced as the result of the enzymatic sialylation, this will mean that  $\beta$ 4GalNAcTI can recognize Neu5,9Ac2 as a substrate and also that SOAT acts on activated CMP-Neu5Ac. In the other case, GM2 or GD2 may also result from the enzymatic reaction meaning that *O*-acetylation occurs directly on the carbohydrate moiety after the sialylation step.

The combination of data from LC-MS and MALDI-QIT-TOF analyses led to the structural characterization of *O*-acetylated gangliosides species expressed by BC cells. In that manner, the position of *O*-acetylated group, the sialic acid residue(s) that carry it, and also the complete structure of *O*-acetylated gangliosides species have been properly identified. In order to supplement this profiling study, two approaches can be developed. In our studies, only mono-*O*-

acetylated sialic acid species were investigated by LC-MS, but the analysis framework could be adapted to the analysis of di- or tri-acetylated sialic acids. Indeed, the 7,9 di-*O*-acetylated form of sialic acid is detected in human tissues and is a target for influenza virus infection in human (Wasik *et al.*, 2017). It would be interesting to investigate whether di- or even tri-*O*-acetylated sialic acid species can be expressed by tumors, since *O*-acetylation by itself can alter cell signaling processes. For example, the *O*-acetylation of GD3 induces the delocalization of GD3 to the cell membrane and leads to the loss of apoptotic properties of GD3 (Knierp *et al.*, 2006). Furthermore, *O*-acetylation of GD3 is essential for the survival of acute lymphoblastic leukemia cells and induces resistance to several drugs like nilotinib and vincristine in acute lymphoblastic leukemia (Parameswaran *et al.*, 2013). The second approach is to extend our analyses to normal and cancer tissues in order to identify specific tumor markers by LC-MS and MALDI-QIT-TOF. The completed profiling pattern will lead to determine specific differences between normal and tumor tissues in order to finely define potential immunotherapeutic targets.

In contrast to our results obtained by immunodetection analysis, *O*AcGD3 is detected in BC cell lines by MALDI-QIT-TOF. In our first publication, because of the absence of *O*AcGD3, we suggested a direct synthesis of *O*AcGD2 from GD2 (Cavdarli *et al.*, 2019). The diversity of *O*-acetylation on sialic acids suggests that *O*-acetylation is the final step occurring in the biosynthetic process. *O*AcGD2, *O*AcGD3, and *O*AcGT3 have been concomitantly identified in cell lines overexpressing GD3 synthase underlining again the importance of substrate availability in the *O*-acetylation process. Besides, GM2/GD2 synthase knock-out mice exhibit an accumulation of *O*AcGD3 and a decreased level of *O*-acetylation inducer Tis 21. Thus, the accumulated GD3 is converted to *O*AcGD3 due to the substrate availability (Furukawa *et al.*, 2008). The possibility of a direct ganglioside *O*-acetylation mechanism is controversial but remains an attractive possibility that would need to be confirmed by *in vitro* *O*-acetylation experiments. Glycosyltransferases are the key elements for ganglioside biosynthesis. As depicted in part III of Results, the differential expression of glycosyltransferases between BC cell lines showed that glycosyltransferases are upregulated in cell lines overexpressing GD3 synthase compared to their

control counterparts, and in cell lines having a triple negative status compared to a luminal status. The same analysis has been performed for CASD1 and SLC33A1 (the acetyl CoA transporter) which are the main enzymes known for their potential role in ganglioside *O*-acetylation. However, their expression level in BC cells, *O*-acetylated gangliosides have been identified in BC cell lines. These results point to the potential existence of at least two pathways for ganglioside *O*-Acetylation: a CASD1-dependent and a CASD1-independent *O*-acetylation pathway, which suggests that further investigations for the identification of new SOATs are required.

The last part of my PhD project aimed to complete preliminary steps for the identification of new genes involved in GD2 *O*-acetylation. Using a high throughput phosphatome/kinome screening assay on MDA-MB-231 GD3S+ cells, we identified 72 hits involved in *O*AcGD2 expression. Many of the genes identified are belonging to the lipid and carbohydrate metabolism pathways or to MAPK/PI3K cell signaling pathways, suggesting to a highly controlled *O*AcGD2 expression in tumor cells. Interestingly, half of the hits identified are *O*AcGD2 repressor genes, whose depletion upregulates *O*AcGD2 expression to a higher level than the basal expression of *O*AcGD2. In the negative control, *O*AcGD2 is totally absent, whereas in *O*AcGD2 downregulating hits, a low expression level of *O*AcGD2 is maintained. There is a finely tuned process regulating *O*AcGD2 expression in cancer cells which requires at least a very low basal level of *O*AcGD2 expression. Besides, the level of *O*AcGD2 in upregulating hits are much higher than the basal level of *O*AcGD2 suggesting an important feedback regulating the level of expression. Indeed, the expression of *O*AcGD2 could be doubled or tripled by downregulating several genes, such as Ceramide kinase CERK. The identification of genes that tightly control *O*AcGD2 biosynthesis is of great interest regarding the therapeutic potential of *O*AcGD2 as a targetable antigen in BC. Besides, validated hits could represent new targets for therapy in combination with 8B6 mAb, since therapeutic combination can enhance anti-tumor treatment efficacy and improve patient outcomes. Dinutuximab has been approved by the FDA as a therapeutic combination with interleukine-2, 13 cis-retinoic acid and GM-CSF in pediatric NB (Dhillon, 2015). A phase 2 trial evidenced that the chemotherapeutic combination of irinotecan, temozolomide supplemented



with dinutuximab induces a better outcome in children with relapse and refractory NB than the combination supplemented with temsirolimus (Mody *et al.*, 2017). Temozolomide is also used as an adjuvant chemotherapeutic agent with radiotherapy in the first line treatment of glioblastoma. It induces improved survival outcome of patients up to 19 months but cannot prevent the high rate of tumor recurrence (Stupp *et al.*, 2005). The chemoresistance to temozolomide is dependent on the presence of cancer stem cells (CSC) in glioblastoma tumors. Cancer Stem cells (CSC) are a subpopulation of tumor cells initiating and promoting tumorigenesis. They are a source of chemotherapeutic resistance to anti-cancer treatment (Fillmore and Kuperwasser, 2008). Thus, targeting specifically CSC should potentiate the effect on tumorigenesis and chemotherapeutic resistance. Fleurence and coworkers have evidenced that therapeutic combination of 8B6 mAb to temozolomide sensitized glioblastoma CSC expressing *O*AcGD2 to temozolomide (Fleurence *et al.*, 2019). In BC, GD2 expression in CSC has been identified by Battula and coworkers. The authors correlated GD2 expression to CD44<sup>high</sup>CD24<sup>low</sup> BC CSC markers showing a correlation between GD2 expression and an increase of tumor malignancy (Battula *et al.*, 2012). In the same line of research, Birkle and coworkers showed that *O*AcGD2 is expressed in CSC and can be used as a biomarker for therapeutic treatment in BC, glioma, acute lymphoid leukemia, acute myeloid leukemia (U.S. Patent No. 10,000,575 issued Jun 19, 2018). As depicted in the patent, *O*AcGD2 expression in CSC correlates with CD44<sup>high</sup>CD24<sup>low</sup> expression in BC. As a conclusion, BC stem cells sustained GD2 and *O*AcGD2 expression and upregulate GD3 synthase expression to promote malignant cancer properties (Battula *et al.*, 2012; Liang *et al.*, 2017).

As a conclusion, this project leads to the identification of *O*AcGD2 as a target for BC immunotherapy. The proper identification of the chemical structure of *O*AcGD2 in different cell lines using several methods give mechanistic insights for the *O*-acetylation of GD2. Indeed, BC cells are characterized by the expression of 9-*O*AcGD2 which can be *O*-acetylated either on the terminal sialic acid residue into *O*-AcNeu5Ac $\alpha$ 2-8Neu5Ac $\alpha$ 2-3LacCer or on the subterminal sialic acid residue, resulting in Neu5Ac $\alpha$ 2-8-*O*-AcNeu5Ac $\alpha$ 2-3LacCer. These first insights into *O*-acetylation mechanisms suggest a direct acetylation of GD2. While the effect of CASD1 still has to be

elucidated, GD3 synthase expression is essential for *O*AcGD2 synthesis, which convinced me of the existence of at least two pathways responsible for GD2 *O*-acetylation. This hypothesis led us to set up a high throughput screening analysis in which we identified 72 genes modulating *O*AcGD2 expression. Our results suggest that *O*-acetylation of gangliosides are finely tuned processes in cancer cells (and likely in normal cells as well), increasing highly the therapeutic potential of this antigen for the treatment of neuroectoderm derived tumors. In this context, two approaches might be held to pursue my work in basic and translational research. The basic research approach requires the identification of new SOATs for the proper understanding of gangliosides *O*-acetylation, for which genome wide screening remains one of the best options. The translational research needs better curative strategy for neuroectoderm derived tumors. These requirements can be fulfilled by defining therapeutic combinations enhancing 8B6 mAb effect on tumors, starting with the validation of hits highlighted by the pilot screening assay.

## REFERENCES

Ahmed, M. and Cheung, N.-K.V. 2014. Engineering anti-GD2 monoclonal antibodies for cancer immunotherapy. *FEBS Lett.*, **588**: 288–297.

Akram, M. 2013. Mini-review on glycolysis and cancer. *J. Cancer Educ. Off. J. Am. Assoc. Cancer Educ.*, **28**: 454–457.

Alvarez-Rueda, N., Desselle, A., Cochonneau, D., Chaumette, T., Clemenceau, B., Leprieur, S., Bougras, G., Supiot, S., Mussini, J.-M., Barbet, J., Saba, J., Paris, F., Aubry, J. and Birklé, S. 2011. A Monoclonal Antibody to O-Acetyl-GD2 Ganglioside and Not to GD2 Shows Potent Anti-Tumor Activity without Peripheral Nervous System Cross-Reactivity. *PLoS ONE*, **6**.

Amin, M.B., Greene, F.L., Edge, S.B., Compton, C.C., Gershewald, J.E., Brookland, R.K., Meyer, L., Gress, D.M., Byrd, D.R. and Winchester, D.P. 2017. The Eighth Edition AJCC Cancer Staging Manual: Continuing to build a bridge from a population-based to a more “personalized” approach to cancer staging. *CA. Cancer J. Clin.*, **67**: 93–99.

Anantharaman, V. and Aravind, L. 2010. Novel eukaryotic enzymes modifying cell-surface biopolymers. *Biol. Direct*, **5**: 1.

Arming, S., Wipfler, D., Mayr, J., Merling, A., Vilas, U., Schauer, R., Schwartz-Albiez, R. and Vlasak, R. 2011. The human Cas1 protein: a sialic acid-specific O-acetyltransferase? *Glycobiology*, **21**: 553–564.

Bannas, P., Hambach, J. and Koch-Nolte, F. 2017. Nanobodies and Nanobody-Based Human Heavy Chain Antibodies As Antitumor Therapeutics. *Front. Immunol.*, **8**: 1603.

Barker, E., Mueller, B.M., Handgretinger, R., Herter, M., Yu, A.L. and Reisfeld, R.A. 1991. Effect of a chimeric anti-ganglioside GD2 antibody on cell-mediated lysis of human neuroblastoma cells. *Cancer Res.*, **51**: 144–149.

Battula, V.L., Shi, Y., Evans, K.W., Wang, R.-Y., Spaeth, E.L., Jacamo, R.O., Guerra, R., Sahin, A.A., Marini, F.C., Hortobagyi, G., Mani, S.A. and Andreeff, M. 2012. Ganglioside GD2 identifies breast cancer stem cells and promotes tumorigenesis. *J. Clin. Invest.*, **122**: 2066–2078.

Baumann, A.-M.T., Bakkers, M.J.G., Buettner, F.F.R., Hartmann, M., Grove, M., Langereis, M.A., de Groot, R.J. and Mühlenhoff, M. 2015. 9-O-Acetylation of sialic acids is catalysed by CASD1 via a covalent acetyl-enzyme intermediate. *Nat. Commun.*, **6**: 7673.

Bigi, A., Morosi, L., Pozzi, C., Forcella, M., Tettamanti, G., Venerando, B., Monti, E. and Fusi, P. 2010. Human sialidase NEU4 long and short are extrinsic proteins bound to outer mitochondrial membrane and the endoplasmic reticulum, respectively. *Glycobiology*, **20**: 148–157.

Boes, M. 2000. Role of natural and immune IgM antibodies in immune responses. *Mol. Immunol.*, **37**: 1141–1149.

Boulianne, G.L., Hozumi, N. and Shulman, M.J. 1984. Production of functional chimaeric mouse/human antibody. *Nature*, **312**: 643–646.

Bruhns, P. 2012. Properties of mouse and human IgG receptors and their contribution to disease models. *Blood*, **119**: 5640–5649.

- Burstein, H.J., Polyak, K., Wong, J.S., Lester, S.C. and Kaelin, C.M. 2004. Ductal carcinoma in situ of the breast. *N. Engl. J. Med.*, **350**: 1430–1441.
- Butor, C., Diaz, S. and Varki, A. 1993. High level O-acetylation of sialic acids on N-linked oligosaccharides of rat liver membranes. Differential subcellular distribution of 7- and 9-O-acetyl groups and of enzymes involved in their regulation. *J. Biol. Chem.*, **268**: 10197–10206.
- Castel, V., Segura, V. and Cañete, A. 2010. Treatment of high-risk neuroblastoma with anti-GD2 antibodies. *Clin. Transl. Oncol. Off. Publ. Fed. Span. Oncol. Soc. Natl. Cancer Inst. Mex.*, **12**: 788–793.
- Cavdarli, S., Dewald, J.H., Yamakawa, N., Guérardel, Y., Terme, M., Le Doussal, J.-M., Delannoy, P. and Groux-Degroote, S. 2019. Identification of 9-O-acetyl-N-acetylneuraminic acid (Neu5,9Ac2) as main O-acetylated sialic acid species of GD2 in breast cancer cells. *Glycoconj. J.*, doi: 10.1007/s10719-018-09856-w.
- Cazet, A., Bobowski, M., Rombouts, Y., Lefebvre, J., Steenackers, A., Popa, I., Guérardel, Y., Le Bourhis, X., Tulasne, D. and Delannoy, P. 2012. The ganglioside G(D2) induces the constitutive activation of c-Met in MDA-MB-231 breast cancer cells expressing the G(D3) synthase. *Glycobiology*, **22**: 806–816.
- Cazet, A., Groux-Degroote, S., Teylaert, B., Kwon, K.-M., Lehoux, S., Slomianny, C., Kim, C.-H., Le Bourhis, X. and Delannoy, P. 2009. GD3 synthase overexpression enhances proliferation and migration of MDA-MB-231 breast cancer cells. *Biol. Chem.*, **390**: 601–609.
- Cerato, E., Birkle, S., Portoukalian, J., Mezazigh, A., Chatal, J.F. and Aubry, J. 1997. Variable region gene segments of nine monoclonal antibodies specific to disialogangliosides (GD2, GD3) and their O-acetylated derivatives. *Hybridoma*, **16**: 307–316.
- Chan, A.C. and Carter, P.J. 2010. Therapeutic antibodies for autoimmunity and inflammation. *Nat. Rev. Immunol.*, **10**: 301–316.
- Chang, T.W., Wu, P.C., Hsu, C.L. and Hung, A.F. 2007. Anti-IgE antibodies for the treatment of IgE-mediated allergic diseases. *Adv. Immunol.*, **93**: 63–119.
- Chanier, T. and Chames, P. 2019. Nanobody Engineering: Toward Next Generation Immunotherapies and Immunoimaging of Cancer. *Antibodies*, **8**: 13.
- Chen, H.Y., Challa, A.K. and Varki, A. 2006. 9-O-acetylation of exogenously added ganglioside GD3. The GD3 molecule induces its own O-acetylation machinery. *J. Biol. Chem.*, **281**: 7825–7833.
- Cheung, N.K., Guo, H.F., Heller, G. and Cheung, I.Y. 2000. Induction of Ab3 and Ab3' antibody was associated with long-term survival after anti-G(D2) antibody therapy of stage 4 neuroblastoma. *Clin. Cancer Res. Off. J. Am. Assoc. Cancer Res.*, **6**: 2653–2660.
- Cheung, N.K., Lazarus, H., Miraldi, F.D., Abramowsky, C.R., Kallick, S., Saarinen, U.M., Spitzer, T., Strandjord, S.E., Coccia, P.F. and Berger, N.A. 1987. Ganglioside GD2 specific monoclonal antibody 3F8: a phase I study in patients with neuroblastoma and malignant melanoma. *J. Clin. Oncol. Off. J. Am. Soc. Clin. Oncol.*, **5**: 1430–1440.
- Cheung, N.K., Saarinen, U.M., Neely, J.E., Landmeier, B., Donovan, D. and Coccia, P.F. 1985. Monoclonal antibodies to a glycolipid antigen on human neuroblastoma cells. *Cancer Res.*, **45**:

2642–2649.

Cheung, N.-K.V., Guo, H., Hu, J., Tassev, D.V. and Cheung, I.Y. 2012. Humanizing murine IgG3 anti-GD2 antibody m3F8 substantially improves antibody-dependent cell-mediated cytotoxicity while retaining targeting in vivo. *Oncoimmunology*, **1**: 477–486.

Chia, J., Goh, G., Racine, V., Ng, S., Kumar, P. and Bard, F. 2012. RNAi screening reveals a large signaling network controlling the Golgi apparatus in human cells. *Mol. Syst. Biol.*, **8**: 629.

Choi, B.D., Cai, M., Bigner, D.D., Mehta, A.I., Kuan, C.-T. and Sampson, J.H. 2011. Bispecific antibodies engage T cells for antitumor immunotherapy. *Expert Opin. Biol. Ther.*, **11**: 843–853.

Clynes, R.A., Towers, T.L., Presta, L.G. and Ravetch, J.V. 2000. Inhibitory Fc receptors modulate in vivo cytotoxicity against tumor targets. *Nat. Med.*, **6**: 443–446.

Cochonneau, D., Terme, M., Michaud, A., Dorvillius, M., Gautier, N., Frikeche, J., Alvarez-Rueda, N., Bougras, G., Aubry, J., Paris, F. and Birklé, S. 2013. Cell cycle arrest and apoptosis induced by O-acetyl-GD2-specific monoclonal antibody 8B6 inhibits tumor growth in vitro and in vivo. *Cancer Lett.*, **333**: 194–204.

Corfield, A.P., Myerscough, N., Warren, B.F., Durdey, P., Paraskeva, C. and Schauer, R. 1999. Reduction of sialic acid O-acetylation in human colonic mucins in the adenoma-carcinoma sequence. *Glycoconj. J.*, **16**: 307–317.

Crespo, P.M., von Muhlinen, N., Iglesias-Bartolomé, R. and Daniotti, J.L. 2008. Complex gangliosides are apically sorted in polarized MDCK cells and internalized by clathrin-independent endocytosis. *FEBS J.*, **275**: 6043–6056.

Daniotti, J.L. and Iglesias-Bartolomé, R. 2011. Metabolic pathways and intracellular trafficking of gangliosides. *IUBMB Life*, **63**: 513–520.

Davies, L.R.L. and Varki, A. 2015. Why Is N-Glycolylneuraminic Acid Rare in the Vertebrate Brain? *Top. Curr. Chem.*, **366**: 31–54.

Deckert, P.M. 2009. Current constructs and targets in clinical development for antibody-based cancer therapy. *Curr. Drug Targets*, **10**: 158–175.

Degroote, S., Wolthoorn, J. and van Meer, G. 2004. The cell biology of glycosphingolipids. *Semin. Cell Dev. Biol.*, **15**: 375–387.

Dhillon, S. 2015. Dinutuximab: first global approval. *Drugs*, **75**: 923–927.

Doronin, I.I., Vishnyakova, P.A., Kholodenko, I.V., Ponomarev, E.D., Ryazantsev, D.Y., Molotkovskaya, I.M. and Kholodenko, R.V. 2014. Ganglioside GD2 in reception and transduction of cell death signal in tumor cells. *BMC Cancer*, **14**: 295.

Elshazzly, M. and Caban, O. 2019. Embryology, Central Nervous System. In: *StatPearls*.

Etchevers, H.C., Dupin, E. and Le Douarin, N.M. 2019. The diverse neural crest: from embryology to human pathology. *Dev. Camb. Engl.*, **146**.

Fillmore, C.M. and Kuperwasser, C. 2008. Human breast cancer cell lines contain stem-like cells



that self-renew, give rise to phenotypically diverse progeny and survive chemotherapy. *Breast Cancer Res. BCR*, **10**: R25.

Fingerhut, R., van der Horst, G.T., Verheijen, F.W. and Conzelmann, E. 1992. Degradation of gangliosides by the lysosomal sialidase requires an activator protein. *Eur. J. Biochem.*, **208**: 623–629.

Fleurence, J., Bahri, M., Fougeray, S., Faraj, S., Vermeulen, S., Pinault, E., Geraldo, F., Oliver, L., Véziers, J., Marquet, P., Rabé, M., Gratas, C., Vallette, F., Pecqueur, C., Paris, F. and Birklé, S. 2019. Impairing temozolomide resistance driven by glioma stem-like cells with adjuvant immunotherapy targeting O-acetyl GD2 ganglioside. *Int. J. Cancer*, doi: 10.1002/ijc.32533.

Fukumoto, S., Mutoh, T., Hasegawa, T., Miyazaki, H., Okada, M., Goto, G., Furukawa, K. and Urano, T. 2000. GD3 synthase gene expression in PC12 cells results in the continuous activation of TrkA and ERK1/2 and enhanced proliferation. *J. Biol. Chem.*, **275**: 5832–5838.

Fürst, W. and Sandhoff, K. 1992. Activator proteins and topology of lysosomal sphingolipid catabolism. *Biochim. Biophys. Acta*, **1126**: 1–16.

Furukawa, Keiko, Aixinjueluo, W., Kasama, T., Ohkawa, Y., Yoshihara, M., Ohmi, Y., Tajima, O., Suzumura, A., Kittaka, D. and Furukawa, Koichi. 2008. Disruption of GM2/GD2 synthase gene resulted in overt expression of 9-O-acetyl GD3 irrespective of Tis21. *J. Neurochem.*, **105**: 1057–1066.

Furukawa, Koichi, Hamamura, K., Aixinjueluo, W. and Furukawa, Keiko. 2006. Biosignals modulated by tumor-associated carbohydrate antigens: novel targets for cancer therapy. *Ann. N. Y. Acad. Sci.*, **1086**: 185–198.

Gelderman, K.A., Tomlinson, S., Ross, G.D. and Gorter, A. 2004. Complement function in mAb-mediated cancer immunotherapy. *Trends Immunol.*, **25**: 158–164.

Gerardy-Schahn, R., Delannoy, P. and Itzstein, M. von. 2015. *SialoGlyco Chemistry and Biology I: Biosynthesis, structural diversity and sialoglycopathologies*.

Giraud, C.G. and Maccioni, H.J.F. 2003. Ganglioside glycosyltransferases organize in distinct multienzyme complexes in CHO-K1 cells. *J. Biol. Chem.*, **278**: 40262–40271.

Govindan, S.V. and Goldenberg, D.M. 2010. New antibody conjugates in cancer therapy. *ScientificWorldJournal*, **10**: 2070–2089.

Gross, N., Beck, D., Portoukalian, J., Favre, S. and Carrel, S. 1989. New anti-GD2 monoclonal antibodies produced from gamma-interferon-treated neuroblastoma cells. *Int. J. Cancer*, **43**: 665–671.

Gu, X., Preuss, U., Gu, T. and Yu, R.K. 1995. Regulation of sialyltransferase activities by phosphorylation and dephosphorylation. *J. Neurochem.*, **64**: 2295–2302.

Gusterson, B.A. and Stein, T. 2012. Human breast development. *Semin. Cell Dev. Biol.*, **23**: 567–573.

Hama, Y., Li, Y.T. and Li, S.C. 1997. Interaction of GM2 activator protein with glycosphingolipids. *J. Biol. Chem.*, **272**: 2828–2833.

Hamers-Casterman, C., Atarhouch, T., Muyldermans, S., Robinson, G., Hamers, C., Songa, E.B., Bendahman, N. and Hamers, R. 1993. Naturally occurring antibodies devoid of light chains. *Nature*, **363**: 446–448.

Hanahan, D. and Weinberg, R.A. 2000. The Hallmarks of Cancer. *Cell*, **100**: 57–70.

Hawley, S.T., Li, Y., An, L.C., Resnicow, K., Janz, N.K., Sabel, M.S., Ward, K.C., Fagerlin, A., Morrow, M., Jagsi, R., Hofer, T.P. and Katz, S.J. 2018. Improving Breast Cancer Surgical Treatment Decision Making: The iCanDecide Randomized Clinical Trial. *J. Clin. Oncol. Off. J. Am. Soc. Clin. Oncol.*, **36**: 659–666.

Heijnen, I.A. and van de Winkel, J.G. 1997. Human IgG Fc receptors. *Int. Rev. Immunol.*, **16**: 29–55.

Hidari, J.K., Ichikawa, S., Furukawa, K., Yamasaki, M. and Hirabayashi, Y. 1994. beta 1-4N-acetylgalactosaminyltransferase can synthesize both asialoglycosphingolipid GM2 and glycosphingolipid GM2 in vitro and in vivo: isolation and characterization of a beta 1-4N-acetylgalactosaminyltransferase cDNA clone from rat ascites hepatoma cell line AH7974F. *Biochem. J.*, **303 ( Pt 3)**: 957–965.

Hoffmann, T.K., Meidenbauer, N., Dworacki, G., Kanaya, H. and Whiteside, T.L. 2000. Generation of tumor-specific T-lymphocytes by cross-priming with human dendritic cells ingesting apoptotic tumor cells. *Cancer Res.*, **60**: 3542–3549.

Horwacik, I., Durbas, M., Boratyn, E., Węgrzyn, P. and Rokita, H. 2013. Targeting GD2 ganglioside and aurora A kinase as a dual strategy leading to cell death in cultures of human neuroblastoma cells. *Cancer Lett.*, **341**: 248–264.

Huwiler, A., Kolter, T., Pfeilschifter, J. and Sandhoff, K. 2000. Physiology and pathophysiology of sphingolipid metabolism and signaling. *Biochim. Biophys. Acta*, **1485**: 63–99.

Hwang, W.Y.K. and Foote, J. 2005. Immunogenicity of engineered antibodies. *Methods San Diego Calif*, **36**: 3–10.

Ishii, A., Ohta, M., Watanabe, Y., Matsuda, K., Ishiyama, K., Sakoe, K., Nakamura, M., Inokuchi, J., Sanai, Y. and Saito, M. 1998. Expression cloning and functional characterization of human cDNA for ganglioside GM3 synthase. *J. Biol. Chem.*, **273**: 31652–31655.

Ito, M. and Yamagata, T. 1986. A novel glycosphingolipid-degrading enzyme cleaves the linkage between the oligosaccharide and ceramide of neutral and acidic glycosphingolipids. *J. Biol. Chem.*, **261**: 14278–14282.

Iwersen, M., Dora, H., Kohla, G., Gasa, S. and Schauer, R. 2003. Solubilisation and properties of the sialate-4-O-acetyltransferase from guinea pig liver. *Biol. Chem.*, **384**: 1035–1047.

Iwersen, M., Vandamme-Feldhaus, V. and Schauer, R. 1998. Enzymatic 4-O-acetylation of N-acetylneuraminic acid in guinea-pig liver. *Glycoconj. J.*, **15**: 895–904.

Janbon, G., Himmelreich, U., Moyrand, F., Improvisi, L. and Dromer, F. 2001. Cas1p is a membrane protein necessary for the O-acetylation of the *Cryptococcus neoformans* capsular polysaccharide. *Mol. Microbiol.*, **42**: 453–467.

Jeckel, D., Karrenbauer, A., Burger, K.N., van Meer, G. and Wieland, F. 1992. Glucosylceramide is synthesized at the cytosolic surface of various Golgi subfractions. *J. Cell Biol.*, **117**: 259–267.

Kakugawa, Y., Wada, T., Yamaguchi, K., Yamanami, H., Ouchi, K., Sato, I. and Miyagi, T. 2002. Up-regulation of plasma membrane-associated ganglioside sialidase (Neu3) in human colon cancer and its involvement in apoptosis suppression. *Proc. Natl. Acad. Sci. U. S. A.*, **99**: 10718–10723.

Kanamori, A., Nakayama, J., Fukuda, M.N., Stallcup, W.B., Sasaki, K., Fukuda, M. and Hirabayashi, Y. 1997. Expression cloning and characterization of a cDNA encoding a novel membrane protein required for the formation of O-acetylated ganglioside: a putative acetyl-CoA transporter. *Proc. Natl. Acad. Sci. U. S. A.*, **94**: 2897–2902.

Kaplon, H. and Reichert, J.M. 2019. Antibodies to watch in 2019. *mAbs*, **11**: 219–238.

Kishimoto, Y., Hiraiwa, M. and O'Brien, J.S. 1992. Saposins: structure, function, distribution, and molecular genetics. *J. Lipid Res.*, **33**: 1255–1267.

Klee, G.G. 2000. Human anti-mouse antibodies. *Arch. Pathol. Lab. Med.*, **124**: 921–923.

Klein, A., Diaz, S., Ferreira, I., Lamblin, G., Roussel, P. and Manzi, A.E. 1997. New sialic acids from biological sources identified by a comprehensive and sensitive approach: liquid chromatography-electrospray ionization-mass spectrometry (LC-ESI-MS) of SIA quinoxalinones. *Glycobiology*, **7**: 421–432.

Klein, A., Henseler, M., Klein, C., Suzuki, K., Harzer, K. and Sandhoff, K. 1994. Sphingolipid activator protein D (sap-D) stimulates the lysosomal degradation of ceramide in vivo. *Biochem. Biophys. Res. Commun.*, **200**: 1440–1448.

Klyuyeva, A., Tuganova, A., Kedishvili, N. and Popov, K.M. 2019. Tissue-specific kinase expression and activity regulate flux through the pyruvate dehydrogenase complex. *J. Biol. Chem.*, **294**: 838–851.

Kniep, B., Kniep, E., Ozkucur, N., Barz, S., Bachmann, M., Malisan, F., Testi, R. and Rieber, E.P. 2006. 9-O-acetyl GD3 protects tumor cells from apoptosis. *Int. J. Cancer*, **119**: 67–73.

Köhler, G. and Milstein, C. 1975. Continuous cultures of fused cells secreting antibody of predefined specificity. *Nature*, **256**: 495–497.

Kolter, T., Proia, R.L. and Sandhoff, K. 2002. Combinatorial Ganglioside Biosynthesis. *J. Biol. Chem.*, **277**: 25859–25862.

Kowalczyk, A., Gil, M., Horwacik, I., Odrowaz, Z., Kozbor, D. and Rokita, H. 2009. The GD2-specific 14G2a monoclonal antibody induces apoptosis and enhances cytotoxicity of chemotherapeutic drugs in IMR-32 human neuroblastoma cells. *Cancer Lett.*, **281**: 171–182.

Kushner, B.H., Cheung, I.Y., Kramer, K., Modak, S. and Cheung, N.-K.V. 2007. High-dose cyclophosphamide inhibition of humoral immune response to murine monoclonal antibody 3F8 in neuroblastoma patients: broad implications for immunotherapy. *Pediatr. Blood Cancer*, **48**: 430–434.

Kushner, B.H. and Cheung, N.K. 1989. GM-CSF enhances 3F8 monoclonal antibody-dependent

cellular cytotoxicity against human melanoma and neuroblastoma. *Blood*, **73**: 1936–1941.

Ladenstein, R., Pötschger, U., Valteau-Couanet, D., Luksch, R., Castel, V., Yaniv, I., Laureys, G., Brock, P., Michon, J.M., Owens, C., Trahair, T., Chan, G.C.F., Ruud, E., Schroeder, H., Beck Popovic, M., Schreier, G., Loibner, H., Ambros, P., Holmes, K., *et al.* 2018. Interleukin 2 with anti-GD2 antibody ch14.18/CHO (dinutuximab beta) in patients with high-risk neuroblastoma (HR-NBL1/SIOPEN): a multicentre, randomised, phase 3 trial. *Lancet Oncol.*, **19**: 1617–1629.

Lahti, J.M., Valentine, M., Xiang, J., Jones, B., Amann, J., Grenet, J., Richmond, G., Look, A.T. and Kidd, V.J. 1994. Alterations in the PITSLRE protein kinase gene complex on chromosome 1p36 in childhood neuroblastoma. *Nat. Genet.*, **7**: 370–375.

Lannert, H., Bünning, C., Jeckel, D. and Wieland, F.T. 1994. Lactosylceramide is synthesized in the lumen of the Golgi apparatus. *FEBS Lett.*, **342**: 91–96.

Liang, Y.-J., Ding, Y., Levery, S.B., Lobaton, M., Handa, K. and Hakomori, S. 2013. Differential expression profiles of glycosphingolipids in human breast cancer stem cells vs. cancer non-stem cells. *Proc. Natl. Acad. Sci. U. S. A.*, **110**: 4968–4973.

Liang, Y.-J., Wang, C.-Y., Wang, I.-A., Chen, Y.-W., Li, L.-T., Lin, C.-Y., Ho, M.-Y., Chou, T.-L., Wang, Y.-H., Chiou, S.-P., Lin, Y.-J., Yu, J., Liang, Y.-J., Wang, C.-Y., Wang, I.-A., Chen, Y.-W., Li, L.-T., Lin, C.-Y., Ho, M.-Y., *et al.* 2017. Interaction of glycosphingolipids GD3 and GD2 with growth factor receptors maintains breast cancer stem cell phenotype. *Oncotarget*, **5**.

Linke, T., Wilkening, G., Sadeghlar, F., Mozcall, H., Bernardo, K., Schuchman, E. and Sandhoff, K. 2001. Interfacial regulation of acid ceramidase activity. Stimulation of ceramide degradation by lysosomal lipids and sphingolipid activator proteins. *J. Biol. Chem.*, **276**: 5760–5768.

Livingston, P.O., Ritter, G. and Calves, M.J. 1989. Antibody response after immunization with the gangliosides GM1, GM2, GM3, GD2 and GD3 in the mouse. *Cancer Immunol. Immunother. CII*, **29**: 179–184.

Magnusson, S.E., Engström, M., Jacob, U., Ulfgren, A.-K. and Kleinau, S. 2007. High synovial expression of the inhibitory FcγRIIb in rheumatoid arthritis. *Arthritis Res. Ther.*, **9**: R51.

Mahajan, V.S., Alsufyani, F., Mattoo, H., Rosenberg, I. and Pillai, S. 2019. Alterations in sialic-acid O-acetylation glycoforms during murine erythrocyte development. *Glycobiology*, **29**: 222–228.

Manches, O., Lui, G., Chaperot, L., Gressin, R., Molens, J.-P., Jacob, M.-C., Sotto, J.-J., Leroux, D., Bensa, J.-C. and Plumas, J. 2003. In vitro mechanisms of action of rituximab on primary non-Hodgkin lymphomas. *Blood*, **101**: 949–954.

Mandal, C., Schwartz-Albiez, R. and Vlasak, R. 2015. Functions and Biosynthesis of O-Acetylated Sialic Acids. *Top. Curr. Chem.*, **366**: 1–30.

Maris, J.M., Hogarty, M.D., Bagatell, R. and Cohn, S.L. 2007. Neuroblastoma. *Lancet Lond. Engl.*, **369**: 2106–2120.

Martina, J.A., Daniotti, J.L. and Maccioni, H.J.F. 1998. Influence of N-Glycosylation and N-Glycan Trimming on the Activity and Intracellular Traffic of GD3 Synthase. *J. Biol. Chem.*, **273**: 3725–3731.

Medlock, K.A. and Merrill, A.H. 1988. Rapid turnover of sphingosine synthesized de novo from [14C]serine by Chinese hamster ovary cells. *Biochem. Biophys. Res. Commun.*, **157**: 232–237.

Meknache, N., Jönsson, F., Laurent, J., Guinnepain, M.-T. and Daëron, M. 2009. Human basophils express the glycosylphosphatidylinositol-anchored low-affinity IgG receptor FcγRIIIB (CD16B). *J. Immunol. Baltim. Md 1950*, **182**: 2542–2550.

Miller-Podraza, H. and Fishman, P.H. 1982. Translocation of newly synthesized gangliosides to the cell surface. *Biochemistry*, **21**: 3265–3270.

Mir, M.A., Mehraj, U., Sheikh, B.A. and Hamdani, S.S. 2019. Nanobodies: The “magic bullets” in therapeutics, drug delivery and diagnostics. *Hum. Antibodies*, doi: 10.3233/HAB-190390.

Mody, R., Naranjo, A., Van Ryn, C., Yu, A.L., London, W.B., Shulkin, B.L., Parisi, M.T., Servaes, S.-E.-N., Diccianni, M.B., Sondel, P.M., Bender, J.G., Maris, J.M., Park, J.R. and Bagatell, R. 2017. Irinotecan-temozolomide with temsirolimus or dinutuximab in children with refractory or relapsed neuroblastoma (COG ANBL1221): an open-label, randomised, phase 2 trial. *Lancet Oncol.*, doi: 10.1016/S1470-2045(17)30355-8.

Monti, E. and Miyagi, T. 2015. Structure and Function of Mammalian Sialidases. *Top. Curr. Chem.*, **366**: 183–208.

Moreau, K., Ravikumar, B., Renna, M., Puri, C. and Rubinsztein, D.C. 2011. Autophagosome precursor maturation requires homotypic fusion. *Cell*, **146**: 303–317.

Morimoto, S., Yamamoto, Y., O'Brien, J.S. and Kishimoto, Y. 1990. Determination of saposin proteins (sphingolipid activator proteins) in human tissues. *Anal. Biochem.*, **190**: 154–157.

Morrison, S.L., Johnson, M.J., Herzenberg, L.A. and Oi, V.T. 1984. Chimeric human antibody molecules: mouse antigen-binding domains with human constant region domains. *Proc. Natl. Acad. Sci. U. S. A.*, **81**: 6851–6855.

Mueller, I., Ehlert, K., Endres, S., Pill, L., Siebert, N., Kietz, S., Brock, P., Garaventa, A., Valteau-Couanet, D., Janzek, E., Hosten, N., Zinke, A., Barthlen, W., Varol, E., Loibner, H., Ladenstein, R. and Lode, H.N. 2018. Tolerability, response and outcome of high-risk neuroblastoma patients treated with long-term infusion of anti-GD2 antibody ch14.18/CHO. *mAbs*, **10**: 55–61.

Mujoo, K., Cheresch, D.A., Yang, H.M. and Reisfeld, R.A. 1987. Disialoganglioside GD2 on human neuroblastoma cells: target antigen for monoclonal antibody-mediated cytolysis and suppression of tumor growth. *Cancer Res.*, **47**: 1098–1104.

Mujoo, K., Kipps, T.J., Yang, H.M., Cheresch, D.A., Wargalla, U., Sander, D.J. and Reisfeld, R.A. 1989. Functional properties and effect on growth suppression of human neuroblastoma tumors by isotype switch variants of monoclonal antiganglioside GD2 antibody 14.18. *Cancer Res.*, **49**: 2857–2861.

Nairn, A.V., York, W.S., Harris, K., Hall, E.M., Pierce, J.M. and Moremen, K.W. 2008. Regulation of glycan structures in animal tissues: transcript profiling of glycan-related genes. *J. Biol. Chem.*, **283**: 17298–17313.

Nelson, M.A., Ariza, M.E., Yang, J.M., Thompson, F.H., Taetle, R., Trent, J.M., Wymer, J., Massey-

- Brown, K., Broome-Powell, M., Easton, J., Lahti, J.M. and Kidd, V.J. 1999. Abnormalities in the p34cdc2-related PITSLRE protein kinase gene complex (CDC2L) on chromosome band 1p36 in melanoma. *Cancer Genet. Cytogenet.*, **108**: 91–99.
- Neve, R.M., Chin, K., Fridlyand, J., Yeh, J., Baehner, F.L., Fevr, T., Clark, L., Bayani, N., Coppe, J.-P., Tong, F., Speed, T., Spellman, P.T., DeVries, S., Lapuk, A., Wang, N.J., Kuo, W.-L., Stilwell, J.L., Pinkel, D., Albertson, D.G., *et al.* 2006. A collection of breast cancer cell lines for the study of functionally distinct cancer subtypes. *Cancer Cell*, **10**: 515–527.
- Nimmerjahn, F. and Ravetch, J.V. 2007. Fc-receptors as regulators of immunity. *Adv. Immunol.*, **96**: 179–204.
- Nomura, T., Takizawa, M., Aoki, J., Arai, H., Inoue, K., Wakisaka, E., Yoshizuka, N., Imokawa, G., Dohmae, N., Takio, K., Hattori, M. and Matsuo, N. 1998. Purification, cDNA cloning, and expression of UDP-Gal: glucosylceramide beta-1,4-galactosyltransferase from rat brain. *J. Biol. Chem.*, **273**: 13570–13577.
- Oiseth, S.J. and Aziz, M.S. 2017. Cancer immunotherapy: a brief review of the history, possibilities, and challenges ahead. *J. Cancer Metastasis Treat.*, **3**: 250.
- Orsi, G., Barbolini, M., Ficarra, G., Tazzioli, G., Manni, P., Petrachi, T., Mastrolia, I., Orvieto, E., Spano, C., Prapa, M., Kaleci, S., D'Amico, R., Guarneri, V., Dieci, M.V., Cascinu, S., Conte, P., Piacentini, F. and Dominici, M. 2017. GD2 expression in breast cancer. *Oncotarget*, **8**: 31592–31600.
- Owens, T.W. and Naylor, M.J. 2013. Breast cancer stem cells. *Front. Physiol.*, **4**.
- Parameswaran, R., Lim, M., Arutyunyan, A., Abdel-Azim, H., Hurtz, C., Lau, K., Müschen, M., Yu, R.K., Itzstein, M. von, Heisterkamp, N. and Groffen, J. 2013. O-acetylated N-acetylneuraminic acid as a novel target for therapy in human pre-B acute lymphoblastic leukemia. *J. Exp. Med.*, **210**: 805–819.
- Perry, R.J. and Ridgway, N.D. 2005. Molecular mechanisms and regulation of ceramide transport. *Biochim. Biophys. Acta*, **1734**: 220–234.
- Rojas, K. and Stuckey, A. 2016. Breast Cancer Epidemiology and Risk Factors. *Clin. Obstet. Gynecol.*, **59**: 651–672.
- Roth, M., Linkowski, M., Tarim, J., Piperdi, S., Sowers, R., Geller, D., Gill, J. and Gorlick, R. 2014. Ganglioside GD2 as a therapeutic target for antibody-mediated therapy in patients with osteosarcoma. *Cancer*, **120**: 548–554.
- Safdari, Y., Farajnia, S., Asgharzadeh, M. and Khalili, M. 2013. Antibody humanization methods - a review and update. *Biotechnol. Genet. Eng. Rev.*, **29**: 175–186.
- Sahagan, B.G., Dorai, H., Saltzgaber-Muller, J., Toneguzzo, F., Guindon, C.A., Lilly, S.P., McDonald, K.W., Morrissey, D.V., Stone, B.A. and Davis, G.L. 1986. A genetically engineered murine/human chimeric antibody retains specificity for human tumor-associated antigen. *J. Immunol. Baltim. Md 1950*, **137**: 1066–1074.
- Sarkar, T.R., Battula, V.L., Werden, S.J., Vijay, G.V., Ramirez-Peña, E.Q., Taube, J.H., Chang, J.T., Miura, N., Porter, W., Sphyris, N., Andreeff, M. and Mani, S.A. 2015. GD3 synthase regulates epithelial-mesenchymal transition and metastasis in breast cancer. *Oncogene*, **34**: 2958–2967.



- Satake, H., Chen, H.Y. and Varki, A. 2003. Genes modulated by expression of GD3 synthase in Chinese hamster ovary cells. Evidence that the Tis21 gene is involved in the induction of GD3 9-O-acetylation. *J. Biol. Chem.*, **278**: 7942–7948.
- Sawada, M., Moriya, S., Saito, S., Shineha, R., Satomi, S., Yamori, T., Tsuruo, T., Kannagi, R. and Miyagi, T. 2002. Reduced sialidase expression in highly metastatic variants of mouse colon adenocarcinoma 26 and retardation of their metastatic ability by sialidase overexpression. *Int. J. Cancer*, **97**: 180–185.
- Schroeder, H.W. and Cavacini, L. 2010. Structure and function of immunoglobulins. *J. Allergy Clin. Immunol.*, **125**: S41-52.
- Schütte, C.G., Lemm, T., Glombitza, G.J. and Sandhoff, K. 1998. Complete localization of disulfide bonds in GM2 activator protein. *Protein Sci. Publ. Protein Soc.*, **7**: 1039–1045.
- Seyrantepe, V., Landry, K., Trudel, S., Hassan, J.A., Morales, C.R. and Pshezhetsky, A.V. 2004. Neu4, a novel human lysosomal lumen sialidase, confers normal phenotype to sialidosis and galactosialidosis cells. *J. Biol. Chem.*, **279**: 37021–37029.
- Sharma, D.K., Choudhury, A., Singh, R.D., Wheatley, C.L., Marks, D.L. and Pagano, R.E. 2003. Glycosphingolipids internalized via caveolar-related endocytosis rapidly merge with the clathrin pathway in early endosomes and form microdomains for recycling. *J. Biol. Chem.*, **278**: 7564–7572.
- Shen, Y., Kohla, G., Lrhorfi, A.L., Sipos, B., Kalthoff, H., Gerwig, G.J., Kamerling, J.P., Schauer, R. and Tiralongo, J. 2004. O-acetylation and de-O-acetylation of sialic acids in human colorectal carcinoma. *Eur. J. Biochem.*, **271**: 281–290.
- Shepherd, A.J., Wilson, N.J. and Smith, K.T. 2003. Characterisation of endogenous retrovirus in rodent cell lines used for production of biologicals. *Biol. J. Int. Assoc. Biol. Stand.*, **31**: 251–260.
- Shibuya, H., Hamamura, K., Hotta, H., Matsumoto, Y., Nishida, Y., Hattori, H., Furukawa, Keiko, Ueda, M. and Furukawa, Koichi. 2012. Enhancement of malignant properties of human osteosarcoma cells with disialyl gangliosides GD2/GD3. *Cancer Sci.*, **103**: 1656–1664.
- Shields, R.L., Namenuk, A.K., Hong, K., Meng, Y.G., Rae, J., Briggs, J., Xie, D., Lai, J., Stadlen, A., Li, B., Fox, J.A. and Presta, L.G. 2001. High resolution mapping of the binding site on human IgG1 for Fc gamma RI, Fc gamma RII, Fc gamma RIII, and FcRn and design of IgG1 variants with improved binding to the Fc gamma R. *J. Biol. Chem.*, **276**: 6591–6604.
- Stupp, R., Mason, W.P., van den Bent, M.J., Weller, M., Fisher, B., Taphoorn, M.J.B., Belanger, K., Brandes, A.A., Marosi, C., Bogdahn, U., Curschmann, J., Janzer, R.C., Ludwin, S.K., Gorlia, T., Allgeier, A., Lacombe, D., Cairncross, J.G., Eisenhauer, E., Mirimanoff, R.O., *et al.* 2005. Radiotherapy plus concomitant and adjuvant temozolomide for glioblastoma. *N. Engl. J. Med.*, **352**: 987–996.
- Sulica, A., Morel, P., Metes, D. and Herberman, R.B. 2001. Ig-binding receptors on human NK cells as effector and regulatory surface molecules. *Int. Rev. Immunol.*, **20**: 371–414.
- Sun, Y.-S., Zhao, Z., Yang, Z.-N., Xu, F., Lu, H.-J., Zhu, Z.-Y., Shi, W., Jiang, J., Yao, P.-P. and Zhu, H.-P. 2017. Risk Factors and Preventions of Breast Cancer. *Int. J. Biol. Sci.*, **13**: 1387–1397.
- Sundaram, K.S. and Lev, M. 1992. Purification and activation of brain sulfotransferase. *J. Biol.*

*Chem.*, **267**: 24041–24044.

Szklarczyk, D., Gable, A.L., Lyon, D., Junge, A., Wyder, S., Huerta-Cepas, J., Simonovic, M., Doncheva, N.T., Morris, J.H., Bork, P., Jensen, L.J. and Mering, C. von. 2019. STRING v11: protein-protein association networks with increased coverage, supporting functional discovery in genome-wide experimental datasets. *Nucleic Acids Res.*, **47**: D607–D613.

Takahashi, K., Proshin, S., Yamaguchi, K., Yamashita, Y., Katakura, R., Yamamoto, K., Shima, H., Hosono, M. and Miyagi, T. 2017. Sialidase NEU3 defines invasive potential of human glioblastoma cells by regulating calpain-mediated proteolysis of focal adhesion proteins. *Biochim. Biophys. Acta Gen. Subj.*, **1861**: 2778–2788.

Takematsu, H., Diaz, S., Stoddart, A., Zhang, Y. and Varki, A. 1999. Lysosomal and Cytosolic Sialic Acid 9-O-Acetyltransferase Activities Can Be Encoded by One Gene via Differential Usage of a Signal Peptide-encoding Exon at the N Terminus. *J. Biol. Chem.*, **274**: 25623–25631.

Terme, M., Dorvillius, M., Cochonneau, D., Chaumette, T., Xiao, W., Diccianni, M.B., Barbet, J., Yu, A.L., Paris, F., Sorkin, L.S. and Birklé, S. 2014. Chimeric antibody c.8B6 to O-acetyl-GD2 mediates the same efficient anti-neuroblastoma effects as therapeutic ch14.18 antibody to GD2 without antibody induced allodynia. *PLoS One*, **9**: e87210.

Tettamanti, G. 2004. Ganglioside/glycosphingolipid turnover: new concepts. *Glycoconj. J.*, **20**: 301–317.

Titus, A.J., Way, G.P., Johnson, K.C. and Christensen, B.C. 2017. Deconvolution of DNA methylation identifies differentially methylated gene regions on 1p36 across breast cancer subtypes. *Sci. Rep.*, **7**: 11594.

Uliana, A.S., Crespo, P.M., Martina, J.A., Daniotti, J.L. and Maccioni, H.J.F. 2006. Modulation of GalT1 and SialT1 Sub-Golgi Localization by SialT2 Expression Reveals an Organellar Level of Glycolipid Synthesis Control. *J. Biol. Chem.*, **281**: 32852–32860.

Vaccaro, A.M., Salvioli, R., Barca, A., Tatti, M., Ciaffoni, F., Maras, B., Siciliano, R., Zappacosta, F., Amoresano, A. and Pucci, P. 1995. Structural analysis of saposin C and B. Complete localization of disulfide bridges. *J. Biol. Chem.*, **270**: 9953–9960.

Valastyan, S. and Weinberg, R.A. 2011. Tumor metastasis: molecular insights and evolving paradigms. *Cell*, **147**: 275–292.

Vandamme-Feldhaus, V. and Schauer, R. 1998. Characterization of the enzymatic 7-O-acetylation of sialic acids and evidence for enzymatic O-acetyl migration from C-7 to C-9 in bovine submandibular gland. *J. Biochem. (Tokyo)*, **124**: 111–121.

Vargo-Gogola, T. and Rosen, J.M. 2007. Modelling breast cancer: one size does not fit all. *Nat. Rev. Cancer*, **7**: 659–672.

Varki, A. 2001. Loss of N-glycolylneuraminic acid in humans: Mechanisms, consequences, and implications for hominid evolution. *Am. J. Phys. Anthropol.*, **Suppl 33**: 54–69.

Veri, M.-C., Gorlatov, S., Li, H., Burke, S., Johnson, S., Stavenhagen, J., Stein, K.E., Bonvini, E. and Koenig, S. 2007. Monoclonal antibodies capable of discriminating the human inhibitory Fcγ3a-

receptor IIB (CD32B) from the activating Fcγ-receptor IIA (CD32A): biochemical, biological and functional characterization. *Immunology*, **121**: 392–404.

Vielhaber, G., Hurwitz, R. and Sandhoff, K. 1996. Biosynthesis, processing, and targeting of sphingolipid activator protein (SAP) precursor in cultured human fibroblasts. Mannose 6-phosphate receptor-independent endocytosis of SAP precursor. *J. Biol. Chem.*, **271**: 32438–32446.

Wallace, M.S., Lee, J., Sorkin, L., Dunn, J.S., Yaksh, T. and Yu, A. 1997. Intravenous lidocaine: effects on controlling pain after anti-GD2 antibody therapy in children with neuroblastoma--a report of a series. *Anesth. Analg.*, **85**: 794–796.

Wang, W., Erbe, A.K., Hank, J.A., Morris, Z.S. and Sondel, P.M. 2015. NK Cell-Mediated Antibody-Dependent Cellular Cytotoxicity in Cancer Immunotherapy. *Front. Immunol.*, **6**.

Wang, Z., Sun, Z., Li, A.V. and Yarema, K.J. 2006. Roles for UDP-GlcNAc 2-epimerase/ManNAc 6-kinase outside of sialic acid biosynthesis: modulation of sialyltransferase and BiP expression, GM3 and GD3 biosynthesis, proliferation, and apoptosis, and ERK1/2 phosphorylation. *J. Biol. Chem.*, **281**: 27016–27028.

Wasik, B.R., Barnard, K.N., Ossiboff, R.J., Khedri, Z., Feng, K.H., Yu, H., Chen, X., Perez, D.R., Varki, A. and Parrish, C.R. 2017. Distribution of O-Acetylated Sialic Acids among Target Host Tissues for Influenza Virus. *mSphere*, **2**.

Watson, C.J. and Khaled, W.T. 2008. Mammary development in the embryo and adult: a journey of morphogenesis and commitment. *Dev. Camb. Engl.*, **135**: 995–1003.

Wilkening, G., Linke, T., Uhlhorn-Dierks, G. and Sandhoff, K. 2000. Degradation of membrane-bound ganglioside GM1. Stimulation by bis(monoacylglycero)phosphate and the activator proteins SAP-B and GM2-AP. *J. Biol. Chem.*, **275**: 35814–35819.

Williams, A.F. and Barclay, A.N. 1988. The immunoglobulin superfamily--domains for cell surface recognition. *Annu. Rev. Immunol.*, **6**: 381–405.

Willison, H.J. and Yuki, N. 2002. Peripheral neuropathies and anti-glycolipid antibodies. *Brain J. Neurol.*, **125**: 2591–2625.

Yamaguchi, K., Hata, K., Koseki, K., Shiozaki, K., Akita, H., Wada, T., Moriya, S. and Miyagi, T. 2005. Evidence for mitochondrial localization of a novel human sialidase (NEU4). *Biochem. J.*, **390**: 85–93.

Yamamoto, A., Haraguchi, M., Yamashiro, S., Fukumoto, S., Furukawa, K., Takamiya, K., Atsuta, M., Shiku, H. and Furukawa, K. 1996. Heterogeneity in the expression pattern of two ganglioside synthase genes during mouse brain development. *J. Neurochem.*, **66**: 26–34.

Yamanami, H., Shiozaki, K., Wada, T., Yamaguchi, K., Uemura, T., Kakugawa, Y., Huijiya, T. and Miyagi, T. 2007. Down-regulation of sialidase NEU4 may contribute to invasive properties of human colon cancers. *Cancer Sci.*, **98**: 299–307.

Yankelevich, M., Kondadasula, S.V., Thakur, A., Buck, S., Cheung, N.-K.V. and Lum, L.G. 2012. Anti-CD3 × anti-GD2 bispecific antibody redirects T-cell cytolytic activity to neuroblastoma targets. *Pediatr. Blood Cancer*, **59**: 1198–1205.

Yu, A.L., Gilman, A.L., Ozkaynak, M.F., London, W.B., Kreissman, S.G., Chen, H.X., Smith, M., Anderson, B., Villablanca, J.G., Matthay, K.K., Shimada, H., Grupp, S.A., Seeger, R., Reynolds, C.P., Buxton, A., Reisfeld, R.A., Gillies, S.D., Cohn, S.L., Maris, J.M., *et al.* 2010. Anti-GD2 antibody with GM-CSF, interleukin-2, and isotretinoin for neuroblastoma. *N. Engl. J. Med.*, **363**: 1324–1334.

Yu, R.K. and Bieberich, E. 2001. Regulation of glycosyltransferases in ganglioside biosynthesis by phosphorylation and dephosphorylation. *Mol. Cell. Endocrinol.*, **177**: 19–24.

Yu, R.K., Macala, L.J., Taki, T., Weinfield, H.M. and Yu, F.S. 1988. Developmental changes in ganglioside composition and synthesis in embryonic rat brain. *J. Neurochem.*, **50**: 1825–1829.

Yusuf, H.K., Schwarzmann, G., Pohlentz, G. and Sandhoff, K. 1987. Oligosialogangliosides inhibit GM2- and GD3-synthesis in isolated Golgi vesicles from rat liver. *Biol. Chem. Hoppe. Seyler*, **368**: 455–462.

Zeng, Y., Fest, S., Kunert, R., Katinger, H., Pistoia, V., Michon, J., Lewis, G., Ladenstein, R. and Lode, H.N. 2005. Anti-neuroblastoma effect of ch14.18 antibody produced in CHO cells is mediated by NK-cells in mice. *Mol. Immunol.*, **42**: 1311–1319.